

Novel Pathways

Suppressing the Deleterious Effects of

Mitochondrial Protein Import Clogging

Gargi Mishra

A Dissertation in Biochemistry and Molecular Biology

Submitted in partial fulfillment of the requirements for the degree of Doctor of Philosophy in the
College of Graduate Studies of State University of New York, Upstate Medical University

Dedication

I dedicate this work to my partner, Nick, whose presence makes my life an equal measure of chaotic and peaceful. I also dedicate this work to my dog, Oreo, for his unconditional love; and whose curiosity for the world around him inspires me to be curious as well.

TABLE OF CONTENTS

LIST OF ABBREVIATIONS.....	7
ABSTRACT	8
LIST OF TABLES AND FIGURES.....	9
CHAPTER 1. INTRODUCTION	11
1.1] MITOCHONDRIAL PROTEIN IMPORT MACHINERIES	15
1.2] DEFECTIVE MITOCHONDRIAL PROTEIN IMPORT IN HEALTH AND DISEASE	31
1.3] MITOCHONDRIAL PROTEIN IMPORT CLOGGING: A SPECIFIC FORM OF MITOCHONDRIAL PROTEIN IMPORT STRESS	34
1.4] MOLECULAR PATHWAYS ACTIVATED IN RESPONSE TO MPOS AND MITOCHONDRIAL PROTEIN IMPORT CLOGGING	46
1.5] MEMBRANELESS ORGANELLES IN THE CONTEXT OF MITOCHONDRIA AND HUMAN HEALTH	67
1.6] THESIS OBJECTIVES.....	76
1.7] REFERENCES FOR CHAPTER 1	78
CHAPTER 2. CELLULAR PROTEOSTASIS DURING MITOCHONDRIAL PROTEIN IMPORT CLOGGING REQUIRES THE MITOCHONDRIAL F-BOX PROTEIN 1 AND DJ-1 HOMOLOG HSP31 IN	94
<i>SACCHAROMYCES CEREVISIAE</i>	94
2.1] ABSTRACT.....	95
2.2] INTRODUCTION	96
2.3] MATERIALS AND METHODS	99
2.4] RESULTS	109
2.5] DISCUSSION	126
2.6] SUPPORTING INFORMATION	135
2.7] LITERATURE CITED.....	136
2.8] SUPPLEMENTAL FIGURES AND OTHER SUPPORTING INFORMATION.....	140
CHAPTER 3. PBP1, THE YEAST HOMOLOG OF HUMAN ATAXIN-2, PROMOTES CELLULAR HOMEOSTASIS AND MITOCHONDRIAL GENOME STABILITY DURING MITOCHONDRIAL PROTEIN IMPORT CLOGGING	149
3.1] ABSTRACT.....	150
3.2] INTRODUCTION	151
3.3] RESULTS.....	157
3.4] DISCUSSION	182
3.5] EXPERIMENTAL PROCEDURES	192
3.6] SUPPORTING INFORMATION	211
3.7] REFERENCES FOR CHAPTER 3	212
3.8] SUPPLEMENTAL FIGURES AND TABLES FOR CHAPTER 3.....	217
CHAPTER 4. DISCUSSION AND FUTURE DIRECTIONS	225
4.1] KEY FINDINGS AND IMMEDIATE FUTURE DIRECTIONS.....	226
4.2] FUTURE DIRECTIONS FOR THE STUDY OF MITOCHONDRIAL BIOGENESIS AND HUMAN HEALTH	234
4.3] REFERENCES FOR CHAPTER 4	236

Acknowledgements

I would like to thank Dr. Xin Jie Chen for being my mentor these past five years. I have learned so much about yeast genetics and mitochondrial biology from him. He has also taught me how to think critically when performing experiments. Thanks also to Xiaowen Wang for training me in yeast-based experiments when I joined the Chen lab. Finally, thank you to all Chen lab members past and present (Liam, Arnav, Nick, Joe, Sanaea, and Eamon), you have all been wonderful peers.

Thank you to Drs. Kane and Knutson for being incredibly helpful members of both my thesis committee as well as my defense committee. Additionally, thank you to the professors who agreed to be on my thesis committee: Dr. Frank Middleton (chair), Dr. Martin Graef from Cornell University (external examiner), and Dr. Auyon Ghosh. Thank you so much to you all for your incredibly helpful feedback!

A huge thank you to the MD-PhD program, our current director Dr. Kane, our current assistant director Dr. Auyon Ghosh, and the past directors: Dr. Dhamoon for his continued mentorship these past six years, as well as Dr. Kotula and Dr. Perl who accepted me into this program. A special shoutout to the program coordinator Andrea Cifonelli who has always been a huge support for me.

Thank you to all members of the Biochemistry and Molecular Biology department, especially Dr. Bruce Knutson and Dr. Ryan Palumbo for always helping me with anything related to molecular biology. A special thank you to Dr. Stephen Hanes for his mentorship when I was applying to the AHA fellowship. Thank you also to Dr. Ebbing de jong and Karen Gentile for all their support in my omics-based experiments. A huge thank you to Sandra Jarvis and Jennifer Dow for helping navigate anything administrative in the Biochemistry department and for their warmth.

Thank you to COGS leadership -our current and past deans, as well as administrative staff: Cherylene Small, Jennifer Brennan, John Gillies, and Shaunna Arnold. Thank you for being so supportive during my training here.

Next, I would like to thank my clinical mentors who allowed me to shadow them during my PhD training years: Dr. Anuradha Duleep, Dr. Geoffrey Henderson, Dr. Dragos Mihaila, Dr. Amit Dhamoon, Dr. Joshua Harrison, Dr. Srikanth Yandrapalli, and Dr. Auyon Ghosh. Clinical preceptorships with these physicians helped expose me to different clinical departments during my PhD years when I was away from medical school, and it was so helpful to observe the clinician-patient dynamics through these mentored experiences.

Next, I would like to thank our funding sources that provided support for making this project possible, namely the National Institutes of Health, and the American Heart Association's predoctoral fellowship. I especially want to thank members in the Central New York (CNY) region that are a part of the American Heart Association, namely Kristy Smorol, Jason Pomeroy, and Heather Evans. These individuals helped introduce me to members of the local community so that I could describe my research project with non-experts. Additionally, I was able to hear from physicians and heart disease patients in the CNY region, which was an invaluable experience.

I would like to now thank folks more personal to my life who have supported my journey so far. First, my parents, my brother, my grandmother, and my other grandparents in heaven for being the best support system I could ask for. Next, I have been blessed with several parental figures both in my personal life, such as my partner's mom, and folks at Upstate, such as Debra Purdy and Katie Daley. I have also been blessed with the best mentors, teachers, and coaches throughout school and in college. Some notable folks who made college an invaluable experience for my life are: Professor Sarah Bacon with whom I did my undergraduate thesis in Biology;

Professor Katie Berry with whom I took Biochemistry courses and realized I loved Biochemistry; and Professor Maria Gomez with whom I took my first 8:35am college course (General Chemistry) and who showed me that thermodynamics wasn't that scary. I also want to thank my coaches in Track and Field and Cross Country who taught me the importance of hard work: Christine (Tina) Lee, Jennifer Adams, and Chris Kibler. After college, I had a once-in-a-lifetime opportunity of spending a year working at the Broad Institute of MIT & Harvard in Dr. Robert Manguso's group: the Tumor Immunotherapy Discovery Engine (TIDE). Rob, Kathleen, and Juan led the most collegial and productive lab, and I learned not only how to perform in vivo genomic screens, but how to also be a good scientist and colleague. Next, I would like to thank all the friends that I have made through different phases of my life so far. They span multiple continents, countries, cities, and time zones, and there are too many to name. But despite being spread out all around the globe, they make space for me in their lives and have brought so much joy and love into my life, I am forever indebted to them.

Finally, I would like to thank my partner Nicholas Frey, and my soul-dog Oreo. They both have supported me every single day and I love and appreciate them very much.

List of Abbreviations

General mitochondrial biology & stress

- **mPOS**: mitochondrial protein overaccumulation stress
- **mtDNA**: mitochondrial DNA
- $\Delta\psi$: mitochondrial membrane potential
- **ROS**: reactive oxygen species
- **UPRmt**: mitochondrial unfolded protein response

Mitochondrial protein import & biogenesis

- **TOM**: translocase of the outer mitochondrial membrane
- **TIM23**: translocase of the inner mitochondrial membrane 23 complex
- **TIM22**: translocase of the inner mitochondrial membrane 22 complex
- **SAM**: sorting and assembly machinery
- **MIM**: mitochondrial import machinery
- **OMM**: outer mitochondrial membrane
- **IMM**: inner mitochondrial membrane
- **IMS**: intermembrane space
- **MTS**: mitochondrial targeting sequence
- **PAM**: presequence translocase-associated motor

Genes, proteins, and pathways central to this thesis

- **AAC2**: ADP/ATP carrier 2
- **ANT**: adenine nucleotide translocator
- **DM**: Aac2^{A128P, A137D} double mutant
- **Mfb1**: mitochondrial F-box protein 1
- **Hsp31**: heat shock protein 31 (DJ-1 homolog)
- **Pbp1**: poly(A)-binding protein-binding protein 1
- **DJ-1**: Parkinson disease protein 7 (human homolog of Hsp31)
- **SG**: Stress granules
- **P bodies**: Processing bodies

Proteostasis & stress responses

- **HSP**: heat shock protein
- **UPS**: ubiquitin-proteasome system
- **SG**: stress granule
- **RQC**: ribosome quality control
- **ISR**: integrated stress response

Genetics & yeast biology

- **WT**: wild type
- **KO**: knockout
- **OE**: overexpression
- Δ : gene deletion
- **ORF**: open reading frame

Abstract

Mitochondria perform diverse cellular functions beyond ATP production, including calcium handling, innate immune signaling, and cell death regulation. Increasing evidence indicates that mitochondrial dysfunction can arise independently of bioenergetic failure. In particular, defects in mitochondrial protein import can cause the toxic accumulation of unimported precursors in the cytosol, triggering mitochondrial precursor overaccumulation stress (mPOS) and ultimately leading to cell death. Because ~99% of the mitochondrial proteome is nuclear encoded, maintaining protein import fidelity is a major cellular challenge. Several human diseases previously attributed solely to impaired mitochondrial function are now understood to arise from protein import defects. One especially deleterious form of import defect occurs when precursor proteins become lodged within the import translocases, a phenomenon termed mitochondrial protein import clogging. In this thesis, I used *Saccharomyces cerevisiae* to identify and characterize cellular pathways that either alleviate mitochondrial protein import clogging or enable adaptation to mPOS. Using genetic screens, transcriptomic profiling, and proteomic approaches, I identified two distinct protective pathways. The first centers on the mitochondrial F-box protein Mfb1 and the cytosolic heat shock protein Hsp31, the yeast homolog of human DJ-1. I show that *MFBI* overexpression rescues growth and import defects under multiple mPOS-inducing conditions, whereas *MFBI* loss exacerbates precursor accumulation, mtDNA instability, and proteostatic stress. Mechanistically, Mfb1 localizes near the mitochondrial protein import machinery and appears to support import competency at the mitochondrial surface, while Hsp31 acts downstream as a cytosolic proteostatic buffer in Mfb1-deficient cells to alleviate mPOS under import clogging conditions. The second pathway involves the RNA-binding proteins Pbp1 and Pab1, key components of stress granules. Through a multicopy suppressor screen, I found that *PBP1* and *PABI* robustly suppress petite colony formation, likely by restoring mitochondrial integrity under severe import clogging conditions. Transcriptomic, proteomic, and RNA interactomic analyses revealed that mitochondrial protein import clogging dramatically reduces the interaction networks of Pbp1. Pbp1 dosage strongly modulates transcriptional programs governing mitochondrial biogenesis, iron homeostasis, and cellular metabolism in a manner dependent on import state. Together, this work defines two complementary adaptive strategies that protect cells from mitochondrial protein import clogging: a mitochondrial surface quality-control pathway mediated by Mfb1, a cytosolic proteostasis pathway involving Hsp31, and a condensate-driven pathway involving Pbp1. These findings establish mechanistic links between mitochondrial protein import fidelity, cytosolic proteostasis, RNA biology, and mitochondrial genome stability, with implications for understanding mitochondrial disease and neurodegenerative disorders.

List of Tables and Figures

Chapter 1. Introduction

Figure 1.1. An overview of mitochondria (singular: mitochondrion).

Figure 1.2. Overview of the TOM complex.

Figure 1.3. Overview of the other OMM import pathways.

Figure 1.4. Subcategories of intermembrane space (IMS) proteins.

Figure 1.5. An overview of the IMM-based import pathways.

Figure 1.6. An overview of mPOS and mitochondrial protein import clogging.

Table 1.1. Outer membrane import complexes and their components.

Table 1.2. Similarities and differences between the TIM23 (presequence) and TIM22 (carrier) import complexes.

Table 1.3. MICOS complex components and their functions.

Table 1.4. Human diseases associated with defects in mitochondrial protein import machineries.

Table 1.5. Disease-associated dominant mutations in ANT1.

Table 1.6. Model systems used to induce mitochondrial protein import clogging and stress.

Table 1.7. Cellular responses triggered by mitochondrial protein import stress.

Table 1.8. Protein quality control pathways acting on the cytosol-mitochondria interface.

Table 1.9. Intramitochondrial protein quality control pathways.

Table 1.10. P bodies and Stress Granules (SGs): Key similarities and differences.

Table 1.11. RNA-protein condensates in the cytosol associated with mitochondria across different species.

Table 1.12. RNA-binding proteins (RBPs) with causative links to neurodegenerative diseases.

Chapter 2. Cellular proteostasis during mitochondrial protein import clogging requires the mitochondrial F-box protein 1 and DJ-1 homolog HSP31 in *Saccharomyces cerevisiae*

Figure 2.1. *MFBI* overexpression rescues cell growth under a variety of stress conditions with mitochondrial protein import defects.

Figure 2.2. Disruption of *MFBI* under import clogging conditions worsens growth defects and decreases mtDNA stability.

Figure 2.3. Mfb1 interactome analysis reveals its presence on the mitochondrial outer membrane in the proximity of the TOM complex and interorganelle contact sites.

Figure 2.4. Disruption of *MFBI* increases the cytosolic retention of mitochondrial proteins under protein import clogging conditions as revealed by TMT-mass spectrometry analysis of cytosolic fractions.

Figure 2.5. Transcriptomic analysis reveals the activation of unique cellular pathways under conditions of protein import clogging and *MFBI* loss.

Figure 2.6. Disruption of *HSP31* creates a synthetic growth defect with *aac2^{A128P, A137D}* and *aac2^{A128P, A137D} mfb1Δ* and increases the levels of ubiquitinated proteins in the cytosol under respiring conditions.

Figure S2.1: A subclone containing only the *MFBI* open reading frame can rescue cell growth defect of a yeast strain expressing *aac2^{A128P}*.

Figure S2.2: Western blot showing localization of the Mfb1-miniTurboID fusion protein to the mitochondrial fraction.

Figure S2.3: Mfb1's interactome as revealed by BioID assay.

Figure S2.4: Downregulated genes in the RNAseq dataset.

Figure S2.5: Characterization of *AMK1*.

Figure S2.6: Disruption of *HSP31* is sufficient to increase levels of ubiquitinated proteins in Triton-insoluble fractions.

Figure S2.7: Hsp31 remains cytosolic, regardless of clogging conditions or Mfb1-deficiency.

Tables for Chapter 2 are available online as part of the manuscript by Mishra et al. 2025 (doi:10.1093/genetics/iyaf279)

Chapter 3. Pbp1, the yeast homolog of human Ataxin-2, promotes cellular homeostasis and mitochondrial genome stability during mitochondrial protein import clogging

Figure 3.1. Multicopy suppressor screen identifies genetic suppressors of mtDNA instability under import clogging conditions.

Figure 3.2. Genetic suppressors of mtDNA loss improve mitochondrial morphology.

Figure 3.3. Protein import clogging-associated growth defects and mtDNA loss is made worse by the disruption of *PBPI* and *PABI*.

Figure 3.4. Pairwise differential expression analysis.

Figure 3.5. Differences in *PBPI* gene dosage affect cellular transcription depending on presence or absence of clogging.

Figure 3.6. Pbp1 protein's localization becomes heterogeneous under respiring conditions, and this is exacerbated by protein import clogging.

Figure 3.7. Pbp1 immunoprecipitation (IP) reveals the types of proteins Pbp1 interacts with under respiring conditions, with or without import clogging.

Figure 3.8. Pathways represented by the proteins associating with Pbp1.

Figure 3.9. RNAs enriched with Pbp1 protein under respiring conditions, with or without protein import clogging.

Figure 3.10. A large fraction of RNAs undergo a reduction in binding to Pbp1 under protein import clogging conditions.

Figure 3.11. Working model for Pbp1's role in maintaining mitochondrial protein import efficiency.

Figure S3.1: Pathways enriched and depleted in Bulk RNAseq (part 1).

Figure S3.2: Pathways enriched and depleted in Bulk RNAseq (part 2).

Figure S3.3. Genotype-Environment Interaction MA plots.

Figure S3.4. Western blot analysis for Pbp1 protein localization and immunoprecipitation.

Figure S3.5. Venn diagram of shared and unique proteins enriched with Pbp1 (IPMS).

Figure S3.6. Global heatmaps of enriched or depleted proteins in the Pbp1 immunoprecipitation (IP-MS).

Figure S3.7. Types of RNA (transcript "biotypes") enriched with Pbp1 in (A) WT background, or (B) DM background.

Figure S3.8. Venn diagram of shared and unique RNAs enriched with Pbp1 (RIPseq).

Figure S3.9. Pathways enriched or depleted in RIPseq for the RNAs associating with Pbp1.

Supplemental Table S3.1. Excel Workbook containing list of strains, plasmids, primers, and reagents.

Chapter 1. Introduction

Gargi Mishra

Portions of this chapter were adapted from Mishra et al. 2023 (Mishra G, Coyne LP, Chen XJ. Adenine nucleotide carrier protein dysfunction in human disease. *IUBMB Life*. 2023;75(11):911-925. doi:10.1002/iub.2767).

All figures in Chapter 1 were prepared using Biorender (Biorender.com).

Mitochondria are double-membraned organelles found in almost all eukaryotic cells (ROGER *et al.* 2017) (Figure 1.1A). They are best known for their role in energy production, a process that generates large amounts of ATP, the primary energy currency of the cell (MITCHELL 1961; ERNSTER AND SCHATZ 1981). However, over the past several years it has become clear that mitochondria play essential roles in many other vital cellular processes, including cellular proliferation, innate immunity, redox homeostasis, calcium signaling, iron-sulfur (Fe-S) cluster assembly, and programmed cell death (STEHLING AND LILL 2013; ORRENIUS *et al.* 2015; SPINELLI AND HAIGIS 2018; TIWARI-HECKLER *et al.* 2022; CHEN *et al.* 2024; LU *et al.* 2025) (Figure 1.1B). These diverse functions underscore the profound importance of mitochondria to cellular and organismal homeostasis.

Ancestors of the modern eukaryotic cell did not always contain mitochondria. Evolutionary and phylogenetic studies suggest that approximately 1.5 billion years ago, a host cell of unknown lineage engulfed an α -proteobacterium or an intracellular symbiont with α -proteobacterial features (MARTIJN *et al.* 2018). This endosymbiotic event is thought to have occurred prior to the emergence of the last eukaryotic common ancestor (LECA), indicating that mitochondria were already an integral component of early eukaryotic cells. Natural selection favored the stable maintenance of this endosymbiont within the host, which gradually transitioned into a bona fide organelle as the host cell evolved into modern eukaryotes (RAVAL *et al.* 2022) (Figure 1.1C).

A defining feature of this transition was extensive genome reduction of the endosymbiont. Many genes were either lost or transferred to the host nuclear genome through endosymbiotic gene transfer, while a small subset was retained within the mitochondrial genome (GRAY 1982; JANOUSKOVEC *et al.* 2017; SUNNUCKS *et al.* 2017). As a result, modern mitochondria harbor

compact genomes, circular or linear depending on the species, that encode a limited number of polypeptides involved primarily in oxidative phosphorylation, as well as ribosomal (rRNA) and transfer RNAs (tRNA). Consequently, the vast majority of mitochondrial proteins, including most components of the oxidative phosphorylation machinery, are now encoded in the nucleus and must be imported into mitochondria (CHACINSKA *et al.* 2009). This reliance on protein import is a defining feature of mitochondrial biogenesis and is essential for mitochondria to execute their diverse cellular functions (NEUPERT AND HERRMANN 2007).

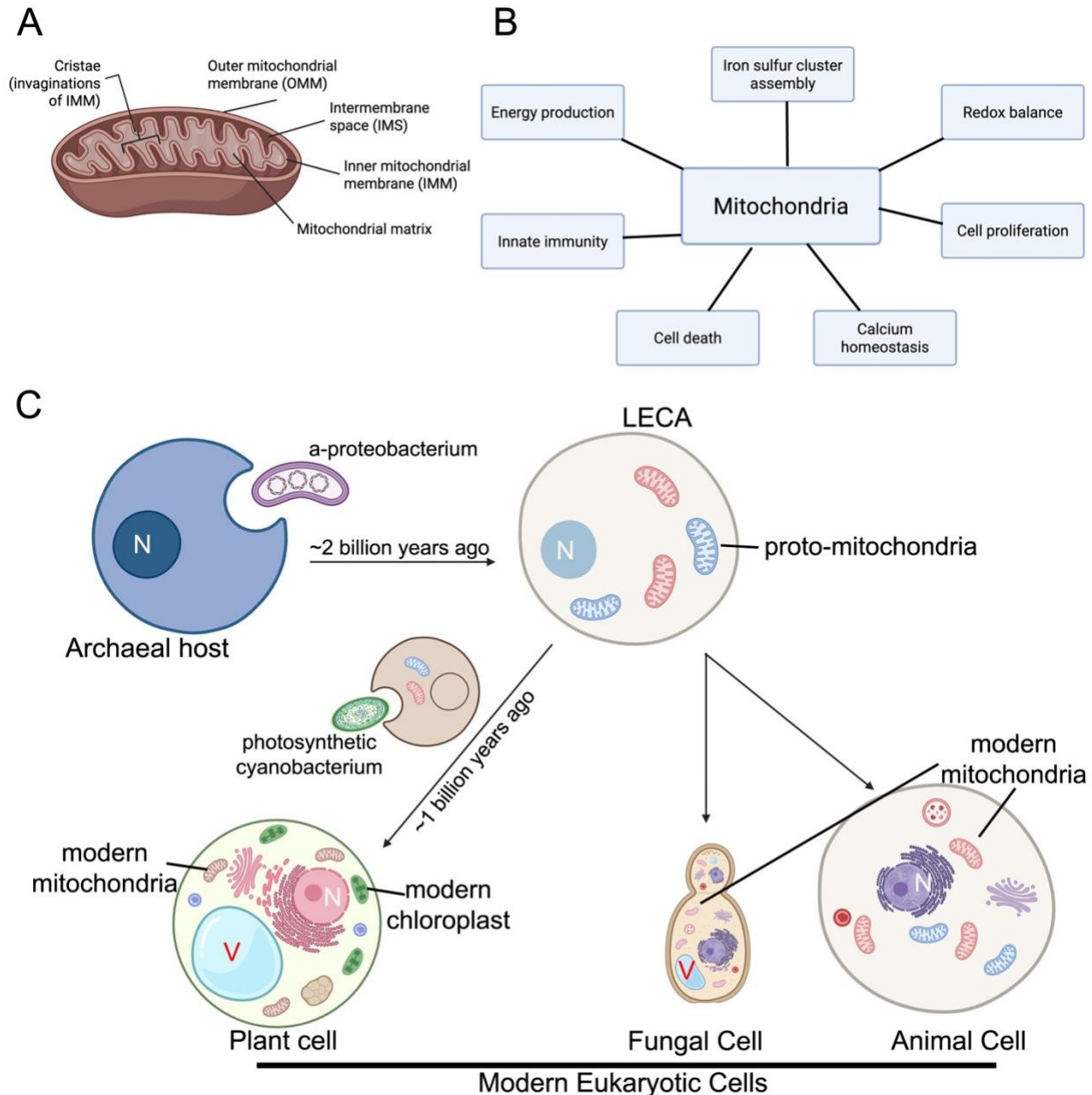


Figure 1.1. An overview of mitochondria (singular: mitochondrion). (A) Mitochondria are double-membraned, and this gives rise to four distinct sub-compartments: outer mitochondrial membrane (OMM), intermembrane space (IMS), inner mitochondrial membrane (IMM), and the matrix. Cristae (singular: crista) are invaginations of the IMM. (B) A diverse set of cellular functions performed by mitochondria. (C) Key evolutionary events that led to the acquisition of mitochondria by modern eukaryotic cells. Plant cells underwent an additional evolutionary event that led to acquisition of chloroplasts in addition to mitochondria. N, nucleus; V, vacuole.

1.1] Mitochondrial protein import machineries

The host cell evolved protein complexes that would be dedicated to the import of nuclear genome-encoded mitochondrial proteins and tRNAs from the cytosol to the four distinct mitochondrial compartments. These included the translocase complexes TOM (translocase of the outer membrane) and TIM (translocase of the inner membrane). TIM can be further subdivided into TIM22 and TIM23 complexes. Other import pathways such as SAM (sorting and assembly machinery), MIA (mitochondrial intermembrane space assembly), and MIM (mitochondrial import complex) also evolved to facilitate the transfer of proteins from the cytosol into the various mitochondrial subcompartments (NEUPERT AND HERRMANN 2007; CHACINSKA *et al.* 2009; WIEDEMANN AND PFANNER 2017).

1.1.a] Overview of the TOM complex

The TOM complex on the outer mitochondrial membrane (OMM) is composed of seven subunits: the entry channel Tom40, three receptors Tom70, Tom22, and Tom20, as well as the three small subunits Tom5, Tom6, and Tom7. In human (*Homo sapiens*), these subunits are correspondingly called TOMM40, TOMM70, TOMM22, TOMM20, TOMM5, TOMM6, and TOMM7 (ENDO AND YAMANO 2010; SAYYED AND MAHALAKSHMI 2022). Based on cryo-EM studies performed in *Neurospora crassa*, *Saccharomyces cerevisiae*, and human cells, it was revealed that the TOM core complex (TOM-CC) is evolutionarily conserved and consists of Tom40, small Tom subunits, and Tom22. This core complex interacts with Tom20 and Tom70 to form the complete TOM complex (BAUSEWEIN *et al.* 2017; TUCKER AND PARK 2019; WANG *et al.* 2020).

Tom40 forms a 19-stranded β -barrel that can form parallel hydrogen bonds leading to barrel closure (LACKEY *et al.* 2014). This channel provides the primary entry gate for

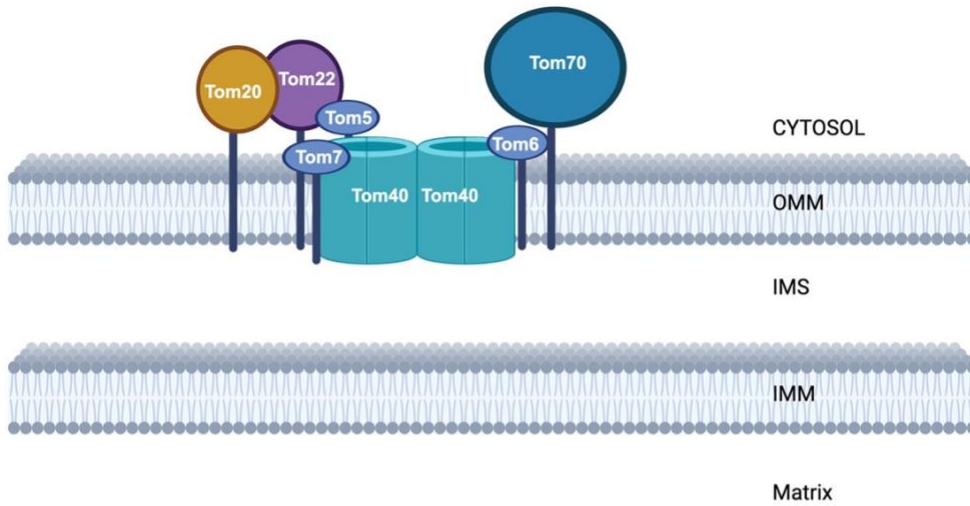
mitochondrial precursor proteins, i.e., preproteins, to translocate from the cytosol and into the intermembrane space (IMS) side of mitochondria. The lumen of Tom40 is highly negatively charged which allows positively charged polypeptides to be translocated. Further, Tom40 can accommodate two alpha-helices to translocate at a time since it has a diameter of 40 angstroms at its longest point. Tom40 can exist as a dimer or a tetramer, and potentially as a trimer in humans and yeast. The transmembrane portion of the Tom40 b-barrel is 90 angstroms and contains a 30-angstroms hydrophobic patch. On the IMS side, Tom40 possesses a positive region, while on the cytosolic side it possesses a negative region (AHTING *et al.* 2001). In the stabilized dimeric state, two Tom22 receptors appear to bind to the Tom40 channels. The tetramer form of Tom40 is thought to arise due to the dimerization of the dimer and stabilized by Tom6. However, the most stable form of Tom40 appears to be a dimer stabilized by two copies of Tom22, Tom5, Tom6, and Tom7 (MODEL *et al.* 2002).

The small Toms, namely Tom5, Tom6, and Tom7 are small, single-pass transmembrane proteins that play essential structural and regulatory roles within the TOM complex. Although they do not function as primary receptors, these subunits are critical for stabilizing Tom40, organizing the TOM core complex, and modulating complex assembly and dynamics. Tom5 is positioned adjacent to the cytosolic entrance of the Tom40 pore and facilitates the efficient transfer of precursor proteins from the surface receptors to the translocation channel, thereby acting as a coupling factor between receptor binding and pore engagement (DIETMEIER *et al.* 1997). Tom6 primarily functions as a stabilizing subunit that promotes oligomerization of Tom40, contributing to the formation and maintenance of dimeric and higher-order TOM assemblies. In contrast, Tom7 plays a more dynamic role and has been implicated in TOM complex remodeling and turnover; loss of Tom7 stabilizes larger TOM assemblies, suggesting that Tom7 promotes complex

disassembly or exchange of Tom40 subunits during biogenesis or quality control (HONLINGER *et al.* 1996). Together, Tom5, Tom6, and Tom7 fine-tune the structural integrity, functional efficiency, and plasticity of the TOM complex, ensuring robust mitochondrial protein import under varying cellular conditions (MEISINGER *et al.* 2001; MODEL *et al.* 2002).

Tom22 is the core complex's primary preprotein receptor (KIEBLER *et al.* 1993). To perform this function, Tom22 utilizes its cytosolic hydrophilic N-terminal subunit. This subunit recognizes the import signal sequence and serves as an interaction site for Tom20 and Tom70. The IMS-exposed C-terminal domain of Tom22 stabilizes the TOM complex and transfers the imported preprotein to the downstream import machinery, primarily the translocase of inner mitochondrial (TIM)23 complex (HONLINGER *et al.* 1995; VAN WILPE *et al.* 1999). Tom20 and Tom70 both contain a single transmembrane alpha-helix at their N-termini which anchors them to the outer mitochondrial membrane (PITT AND BUCHANAN 2021). Tom20 acts as the receptor for preproteins containing an N-terminal signal sequence, while Tom70 serves as the receptor for preproteins with an internal targeting sequence (BRIX *et al.* 1999; BRIX *et al.* 2000). Tom20's cytosolic C-terminal sequence creates an alpha-helix containing a hydrophobic groove to interact with the presequence peptide of a mitochondrial preprotein (ABE *et al.* 2000). The cytosolic domain of Tom70 is a lot more complex and composed of 26 alpha-helices forming a suprahelical structure that interacts with various cytosolic proteins, including heat shock proteins Hsp70 (yeast) or the chaperone complex of Hsp70 and Hsp90 (human) to deliver preproteins to Tom70 and TOMM70 respectively (YOUNG *et al.* 2003) (Figure 1.2, Table 1.1).

A



B

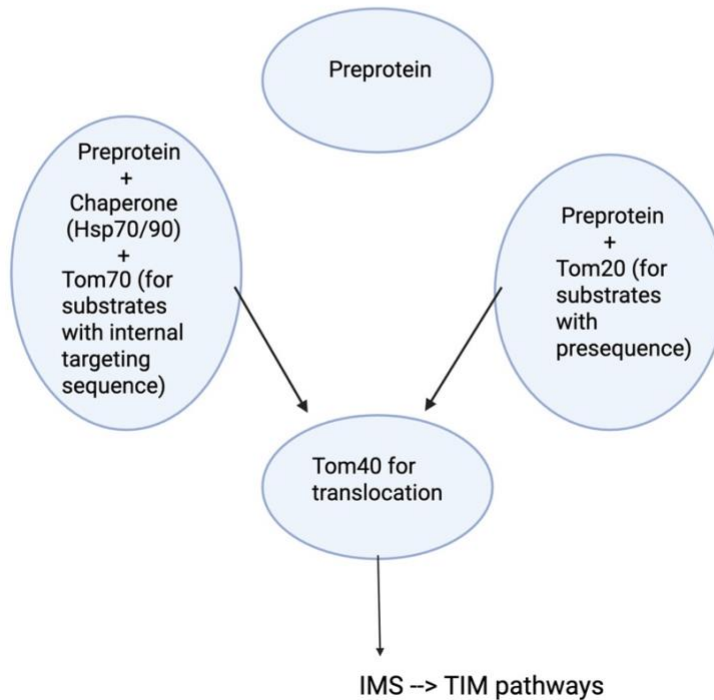


Figure 1.2. Overview of the TOM complex. (A) Main components of the TOM translocase complex. The translocase channel is formed by Tom40. Membrane-anchored receptors on the OMM consist of Tom20, Tom22, and Tom70. Small Tom subunits Tom5, Tom6, Tom7 support the stability of the translocase complex. (B) The logic of mitochondrial protein import. Nascent preprotein interacts with OMM receptors with or without being escorted by the cytosolic chaperones. The receptors (Tom20, Tom22, or Tom70) with escort the nascent preprotein to Tom40 for translocation across the OMM to deliver preprotein to the IMS. Here, the preprotein can either be imported further by the TIM pathways to reach the IMM or the matrix, or it can stay in the IMS.

Table 1.1. Outer membrane import complexes and their components.

Subunit	Localization	Structural Features	Primary Function	Notes
Tom40	OMM	19-stranded β -barrel	Import channel	Negatively charged lumen
Tom22	OMM	Single-pass TM + cytosolic & IMS domains	Core receptor & scaffold	Couples TOM to TIM23
Tom20	OMM	N-term TM, C-term receptor	Presequence recognition	Hydrophobic groove
Tom70	OMM	N-term TM, TPR-rich cytosolic domain	Internal signal receptor	Chaperone docking
Tom5	OMM	Single-pass TM	Substrate hand-off	Couples receptors to pore
Tom6	OMM	Single-pass TM	Complex stabilization	Promotes oligomerization
Tom7	OMM	Single-pass TM	Remodeling & turnover	Regulates TOM dynamics

1.1.b] Overview of the MIM and SAM pathways for mitochondrial outer membrane protein insertion

Not all mitochondrial proteins utilize the TOM complex for translocating across the OMM. The mitochondrial import (MIM) complex acts as the primary translocase for the insertion of single-pass and multi-spanning alpha-helical proteins into the OMM (BECKER *et al.* 2011; DIMMER *et al.* 2012; DOAN *et al.* 2020) (Figure 1.3A). MIM complex also promotes the import of signal-anchored and tail-anchored proteins (WALTHER AND RAPAPORT 2009). Well-known substrates of the MIM complex include the signal-anchored receptors Tom20 and Tom70 as well as the tail-anchored proteins Tom5, Tom6, and Tom7, emphasizing the importance of MIM in TOM complex biogenesis (POPOV-CELEKETIC *et al.* 2008; DIMMER *et al.* 2012). The MIM complex consists of multiple copies of Mim1 as well as up to two copies of Mim2. MIM complex is subdivided into three populations: MIM interacting with TOM allows Tom70-dependent import of multispanning and some signal-anchored proteins, free MIM complexes promote Tom70-independent import of single-spanning proteins, and MIM interacting with the sorting and assembly machinery (SAM)

delivers small Tom proteins for their assembly with the beta-barrel of Tom40 (POPOV-CELEKETIC *et al.* 2008; ENDO AND YAMANO 2010; BECKER *et al.* 2011; DIMMER *et al.* 2012).

As alluded, the sorting and assembly machinery (SAM) complex plays a role in the insertion of beta-barrel precursor proteins into the OMM (HOPPINS AND NARGANG 2004; WIEDEMANN *et al.* 2004). The SAM complex, composed of the beta-barrel Sam50 and peripheral components Sam35 and Sam37, is required for the maturation of Tom40 and its insertion into the OMM (CHAN AND LITHGOW 2008; BECKER *et al.* 2010). Other beta-barrel precursors first interact with Tom70 and are then transferred over to the SAM complex for insertion into the OMM (BECKER *et al.* 2008) (Figure 1.3B).

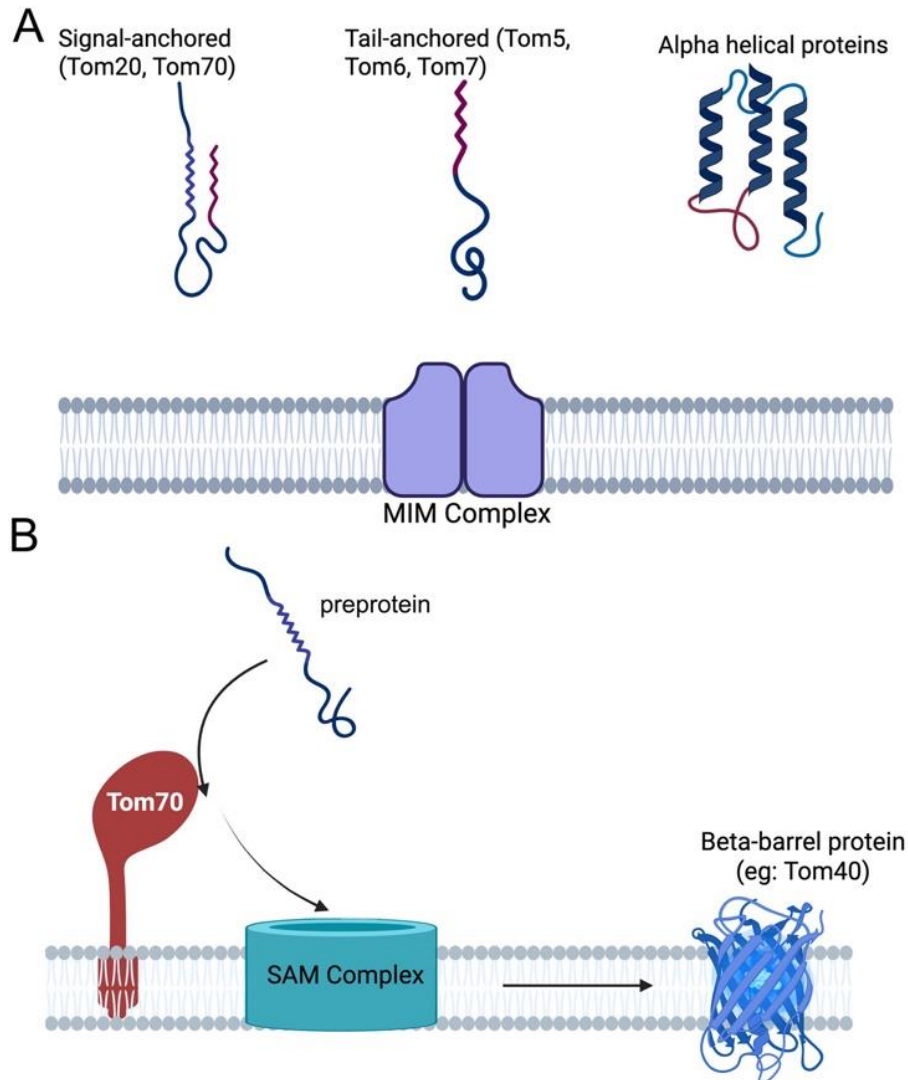


Figure 1.3. Overview of the other OMM import pathways. (A) The MIM pathway is responsible for the biogenesis of several TOM complex subunits. Additionally, the MIM pathway takes part importing alpha-helical proteins into the OMM in either a Tom70-dependent, or Tom70-independent manner. **(B)** The SAM complex plays a role in the biogenesis of the TOM complex's translocase subunit, namely Tom40, a beta-barrel protein. SAM complex imports other beta-barrel proteins into the OMM as well in a Tom70-dependent manner.

1.1.c] Overview of the MIA pathway for the import of intermembrane space proteins

The mitochondrial intermembrane space (IMS) is a topological space enclosed by the outer and inner mitochondrial membranes. It houses proteins involved in a variety of different processes such as the electron transport chain, lipid and metal ion homeostasis, redox signaling, and calcium signaling. IMS proteins only amount to about 5% of the entire mitochondrial proteome, however

their import is highly regulated (HERRMANN AND RIEMER 2010). Proteins destined for the IMS can be classified into three distinct groups based on the way they are sorted (Figure 1.4). The first group consists of proteins that possess bipartite presequences. Proteins with bipartite presequences utilize an N-terminal matrix targeting signal sequence that causes them to reach the TIM23 complex present on the inner membrane which is followed by a hydrophobic sorting domain that integrates into the inner membrane. The hydrophobic domains of these proteins integrate into the inner membrane by lateral diffusion and then mitochondrial proteases cleave the N-terminal presequence as well as within or at the IMS-facing surface of the inner membrane, allowing the mature and soluble protein to be released into the IMS (GOMES *et al.* 2017; HANSEN AND HERRMANN 2019). A prime example of a bipartite presequence containing soluble IMS protein is cytochrome b2 (GLICK *et al.* 1992). The second class of IMS proteins are soluble proteins imported independently of being targeted to the TIM23 complex. Proteins in this category lack N-terminal targeting signals, possess low molecular weight, and contain cysteine residues that allow for cofactor binding and disulfide bridge formation (LUTZ *et al.* 2003). These proteins are imported into the IMS via the mitochondrial intermembrane space assembly (MIA) pathway. The key effectors of this pathway are two IMS proteins namely the oxidoreductase Mia40 and a sulfhydryl oxidase Erv1. The substrates of Mia40 are first translocated via the TOM complex to enter the IMS. The cysteine residue on these substrates binds to Mia40 via a disulfide intermediate. Nucleophilic attack causes the intermolecular disulfide bond to be substituted for an intramolecular disulfide bond within the substrate protein. Mia40 is reoxidized via an electron transfer from Erv1. This process is called the ‘disulfide relay’ and is one of the major import pathways for IMS proteins, an example substrate of this pathway is the protein Atp23 (MESECKE *et al.* 2005). Proteins such as the yeast thiol peroxidase Gpx3 were also found to also re-oxidize Mia40 (FISCHER *et al.*

2013). The third and final class of IMS proteins neither possess bipartite presequences nor require Mia40 for import. Instead, these proteins utilize unconventional modes of import, the most common route being their import via Tom40 into IMS, followed by their arrest in a stable folded state that prevents their retrotranslocation, a prime example of this kind being cytochrome c (DIEKERT *et al.* 1999; EDWARDS *et al.* 2021).

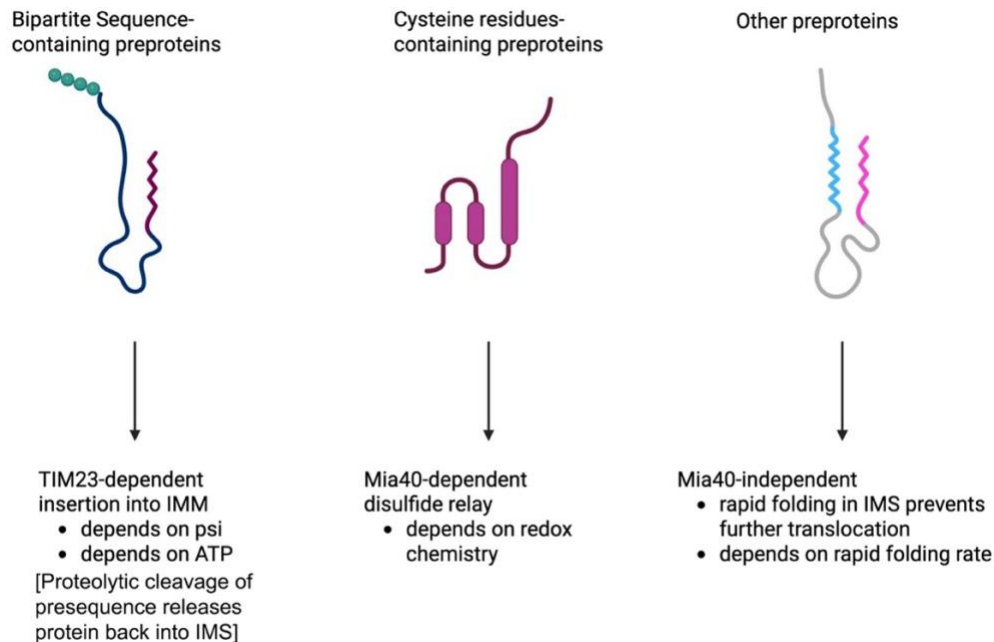


Figure 1.4. Subcategories of intermembrane space (IMS) proteins. From left to right: bipartite presequence-containing proteins (example, cytochrome B2), cysteine residues-containing proteins (example, Atp23), kinetically folding proteins (example, cytochrome c).

1.1.d] Overview of TIM22 and TIM23 complexes for mitochondrial inner membrane and matrix protein import

Two subcompartments exist downstream of OMM and IMS, namely the inner membrane (IMM) and the matrix. The TIM23 complex facilitates the import of soluble proteins belonging to the mitochondrial matrix, as well as IMM proteins whose precursors contain cleavable presequences. On the other hand, the TIM22 complex facilitates the import of mitochondrial carrier proteins, which is a family of proteins that resides in the IMM and whose members act as

channels and transporters of various solutes. Below, is an overview of what we know about these two import machineries (Figure 1.5, Table 1.2).

The TIM23 core complex in yeast is composed of three major subunits, namely Tim17, Tim44, and Tim23 (JAIN *et al.* 2025). Various chaperones, ATPases, nucleotide exchange factors, and motor proteins also take part in facilitating the function of this complex. The human TIM23 complex is highly conserved with that in yeast, but with subtle differences. For instance, humans have multiple TIM23 complexes due to having multiple Tim17 isoforms (RAINBOLT *et al.* 2013; PFANNER *et al.* 2019). The substrates of the TIM23 complex include nuclear-encoded proteins that contain an N-terminal cleavable presequence and are destined for the IMM or the matrix (NEUPERT AND HERRMANN 2007; CHACINSKA *et al.* 2009; HOMBERG *et al.* 2023). In contrast, mitochondrially encoded proteins are synthesized within the organelle and inserted into the inner membrane by dedicated insertases such as Oxa1 rather than by the TIM23 translocase (HELL *et al.* 2001; KRUGER *et al.* 2012).

After the initial steps of the preprotein being escorted by cytosolic chaperones to the OMM and being guided by the receptors Tom22 and Tom20 to the OMM translocase channel Tom40, the preprotein is shuttled into the IMS. Within the IMS, Tim50 interacts with the presequence present on the preprotein to guide it to the IMS domain of Tim23 (CHACINSKA *et al.* 2009). For substrates destined for the mitochondrial matrix that require complete unfolding, the TIM23 complex associates with the presequence translocase-associated motor (PAM). The PAM complex employs mitochondrial Hsp70 (mtHsp70), whose ATP-dependent binding and release cycles generate a pulling force that drives preprotein translocation across the inner membrane, in conjunction with the membrane potential ($\Delta\psi$). Pam18 and Pam16 regulate and stabilize mtHsp70 activity, while the nucleotide exchange factor Mge1 promotes ADP-ATP exchange (MIAO *et al.*

1997; FRAZIER *et al.* 2004). Upon arrival in the matrix, the targeting presequence is cleaved by the mitochondrial processing peptidase (MPP) (CHACINSKA *et al.* 2005; NEUPERT AND HERRMANN 2007).

In contrast, TIM23 substrates containing hydrophobic transmembrane domains are sorted into the inner membrane via a stop-transfer mechanism. These precursors are laterally released into the inner membrane while still engaged with the TIM23 core complex, which dissociates from the PAM motor upon recognition of hydrophobic segments. This lateral insertion process is facilitated by the regulatory subunits Tim21 and Mgr2 (VAN DER LAAN *et al.* 2006; IEVA *et al.* 2014). Following insertion, transmembrane segments may be further stabilized or integrated from the matrix side with the assistance of Oxa1 (HOMBERG *et al.* 2023). Lastly, some substrates of the TIM23 complex are soluble IMS proteins (NEUPERT AND HERRMANN 2007). The precursors of these proteins first get laterally sorted into the IMM, and then via proteolytic cleavage by inner membrane peptidase (IMP) get released as soluble IMS resident proteins (GLICK *et al.* 1992). On a structural level, recent cryo-EM studies have refined the preexisting model for how the TIM23 complex translocates its substrates. Previously, it was believed that Tim23 forms an aqueous pore, with Tim17 as its stabilizing interactor (TRUSCOTT *et al.* 2001). However, insights from cryo-EM revealed that Tim23-Tim17 form a heterodimer in a manner that creates open lateral cavities facing the lipid bilayer. This suggests that the substrates of the TIM23 complex interact with the Tim23-Tim17 core complex on one side, and with the lipid bilayer on the other side. Furthermore, Mgr2 could be modeled into this complex structure and was found to seal off the lateral opening of Tim17 toward the lipid bilayer. Altogether, these cryo-EM studies in conjunction with cross-linking studies in mitochondria showed how the components of the TIM23 complex handle the

import of both matrix proteins, as well as the lateral sorting of IMM proteins (SIM *et al.* 2023; WANG *et al.* 2024b).

The TIM22 complex is responsible for importing mitochondrial carrier proteins, mitochondrial carrier proteins, as well as Tim17 and Tim23 family proteins, into the IMM (SIRRENBURG *et al.* 1996; REHLING *et al.* 2003). Mitochondrial carrier protein family, or the solute carrier family 25 (SLC25), is composed of several solute-carrying channels. In yeast, there are 35 mitochondrial carrier proteins, while in humans there are at least 53. All members of this family, in both human and yeast, share structural commonalities which include: six transmembrane alpha helices, tripartite organization, and a central substrate binding motif. Furthermore, mitochondrial carrier proteins lack a cleavable presequence and instead carry internal signal sequences for import, which is why they are imported by the TIM22 complex instead of the TIM23 complex (PALMIERI 2004; PALMIERI 2013).

In yeast, the TIM22 complex is composed of a “channel”-forming Tim22, the small Tims (Tim9, Tim10, and Tim12), Sdh3, Tim 18, and Tim54. In humans, the TIM22 complex does not contain homologs for yeast Tim54 or Tim18. Instead, it contains the proteins Tim29 and acylglycerol kinase (AGK), both of which stabilize and regulate the complex activity. Furthermore, the human TIM22 complex interacts with the mitochondrial cristae organizing structure (MICOS) complex, while the yeast TIM22 does not. Despite the slight differences in composition, both yeast and human TIM22 complexes showcase a similar structure. In both species, the complex consists of a membrane-embedded Tim22 core (consisting of four transmembrane helical segments arranged as hairpins), with the small Tim proteins (Tim9/Tim10) surrounding this core from the IMS side as hexamers or mixed oligomers. Finally, species-specific subunits (Tim54/Tim18/Sdh3 in yeast; Tim29/AGK in human) take part to stabilize the Tim22

core and link it to the neighboring complexes (WIEDEMANN AND PFANNER 2017; PFANNER *et al.* 2019). Based on recent structural studies, it is important to note that Tim22 does not form an aqueous pore. Instead, it forms a hydrophobic, membrane-embedded cavity that opens laterally toward the lipid bilayer (QI *et al.* 2021; VALPADASHI *et al.* 2021; ZHANG *et al.* 2021b). This is similar to the lateral cavity formed by Tim23, suggesting a similar conserved import process for both these complexes.

Substrates of the TIM22 complex, i.e. precursors of mitochondrial carrier proteins (or ‘carrier preproteins’), first interact with the Tom70 receptor on the OMM which transfers them over to the Tom40 channel for translocation across the OMM (SIRRENBURG *et al.* 1996). Once these preproteins reach the IMS, the small Tim protein chaperone (sTims) complex composed of Tim9 and Tim10 interact with the hydrophobic patches of carrier preproteins to prevent them from aggregating and stalling protein import. With the support of Tim9/Tim10, carrier preproteins are transferred toward the central core subunit Tim22 (CURRAN *et al.* 2002). Insertion of the carrier preprotein into the membrane cavity of Tim22 requires an intact mitochondrial membrane potential. Once the integral membrane segments of the preproteins have assembled within the membrane cavity of Tim22, the preprotein is laterally released into the IMM (BOLENDER *et al.* 2008; JAIN *et al.* 2025).

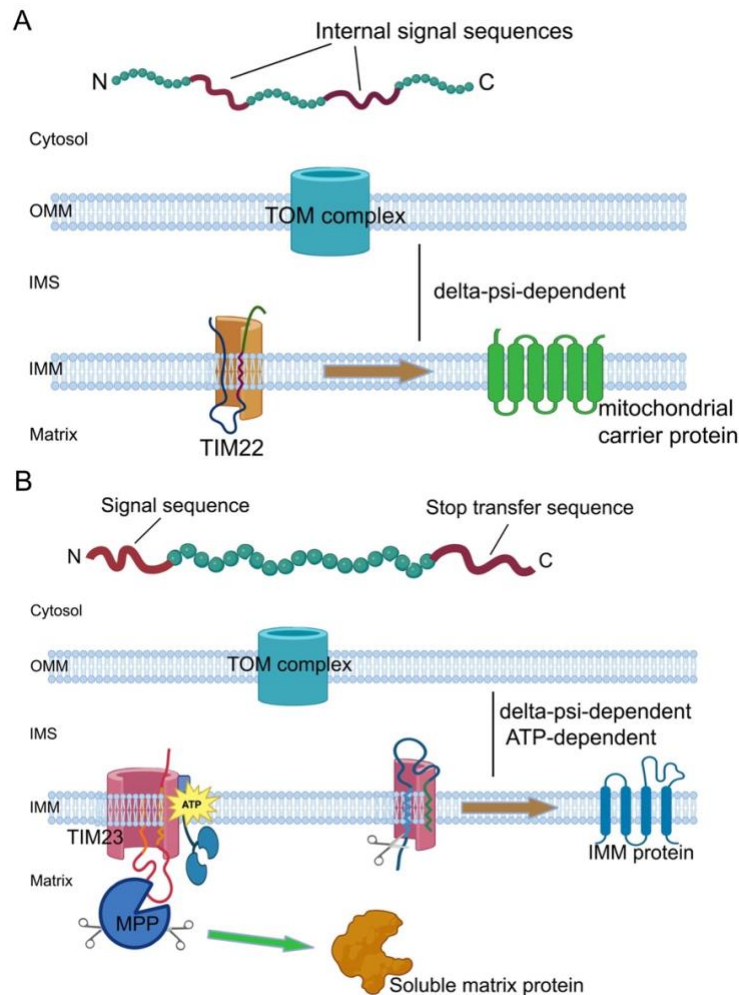


Figure 1.5. An overview of the IMM-based import pathways. (A) TIM22 complex, or the carrier protein import pathway, relies of mitochondrial membrane potential ($\Delta\psi$) to import hydrophobic mitochondrial carrier preproteins with internal targeting sequences for their insertion in the IMM. **(B)** TIM23 complex, or the presequence protein import pathway, relies on both $\Delta\psi$ and cellular energy (ATP) to import bipartite presequence containing proteins destined to be in the IMM, mitochondrial matrix, or the IMS.

Table 1.2. Similarities and differences between the TIM23 (presequence) and TIM22 (carrier) import complexes.

Feature	TIM23	TIM22
Primary substrates	Matrix & presequence-containing IMM proteins	Carrier proteins (SLC25 family)
Targeting signal	N-terminal cleavable presequence	Internal targeting signals
Energy requirement	$\Delta\psi + \text{ATP}$ (PAM motor)	$\Delta\psi$ only
IMS chaperones	Tim50, PAM-associated factors	Tim9/Tim10
Insertion mode	Translocation or lateral sorting	Lateral release
Channel type	Lateral cavity	Lateral cavity
Example substrates	Cox4, Mge1, Mdj1, Pim1, cytochrome b_2	Aac2, Sal1

1.1.f] Overview of MICOS complex in coordinating import of mitochondrial proteins destined for different mitochondrial compartments

The inner mitochondrial membrane is not always run parallel to the outer mitochondrial membrane. Instead, the IMM forms invaginations that increase its overall surface area and are instrumental in increasing the efficacy of oxidative phosphorylation. These invaginations of the IMM are called ‘cristae’. Furthermore, there are regions along the mitochondrial structure where the OMM and IMM have increased proximity which essentially forms a ‘contact site’. These sites facilitate improved lipid transfer, preprotein import, and increased TOM-TIM complexes alignment. A complex of several proteins is enriched in areas of the IMM around where cristae form (i.e., at cristae junctions), as well as at OMM-IMM contact sites. This complex refers to MICOS, which stands for mitochondria contact site and cristae organizing system (Table 1.3). MICOS serves three main functions. First, it organizes cristae architecture. The proteins Mic60 and Mic10 form the core cristae junction ring. Loss of MICOS collapses cristae and leads to an ‘onion-like stacks’ phenotype as observed on electron microscopy. Second, MICOS forms and stabilizes OMM-IMM contact sites via interacting with several other complexes to promote lipid transfer. Third, due to its interactions with other proteins, the MICOS complex can position import machineries to be better coordinated for protein import (PFANNER *et al.* 2014; FRIEDMAN *et al.* 2015; RAMPELT *et al.* 2017).

MICOS promotes mitochondrial protein import via several key interactions. The Mic60 subcomplex of MICOS interacts with TOM and SAM complexes, forming the mitochondrial intermembrane space bridging, or MIB, complex (TANG *et al.* 2020). This interaction aligns TOM with the inner membrane and positions TIM23 and TIM22 nearby, so that preproteins don’t diffuse randomly in the IMS, and instead can be shuttled to the correct sequential import pathway. MICOS

also interacts with TIMs. However, this appears to play out differently by species. In humans, it was shown that MICOS physically associates with human TIM22 complex and that loss of MICOS subunits impairs carrier protein import, but not presequence protein import (CALLEGARI *et al.* 2019). On the other hand in yeast, it was shown that MICOS preferentially interacts with the TIM23 complex since loss of MICOS subunits causes defective import of presequence proteins. Despite species-level differences, it is clear that MICOS is enriched near import machineries to facilitate the transfer of preproteins from the OMM to the IMM. Furthermore, the role of MICOS in maintaining cristae architecture indirectly promotes protein import since intact cristae organization ensures an optimal mitochondrial membrane potential that promotes protein import via both TIM22 and TIM23 complexes (STEPHAN *et al.* 2020). Finally, recent studies have suggested that MICOS is a hub not only for promoting cristae organization and protein import but also takes part in quality control. Complexome studies as well as direct protein-interaction studies have suggested that MICOS is in close vicinity to i/m-AAA proteases and may take part in promoting Omal-mediated clearance of stalled preproteins (DEN BRAVE *et al.* 2024). While these may be indirect interactions requiring further study, it is interesting to consider the possibility that MICOS can be an organizing center that ensures efficient mitochondrial biogenesis, bioenergetic landscape, and protein quality control.

Table 1.3. MICOS complex components and their functions.

MICOS Function	Mechanism	Impact on Import
Cristae organization	Mic60/Mic10 junction ring	Maintains $\Delta\psi$
Contact site formation	OMM-IMM tethering	Reduces IMS diffusion
Import coordination	MIB complex	Aligns TOM-TIM
Lipid transfer	Contact site stabilization	Supports membrane integrity
Quality control	Proximity to proteases	Clearance of stalled substrates

1.2] Defective mitochondrial protein import in health and disease

Given the vast number of machineries involved in mitochondrial protein import, there are many stages at which protein import can become defective. Below is an overview of the ways in which mitochondrial protein import defects occur, as well as a discussion of the consequences of defective mitochondrial protein import.

1.2.a] Mitochondrial protein import defects due to mutations in the import machineries

Several components of the protein import machineries have been found to carry mutations that can impair the efficient translocation of nuclear-encoded mitochondrial proteins. These mutations can occur in the chaperones, import translocases, or in motor proteins that support the translocation processes.

For instance, mutations in the mitochondrial chaperone *HSP60* have been found to cause spastic paraplegia-13, as well as a disorder termed atypical mitochondrial disease involving multisystem failure (AGSTERIBBE *et al.* 1993; BRIONES *et al.* 1997). Hsp60 is involved in the folding of mitochondrial matrix proteins once they have been imported. Thus, its loss of function drastically disrupts the matrix proteome, leading to loss of mitochondrial integrity and activation of apoptosis. Another chaperone, namely *DNAJC19*, the human homolog of yeast *TIM14*, is mutated in a disease called dilated cardiomyopathy with ataxia, or DCMA syndrome (DAVEY *et al.* 2006).

As previously mentioned, mutations in subunits of the translocase complexes are also associated with various diseases. Mutations in Tim22, the core subunit of the TIM22 complex, have been reported to cause early-onset mitochondrial myopathy (PACHEU-GRAU *et al.* 2018). While mutations in Tim50, a component of the TIM23 complex, has been linked to several forms

of mitochondrial disease such as optic atrophy, neutropenia, cardiomyopathy, Leigh syndrome, and persistent 3-methylglutaconic aciduria (3-MGA-uria) (TORT *et al.* 2019).

Lastly, besides causing mitochondrial disease, several neurodegenerative and cardiovascular diseases can also be linked to defects in the mitochondrial protein import machineries. For instance, downregulation of Tom20 and Tim23 can cause complex-I defects and contribute to neurodegeneration in Parkinson’s disease models. Several components of the TOM complex are implicated in cardiovascular disease. Myocardial ischemia can downregulate Tom20 receptor levels, while cardiac hypertrophy and diabetic cardiomyopathy decreases Tom70 levels. Finally, several genetic variants of the translocase channel Tom40 were found to correlate with cardiac arrhythmia and cardiac aging (MIDDELBERG *et al.* 2011; WANG *et al.* 2019). These examples underscore the profound significance of mitochondrial protein import process in organismal health (Table 1.4).

Table 1.4. Human diseases associated with defects in mitochondrial protein import machineries.

Affected Protein	Yeast Homolog	Import Step Affected	Disease / Phenotype
HSP60	Hsp60	Matrix protein folding	Spastic paraplegia-13; multisystem mitochondrial disease
DNAJC19	Tim14 (Pam18)	TIM23/PAM motor	Dilated cardiomyopathy with ataxia (DCMA)
TIM22	Tim22	Carrier protein insertion	Early-onset mitochondrial myopathy
TIM50	Tim50	Presequence recognition	Optic atrophy; Leigh syndrome; 3-MGA-uria
TOM20	Tom20	OMM receptor	Neurodegeneration (PD models)
TOM70	Tom70	OMM receptor	Cardiomyopathy; hypertrophy
TOMM40	Tom40	OMM translocation pore	Cardiac arrhythmia; cardiac aging

1.2.b] Mitochondrial protein import defects due to mtDNA damage

Numerous mitochondrial diseases can be caused by mutations in the mitochondrial genome or mtDNA. Many of the mtDNA mutations disrupt genes that encode subunits of the electron transport chain (ETC) leading to a gross reduction in ATP production, or of noncoding RNAs involved in mitochondrial protein synthesis which disrupts mitochondrial function (WALLACE

1999). Additionally, mtDNA damage reduces the mitochondrial membrane potential, which impairs protein import since both TIM22 and TIM23 complexes rely on the membrane potential for translocating preproteins across the inner membrane (NEUPERT AND HERRMANN 2007; GORMAN *et al.* 2016; WIEDEMANN AND PFANNER 2017).

In line with this, many mechanistic studies have demonstrated that mtDNA damage impairs protein import. Targeted double strand breaks in the mitochondrial genome (mtDSBs) were shown to cause mislocalization of nuclear-encoded mitochondrial proteins in a human cell culture model (FU *et al.* 2023). Similarly, in a yeast model it was shown that cells lacking intact mtDNA showed reduced import of the precursor Cox4 (GARIPLER AND DUNN 2013). Many other studies have also shown that mtDNA damage activates stress response pathways that are characteristically activated due to impaired mitochondrial protein import (ARNOULD *et al.* 2003; WEIDBERG AND AMON 2018). Thus, damage to mtDNA directly leads to impaired protein import into mitochondria.

1.2.c] Mitochondrial protein import defects due to perturbations in nuclear-encoded mitochondrial proteins and the discovery of mPOS

In addition to mutations that disrupt the import machinery or damage mtDNA, import defects can also be caused by perturbations to the nuclear-encoded preproteins requiring import into mitochondria. These perturbations could be caused by mutations that cause a preprotein to misfold and stall along the import canal. Alternatively, these perturbations could be due to overloading by a highly expressed preprotein that competes with the ability of other mitochondrial preproteins to be imported.

Depending on the severity with which a mutant protein stalls during import, or the degree by which an overexpressed preprotein outcompetes the import of other proteins, the severity of the protein import defect can vary. However, the outcome of the import defect is the overaccumulation

of unimported mitochondrial preproteins in the cytosol. This form of cytosolic proteostatic stress is termed mitochondrial precursor overaccumulation stress, or mPOS (WANG AND CHEN 2015). The accumulation of unimported preproteins in the cytosol leads to the formation of toxic aggregates, which is a hallmark of mPOS (LIU *et al.* 2019). Ultimately, if mPOS cannot be resolved, it ultimately leads to cell death (COYNE AND CHEN 2018) (Figure 1.6A).

1.3] Mitochondrial protein import clogging: a specific form of mitochondrial protein import stress

The discovery of mPOS was a paradigm shift in understanding mitochondrial homeostasis and how it affects cellular health. This is because the discovery of mPOS showed that mitochondria-associated diseases are not only caused by bioenergetic defects but can be independently caused by severe defects in protein quality control. This required a re-evaluation of several dominant mitochondrial diseases that were previously thought to be due to bioenergetic defects. Studies showed that several dominant mitochondrial diseases occurring due to mutations in nuclear-encoded mitochondrial proteins occur not due to loss of function, but due to toxic gain of function that involves the mutant preprotein getting stuck on the translocases on the OMM or IMM during protein import (COYNE *et al.* 2023) (Figure 1.6B). The process by which a mutant preprotein misfolds and stalls along the import canal is called mitochondrial protein import clogging, or simply ‘clogging’, and the stalled mutant preprotein is referred to as a ‘clogger’.

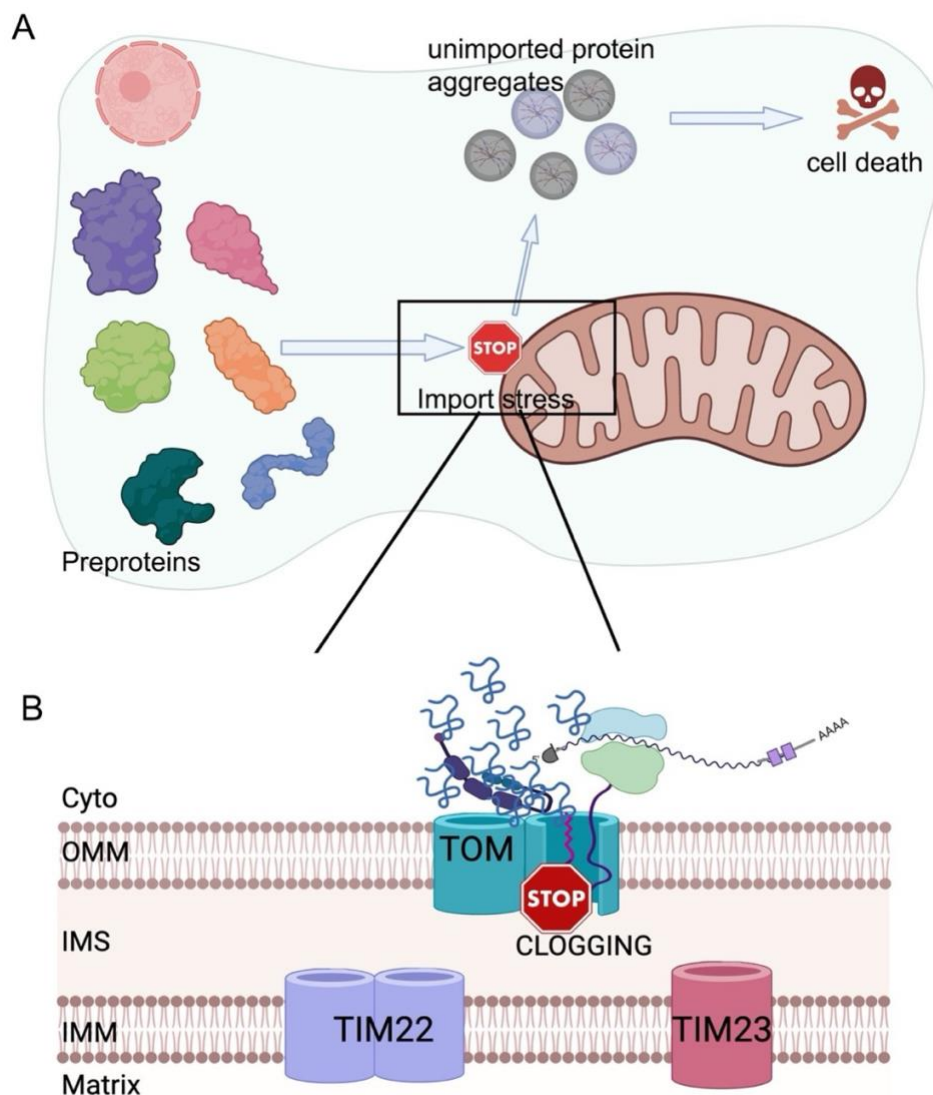


Figure 1.6. An overview of mPOS and mitochondrial protein import clogging. (A) Mitochondrial precursor overaccumulation stress (mPOS) can be triggered by various forms of protein import stress, and results in the accumulation of unimported mitochondrial proteins in the cytosol. These unimported proteins, if unable to get turned over, can form toxic protein aggregates, and eventually cause cell death. **(B)** An inset from (A) showing that mitochondrial protein import clogging is a specific form of protein import stress that can induce mPOS. Clogging occurs when a precursor protein stalls along the protein import pathway, either at the TOM translocase, or at the IMM translocases TIM22 or TIM23 complexes.

1.3.a] Adenine Nucleotide Translocase in the context of human physiology, disease, and mitochondrial protein import clogging

Adenine nucleotide translocase (ANT) is a nuclear-encoded, multi-pass inner mitochondrial membrane (IMM) carrier that catalyzes ADP/ATP exchange across the IMM. During oxidative phosphorylation, ANT imports ADP^{3-} into the matrix in exchange for exporting

newly synthesized ATP⁴⁻ to the intermembrane space, a 1:1 electrogenic antiport that is strongly driven by the IMM membrane potential (PALMIERI *et al.* 1993). ANT is a member of the SLC25 family of mitochondrial carriers, a large group of IMM transporters that collectively mediate the exchange of diverse metabolites (KUNJI *et al.* 2020). In humans, ANT is encoded by four paralogs (ANT1-ANT4). ANT1 (SLC25A4) is the most extensively studied and is enriched in energetically demanding tissues such as heart and skeletal muscle, whereas ANT2 is more prominent in proliferative tissues, ANT3 is broadly expressed, and ANT4 is primarily expressed in testis and germ cells (STEPIEN *et al.* 1992; DOLCE *et al.* 2005). Mammals also express several ANT-related, Ca²⁺-regulated nucleotide carriers (SLC25A23/24/25; APC/SCaMC family) that contain EF-hand motifs and mediate Ca²⁺-dependent transport of cytosolic Mg²⁺-ATP in exchange for matrix phosphate, providing an additional route to modulate mitochondrial adenine nucleotide pools (DEL ARCO AND SATRUSTEGUI 2004; FIERMONTE *et al.* 2004).

Mitochondrial carrier proteins are highly conserved throughout evolution. In the budding yeast *Saccharomyces cerevisiae*, ANT is encoded by three AAC (ADP/ATP carrier) genes: *AAC1*, *AAC2* and *AAC3*. Under aerobic conditions, *Aac2* is the major isoform expressed and *Aac1* is poorly expressed. *Aac3* is expressed only under anaerobic conditions, likely playing a role in the reversal of ATP (matrix)/ADP(cytosol) exchange to sustain mitochondrial biogenesis in the absence of ATP synthesis inside mitochondria. *S. cerevisiae* has only one Ca²⁺-dependent mitochondrial carrier protein, named *Sa11* (for Suppressor of *aac2*-lethality), which has been shown to functionally interact with *Aac2* (CHEN 2004).

In addition to its canonical role in ADP/ATP exchange that supports oxidative phosphorylation (the R function), the yeast ADP/ATP carrier *Aac2* has been shown to perform an

additional function essential for cell viability that is genetically separable from respiration. Studies from the Chen laboratory demonstrated that Aac2 and Aac3, but not Aac1, are required for survival even under fermentative conditions, defining a distinct “viability” (V) function independent of oxidative phosphorylation. Because mitochondrial respiration is dispensable under these conditions, loss of V function is thought to impair a process critical for mitochondrial biogenesis. Genetic suppression by the Ca²⁺-dependent carrier Sall1 and by the human carrier SLC25A25 suggests partial functional overlap in maintaining mitochondrial adenine nucleotide homeostasis. Consistent with this idea, the V function of Aac2 is required for mitochondrial protein synthesis and mitochondrial DNA maintenance, although whether this activity reflects a specialized transport mode or a transport-independent role remains unresolved (CHEN 2004; KUCEJOVA *et al.* 2008).

Beyond its role in nucleotide exchange, Aac2 physically associates with respiratory supercomplexes and the TIM23 protein translocase, interactions that appear to be evolutionarily conserved (DIENHART AND STUART 2008; LU *et al.* 2017). Loss of Aac2 in yeast compromises complex IV activity and reduces translation of mitochondrially encoded respiratory subunits, indicating that Aac2 contributes to oxidative phosphorylation not only by supplying adenine nucleotides but also by influencing respiratory chain biogenesis through physical and functional coupling to mitochondrial protein import and translation machinery (MULLER *et al.* 1996; FONTANESI *et al.* 2004; OGUNBONA *et al.* 2018).

ANT has also been implicated in regulation of the mitochondrial permeability transition pore (mPTP), although its precise role remains controversial. Pharmacological and genetic studies have suggested that ANT can modulate the calcium sensitivity of permeability transition, while

mouse models lacking multiple ANT isoforms display increased calcium requirements for mPTP induction (KOKOSZKA *et al.* 2004; KARCH *et al.* 2019). Conflicting electrophysiological and biochemical findings have led to differing interpretations as to whether ANT constitutes a structural component of the pore or instead acts as a regulatory factor. Current evidence supports a model in which ANT contributes to mPTP regulation in a context-dependent manner, potentially acting alongside other proteins with partial redundancy (BRUSTOVETSKY 2020).

Mutations in human ANT isoforms have been associated with various pathologies affecting different organ systems. Mutations in the *SLC25A4* gene (encoding ANT1) can lead to complete loss of nucleotide transport activity, which is in many cases manifested by hypertrophic cardiomyopathy and myopathy (PALMIERI *et al.* 2005). Interestingly, missense mutations in *ANT1* have also been found to cause diseases including (1) autosomal dominant Progressive External Ophthalmoplegia (adPEO), (2) neuropsychiatric disturbances such as seizures, encephalopathies, and deafness; (3) musculoskeletal pathologies such as skeletal muscle dysfunction, and dystonia; and (4) cardiomyopathy (KAUKONEN *et al.* 2000; SICILIANO *et al.* 2003; KAWAMATA *et al.* 2011; THOMPSON *et al.* 2016; KASHIKI *et al.* 2022) (Table 1.5).

Table 1.5. Disease-associated dominant mutations in ANT1.

<i>ANT1</i> mutation	Conserved mutation in Yeast <i>AAC2</i>	Clinical Phenotype
A90D	A106D	adPEO, neuropsychiatric disease
L98P	M114P	adPEO
A114P	A128P	Dementia
A123D	A137D	Hypertrophic cardiomyopathy
R80H	R96H	Infantile encephalopathy
R235G	R252G	Infantile mitochondrial disease

Genetic and preclinical studies have established a central role for ANT1 in mitochondrial physiology and disease. Deletion of the *SLC25A4* gene encoding ANT1 generated the first mouse model of a mitochondrial disorder and resulted in cardiomyopathy, mitochondrial myopathy,

exercise intolerance, and lactic acidosis (GRAHAM *et al.* 1997). ANT1-deficient mice exhibit respiratory deficiency accompanied by mitochondrial proliferation, likely reflecting compensatory activation of mitochondrial biogenesis pathways. These animals also display increased reactive oxygen species production, mitochondrial DNA instability, and defects in mitochondrial quality control, including reduced mitophagy, underscoring the importance of ANT1 for maintaining mitochondrial homeostasis (ESPOSITO *et al.* 1999; MURDOCK *et al.* 1999; HOSHINO *et al.* 2019). Subsequent studies demonstrated that loss of ANT1 leads to progressive cardiomyopathy with age. Importantly, loss-of-function mutations in SLC25A4 were later identified in humans with autosomal recessive myopathy and cardiomyopathy, validating insights gained from these animal models (VON RENESSE *et al.* 2019).

In addition to complete loss of ANT1, defects in ANT1 biogenesis can arise indirectly through disruption of mitochondrial protein import. Sengers syndrome, a multisystem disorder characterized by hypertrophic cardiomyopathy, congenital cataracts, and skeletal myopathy, is caused by mutations in acylglycerol kinase (AGK), a core subunit of the TIM22 carrier import pathway. Because ANT1 relies on TIM22 for insertion into the inner mitochondrial membrane, AGK mutations result in secondary ANT1 deficiency (SENGERS *et al.* 1975; SENEGERS *et al.* 1985; MAYR *et al.* 2012). Given that TIM22 mediates the import of multiple mitochondrial carriers, it is likely that impaired carrier import and broader proteostatic stress contribute to disease pathogenesis in this context.

Altered ANT1 expression levels, rather than complete loss, have also been implicated in disease. Reduced ANT expression has been linked to pulmonary pathologies, including chronic obstructive pulmonary disease and idiopathic pulmonary fibrosis, where ANT1 deficiency

promotes cellular senescence and fibrotic remodeling in experimental models (KLIMENT *et al.* 2021; SUI *et al.* 2023). Conversely, ANT1 overexpression has been associated with muscle and cardiac phenotypes. In facioscapulohumeral dystrophy (FSHD), transcriptional derepression of the SLC25A4 locus leads to elevated ANT1 expression, and experimental overexpression of ANT1 is sufficient to drive progressive skeletal muscle wasting in mice (LAOUDJ-CHENIVESSE *et al.* 2005; LIM *et al.* 2020; MOCCIARO *et al.* 2021; ARBOGAST *et al.* 2022). Emerging evidence suggests that excessive ANT1 may induce mitochondrial protein import stress and cytosolic proteostatic imbalance, providing a potential mechanistic link between altered ANT1 dosage and muscle pathology (WANG *et al.* 2022a). Together, these studies demonstrate that both loss and gain of ANT1 function disrupt mitochondrial homeostasis and tissue physiology. They further highlight that precise regulation of ANT1 expression and import is critical for mitochondrial health, setting the stage for understanding how pathogenic ANT1 variants induce mitochondrial protein import stress and precursor overaccumulation.

Dominant missense mutations in SLC25A4 (ANT1) are a well-established cause of autosomal dominant progressive external ophthalmoplegia (adPEO), a multisystem mitochondrial disorder characterized by adult- or late-onset muscle weakness, particularly affecting extraocular muscles, exercise intolerance, sensory ataxia, cardiomyopathy, and myopathy (KAUKONEN *et al.* 2000; NAPOLI *et al.* 2001; DESCHAUER *et al.* 2005). Skeletal muscle from affected individuals commonly exhibits multiple mitochondrial DNA (mtDNA) deletions and mild defects in respiratory chain function. Pathogenic missense mutations associated with adPEO include A90D, L98P, A114P, D104G, and V289M (KAUKONEN *et al.* 2000; KOMAKI *et al.* 2002; SICILIANO *et al.* 2003; DESCHAUER *et al.* 2005; KAWAMATA *et al.* 2011). Although the V289M variant was initially identified as a *de novo* mutation in an adPEO patient, subsequent studies revealed that the same

individual also harbored a pathogenic mutation in POLG1, complicating attribution of disease causality to the ANT1 variant alone and leaving the pathogenicity of ANT1^{V289M} unresolved (GALASSI *et al.* 2008).

The clinical manifestations associated with dominant ANT1 mutations are heterogeneous and extend beyond classical adPEO. The A90D and L98P variants have been linked to neuropsychiatric phenotypes, including schizoaffective and bipolar disorders, while the A114P mutation has been associated with dementia (SIMONCINI *et al.* 2017). More severe early-onset disease has been described for other dominant mutations: de novo R80H and R235G substitutions cause infantile-onset mitochondrial disease with epileptic encephalopathy and skeletal muscle atrophy (THOMPSON *et al.* 2016). The R80H mutation has additionally been associated with mitochondrial DNA depletion syndrome, presenting with profound hypotonia, respiratory insufficiency, and in some cases hypertrophic cardiomyopathy. By contrast, a recently described dominant K33Q mutation causes a relatively mild childhood-onset skeletal myopathy without cardiomyopathy or ophthalmoplegia, despite normal ANT1 protein abundance in patient muscle biopsies (KING *et al.* 2018). This observation suggests that residual wild-type ANT1 activity, together with compensation by other ANT isoforms, can modulate disease severity in the presence of dominant mutations.

Collectively, dominant missense mutations in SLC25A4 produce clinical phenotypes that are mechanistically and clinically distinct from recessive loss-of-function mutations, often resulting in more severe and complex disease. The budding yeast *Saccharomyces cerevisiae* has proven to be a powerful model system for dissecting the molecular basis of these dominant disorders due to the high conservation of mitochondrial pathways and the ability of yeast cells to

survive without oxidative phosphorylation on fermentable carbon sources. Early yeast studies established the fundamental biochemical properties of ANT, while more recent work has leveraged this system to interrogate dominant pathogenic mechanisms.

To this end, multiple dominant ANT1 mutations associated with adPEO have been modeled in yeast by introducing equivalent substitutions into the orthologous ADP/ATP carrier Aac2, including ANT1^{L98P}, ANT1^{A90D}, ANT1^{A114P}, and ANT1^{V289M} (corresponding to Aac2^{M114P}, Aac2^{A106D}, Aac2^{A128P}, and Aac2^{S303M}, respectively). Although the ANT1^{D104G} mutation does not map directly onto Aac2, chimeric complementation approaches have confirmed its pathogenicity in yeast. These mutant *aac2* alleles consistently exhibit impaired respiratory growth on non-fermentable carbon sources, even when expressed alongside wild-type *AAC2*, indicating dominant interference with mitochondrial function (KAUKONEN *et al.* 2000; FONTANESI *et al.* 2004; PALMIERI *et al.* 2005). Similar dominant effects were observed for *aac2* mutations modeling the early-onset ANT1^{R80H} and ANT1^{R235G} alleles (DALLABONA *et al.* 2017). Notably, expression of a catalytically inactive Aac2 variant corresponding to the cardiomyopathy-associated ANT1^{A123D} mutation caused a greater reduction in complex IV activity than complete loss of *AAC2*, providing strong evidence for a gain-of-toxicity mechanism (OGUNBONA *et al.* 2018). Together, these studies demonstrate that dominant ANT1 mutations compromise mitochondrial function not simply through loss of transport activity, but by exerting deleterious effects that broadly perturb mitochondrial homeostasis.

What is the molecular basis of mutant Aac2-induced mitochondrial protein import defects? Several mechanisms were initially proposed, including reduced membrane potential, misfolding-induced proteostatic stress at the inner mitochondrial membrane leading to TIM22 destabilization,

or other indirect consequences of mitochondrial dysfunction (WANG *et al.* 2008; LIU *et al.* 2015; COYNE AND CHEN 2019). However, published and unpublished work from the Chen lab demonstrated that expression of pathogenic Ant1 variants in human cells robustly induces mitochondrial precursor overaccumulation stress (mPOS) without reducing membrane potential or destabilizing the TIM22 complex, arguing against these indirect mechanisms as primary drivers of mPOS (LIU *et al.* 2019). Subsequent studies revealed that pathogenic Aac2 and ANT1 proteins directly clog mitochondrial protein import translocases, providing a direct mechanistic explanation for mPOS. In both yeast and human cells, mutant Aac2/ANT1 exhibited increased association with protein translocase channels, consistent with cytosolic proteomic signatures of precursor accumulation. Strikingly, mutant Aac2, particularly variants carrying multiple dominant substitutions, failed to efficiently traverse the TOM complex when imported *in vitro* into fully energized wild-type yeast mitochondria (COYNE *et al.* 2023). These findings demonstrate that the intrinsic biophysical properties of the mutant carrier, rather than secondary mitochondrial damage, underlie the clogging phenotype. Obstruction at the TOM complex is therefore sufficient to impede mitochondrial protein import and trigger mPOS.

Although the precise import step that fails to accommodate mutant Aac2/ANT1 remains unresolved, available evidence implicates the TOM complex. Three non-mutually exclusive models have been proposed. First, introduction of proline or aspartate residues into transmembrane α -helices may disrupt formation of the characteristic carrier “hairpin loop” during TOM engagement, creating steric constraints incompatible with passage through the Tom40 pore. Second, these substitutions may alter interactions between the carrier preprotein and the interior surface of the Tom40 channel, impairing translocation. Third, mutant carriers may fail to productively associate with the small Tim chaperones, resulting in their retention at the TOM exit

site. This latter model is supported by the observation that carrier proteins retain partial secondary structure while bound to small Tim chaperones (WEINHAUPL *et al.* 2018). Discriminating among these possibilities will require further mechanistic investigation.

Importantly, import clogging represents a conserved gain-of-toxicity mechanism. Pathogenic ANT1 variants similarly associate with the TOM complex and induce mPOS in human cells without compromising membrane potential, reinforcing the conclusion that mutant ANT1 directly obstructs protein import. This mechanism was further validated *in vivo* using a mouse model expressing a “super-clogger” ANT1 variant harboring two dominant missense mutations (A123D and A137D). These mice developed mitochondrial myopathy accompanied by import clogging and mPOS, phenotypes reminiscent of adPEO patient muscle pathology (PALMIERI *et al.* 2005; KAWAMATA *et al.* 2011; COYNE *et al.* 2023). Although the super-clogger model does not fully recapitulate human adPEO, these findings strongly support a contributory role for protein import clogging and mPOS in disease pathogenesis. More broadly, the clustering of clogging-associated mutations within the transmembrane α -helices of SLC25A4 highlights the importance of these domains in maintaining import competence. The presence of pathogenic mutations within transmembrane helices of related carriers, including SLC25A24 and SLC25A25, further raises the possibility that import clogging contributes to disease beyond ANT1 (EHMKE *et al.* 2017; WRITZL *et al.* 2017; JABALAMELI *et al.* 2021). Together, yeast Aac2 and human ANT1 provide a powerful, clinically relevant model for dissecting mitochondrial protein import clogging.

1.3.b] Other model systems for studying mitochondrial protein import clogging and stress

Besides ANT1/Aac2 as a system for the study of mitochondrial protein import clogging and mPOS, other models have also been utilized. These include the artificially generated clogger

protein models as well as models that overexpress mitochondrial proteins containing bipartite signal sequences to induce import stress. Both these types of systems allowed the discovery of novel response pathways to import clogging (Table 1.6).

Table 1.6. Model systems used to induce mitochondrial protein import clogging and stress.

Model System	Perturbation	Import Step Affected	Outcome	Pathway Discovered
ANT1/Aac2 mutants	Misfolded carrier	TOM or TIM (mutation dependent)	mPOS	Import clogging
b ₂ -DHFR fusion	Folding during import	IMS/TOM	Toxic stalling	mitoTAD
TIM23 substrate overexpression	Import saturation	TIM23 → TOM preprotein backlog	Import arrest	mitoCPR

In the former model, researchers inserted a dihydrofolate reductase (DHFR) moiety between the presequence and heme binding domain of cytochrome b₂. Two versions of cytochrome b₂, either carrying (*b2*) or lacking (*b2Δ*) were generated. Thus, b₂-DHFR-HB was inserted into the IMM, while *b2Δ*-DHFR-HB, which lacked the hydrophobic signal, was transported into the matrix. Ligand binding caused the DHFR moiety at the C-terminal end to fold rapidly while the mitochondrial fusion preprotein is being translocated. Using this system, researchers were able to identify the mitochondrial translocation associated degradation (mitoTAD) pathway (MARTENSSON *et al.* 2019) which will be discussed in detail in section 1.4.b.

In the latter system, researchers overexpressed mitochondrial protein precursors that contain a bipartite signal and are substrates of the TIM23 complex. The overexpression of such precursors saturated the Tim23 translocon and interrupted any further mitochondrial protein import from occurring. Furthermore, this led to the arrest of mitochondrial precursors at the OMM in the vicinity of the TOM complex and within the TOM translocase. The authors of this study concluded that the lateral diffusion of mature TIM23 substrates into the IMM is a rate-limiting step of mitochondrial protein import. Additionally, they were able to identify a novel response to protein

import stress that they termed mitochondrial compromised protein import response (mitoCPR) (WEIDBERG AND AMON 2018) which will also be discussed in detail in section 1.4.b.

1.4] Molecular pathways activated in response to mPOS and mitochondrial protein import clogging

1.4.a] Stress signaling in response to mitochondrial protein import defects

Overaccumulation of mitochondrial precursors in the cytosol (mPOS) results in a significant proteostatic burden for the cytosol. If left unchecked, the presence of unimported and aggregated preproteins can trigger cell death (COYNE AND CHEN 2018). To prevent this and reestablish homeostasis, the cell activates many molecular pathways that act either at the transcriptional or translational levels (Table 1.7).

Table 1.7. Cellular responses triggered by mitochondrial protein import stress.

Pathway	Trigger	Primary Effect	Key Features
mPOS response	Cytosolic precursor accumulation (mPOS)	Translation repression, proteostasis	Defined by precursor aggregation
UPRam	Protein mistargeting	↓ Translation, ↑ proteasome	Immunoproteasome function
ISRmt	Import stress, ETC defects	eIF2 α -P, ATF4 induction	HRI-DELE1-OMA1 axis
HSR	Proteotoxic stress	Chaperone induction	HSF1-driven
OSR	ROS accumulation	Antioxidant response	YAP1, SOD2
RTG (yeast)	Mitochondrial dysfunction	Metabolic rewiring	Rtg1/3-dependent

In the context of mPOS, it was found that the cytosolic stress induced by overexpression of a clinically relevant mutant mitochondrial preprotein can be suppressed by several genes that repress ribosomal biogenesis and cap-dependent translation, while simultaneously promoting cap-independent translation. Additionally, genes involved in TOR signaling and increased protein chaperoning and proteasomal degradation were found to suppress mPOS (WANG AND CHEN 2015). The finding of mPOS was further validated in human cells (LIU *et al.* 2019) and in a mouse model

(WANG *et al.* 2022a), suggesting that this form of proteostatic stress induced by perturbation of mitochondrial protein import is conserved across species, and may be implicated in the pathogenesis of various human diseases (PALMER *et al.* 2021).

A related but distinct cytosolic stress response was uncovered by the Chacinska group using a yeast model defective in the mitochondrial intermembrane space import and assembly (MIA) pathway. Disruption of the MIA complex led to cytosolic mistargeting of mitochondrial proteins and activation of a novel stress response termed the unfolded protein response activated by mistargeting of proteins (UPRam) (WROBEL *et al.* 2015). UPRam is characterized by reduced cytosolic protein synthesis coupled with increased proteasomal activity. Importantly, this pathway is conserved in human cells and depends on activation of the immunoproteasome and the small heat shock protein HSPB1 (KIM *et al.* 2023).

Another major responder to mitochondrial protein import stress is the integrated stress response activated by mitochondrial damage (ISR_{mt}). To contextualize ISR_{mt}, it is useful to first describe the integrated stress response (ISR). The ISR is a conserved pathway that maintains cellular homeostasis under diverse stress conditions, including proteotoxic stress, viral infection, and nutrient deprivation. These stressors activate one or more stress-responsive kinases, namely HRI, PKR, GCN2, or PERK, which phosphorylate the α subunit of eukaryotic initiation factor 2 (eIF2 α). Phosphorylation of eIF2 α reduces global cytosolic protein synthesis while selectively enhancing translation of specific stress-responsive mRNAs, thereby promoting adaptation or, in cases of prolonged stress, programmed cell death (HARDING *et al.* 2003; WEK *et al.* 2006).

Recent studies have elucidated the molecular mechanisms underlying ISR^{mt}. Using cell culture models, two seminal studies demonstrated that mitochondrial dysfunction and import stress

induced by electron transport chain inhibitors activate ISR^{mt} via the kinase heme-regulated eIF2 α kinase (HRI). In this pathway, mitochondrial stress activates the protease OMA1, which cleaves the mitochondrial protein DELE1. The resulting short DELE1 fragment (S-DELE1) accumulates in the cytosol, where it binds and activates HRI, leading to eIF2 α phosphorylation. In parallel, the uncleaved long form of DELE1 (L-DELE1) can oligomerize and accumulate on the mitochondrial surface during protein import stress and iron dyshomeostasis, where it also activates HRI. In addition to HRI, the kinase GCN2 may be engaged under conditions of amino acid deprivation secondary to mitochondrial dysfunction (FESSLER *et al.* 2020; GUO *et al.* 2020). PERK and PKR have likewise been reported to respond to certain forms of mitochondrial stress (SILVA *et al.* 2009; TOUVIER *et al.* 2015; ZHANG *et al.* 2021a), although how cells selectively engage specific ISR kinases in response to distinct mitochondrial insults remains an open question.

Regardless of the activated kinase, eIF2 α phosphorylation causes increased translation of the transcription factor ATF4 which relocates to the nucleus to initiate the ISR's transcriptional program. ATF4 activates genes (such as ATF5, GDF15, FGF21, and MTHFD2) that increase the expression of stress-responsive proteins, such as amino acid transporters and metabolic enzymes (FAN *et al.* 2014; NILSSON *et al.* 2014; FIORESE *et al.* 2016; FUJITA *et al.* 2016; KLIEWER AND MANGELSDORF 2019). This concludes the first stage of ISR^{mt}. In the second phase, mTORC1 activation, increases de novo serine synthesis, glucose absorption, and glutathione production occur (NIKKANEN *et al.* 2016; KHAN *et al.* 2017; WANG *et al.* 2022b). Finally, in the third stage of ISR^{mt}, the transcription of ATF3 and the activation of another stress response pathway UPR^{mt} occurs. ATF3 can either contribute to cellular survival or apoptosis, and the outcome depends on the severity of the cellular stress (BUENO *et al.* 2018; HATHAZI *et al.* 2020). UPR^{mt} will be discussed in detail later, but briefly, its activation causes an increase in the expression of

mitochondrial chaperones to aid in import, folding and turnover of mitochondrial proteins (ZHAO *et al.* 2002).

Mitochondrial protein import stress can also activate the heat shock response (HSR), which contributes to the triage of misfolded, unimported mitochondrial precursors. Import defects activate Heat Shock Factor 1 (HSF-1), leading to transcription of molecular chaperones, including HSP70 and HSP90, both of which play central roles in mitochondrial protein import, as well as small heat shock proteins such as HSPB7, HSP12, and HSP26, and additional cytosolic chaperones including HSP40 and TRiC subunits. These chaperones function either by refolding mislocalized proteins or by acting as holdases to prevent aggregation prior to degradation (LABBADIA AND MORIMOTO 2015; WANG AND CHEN 2015; WROBEL *et al.* 2015).

Another consequence of mitochondrial protein import stress is an increase in reactive oxygen species (ROS) (LEVY *et al.* 2019). This can occur either be due to misassembled respiratory complexes which allow the leakage of electrons, or it can occur independently due to loss of iron homeostasis (PATIL *et al.* 2013; GALARIS *et al.* 2019). Interestingly, increased ROS can further destabilize mitochondrial handling of iron (CHEN *et al.* 2023). Increased ROS can be detrimental for several cellular processes, and thus the oxidative stress response (OSR) can become activated in response to mitochondrial protein import stress. Interestingly, the effectors of OSR include the HSR-associated transcription factor HSF-1 and the ISR^{mt}-associated protein OMA1 (MORIMOTO 2011; BAKER *et al.* 2014; SIES AND JONES 2020). Furthermore, studies in yeast model systems have described the upregulation of antioxidant genes such as YAP1 and SOD2 that are activated in response to import defects (STEPHEN *et al.* 1995; WANG AND CHEN 2015).

Finally, mitochondrial protein import stress intersects with mitochondria-to-nucleus retrograde signaling (RTG), a pathway first characterized in yeast by Butow and colleagues. In *Saccharomyces cerevisiae*, the RTG response is activated by compromised mitochondrial function, including loss of mitochondrial DNA (ρ^0 cells), respiratory chain defects, or broader bioenergetic impairments. Under these conditions, the cytosolic sensor Rtg2 promotes nuclear translocation of the Rtg1-Rtg3 transcription factor heterodimer, inducing a transcriptional program that upregulates metabolic enzymes such as the peroxisomal citrate synthase CIT2. This response supports anaplerotic flux, α -ketoglutarate and glutamate production, and nitrogen and carbon metabolism in cells with dysfunctional mitochondria (LIAO AND BUTOW 1993; LIU AND BUTOW 2006; JAZWINSKI 2013).

1.4.b] Quality control in the cytosol and at the cytosol-mitochondria interface

In addition to transcriptional and translational reprogramming that occurs in response to mPOS, several molecular pathways get activated to tackle the buildup of unimported preproteins in the cytosol, as well as to clear the mitochondrial protein import translocases that contain clogged preproteins (Table 1.8). Some of these pathways are the downstream effectors of the stress response pathways discussed previously, while others appear to be activated independently. Below is a discussion of the molecular mechanisms underlying these pathways.

Table 1.8. Protein quality control pathways acting on the cytosol-mitochondria interface.

Pathway	Location	Trigger	Primary Function
mitoCPR	OMM	Import saturation	Clear TOM clogging
mitoTAD	OMM	Basal surveillance	Remove stalled precursors
MAD	OMM	Mislocalized OMM proteins	Proteasomal extraction
RQC	Cytosol	Ribosome collision	Abort stalled translation
mitoRQC	OMM-bound ribosomes	Vectorial translation stalling	Prevent toxic CAT tails
MitoStores	Cytosol	Import overload	Buffer precursors
ER-SURF / GET	ER-mitochondria contacts	Hydrophobic precursors	Reroute & buffer
MDVs / MDCs / SPOTs	Cytosol	Stress / infection	Vesicular clearance
Mitophagy	Organelle	Irreversible mitochondrial damage	Degrade damaged mitochondria

The proteasome is a large protein complex present in the cytosol, that takes part in targeted degradation of proteins that have either been misfolded, mistargeted or damaged. It consists of a 20S core subunit, and a 19S regulatory subunit. Both these units together form the 26S proteasomal machinery. Proteins that have been post-translationally modified with several ubiquitin tags by E3 ligase enzymes get recognized by the 19S regulatory cap which unfolds and deubiquitinates the substrate proteins. After this step, the substrate proteins are escorted to the beta-barrel portion of the 20S core where protein degradation takes place in an ATP-dependent manner (HERSHKO AND CIECHANOVER 1998; BARD *et al.* 2018). In recent years, a growing body of literature has described how mitochondrial dysfunction coordinates with proteasomal activity in the cytosol. Several molecular pathways have been defined through which unimported or clogged mitochondrial proteins become ubiquitinated and subsequently delivered to the proteasome for degradation.

The first pathway to be described was the mitochondrial compromised protein import response (mitoCPR), identified by the Amon group (WEIDBERG AND AMON 2018). By overexpressing bipartite signal-containing mitochondrial preproteins, the authors saturated the TIM23 complex and induced protein import stress in a yeast model. Using this system, they identified the protein Cis1 at the outer mitochondrial membrane (OMM), where it interacts with

the TOM complex and recruits the AAA-ATPase Msp1. Msp1 dislocates clogged preproteins from the Tom40 channel, thereby improving protein import efficiency, and escorts the extracted proteins to the proteasome for degradation. The Weidberg group later demonstrated that this pathway is conserved in humans, as ATAD1, the human homolog of yeast Msp1, can extract stalled preproteins from the TOM complex and facilitate clearance of import channels (KIM *et al.* 2024).

In addition to this stress-induced system, a related pathway operates under basal, unstressed conditions to survey the OMM and remove stalled preproteins. This pathway, termed mitochondrial translocation-associated degradation (mitoTAD), was described by the Becker group in yeast (MARTENSSON *et al.* 2019). The authors found that Ubx2, a sensor of polyubiquitinated proteins, associates with the OMM translocase channel Tom40. Upon sensing stalled preproteins, Ubx2 recruits the AAA-ATPase Cdc48, which, similar to Msp1, dislocates preproteins and promotes their delivery to the cytosolic proteasome for degradation.

While the discovery of the Cis1-Msp1 and Ubx2-Cdc48 systems significantly advanced the mitochondrial quality control field, the identity of the E3 ligase responsible for ubiquitinating stalled preproteins at the TOM complex initially remained unclear. This question was resolved by the Becker group, who identified the E3 ligase Rsp5 in yeast as the factor that ubiquitinates clogged mitochondrial preproteins at the TOM complex, thereby enabling recognition by Ubx2 and extraction by Cdc48. Additional factors, including Pth2 and Dsk2, also appear to participate in sensing Rsp5-ubiquitinated substrates and facilitating their proteasomal degradation (SCHULTE *et al.* 2023).

A third pathway coordinating mitochondrial protein quality control with the proteasome is the mitochondria-associated degradation (MAD) pathway. This pathway also employs the adaptor

protein Doa1, which, similar to Ubx2, recruits Cdc48 to extract stalled OMM proteins (KARBOWSKI AND YOULE 2011; TAYLOR AND RUTTER 2011; WU *et al.* 2016). In mammalian systems, E3 ligases such as MARCH5 and MULAN have been shown to ubiquitinate stalled mitochondrial preproteins at the OMM (AMBIVERO *et al.* 2014; SHIIBA *et al.* 2020). Whether additional E3 ligases contribute to ubiquitination of stalled mitochondrial preproteins in yeast and mammalian systems remains an important area for future investigation.

A fourth pathway that coordinates protein clearance with the proteasomal machinery is the ribosome quality control (RQC) pathway. This pathway is activated when protein translation stalls. Translational stalling can occur on both free cytosolic ribosomes as well as membrane-bound ribosomes, including those associated with the endoplasmic reticulum or the outer mitochondrial membrane (OMM). Severe and chronic mitochondrial protein import saturation or clogging can lead to accumulation of unimported precursors in the cytosol, ultimately resulting in mitochondrial precursor overaccumulation stress (mPOS). These aggregated precursors can sequester chaperones and components of the translational machinery, disrupting cytosolic translation and promoting widespread ribosomal stalling and collisions on free cytosolic ribosomes, thereby activating the RQC pathway (JOAZEIRO 2019). Similarly, for OMM-bound ribosomes engaged in protein import-coupled (vectorial) translation of nuclear-encoded mitochondrial proteins, slowed or clogged import through the TOM and TIM complexes can induce ribosomal collisions. Stalling of OMM-bound ribosomes triggers a specialized form of RQC termed mitochondrial RQC (mitoRQC) (IZAWA *et al.* 2017).

In the canonical cytosolic RQC pathway, ribosomal collisions on stalled 80S ribosomes are recognized by an E3 ubiquitin ligase. In yeast, the E3 ligase Hel2 recognizes collided

ribosomes, whereas in mammals this role is performed by ZNF598. In both systems, the E3 ligase ubiquitinates ribosomal proteins on the 40S subunit, initiating recruitment of downstream RQC factors. The stalled 80S ribosome is subsequently split into its 40S and 60S subunits by the coordinated action of Dom34 (Pelota in mammals), Hbs1, and Rli1 (ABCE1 in mammals). The 40S subunit is targeted for degradation, while the 60S subunit remains bound to the nascent polypeptide and peptidyl-tRNA. Core RQC components then act on this 60S-nascent chain-tRNA complex. In yeast, Rqc2 (Tae2; NEMF in mammals) binds the complex, while the E3 ubiquitin ligase Ltn1 (Listerin in mammals) ubiquitinates the nascent polypeptide. Rqc2 catalyzes the addition of non-templated alanine and threonine residues, termed CAT tails, to the C-terminus of the stalled polypeptide. CAT tailing promotes further ubiquitination by Ltn1. The polyubiquitinated nascent chain is then recognized by Cdc48 (p97 in mammals), which, together with its cofactors Ufd1 and Npl4, extracts the ubiquitinated polypeptide from the 60S-peptidyl-tRNA complex and delivers it to the 26S proteasome for degradation (FILBECK *et al.* 2022; LI *et al.* 2025).

In mitoRQC, several steps of this pathway are modified. Unrestricted CAT tail addition can predispose stalled mitochondrial polypeptides to aggregation, potentially exacerbating mPOS under conditions of mitochondrial import stress. To prevent this outcome, the cytosolic protein Vms1 is recruited to the mitochondrial surface, where it inhibits Rqc2 activity and limits CAT tail formation on OMM-bound ribosomes. Vms1 also functions as a peptidyl-tRNA hydrolase, enabling translation termination and release of the nascent polypeptide. Released polypeptides may then be imported into mitochondria if import is permissible, or alternatively targeted to the cytosolic proteasome through the actions of Ltn1, Cdc48, and associated cofactors. Aberrant polypeptides that enter mitochondria are subsequently handled by intramitochondrial quality

control pathways (IMiQ). In the absence of Vms1, CAT-tailed mitochondrial proteins accumulate and aggregate within mitochondria, leading to severe mitochondrial proteostasis failure (IZAWA *et al.* 2017; BERTRAM *et al.* 2025). Recent studies have shown that up to 20% of nuclear-encoded mitochondrial proteins are imported co-translationally, a substantially higher fraction than previously appreciated (ZHU *et al.* 2025). This finding underscores the physiological importance of mitoRQC in managing stalled nascent chains at the OMM during mitochondrial protein import stress.

Another arm of cytosolically-acting mitochondrial quality control is the yeast vacuole/mammalian lysosome (LI AND KANE 2009; TRIVEDI *et al.* 2020). Although many mechanistic details of the reciprocal relationship between mitochondria and the vacuole/lysosome remain active areas of investigation, it is well established that a specialized form of selective autophagy, called mitophagy, plays a central role in removing dysfunctional mitochondria (ONISHI *et al.* 2021). In broad terms, autophagy refers to the process by which cells degrade and recycle their own components, particularly under conditions of metabolic stress such as nutrient deprivation. During autophagy, cytoplasmic material is sequestered into double-membrane autophagosomes and delivered to the vacuole in yeast or the lysosome in mammalian cells, where the cargo is degraded and recycled (MIZUSHIMA AND KOMATSU 2011).

Autophagy provides multiple benefits for cellular homeostasis, including turnover of damaged proteins and organelles, maintenance of amino acid and energy balance, elimination of intracellular pathogens, and mitigation of age-associated declines in cellular fitness (GOMEZ-VIRGILIO *et al.* 2022). Mitophagy, specifically, is the selective recognition, isolation, and degradation of dysfunctional or superfluous mitochondria. By clearing damaged mitochondria that

could otherwise generate reactive oxygen species, lose membrane potential, or accumulate misfolded proteins, mitophagy serves as a key quality-control mechanism that preserves mitochondrial population fitness and protects overall cellular physiology (YOULE AND NARENDRA 2011).

In yeast, mitophagy is regulated by Atg32, a single-pass outer mitochondrial membrane protein that functions as the canonical mitophagy receptor in *Saccharomyces cerevisiae*. Under respiratory growth and starvation or post-log phase conditions, Atg32 is induced and recruits mitochondria to the core autophagy machinery by binding the scaffold protein Atg11 and the ubiquitin-like protein Atg8 on forming autophagosomes. Through these interactions, Atg32 marks damaged or dispensable mitochondria for selective sequestration into mitophagosomes and subsequent delivery to the vacuole for degradation. Genetic screens for mutants defective in mitochondrial turnover first identified *ATG32* as essential for mitophagy, and loss of Atg32 largely abolishes mitophagy in yeast. Later work showed that Atg32 activity is tightly controlled by post-translational modifications: for example, phosphorylation of serine residues in its cytosolic domain by casein kinase 2 (CK2) promotes Atg11 binding and mitophagy induction, whereas additional regulatory inputs modulate Atg32 stability and turnover at the mitochondrial surface. Together, these studies established Atg32-dependent mitophagy as a central vacuolar quality-control pathway that adjusts the mitochondrial population in response to metabolic cues and mitochondrial damage in yeast. Other factors also modulate mitophagy in yeast (KANKI AND KLIONSKY 2008; SUZUKI 2013; INNOKENTEV AND KANKI 2021). For example, Atg33 contributes to mitophagy during post-logarithmic growth, particularly under stationary-phase conditions, but Atg32 remains the primary and essential receptor required for selective mitophagy in *S. cerevisiae* (FUKUDA AND KANKI 2018).

In mammals, several mitophagy-associated pathways have been described, including both ubiquitin-driven and receptor-mediated mechanisms. The best-characterized pathway is the PINK1-Parkin system, in which loss of mitochondrial membrane potential prevents the import and proteolytic turnover of the kinase PINK1, allowing it to accumulate on the outer mitochondrial membrane. There, PINK1 phosphorylates ubiquitin (Ser65) on OMM-anchored substrates and phosphorylates Parkin itself, thereby activating Parkin's E3 ligase activity. Activated Parkin then ubiquitinates a broad set of OMM proteins, including TOM20, TOM70, MFN1/2, VDACs, LETM1, NDUFA10, and others, to drive mitophagy. These ubiquitin chains are recognized by autophagy adaptors such as OPTN and NDP52, which bridge damaged mitochondria to LC3-decorated autophagosomal membranes and promote lysosomal turnover (KANE *et al.* 2014; PALIKARAS *et al.* 2018; PICKLES *et al.* 2018; CALLEGARI *et al.* 2025).

Parallel “receptor-mediated” mitophagy pathways rely on OMM proteins such as BNIP3, NIX/BNIP3L, and FUNDC1, which harbor LC3-interacting regions (LIRs) and can directly recruit autophagic membranes to stressed mitochondria during hypoxia, erythroid maturation, or developmental remodeling. The activity of these receptors is tuned by phosphorylation and other post-translational modifications, for instance, hypoxia-induced, HIF-1 α -dependent upregulation and dephosphorylation of BNIP3 and NIX, or phosphoregulation of FUNDC1, enhance their mitophagy receptor function (LI *et al.* 2021).

Recent studies have additionally identified the mitochondrial F-box protein FBXL4 as a critical brake on BNIP3/NIX-dependent mitophagy: FBXL4 forms an SCF^{FBXL4} ubiquitin ligase complex on the outer membrane that ubiquitylates BNIP3 and NIX and targets them for degradation, thereby restraining basal mitophagy (CAO *et al.* 2023; NGUYEN-DIEN *et al.* 2023).

Loss-of-function FBXL4 mutations or FBXL4 deletion cause accumulation of BNIP3 and NIX, hyperactivation of steady-state mitophagy, mitochondrial loss, and contribute to encephalomyopathic mitochondrial DNA depletion syndrome 13 (MTDPS13), a severe pediatric disorder characterized by early-onset encephalopathy and mtDNA depletion (BONNEN *et al.* 2013; BALLOUT *et al.* 2019; ELCOCKS *et al.* 2023).

Additional modulators such as the Parkinson's disease-linked F-box protein Fbxo7 can facilitate PINK1-Parkin mitophagy in some experimental systems, although recent systematic studies indicate that Fbxo7 is not strictly required for Parkin-dependent mitochondrial turnover, underscoring that multiple partially redundant mitophagy axes cooperate to maintain mitochondrial integrity in mammalian cells (BURCHELL *et al.* 2013; KRAUS *et al.* 2023). In addition to FBXO7, other mitochondrial E3 ligases intersect with the PINK1-Parkin pathway. For example, the OMM ligase MARCH5/MITOL generates basal ubiquitin signals on impaired mitochondria that facilitate PINK1-dependent phosphorylation of ubiquitin and efficient Parkin recruitment, and MARCH5 itself becomes a Parkin substrate during mitophagy (KOYANO *et al.* 2019). In parallel, MARCH5 also regulates Parkin-independent, receptor-mediated mitophagy by ubiquitinating and degrading the mitophagy receptor FUNDC1 under hypoxic conditions, thereby fine-tuning mitophagy sensitivity (CHEN *et al.* 2017).

Vesicular quality control pathways in the cytosol act in a mitophagy-independent manner to promote clearance of unimported mitochondrial preproteins (UOSELIS *et al.* 2023). These include mitochondria-derived vesicles (MDVs), mitochondria-derived compartments (MDCs), and structures positive for outer mitochondrial membrane (SPOTs). MDVs are small vesicular structures that require the mitochondrial fission protein DRP1 to bud off from mitochondria under

basal conditions, while requiring PINK1/Parkin for their formation under oxidative stress conditions. MDVs carry selected mitochondria cargo such as oxidatively damaged proteins to the lysosome for degradation. The machinery required to deliver them to the lysosome has not yet been delineated (SOUBANNIER *et al.* 2012; KONIG *et al.* 2021). MDCs are slightly larger than MDVs and were discovered to form in yeast in response to cytosolic amino acid overload and membrane damage. MDC formation occurs at ER-mitochondrial contact sites and involves the removal of membrane compartments carrying the OMM and selective mitochondrial cargo proteins (HUGHES *et al.* 2016; SCHULER *et al.* 2021; WILSON *et al.* 2024). It is unclear whether fission proteins cause MDC release from the OMM. However, it was recently found that MDC formation requires the protein subunits that form the ER-mitochondrial contact structure (ERMES), as well as the GTPase Gem1 (ENGLISH *et al.* 2020). Unlike MDVs, MDCs have not been shown to form in mammalian systems yet. Lastly, SPOTs, as their name suggests, are large mitochondrial-derived single-membrane structures that contain outer mitochondrial membrane segments. These were observed to form in response to *Toxoplasma gondii* infection in stably transfected mammalian cells (LI *et al.* 2022). The toxoplasma protein TgMAF1 interacts with TOM70 and SAM50 at the OMM. TOM70 is a versatile outer membrane receptor important for many downstream protein import pathways, while SAM50 is a component of the outer-inner mitochondrial intermembrane space (MIB) complex that anchors cristae to the OMM creating OMM-IMM contact sites. TgMAF1 interaction with TOM70/SAM50 destabilizes the MIB complex and causes detachment of segments of the outer membrane leading to formation of SPOT. SPOT formation aids in *Toxoplasma*'s growth within the host cell, since SPOTs are enriched for protein import machineries that play roles in antimicrobial defense (LI *et al.* 2022). It is currently

unclear whether *Toxoplasma* utilizes a conserved cellular pathway for the removal of dysfunctional mitochondrial proteins, or whether it specifically activates SPOT formation.

Besides the utilization of membranous organelles such as vacuoles/lysosomes, and smaller vesicular compartments such as MDVs, MDCs, and SPOTs, the cells have evolved other means to sequester and degrade unimported mitochondrial preproteins. One of these pathways, called MitoStore, involves the chaperone-controlled buffering of mitochondrial precursors in the cytosol (KRAMER *et al.* 2023). This pathway, identified by the Hermann group in *Saccharomyces cerevisiae* or yeast, was shown to be active during physiological growth on nonfermentable carbon sources, as well as during conditions of protein import clogging. The Hermann group showed that MitoStores are formed whenever protein import machineries cannot keep up with nuclear-encoded mitochondrial preprotein synthesis. Furthermore, the mitochondrial preproteins sequestered by MitoStores appears to be selective and includes matrix-destined preproteins that carry an N-terminal targeting sequence. When protein import is slowed down during clogging, or there is an upregulating of mitochondrial biogenesis that exceeds the number of mitochondrial translocases such as during respiratory growth, the cytosolic heat shock proteins Hsp42 and Hsp104 interact with the accumulating preproteins in the cytosol and prevent their accumulation into toxic aggregates. This transient buffering allows cytosolic proteostasis to be re-established until these precursors can eventually get imported, or degraded (KRAMER *et al.* 2023).

An unsung hero that ensures mitochondrial quality control in the cytosol is the organelle called Endoplasmic Reticulum (ER), which plays important roles for cellular homeostasis. The ER is a continuous single-membrane system and continuous with the nuclear envelope (which comprises of a double membrane). The ER membrane contains integral membrane as well as

membrane-bound proteins, and the ER lumen contains soluble proteins (SCHWARZ AND BLOWER 2016). Protein import into ER uses a translocation-based system similar in many ways to mitochondrial protein import. Furthermore, certain mitochondrial quality control proteins, such as Ubx2 and Cdc48 of mitoTAD, are utilized by the ER protein quality control pathway ERAD (ER-associated degradation) (RAPOPORT 2008; KRSHNAN *et al.* 2022). Interestingly, there exist similarities in the targeting signals present on ER and mitochondrial proteins, which can sometimes mistarget mitochondrial proteins to the ER surface (KUNZE AND BERGER 2015). For instance, the guided entry of tail-anchored proteins (GET) pathway is tasked with delivering tail-anchored ER preproteins to the ER membrane for insertion (WANG *et al.* 2011). However, the GET pathway can mistarget mitochondrial outer membrane proteins to the ER (VITALI *et al.* 2018). Furthermore, during conditions of mitochondrial protein import stress, the GET pathway can escort unimported mitochondrial carrier proteins to the ER (XIAO *et al.* 2021). Since mitochondrial carrier proteins are extremely hydrophobic, the membranous surface of the ER buffers them against forming aggregates. Lastly, the GET pathway sometimes targets tail-anchored ER proteins to the mitochondrial surface for import. These mistargeted ER proteins get extracted by Msp1, and re-associate with the GET pathway components to be correctly targeted to the ER (MATSUMOTO *et al.* 2019).

For the two situations when mitochondrial proteins end up on the ER surface due to GET, another pathway termed ER-surface-mediated protein targeting to mitochondria (ER-SURF) ensures that hydrophobic precursors such as mitochondrial carrier proteins which get mistargeted to the ER surface can get relocated to the mitochondrial surface for import. The ER-bound J-protein Djpl retrieves mitochondrial precursors from the ER surface and delivers them to mitochondria at pre-existing ER-mitochondria contact sites (HANSEN *et al.* 2018). These contact

sites include the ERMES complex, as well as the Tom70-Lam6-Djp1 bridges (ELBAZ-ALON *et al.* 2014). These sites create two parallel and partially redundant types of ER-mitochondria delivery routes. Due to the presence of ER-SURF, the ER can act as a “holding platform” for retargeting of proteins, instead of a mislocalized dead end. This rerouting for protein import helps improve mitochondrial biogenesis and helps reduce proteostatic stress in the cytosol.

1.4.c] Quality control within mitochondria

In addition to nuclear-, cytosolic-, vacuolar-, and ER-driven processes that respond to import clogging and mPOS, several pathways act within mitochondria to ensure mitochondrial proteostasis. These pathways can help triage proteins that are synthesized within mitochondria on mitochondrial ribosomes (mitoribosomes), as well as nuclear-encoded mitochondrial proteins that get imported into various mitochondrial subcompartments. The main types of pathways in this sector include AAA+ proteases anchored in the inner membrane, proteases in the mitochondrial matrix, as well as mitochondrial sequestration compartments (Table 1.9). Below is a brief overview of these pathways.

Table 1.9. Intramitochondrial protein quality control pathways.

Protease / System	Location	Substrates	Key Functions	Disease Links
Yme1 / YME1L	IMM (IMS-facing)	Stalled TIM23/IMS/IMM proteins	Basal QC, OPA1 processing	Optic atrophy
Yta12/Yta10 (AFG3L2/SPG7)	IMM (matrix-facing)	Matrix & IMM proteins	Ribosome maturation, QC	SCA28
Oma1	IMM	Stress-damaged proteins, OPA1	Stress-induced remodeling	Neurodegeneration
Pim1 / LonP1	Matrix	Oxidized/misfolded proteins	mtDNA maintenance	CODAS, myopathy
ClpX/ClpP	Matrix (humans)	Aggregation-prone proteins	Translation fidelity	Mitochondrial disease

The yeast Yme1 (or YME1L in mammals) is an intermembrane space-facing protease anchored within the IMM (i-AAA) which plays a role in degrading misfolded or unassembled IMS and IMM proteins (SCHREINER *et al.* 2012). Yme1's major substrates are preproteins that stall in the Tim23 translocase (LEONHARD *et al.* 1996). However, recent evidence suggests that clogged proteins in the IMS on their way to Tim22 can also be subjected to degradation by Yme1 (COYNE *et al.* 2023). The yeast YTA12/YTA10 (AFG3L2/SPG7 in mammals) complex is the matrix-facing protease anchored in the IMM (m-AAA) that performs ATP-dependent extraction and degradation of misfolded matrix and IMM proteins (LEONHARD *et al.* 1996). YTA12/YTA10 activity is required for the maturation of mitoribosomal subunits (DE SILVA *et al.* 2015). Mutations in human AFG3L2 cause a form of neurodegenerative disease called spinocerebellar ataxia type 28 (SCA28) (PIERSON *et al.* 2011; TULLI *et al.* 2019), underscoring the importance of mitochondrial proteostasis in human health.

Another protease present in the IMM, namely Oma1, is also involved in protein quality control. Oma1 is an M48-type zinc metallopeptidase activated in response to a variety of stressors such as membrane depolarization, redox imbalance, and impaired protein homeostasis. It is conserved across species, from bacteria to yeast and humans. Oma1 regulates mitochondrial dynamics by mediating the proteolytic cleavage of the inner membrane shaping protein Opa1 (BOHOVYCH *et al.* 2014). As mentioned previously, it is part of the intramitochondrial quality control network, where it helps clear stalled protein import intermediates or misfolded proteins. Oma1's activity is linked to various signaling pathways including the integrated stress response (ISR) via the protein DELE1 (FESSLER *et al.* 2020; GUO *et al.* 2020). Furthermore, Oma1 acts as a metabolic safeguard and influences the balance between glycolysis and oxidative phosphorylation (QUIROS *et al.* 2015). Finally, there appears to be an interplay between the

functions of Oma1 and Yme1. Both these proteins are crucial for maintaining balanced proteostasis by regulating fission/fusion dynamics, primarily through cleaving Opa1, and for general organelle quality control. Specifically, Yme1 performs the basal constitutive cleavage of Opa1, maintaining a balance of long and short forms of Opa1, which favors mitochondrial fusion. On the other hand, Oma1 cleaves Opa1 only into short forms, triggering mitochondrial fragmentation during times of stress. Interestingly, these proteins are reciprocally degraded in a coordinated manner. Mitochondrial membrane depolarization triggers Yme1-dependent degradation of Oma1, while ATP depletion with concurrent membrane depolarization causes Oma1 to stabilize and degrade Yme1, resulting in mitochondria remaining fragmented. This adaptation helps prevent the fusion of damaged mitochondria with other healthy mitochondria in the cell. This interplay ensures mitochondria can fuse for energy production and repair, or fragment to isolate damaged portions (GRIPARIC *et al.* 2007; HEAD *et al.* 2009; RAINBOLT *et al.* 2016). An imbalance in human OMA1/YME1L is linked to neurodegenerative diseases such as Charcot-Marie-Tooth disease, optic atrophy, and metabolic disorders (QUIROS *et al.* 2015), highlighting their importance in mitochondrial and cellular homeostasis.

The yeast Pim1 (LonP1 in humans) and human ClpX/ClpP complex are the resident proteases of the mitochondrial matrix. Pim1/LonP1 is involved in degrading oxidized, misfolded, or unassembled matrix proteins (SZCZEPANOWSKA AND TRIFUNOVIC 2022). This protease is also important for optimal mtDNA replication and nucleoid maintenance (LU *et al.* 2007). Pim1/LonP1 expression gets upregulated as part of the UPR^{mt} response (TORRES *et al.* 2024). With relevance to physiology, denervation-induced muscle disuse in mice leads to a marked decrease in the mitochondrial matrix protease LONP1, which impairs mitochondrial protein quality control, promotes mitochondrial dysfunction, and exacerbates skeletal muscle atrophy (XU *et al.* 2022).

Several human diseases are also linked to LonP1 loss of function. These include CODAS syndrome (cerebral, ocular, dental, auricular, and skeletal abnormalities) and a form of infantile mitochondrial disease manifesting with lactic acidosis, hypotonia, neurodegeneration, and energy failure (STRAUSS *et al.* 2015; NIMMO *et al.* 2019). Acquired loss of LonP1 function also occurs in various human diseases. This includes chronic kidney disease and aging (GONG *et al.* 2021; HE *et al.* 2022).

The ClpX/ClpP system in humans provides another avenue for protease activity in the mitochondrial matrix. ClpX acts as a chaperone, while its binding partner ClpP performs the function of a protease. Interestingly, while bacteria have an ortholog for human ClpX/ClpP complex, baker's yeast (*Saccharomyces cerevisiae*) does not. Yeast possess an ortholog for human ClpX, which is called Mcx1. However, they lack the ortholog for ClpP. Mcx1 functions as an unfoldase and is responsible for activating the heme synthesis enzyme in yeast called Hem1. But without its protease binding partner, Mcx1 is unable to take part in protein quality control in the matrix. In humans and other organisms that possess both, ClpX and ClpP are able to degrade aggregation-prone matrix proteins, as well as maintain the assembly and translation fidelity of mitoribosomes (VAN DYCK *et al.* 1998; SZCZEPANOWSKA *et al.* 2016; KARDON *et al.* 2020; LUO *et al.* 2021).

In addition to mitochondrial proteases, several other proteins take part in sequestering or compartmentalizing misfolded mitochondrial proteins within mitochondria. Three well-described systems in yeast include intramitochondrial sequestration compartment (IMiQ), Var1 bodies, and Hsp78 foci. IMiQ act as a damage-sequestering compartment inside mitochondria for aggregation-prone or misfolded IMM and matrix proteins that cannot be degraded in a timely manner due to

saturation of mitochondrial protease capacity. Misfolded matrix proteins as well as extracted IMM proteins get transported into “inclusion bodies” inside mitochondria. Furthermore, IMiQ aggregate deposits do not get transferred to daughter cells during cell division, and their detoxification requires the presence of an intact mitochondrial fission machinery (BRUDEREK *et al.* 2018). Similar to IMiQ, it was found that Var1 bodies and Hsp78 foci are found within mitochondria, carrying distinct aggregated contents. Var1 is a mitoribosomal protein that transitions from a soluble to an insoluble form during times of acute stress. The AAA chaperone Hsp78 is a mitochondrial disaggregase that forms foci containing transiently aggregated mitochondrial proteins to promote their folding, or degradation by Pim1 if protein folding fails (BERTGEN *et al.* 2024).

Besides proteases and sequestration compartments, the major stress-signaling pathway activated by intramitochondrial dysfunction is the mitochondrial unfolded protein response (UPR^{mt}). This pathway is triggered by diverse mitochondrial insults, including accumulation of unprocessed presequence-containing proteins, defects in inner membrane and matrix proteases, protein import failure due to loss of membrane potential, and proteotoxic stress within the mitochondrial matrix or inner membrane. In response, the UPR^{mt} induces transcriptional programs that increase the expression of mitochondrial chaperones, proteases, and metabolic adaptation factors to restore organellar proteostasis (SHILKA AND HAYNES 2018).

In mammals, increasing evidence suggests that the UPR^{mt} is mechanistically intertwined with the integrated stress response activated by mitochondrial dysfunction (ISR^{mt}). A central point of convergence between these pathways is the transcription factor ATF4, which is induced downstream of eIF2 α phosphorylation and is required for many UPR^{mt}-associated transcriptional outputs (Fessler *et al.* 2020). However, downstream of ATF4 the pathways diverge: UPR^{mt}

signaling engages the mitochondrial stress-responsive transcription factor ATF5 to specifically promote mitochondrial proteostasis, whereas the broader ISR activates additional transcription factors, such as CHOP, that coordinate more general cytosolic stress adaptation and cell fate decisions (FIORESE *et al.* 2016; PAKOS-ZEBRUCKA *et al.* 2016). Thus, while UPR^{mt} can be viewed as a mitochondria-biased arm of the ISR^{mt}, it retains specialized features that couple intramitochondrial protein homeostasis to nucleus-driven adaptive responses. In this way, UPR^{mt} serves as a critical link between local quality-control mechanisms within mitochondria and global cellular programs that adjust mitochondrial biogenesis, metabolism, and stress tolerance.

1.5] Membraneless organelles in the context of mitochondria and human health

After reviewing the multitude of molecular pathways and machineries involved in mitochondrial biogenesis and protein quality control, I would like to conclude this introductory chapter by discussing the existence of membraneless organelles, which are biomolecular condensates that arise through liquid-liquid phase separation (LLPS) (BANANI *et al.* 2017; LI *et al.* 2024b). These condensates may participate in maintaining global cellular homeostasis. Membraneless organelles can form in several cellular compartments, including the nucleus, the cytoplasm, and even within the luminal spaces of membrane-bound organelles (HYMAN *et al.* 2014; ALBERTI AND HYMAN 2021). Well-established examples include the nucleolus, Cajal bodies, and paraspeckles in the nucleus, P-bodies, stress granules, and germ granules in the cytosol, RNA granules in mitochondria, and multichaperone condensates in the ER (SHETH AND PARKER 2003; BRANGWYNNE *et al.* 2009; MACHYNA *et al.* 2014; ANTONICKA AND SHOUBRIDGE 2015; FERIC *et al.* 2016; PROTTER AND PARKER 2016; FOX *et al.* 2018; LEDER *et al.* 2025). Through the formation, dissolution, and exchange of components among these structures, cells dynamically reorganize their proteome and transcriptome to adapt to changing physiological demands. Although

historically viewed primarily through the lens of RNA metabolism and stress responses, several cytosolic biomolecular condensates exhibit intimate spatial and functional relationships with mitochondria. These connections are increasingly appreciated in both yeast and mammalian systems, revealing new routes through which mitochondrial dysfunction can influence cytoplasmic organization, cellular stress adaptation, and human disease.

1.5.a] P-bodies and stress granules: discovery, composition, and function

P-bodies and stress granules are among the best-characterized membraneless organelles in the cytoplasm. P-bodies, or processing bodies, were first described as cytoplasmic foci enriched for mRNA decay factors, deadenylases, decapping activities, and translational repressors. Work from Roy Parker's laboratory (SHETH AND PARKER 2003; COLLER AND PARKER 2005) established that P-bodies are dynamic sites of mRNA sequestration and decay where mRNAs are silenced or degraded. Core protein components of P bodies include the deadenylation complex Ccr4-Not, Lsm1-7, decapping coactivator and enzyme Dcp1/2, decapping activators such as Edc3 and DDX6 (or Dhh1 in yeast), 5'-3' exoribonuclease Xrn1, and RNA binding proteins (RBPs) involved in translational repression (SHETH AND PARKER 2003; PARKER AND SHETH 2007).

Stress granules (SGs), were characterized initially in mammalian cells by Nancy Kedersha and Paul Anderson (KEDERSHA *et al.* 1999; KEDERSHA *et al.* 2000) and were shown to form when translation initiation is inhibited, leading to the accumulation of stalled pre-initiation complexes (KEDERSHA *et al.* 2002). The Parker lab contributed to the stress granule field as well by characterizing the proteome and transcriptome of SG cores under a variety of stressors (BUCHAN AND PARKER 2009; JAIN *et al.* 2016; WHEELER *et al.* 2016; KHONG *et al.* 2017). SGs function to "hold" poly-A mRNA transcripts when cellular stress prevents translation from occurring and release these mRNAs back into the cytosol when the cellular stress has resolved (ANDERSON AND

KEDERSHA 2008). In mammals, SGs recruit RNA-binding proteins such as G3BP1, G3BP2, TIA-1/TIAR, and PABPC1, and act as triage centers for mRNAs during acute stress. In yeast, core proteins associated with SG formation include RNA-binding proteins such as Pab1, Pbp1, Pub1, nucleation factors such as Lsm7 (LINDSTROM *et al.* 2022), and translation initiation factors such as eIF4E, eIF4G, and eIF3 (BUCHAN AND PARKER 2009). PUF family proteins such as Puf2 appear to also sequester into SGs under certain stress conditions (HSIAO *et al.* 2020). Recent studies have utilized more sophisticated approaches to isolate SGs and identified a greater number of protein components of these organelles (DEMESHKINA AND FERRE-D'AMARE 2025). Finally, it is very important to note that different stressors can cause distinct sets of proteins to be sequestered within SGs (AULAS *et al.* 2017; MARKMILLER *et al.* 2018).

P bodies (PBs) are present constitutively in cells. However, they grow in size and number during conditions of cellular stress. On the other hand, SGs are formed only in response to cellular stressors such as nutrient deprivation, heat shock, viral infection, UV irradiation, translational stalling, electron transport chain (ETC) toxins, increased oxidative stress, etc. While considered distinct entities with distinct composition and function, PBs and stress granules SGs physically and functionally interact with one another. A subset of PBs and SGs can “dock” on one another during times of stress, allowing for the exchange of protein and RNA contents. During such an interaction, SGs can sort the mRNAs requiring degradation and shuttle them to PBs for turnover. This makes PBs and SGs dynamic partners in ensuring timely repression or turnover of mRNA, versus sequestration of mRNA transcripts that may require translation later, respectively (KEDERSHA *et al.* 2005; KEDERSHA AND ANDERSON 2007; BUCHAN *et al.* 2008) (Table 1.10).

Table 1.10. P bodies and Stress Granules (SGs): Key similarities and differences.

Feature	P bodies	Stress granules
Basal presence	Yes	No
Trigger	Constitutive	Acute stress
Primary function	mRNA decay/repression	mRNA storage
Core proteins	Dcp1/2, Xrn1	Pab1, G3BP, eIFs
Interaction	Dock with SGs	Dock with PBs

1.5.b] Functional relevance of P bodies, Stress granules, and other molecular condensates in proximity to mitochondria

P bodies (PBs) and stress granules (SGs) both appear in close proximity to mitochondria. Often this occurs while mRNA is being trafficked along an energy-consuming microtubule (LIAO *et al.* 2019; LIU *et al.* 2025). PBs and SGs also tend to appear in vicinity of ER-mitochondria contact sites, which is where lipid transfer and calcium signaling occur (MORE AND JOSEPH 2025). Finally, in response to ETC poisons such as sodium azide and sodium arsenite, SGs are found to form in the vicinity of mitochondria (KEDERSHA *et al.* 1999; KEDERSHA *et al.* 2000; BASU *et al.* 2017; EIERMANN *et al.* 2022). The physiological relevance of these poison-induced SGs in the context of mitochondrial biogenesis, function, or quality control is unclear. However, what is known is that the metabolic stress caused by the disruption of the ETC leads to translational arrest in an eIF2a phosphorylation-independent manner and the coalescing of stalled translation complexes into cytosolic SGs that require Thioredoxin 1 (Trx1) for assembly (SHENTON *et al.* 2006; GROUSL *et al.* 2009).

Another useful hint about the functional interaction between SG and mitochondria came from a study conducted in a mammalian cell culture system where the authors induced SGs by nutrient deprivation and found that SGs reduce mitochondrial permeability by depleting VDAC expression on the OMM. This reduces the import of fatty acids into mitochondria, and thus limits

beta oxidation of fatty acids (FAO). Reduced FAO leads to a reduction in oxidative stress and is thus protective under times of starvation or another acute stress. Furthermore, the authors of this study showed that cells derived from patients diagnosed with amyotrophic lateral sclerosis could not form functional SGs and thus displayed uncontrolled FAO during long-term starvation (AMEN AND KAGANOVICH 2021). Altogether, this study highlighted that SGs could modulate metabolic processes within mitochondria in a clinically relevant manner.

In addition to these well-characterized membraneless organelles, another type of condensate was recently discovered in a worm *Caenorhabditis elegans* model to form on the mitochondrial surface and was termed mitochondria-associated translation organelles (MATOs). As the name suggests, MATOs mediate local synthesis of nuclear-encoded mitochondrial proteins and require the RNA-binding protein LARP-1 for their formation. LARP-1 provides a scaffold to assemble the translational machinery and various other RNA-binding proteins via LLPS into MATOs that associate with the TOM complex on the mitochondrial surface. In worms that lack LARP-1, mitochondria lose cristae organization and the ability to generate ATP efficiently (BAI *et al.* 2025).

Another form of condensate in the vicinity of mitochondria was characterized by work done by the Benjamin Tu group. This group found that when the growth media of yeast cells is switched from a fermentable carbon source such as glucose to a non-fermentable carbon source such as lactate, Pbp1-containing foci appear “peri-mitochondrially” (YANG *et al.* 2019). They termed these foci ‘nebulous assemblies’ since they were smaller and less sharp appearing in comparison to the well-described classical SGs (SWISHER AND PARKER 2010; WHEELER *et al.* 2016). Benjamin Tu’s group also found that Pbp1 associates with Puf3 to mediate the translation of several nuclear-encoded mitochondrial mRNAs, and that Pbp1 and Mkt1 form a complex to

support other respiratory growth adaptations such as TORC1-dependent autophagy in yeast (VAN DE POLL *et al.* 2023; CABALLERO *et al.* 2025) (Table 1.11).

Table 1.11. RNA-protein condensates in the cytosol associated with mitochondria across different species.

Condensate	Organism	Location	Function
SGs	Conserved across species	Near mitochondria	Translation arrest
P bodies	Conserved across species	Cytosolic, near SGs	RNA processing/turnover
MATOs	<i>C. elegans</i> (Roundworm)	OMM/TOM	Local translation
Pbp1 nebulous assemblies	<i>S. cerevisiae</i> (Yeast)	Perimitochondrial	Respiratory adaptation

1.5.c] Diseases associated with RNA-binding proteins: Spotlight on Ataxin-2

Condensates such as P-bodies and SGs are composed of both RNA and protein components. For such condensates to form via LLPS, the RNA-binding proteins (RBPs) act as a scaffold or nucleation site to sequester the other components which may include ribosomal subunits, ribosomal proteins, RNA species, and stress-specific proteins (BANANI *et al.* 2017). Many RBPs have been implicated in human diseases ranging from cardiovascular and metabolic diseases, cancer, and neurodegeneration (GEBAUER *et al.* 2021; ABORODE *et al.* 2025). RBPs possess intrinsically disordered or low-complexity regions that promote liquid-liquid phase separation and assembly into ribonucleoprotein (RNP) granules, such as stress granules and P bodies. While these assemblies are normally dynamic and reversible, disease-associated mutations can alter their material properties, leading to aberrant persistence, impaired disassembly, or pathological aggregation. As a result, defects in RNA metabolism, translational control, and proteostasis frequently emerge as shared features especially across neurodegenerative diseases (CONLON AND MANLEY 2017) (Table 1.12).

Table 1.12. RNA-binding proteins (RBPs) with causative links to neurodegenerative diseases.

RBP	Condensate	Disease
Ataxin-2	SGs	SCA2, Amyotrophic Lateral Sclerosis (ALS), Parkinsonism
TDP-43	SGs	ALS, Frontotemporal Dementia (FTD)
FUS	SGs	ALS
hnRNPA1	SGs	Multisystem proteinopathy (MSP), ALS, FTD, Inclusion body myopathy (hIBM)

Across disorders such as amyotrophic lateral sclerosis (ALS), frontotemporal dementia (FTD), and spinocerebellar ataxias, disease-linked RBPs often localize to stress granules or related condensates and disrupt their normal dynamics (KHALFALLAH *et al.* 2018; DUDMAN AND QI 2020; KOPPENOL *et al.* 2023; KUMAR *et al.* 2023). In several cases, mutations enhance granule assembly or reduce granule fluidity, converting adaptive stress responses into chronic, maladaptive states. This shift can simultaneously cause loss of normal nuclear or cytosolic RNA-processing functions and toxic gain-of-function effects through sequestration of RNAs, translation factors, or quality-control proteins. These observations have led to the emerging view that dysregulated RNP condensates serve as central hubs where disturbances in RNA metabolism, stress signaling, and proteostasis converge to drive neurodegeneration (NASKAR *et al.* 2023; DESAI *et al.* 2026). Among disease-associated RBPs, Ataxin-2 occupies a unique position due to its modular architecture, its ability to regulate RNA metabolism and translation, and the striking relationship between polyglutamine repeat length and disease risk (OSTROWSKI *et al.* 2017; COSTA *et al.* 2024; LI *et al.* 2024a). Ataxin-2 and its yeast ortholog, Pbp1, are conserved components of stress-responsive RNP granules, making them powerful models for understanding how alterations in condensate behavior can translate into cellular dysfunction and human disease.

Ataxin-2 is a conserved RBP that contains extended intrinsically disordered regions, RNA-interacting domains, and a polyglutamine (polyQ) tract encoded by CAG repeats. These features enable Ataxin-2 to participate in dynamic ribonucleoprotein (RNP) assemblies, including stress

granules, but also render it vulnerable to disease-associated alterations in condensate behavior (COSTA *et al.* 2024). Pathogenic expansion of the Ataxin-2 polyQ tract is the primary genetic cause of Spinocerebellar ataxia type 2 (SCA2) (PULST *et al.* 1996; SANPEI *et al.* 1996). In unaffected individuals, the ATXN2 CAG repeat length typically ranges between ~22 and 32 repeats, whereas expansions greater than 35 repeats are strongly associated with SCA2 (COSTA *et al.* 2024). Clinically, SCA2 is characterized by progressive cerebellar ataxia, dysarthria, and neurodegeneration affecting Purkinje cells and other neuronal populations (VELAZQUEZ-PEREZ *et al.* 2017). At the molecular level, polyQ expansion promotes Ataxin-2 misfolding, altered subcellular localization, and increased aggregation propensity, consistent with other polyglutamine expansion disorders. Importantly, disease-associated Ataxin-2 expansions disrupt normal RNA-binding and translational regulatory functions while simultaneously promoting toxic gain-of-function effects (WANG *et al.* 2024a). Expanded Ataxin-2 exhibits enhanced incorporation into stress granules and reduced granule dynamics, suggesting that pathological solidification of normally liquid-like RNP assemblies contributes to neuronal dysfunction in SCA2 (PETRAUSKAS *et al.* 2024).

Beyond classical SCA2, Ataxin-2 repeat length functions as a dosage-sensitive disease modifier in other neurodegenerative contexts. Intermediate polyQ expansions, often defined as ~27–33 glutamines, do not cause SCA2 outright but significantly increase the risk and lower the age of onset of Amyotrophic lateral sclerosis (ALS) (YU *et al.* 2011; SPROVIERO *et al.* 2017). These intermediate expansions highlight an important conceptual distinction: relatively subtle changes in Ataxin-2 structure and condensate behavior can predispose neurons to degeneration without producing an overt ataxia syndrome. Mechanistically, Ataxin-2 has been shown to genetically and physically interact with other ALS-linked RBPs, particularly TDP-43.

Intermediate expansions enhance Ataxin-2–dependent stress granule assembly and can exacerbate TDP-43 toxicity, supporting a model in which altered RNP granule dynamics sensitize cells to additional proteostatic or stress-related insults (HART AND GITLER 2012; WIJEGUNAWARDANA *et al.* 2025). These findings place Ataxin-2 at a convergence point between RNA metabolism, stress granule biology, and ALS pathogenesis.

Emerging evidence also implicates Ataxin-2 in Parkinsonian syndromes and related movement disorders. Although less well characterized than its roles in SCA2 and ALS, certain Ataxin-2 expansions or variants have been associated with Parkinsonism, suggesting that dysregulation of Ataxin-2-dependent RNA and protein homeostasis may broadly influence neuronal vulnerability across multiple disease contexts (XU *et al.* 2024; WANG *et al.* 2025). These observations reinforce the idea that Ataxin-2 is not a single-disease protein, but rather a pleiotropic regulator whose perturbation can manifest as distinct neurodegenerative phenotypes depending on repeat length, genetic background, and cellular context.

The budding yeast ortholog of Ataxin-2, Pbp1, has provided valuable mechanistic insight into conserved Ataxin-2 functions. Pbp1 localizes to stress granules and P bodies, interacts with multiple RNA-binding proteins, and regulates translation and stress adaptation (BUCHAN *et al.* 2008; SWISHER AND PARKER 2010; BUCHAN *et al.* 2011). Notably, recent work has demonstrated that Pbp1 forms perimitochondrial condensates under respiratory growth conditions, linking Ataxin-2 family proteins to mitochondrial function and metabolic remodeling (YANG *et al.* 2019). These findings suggest that Ataxin-2-dependent condensate behavior may influence not only RNA metabolism but also mitochondrial homeostasis, providing a conceptual bridge between RNP granule biology, cellular stress responses, and neurodegenerative disease.

1.6] Thesis Objectives

Mitochondrial protein import clogging and the resulting mitochondrial precursor overaccumulation stress (mPOS) have emerged as central drivers of cellular dysfunction in both yeast and mammalian systems (WANG AND CHEN 2015; LIU *et al.* 2019; COYNE *et al.* 2023). Work over the past decade has established that pathogenic mutations in nuclear-encoded mitochondrial proteins can induce severe proteostatic stress independent of bioenergetic failure, reframing how mitochondrial disease mechanisms are understood. While several cellular pathways that respond to import clogging and mPOS have been described, much less is known about endogenous mechanisms that actively restore mitochondrial protein import competence, alleviate precursor stress, or improve mitochondrial quality and cell viability under clogging conditions.

The overarching goal of this thesis was to identify and characterize novel cellular pathways that mitigate mitochondrial protein import clogging and mPOS, with the long-term aim of uncovering conserved mechanisms that could be leveraged to improve mitochondrial function in disease contexts. To address this goal, we employed unbiased multicopy suppressor genetic screens in *Saccharomyces cerevisiae* using established models of mitochondrial protein import clogging. These screens were designed to identify factors whose increased dosage improves growth, mitochondrial function, or cellular fitness in the presence of pathogenic import stress. Through this approach, we identified two previously unappreciated pathways that suppress mitochondrial protein import clogging and mPOS:

1. An F-box protein-dependent pathway centered on Mfb1, which improves mitochondrial protein import competence and mitochondrial quality under clogging conditions.

2. A condensate-associated pathway involving the RNA-binding protein Pbp1, revealing an unexpected role for RNA granule biology in supporting mitochondrial protein import and proteostasis.

In this thesis, we describe the genetic, molecular, biochemical, proteomic, and imaging-based approaches used to define these pathways and elucidate their mechanisms of action. We further explore how these pathways intersect with known mitochondrial quality-control networks and stress-response systems to promote mitochondrial integrity, including effects on protein import efficiency, proteostasis, and mitochondrial DNA maintenance. Collectively, this work expands the conceptual framework of mitochondrial protein import quality control by uncovering new layers of regulation that act upstream of, or parallel to, canonical degradation and stress-signaling pathways. By identifying cellular mechanisms that actively improve mitochondrial import competence rather than merely responding to its failure, this thesis provides insights with potential relevance for the development of therapeutic strategies aimed at mitigating mitochondrial dysfunction in human disease.

1.7] References for Chapter 1

- Abe, Y., T. Shodai, T. Muto, K. Mihara, H. Torii *et al.*, 2000 Structural basis of presequence recognition by the mitochondrial protein import receptor Tom20. *Cell* 100: 551-560.
- Aborode, A. T., O. A. Abass, S. Nasiru, M. U. Eigbobo, S. Nefishatu *et al.*, 2025 RNA binding proteins (RBPs) on genetic stability and diseases. *Glob Med Genet* 12: 100032.
- Agsteribbe, E., A. Huckriede, M. Veenhuis, M. H. Ruiters, K. E. Niezen-Koning *et al.*, 1993 A fatal, systemic mitochondrial disease with decreased mitochondrial enzyme activities, abnormal ultrastructure of the mitochondria and deficiency of heat shock protein 60. *Biochem Biophys Res Commun* 193: 146-154.
- Ahting, U., M. Thieffry, H. Engelhardt, R. Hegerl, W. Neupert and S. Nussberger, 2001 Tom40, the pore-forming component of the protein-conducting TOM channel in the outer membrane of mitochondria. *J Cell Biol* 153: 1151-1160.
- Alberti, S., and A. A. Hyman, 2021 Biomolecular condensates at the nexus of cellular stress, protein aggregation disease and ageing. *Nat Rev Mol Cell Biol* 22: 196-213.
- Ambivero, C. T., L. Cilenti, S. Main and A. S. Zervos, 2014 Mulan E3 ubiquitin ligase interacts with multiple E2 conjugating enzymes and participates in mitophagy by recruiting GABARAP. *Cell Signal* 26: 2921-2929.
- Amen, T., and D. Kaganovich, 2021 Stress granules inhibit fatty acid oxidation by modulating mitochondrial permeability. *Cell Rep* 35: 109237.
- Anderson, P., and N. Kedersha, 2008 Stress granules: the Tao of RNA triage. *Trends Biochem Sci* 33: 141-150.
- Antonicka, H., and E. A. Shoubridge, 2015 Mitochondrial RNA Granules Are Centers for Posttranscriptional RNA Processing and Ribosome Biogenesis. *Cell Rep* 10: 920-932.
- Arbogast, S., H. Kotzur, C. Frank, N. Compagnone, T. Sutra *et al.*, 2022 ANT1 overexpression models: Some similarities with facioscapulohumeral muscular dystrophy. *Redox Biol* 56: 102450.
- Arnould, T., L. Mercy, A. Houbion, S. Vankoningsloo, P. Renard *et al.*, 2003 mtCLIC is up-regulated and maintains a mitochondrial membrane potential in mtDNA-depleted L929 cells. *FASEB J* 17: 2145-2147.
- Aulas, A., M. M. Fay, S. M. Lyons, C. A. Achorn, N. Kedersha *et al.*, 2017 Stress-specific differences in assembly and composition of stress granules and related foci. *J Cell Sci* 130: 927-937.
- Bai, Y., T. Ma, S. Zhao, S. Li, X. Wang *et al.*, 2025 Mitochondria-associated condensates maintain mitochondrial homeostasis and promote lifespan. *Nat Aging* 5: 1983-2002.
- Baker, M. J., P. A. Lampe, D. Stojanovski, A. Korwitz, R. Anand *et al.*, 2014 Stress-induced OMA1 activation and autocatalytic turnover regulate OPA1-dependent mitochondrial dynamics. *EMBO J* 33: 578-593.
- Ballout, R. A., C. Al Alam, P. E. Bonnen, M. Huemer, A. W. El-Hattab and R. Shbarou, 2019 FBXL4-Related Mitochondrial DNA Depletion Syndrome 13 (MTDPS13): A Case Report With a Comprehensive Mutation Review. *Front Genet* 10: 39.
- Banani, S. F., H. O. Lee, A. A. Hyman and M. K. Rosen, 2017 Biomolecular condensates: organizers of cellular biochemistry. *Nat Rev Mol Cell Biol* 18: 285-298.
- Bard, J. A. M., E. A. Goodall, E. R. Greene, E. Jonsson, K. C. Dong and A. Martin, 2018 Structure and Function of the 26S Proteasome. *Annu Rev Biochem* 87: 697-724.
- Basu, M., S. C. Courtney and M. A. Brinton, 2017 Arsenite-induced stress granule formation is inhibited by elevated levels of reduced glutathione in West Nile virus-infected cells. *PLoS Pathog* 13: e1006240.
- Bausewein, T., D. J. Mills, J. D. Langer, B. Nitschke, S. Nussberger and W. Kuhlbrandt, 2017 Cryo-EM Structure of the TOM Core Complex from *Neurospora crassa*. *Cell* 170: 693-700 e697.

- Becker, T., B. Guiard, N. Thornton, N. Zufall, D. A. Stroud *et al.*, 2010 Assembly of the mitochondrial protein import channel: role of Tom5 in two-stage interaction of Tom40 with the SAM complex. *Mol Biol Cell* 21: 3106-3113.
- Becker, T., F. N. Vogtle, D. Stojanovski and C. Meisinger, 2008 Sorting and assembly of mitochondrial outer membrane proteins. *Biochim Biophys Acta* 1777: 557-563.
- Becker, T., L. S. Wenz, V. Kruger, W. Lehmann, J. M. Muller *et al.*, 2011 The mitochondrial import protein Mim1 promotes biogenesis of multispinning outer membrane proteins. *J Cell Biol* 194: 387-395.
- Bertgen, L., J. E. Bokenkamp, T. Schneckmann, C. Koch, M. Raschle *et al.*, 2024 Distinct types of intramitochondrial protein aggregates protect mitochondria against proteotoxic stress. *Cell Rep* 43: 114018.
- Bertram, N., T. Izawa, F. Thoma, S. Schwenkert, S. Duvezin-Caubet *et al.*, 2025 Delayed protein translocation protects mitochondria against toxic CAT-tailed proteins. *Mol Cell* 85: 4082-4092 e4087.
- Bohovych, I., G. Donaldson, S. Christianson, N. Zahayko and O. Khalimonchuk, 2014 Stress-triggered activation of the metalloprotease Oma1 involves its C-terminal region and is important for mitochondrial stress protection in yeast. *J Biol Chem* 289: 13259-13272.
- Bolender, N., A. Sickmann, R. Wagner, C. Meisinger and N. Pfanner, 2008 Multiple pathways for sorting mitochondrial precursor proteins. *EMBO Rep* 9: 42-49.
- Bonnen, P. E., J. W. Yarham, A. Besse, P. Wu, E. A. Faqeih *et al.*, 2013 Mutations in FBXL4 cause mitochondrial encephalopathy and a disorder of mitochondrial DNA maintenance. *Am J Hum Genet* 93: 471-481.
- Brangwynne, C. P., C. R. Eckmann, D. S. Courson, A. Rybarska, C. Hoegge *et al.*, 2009 Germline P granules are liquid droplets that localize by controlled dissolution/condensation. *Science* 324: 1729-1732.
- Briones, P., M. A. Vilaseca, A. Ribes, A. Vernet, M. Lluch *et al.*, 1997 A new case of multiple mitochondrial enzyme deficiencies with decreased amount of heat shock protein 60. *J Inher Metab Dis* 20: 569-577.
- Brix, J., S. Rudiger, B. Bukau, J. Schneider-Mergener and N. Pfanner, 1999 Distribution of binding sequences for the mitochondrial import receptors Tom20, Tom22, and Tom70 in a presequence-carrying preprotein and a non-cleavable preprotein. *J Biol Chem* 274: 16522-16530.
- Brix, J., G. A. Ziegler, K. Dietmeier, J. Schneider-Mergener, G. E. Schulz and N. Pfanner, 2000 The mitochondrial import receptor Tom70: identification of a 25 kDa core domain with a specific binding site for preproteins. *J Mol Biol* 303: 479-488.
- Bruderek, M., W. Jaworek, A. Wilkening, C. Rub, G. Cenini *et al.*, 2018 IMiQ: a novel protein quality control compartment protecting mitochondrial functional integrity. *Mol Biol Cell* 29: 256-269.
- Brustovetsky, N., 2020 The Role of Adenine Nucleotide Translocase in the Mitochondrial Permeability Transition. *Cells* 9.
- Buchan, J. R., D. Muhlrad and R. Parker, 2008 P bodies promote stress granule assembly in *Saccharomyces cerevisiae*. *J Cell Biol* 183: 441-455.
- Buchan, J. R., and R. Parker, 2009 Eukaryotic stress granules: the ins and outs of translation. *Mol Cell* 36: 932-941.
- Buchan, J. R., J. H. Yoon and R. Parker, 2011 Stress-specific composition, assembly and kinetics of stress granules in *Saccharomyces cerevisiae*. *J Cell Sci* 124: 228-239.
- Bueno, M., J. Brands, L. Voltz, K. Fiedler, B. Mays *et al.*, 2018 ATF3 represses PINK1 gene transcription in lung epithelial cells to control mitochondrial homeostasis. *Aging Cell* 17.
- Burchell, V. S., D. E. Nelson, A. Sanchez-Martinez, M. Delgado-Camprubi, R. M. Ivatt *et al.*, 2013 The Parkinson's disease-linked proteins Fbxo7 and Parkin interact to mediate mitophagy. *Nat Neurosci* 16: 1257-1265.
- Caballero, D., B. M. Sutter, Z. Xing, C. Wang, E. Choo *et al.*, 2025 The yeast Mkt1/Pbp1 complex promotes adaptive responses to respiratory growth. *J Cell Biol* 224.
- Callegari, S., N. S. Kirk, Z. Y. Gan, T. Dite, S. A. Cobbold *et al.*, 2025 Structure of human PINK1 at a mitochondrial TOM-VDAC array. *Science* 388: 303-310.

- Callegari, S., T. Muller, C. Schulz, C. Lenz, D. C. Jans *et al.*, 2019 A MICOS-TIM22 Association Promotes Carrier Import into Human Mitochondria. *J Mol Biol* 431: 2835-2851.
- Cao, Y., J. Zheng, H. Wan, Y. Sun, S. Fu *et al.*, 2023 A mitochondrial SCF-FBXL4 ubiquitin E3 ligase complex degrades BNIP3 and NIX to restrain mitophagy and prevent mitochondrial disease. *EMBO J* 42: e113033.
- Chacinska, A., C. M. Koehler, D. Milenkovic, T. Lithgow and N. Pfanner, 2009 Importing mitochondrial proteins: machineries and mechanisms. *Cell* 138: 628-644.
- Chacinska, A., M. Lind, A. E. Frazier, J. Dudek, C. Meisinger *et al.*, 2005 Mitochondrial presequence translocase: switching between TOM tethering and motor recruitment involves Tim21 and Tim17. *Cell* 120: 817-829.
- Chan, N. C., and T. Lithgow, 2008 The peripheral membrane subunits of the SAM complex function codependently in mitochondrial outer membrane biogenesis. *Mol Biol Cell* 19: 126-136.
- Chen, T. H., H. C. Wang, C. J. Chang and S. Y. Lee, 2024 Mitochondrial Glutathione in Cellular Redox Homeostasis and Disease Manifestation. *Int J Mol Sci* 25.
- Chen, X. J., 2004 Sallp, a calcium-dependent carrier protein that suppresses an essential cellular function associated With the Aac2 isoform of ADP/ATP translocase in *Saccharomyces cerevisiae*. *Genetics* 167: 607-617.
- Chen, Y., X. Guo, Y. Zeng, X. Mo, S. Hong *et al.*, 2023 Oxidative stress induces mitochondrial iron overload and ferroptotic cell death. *Sci Rep* 13: 15515.
- Chen, Z., S. Siraj, L. Liu and Q. Chen, 2017 MARCH5-FUNDC1 axis fine-tunes hypoxia-induced mitophagy. *Autophagy* 13: 1244-1245.
- Coller, J., and R. Parker, 2005 General translational repression by activators of mRNA decapping. *Cell* 122: 875-886.
- Conlon, E. G., and J. L. Manley, 2017 RNA-binding proteins in neurodegeneration: mechanisms in aggregate. *Genes Dev* 31: 1509-1528.
- Costa, R. G., A. Conceicao, C. A. Matos and C. Nobrega, 2024 The polyglutamine protein ATXN2: from its molecular functions to its involvement in disease. *Cell Death Dis* 15: 415.
- Coyne, L. P., and X. J. Chen, 2018 mPOS is a novel mitochondrial trigger of cell death - implications for neurodegeneration. *FEBS Lett* 592: 759-775.
- Coyne, L. P., and X. J. Chen, 2019 Consequences of inner mitochondrial membrane protein misfolding. *Mitochondrion* 49: 46-55.
- Coyne, L. P., X. Wang, J. Song, E. de Jong, K. Schneider *et al.*, 2023 Mitochondrial protein import clogging as a mechanism of disease. *Elife* 12.
- Curran, S. P., D. Leuenberger, W. Oppliger and C. M. Koehler, 2002 The Tim9p-Tim10p complex binds to the transmembrane domains of the ADP/ATP carrier. *EMBO J* 21: 942-953.
- Dallabona, C., E. Baruffini, P. Goffrini and T. Lodi, 2017 Dominance of yeast aac2(R96H) and aac2(R252G) mutations, equivalent to pathological mutations in ant1, is due to gain of function. *Biochem Biophys Res Commun* 493: 909-913.
- Davey, K. M., J. S. Parboosingh, D. R. McLeod, A. Chan, R. Casey *et al.*, 2006 Mutation of DNAJC19, a human homologue of yeast inner mitochondrial membrane co-chaperones, causes DCMA syndrome, a novel autosomal recessive Barth syndrome-like condition. *J Med Genet* 43: 385-393.
- De Silva, D., Y. T. Tu, A. Amunts, F. Fontanesi and A. Barrientos, 2015 Mitochondrial ribosome assembly in health and disease. *Cell Cycle* 14: 2226-2250.
- del Arco, A., and J. Satrustegui, 2004 Identification of a novel human subfamily of mitochondrial carriers with calcium-binding domains. *J Biol Chem* 279: 24701-24713.
- Demeshkina, N. A., and A. R. Ferre-D'Amare, 2025 Large-scale purifications reveal yeast and human stress granule cores are heterogeneous particles with complex transcriptomes and proteomes. *Cell Rep* 44: 115738.
- den Brave, F., U. Schulte, B. Fakler, N. Pfanner and T. Becker, 2024 Mitochondrial complexome and import network. *Trends Cell Biol* 34: 578-594.

- Desai, M., K. Gulati, M. Agrawal, S. Ghumra and P. K. Sahoo, 2026 Stress granules: Guardians of cellular health and triggers of disease. *Neural Regen Res* 21: 588-597.
- Deschauer, M., G. Hudson, T. Muller, R. W. Taylor, P. F. Chinnery and S. Zierz, 2005 A novel ANT1 gene mutation with probable germline mosaicism in autosomal dominant progressive external ophthalmoplegia. *Neuromuscul Disord* 15: 311-315.
- Diekert, K., G. Kispal, B. Guiard and R. Lill, 1999 An internal targeting signal directing proteins into the mitochondrial intermembrane space. *Proc Natl Acad Sci U S A* 96: 11752-11757.
- Dienhart, M. K., and R. A. Stuart, 2008 The yeast Aac2 protein exists in physical association with the cytochrome bc1-COX supercomplex and the TIM23 machinery. *Mol Biol Cell* 19: 3934-3943.
- Dietmeier, K., A. Honlinger, U. Bomer, P. J. Dekker, C. Eckerskorn *et al.*, 1997 Tom5 functionally links mitochondrial preprotein receptors to the general import pore. *Nature* 388: 195-200.
- Dimmer, K. S., D. Papic, B. Schumann, D. Sperl, K. Krumpel *et al.*, 2012 A crucial role for Mim2 in the biogenesis of mitochondrial outer membrane proteins. *J Cell Sci* 125: 3464-3473.
- Doan, K. N., A. Grevel, C. U. Martensson, L. Ellenrieder, N. Thornton *et al.*, 2020 The Mitochondrial Import Complex MIM Functions as Main Translocase for alpha-Helical Outer Membrane Proteins. *Cell Rep* 31: 107567.
- Dolce, V., P. Scarzia, D. Iacopetta and F. Palmieri, 2005 A fourth ADP/ATP carrier isoform in man: identification, bacterial expression, functional characterization and tissue distribution. *FEBS Lett* 579: 633-637.
- Dudman, J., and X. Qi, 2020 Stress Granule Dysregulation in Amyotrophic Lateral Sclerosis. *Front Cell Neurosci* 14: 598517.
- Edwards, R., R. Eaglesfield and K. Tokatlidis, 2021 The mitochondrial intermembrane space: the most constricted mitochondrial sub-compartment with the largest variety of protein import pathways. *Open Biol* 11: 210002.
- Ehmke, N., L. Graul-Neumann, L. Smorag, R. Koenig, L. Segebrecht *et al.*, 2017 De Novo Mutations in SLC25A24 Cause a Craniosynostosis Syndrome with Hypertrichosis, Progeroid Appearance, and Mitochondrial Dysfunction. *Am J Hum Genet* 101: 833-843.
- Eiermann, N., G. Stoecklin and B. Jovanovic, 2022 Mitochondrial Inhibition by Sodium Azide Induces Assembly of eIF2alpha Phosphorylation-Independent Stress Granules in Mammalian Cells. *Int J Mol Sci* 23.
- Elbaz-Alon, Y., E. Rosenfeld-Gur, V. Shinder, A. H. Futerman, T. Geiger and M. Schuldiner, 2014 A dynamic interface between vacuoles and mitochondria in yeast. *Dev Cell* 30: 95-102.
- Elcocks, H., A. J. Brazel, K. R. McCarron, M. Kaulich, K. Husnjak *et al.*, 2023 FBXL4 ubiquitin ligase deficiency promotes mitophagy by elevating NIX levels. *EMBO J* 42: e112799.
- Endo, T., and K. Yamano, 2010 Transport of proteins across or into the mitochondrial outer membrane. *Biochim Biophys Acta* 1803: 706-714.
- English, A. M., M. H. Schuler, T. Xiao, B. Kornmann, J. M. Shaw and A. L. Hughes, 2020 ER-mitochondria contacts promote mitochondrial-derived compartment biogenesis. *J Cell Biol* 219.
- Ernster, L., and G. Schatz, 1981 Mitochondria: a historical review. *J Cell Biol* 91: 227s-255s.
- Esposito, L. A., S. Melov, A. Panov, B. A. Cottrell and D. C. Wallace, 1999 Mitochondrial disease in mouse results in increased oxidative stress. *Proc Natl Acad Sci U S A* 96: 4820-4825.
- Fan, J., J. Ye, J. J. Kamphorst, T. Shlomi, C. B. Thompson and J. D. Rabinowitz, 2014 Quantitative flux analysis reveals folate-dependent NADPH production. *Nature* 510: 298-302.
- Feric, M., N. Vaidya, T. S. Harmon, D. M. Mitrea, L. Zhu *et al.*, 2016 Coexisting Liquid Phases Underlie Nucleolar Subcompartments. *Cell* 165: 1686-1697.
- Fessler, E., E. M. Eckl, S. Schmitt, I. A. Mancilla, M. F. Meyer-Bender *et al.*, 2020 A pathway coordinated by DELE1 relays mitochondrial stress to the cytosol. *Nature* 579: 433-437.
- Fiermonte, G., F. De Leonadis, S. Todisco, L. Palmieri, F. M. Lasorsa and F. Palmieri, 2004 Identification of the mitochondrial ATP-Mg/Pi transporter. Bacterial expression, reconstitution, functional characterization, and tissue distribution. *J Biol Chem* 279: 30722-30730.

- Filbeck, S., F. Cerullo, S. Pfeffer and C. A. P. Joazeiro, 2022 Ribosome-associated quality-control mechanisms from bacteria to humans. *Mol Cell* 82: 1451-1466.
- Fiorese, C. J., A. M. Schulz, Y. F. Lin, N. Rosin, M. W. Pellegrino and C. M. Haynes, 2016 The Transcription Factor ATF5 Mediates a Mammalian Mitochondrial UPR. *Curr Biol* 26: 2037-2043.
- Fischer, M., S. Horn, A. Belkacemi, K. Kojer, C. Petrunger *et al.*, 2013 Protein import and oxidative folding in the mitochondrial intermembrane space of intact mammalian cells. *Mol Biol Cell* 24: 2160-2170.
- Fontanesi, F., L. Palmieri, P. Scarcia, T. Lodi, C. Donnini *et al.*, 2004 Mutations in AAC2, equivalent to human adPEO-associated ANT1 mutations, lead to defective oxidative phosphorylation in *Saccharomyces cerevisiae* and affect mitochondrial DNA stability. *Hum Mol Genet* 13: 923-934.
- Fox, A. H., S. Nakagawa, T. Hirose and C. S. Bond, 2018 Paraspeckles: Where Long Noncoding RNA Meets Phase Separation. *Trends Biochem Sci* 43: 124-135.
- Frazier, A. E., J. Dudek, B. Guiard, W. Voos, Y. Li *et al.*, 2004 Pam16 has an essential role in the mitochondrial protein import motor. *Nat Struct Mol Biol* 11: 226-233.
- Friedman, J. R., A. Mourier, J. Yamada, J. M. McCaffery and J. Nunnari, 2015 MICOS coordinates with respiratory complexes and lipids to establish mitochondrial inner membrane architecture. *Elife* 4.
- Fu, Y., O. Sacco, E. DeBitetto, E. Kanshin, B. Ueberheide and A. Sfeir, 2023 Mitochondrial DNA breaks activate an integrated stress response to reestablish homeostasis. *Mol Cell* 83: 3740-3753 e3749.
- Fujita, Y., Y. Taniguchi, S. Shinkai, M. Tanaka and M. Ito, 2016 Secreted growth differentiation factor 15 as a potential biomarker for mitochondrial dysfunctions in aging and age-related disorders. *Geriatr Gerontol Int* 16 Suppl 1: 17-29.
- Fukuda, T., and T. Kanki, 2018 Mechanisms and Physiological Roles of Mitophagy in Yeast. *Mol Cells* 41: 35-44.
- Galaris, D., A. Barbouti and K. Pantopoulos, 2019 Iron homeostasis and oxidative stress: An intimate relationship. *Biochim Biophys Acta Mol Cell Res* 1866: 118535.
- Galassi, G., E. Lamantea, F. Invernizzi, F. Tavani, I. Pisano *et al.*, 2008 Additive effects of POLG1 and ANT1 mutations in a complex encephalomyopathy. *Neuromuscul Disord* 18: 465-470.
- Garipler, G., and C. D. Dunn, 2013 Defects associated with mitochondrial DNA damage can be mitigated by increased vacuolar pH in *Saccharomyces cerevisiae*. *Genetics* 194: 285-290.
- Gebauer, F., T. Schwarzl, J. Valcarcel and M. W. Hentze, 2021 RNA-binding proteins in human genetic disease. *Nat Rev Genet* 22: 185-198.
- Glick, B. S., A. Brandt, K. Cunningham, S. Muller, R. L. Hallberg and G. Schatz, 1992 Cytochromes c1 and b2 are sorted to the intermembrane space of yeast mitochondria by a stop-transfer mechanism. *Cell* 69: 809-822.
- Gomes, F., F. R. Palma, M. H. Barros, E. T. Tsuchida, H. G. Turano *et al.*, 2017 Proteolytic cleavage by the inner membrane peptidase (IMP) complex or Oct1 peptidase controls the localization of the yeast peroxiredoxin Prx1 to distinct mitochondrial compartments. *J Biol Chem* 292: 17011-17024.
- Gomez-Virgilio, L., M. D. Silva-Lucero, D. S. Flores-Morelos, J. Gallardo-Nieto, G. Lopez-Toledo *et al.*, 2022 Autophagy: A Key Regulator of Homeostasis and Disease: An Overview of Molecular Mechanisms and Modulators. *Cells* 11.
- Gong, W., J. Song, J. Liang, H. Ma, W. Wu *et al.*, 2021 Reduced Lon protease 1 expression in podocytes contributes to the pathogenesis of podocytopathy. *Kidney Int* 99: 854-869.
- Gorman, G. S., P. F. Chinnery, S. DiMauro, M. Hirano, Y. Koga *et al.*, 2016 Mitochondrial diseases. *Nat Rev Dis Primers* 2: 16080.
- Graham, B. H., K. G. Waymire, B. Cottrell, I. A. Trounce, G. R. MacGregor and D. C. Wallace, 1997 A mouse model for mitochondrial myopathy and cardiomyopathy resulting from a deficiency in the heart/muscle isoform of the adenine nucleotide translocator. *Nat Genet* 16: 226-234.
- Gray, M. W., 1982 Mitochondrial genome diversity and the evolution of mitochondrial DNA. *Can J Biochem* 60: 157-171.
- Griparic, L., T. Kanazawa and A. M. van der Bliek, 2007 Regulation of the mitochondrial dynamin-like protein Opa1 by proteolytic cleavage. *J Cell Biol* 178: 757-764.

- Grousl, T., P. Ivanov, I. Frydlova, P. Vasicova, F. Janda *et al.*, 2009 Robust heat shock induces eIF2 α -phosphorylation-independent assembly of stress granules containing eIF3 and 40S ribosomal subunits in budding yeast, *Saccharomyces cerevisiae*. *J Cell Sci* 122: 2078-2088.
- Guo, X., G. Aviles, Y. Liu, R. Tian, B. A. Unger *et al.*, 2020 Mitochondrial stress is relayed to the cytosol by an OMA1-DELE1-HRI pathway. *Nature* 579: 427-432.
- Hansen, K. G., N. Aviram, J. Laborenz, C. Bibi, M. Meyer *et al.*, 2018 An ER surface retrieval pathway safeguards the import of mitochondrial membrane proteins in yeast. *Science* 361: 1118-1122.
- Hansen, K. G., and J. M. Herrmann, 2019 Transport of Proteins into Mitochondria. *Protein J* 38: 330-342.
- Harding, H. P., Y. Zhang, H. Zeng, I. Novoa, P. D. Lu *et al.*, 2003 An integrated stress response regulates amino acid metabolism and resistance to oxidative stress. *Mol Cell* 11: 619-633.
- Hart, M. P., and A. D. Gitler, 2012 ALS-associated ataxin 2 polyQ expansions enhance stress-induced caspase 3 activation and increase TDP-43 pathological modifications. *J Neurosci* 32: 9133-9142.
- Hathazi, D., H. Griffin, M. J. Jennings, M. Giunta, C. Powell *et al.*, 2020 Metabolic shift underlies recovery in reversible infantile respiratory chain deficiency. *EMBO J* 39: e105364.
- He, Y., Q. Ding, W. Chen, C. Lin, L. Ge *et al.*, 2022 LONP1 downregulation with ageing contributes to osteoarthritis via mitochondrial dysfunction. *Free Radic Biol Med* 191: 176-190.
- Head, B., L. Griparic, M. Amiri, S. Gandre-Babbe and A. M. van der Blik, 2009 Inducible proteolytic inactivation of OPA1 mediated by the OMA1 protease in mammalian cells. *J Cell Biol* 187: 959-966.
- Hell, K., W. Neupert and R. A. Stuart, 2001 Oxa1p acts as a general membrane insertion machinery for proteins encoded by mitochondrial DNA. *EMBO J* 20: 1281-1288.
- Herrmann, J. M., and J. Riemer, 2010 The intermembrane space of mitochondria. *Antioxid Redox Signal* 13: 1341-1358.
- Hershko, A., and A. Ciechanover, 1998 The ubiquitin system. *Annu Rev Biochem* 67: 425-479.
- Homberg, B., P. Rehling and L. D. Cruz-Zaragoza, 2023 The multifaceted mitochondrial OXA insertase. *Trends Cell Biol* 33: 765-772.
- Honlinger, A., U. Bomer, A. Alconada, C. Eckerskorn, F. Lottspeich *et al.*, 1996 Tom7 modulates the dynamics of the mitochondrial outer membrane translocase and plays a pathway-related role in protein import. *EMBO J* 15: 2125-2137.
- Honlinger, A., M. Kubrich, M. Moczko, F. Gartner, L. Mallet *et al.*, 1995 The mitochondrial receptor complex: Mom22 is essential for cell viability and directly interacts with preproteins. *Mol Cell Biol* 15: 3382-3389.
- Hoppins, S. C., and F. E. Nargang, 2004 The Tim8-Tim13 complex of *Neurospora crassa* functions in the assembly of proteins into both mitochondrial membranes. *J Biol Chem* 279: 12396-12405.
- Hoshino, A., W. J. Wang, S. Wada, C. McDermott-Roe, C. S. Evans *et al.*, 2019 The ADP/ATP translocase drives mitophagy independent of nucleotide exchange. *Nature* 575: 375-379.
- Hsiao, W. Y., Y. T. Wang and S. W. Wang, 2020 Fission Yeast Puf2, a Pumilio and FBF Family RNA-Binding Protein, Links Stress Granules to Processing Bodies. *Mol Cell Biol* 40.
- Hughes, A. L., C. E. Hughes, K. A. Henderson, N. Yazvenko and D. E. Gottschling, 2016 Selective sorting and destruction of mitochondrial membrane proteins in aged yeast. *Elife* 5.
- Hyman, A. A., C. A. Weber and F. Julicher, 2014 Liquid-liquid phase separation in biology. *Annu Rev Cell Dev Biol* 30: 39-58.
- Ieva, R., S. G. Schrempp, L. Opalinski, F. Wollweber, P. Hoss *et al.*, 2014 Mgr2 functions as lateral gatekeeper for preprotein sorting in the mitochondrial inner membrane. *Mol Cell* 56: 641-652.
- Innokentev, A., and T. Kanki, 2021 Mitophagy in Yeast: Molecular Mechanism and Regulation. *Cells* 10.
- Izawa, T., S. H. Park, L. Zhao, F. U. Hartl and W. Neupert, 2017 Cytosolic Protein Vms1 Links Ribosome Quality Control to Mitochondrial and Cellular Homeostasis. *Cell* 171: 890-903 e818.
- Jabalumeli, M. R., F. M. Fitzpatrick, R. Colombo, S. A. Howles, G. Leggatt *et al.*, 2021 Exome sequencing identifies a disease variant of the mitochondrial ATP-Mg/Pi carrier SLC25A25 in two families with kidney stones. *Mol Genet Genomic Med* 9: e1749.

- Jain, N., A. Chacinska and P. Rehling, 2025 Understanding mitochondrial protein import: a revised model of the presequence translocase. *Trends Biochem Sci* 50: 585-595.
- Jain, S., J. R. Wheeler, R. W. Walters, A. Agrawal, A. Barsic and R. Parker, 2016 ATPase-Modulated Stress Granules Contain a Diverse Proteome and Substructure. *Cell* 164: 487-498.
- Janouskovec, J., D. V. Tikhonenkov, F. Burki, A. T. Howe, F. L. Rohwer *et al.*, 2017 A New Lineage of Eukaryotes Illuminates Early Mitochondrial Genome Reduction. *Curr Biol* 27: 3717-3724 e3715.
- Jazwinski, S. M., 2013 The retrograde response: when mitochondrial quality control is not enough. *Biochim Biophys Acta* 1833: 400-409.
- Joazeiro, C. A. P., 2019 Mechanisms and functions of ribosome-associated protein quality control. *Nat Rev Mol Cell Biol* 20: 368-383.
- Kane, L. A., M. Lazarou, A. I. Fogel, Y. Li, K. Yamano *et al.*, 2014 PINK1 phosphorylates ubiquitin to activate Parkin E3 ubiquitin ligase activity. *J Cell Biol* 205: 143-153.
- Kanki, T., and D. J. Klionsky, 2008 Mitophagy in yeast occurs through a selective mechanism. *J Biol Chem* 283: 32386-32393.
- Karbowski, M., and R. J. Youle, 2011 Regulating mitochondrial outer membrane proteins by ubiquitination and proteasomal degradation. *Curr Opin Cell Biol* 23: 476-482.
- Karch, J., M. J. Bround, H. Khalil, M. A. Sargent, N. Latchman *et al.*, 2019 Inhibition of mitochondrial permeability transition by deletion of the ANT family and CypD. *Sci Adv* 5: eaaw4597.
- Kardon, J. R., J. A. Moroco, J. R. Engen and T. A. Baker, 2020 Mitochondrial ClpX activates an essential biosynthetic enzyme through partial unfolding. *Elife* 9.
- Kashiki, T., J. Kido, K. Momosaki, S. Kusunoki, S. Ozasa *et al.*, 2022 Mitochondrial DNA depletion syndrome with a mutation in SLC25A4 developing epileptic encephalopathy: A case report. *Brain Dev* 44: 56-62.
- Kaukonen, J., J. K. Juselius, V. Tiranti, A. Kyttala, M. Zeviani *et al.*, 2000 Role of adenine nucleotide translocator 1 in mtDNA maintenance. *Science* 289: 782-785.
- Kawamata, H., V. Tiranti, J. Magrane, C. Chinopoulos and G. Manfredi, 2011 adPEO mutations in ANT1 impair ADP-ATP translocation in muscle mitochondria. *Hum Mol Genet* 20: 2964-2974.
- Kedersha, N., and P. Anderson, 2007 Mammalian stress granules and processing bodies. *Methods Enzymol* 431: 61-81.
- Kedersha, N., S. Chen, N. Gilks, W. Li, I. J. Miller *et al.*, 2002 Evidence that ternary complex (eIF2-GTP-tRNA(i)(Met))-deficient preinitiation complexes are core constituents of mammalian stress granules. *Mol Biol Cell* 13: 195-210.
- Kedersha, N., M. R. Cho, W. Li, P. W. Yacono, S. Chen *et al.*, 2000 Dynamic shuttling of TIA-1 accompanies the recruitment of mRNA to mammalian stress granules. *J Cell Biol* 151: 1257-1268.
- Kedersha, N., G. Stoecklin, M. Ayodele, P. Yacono, J. Lykke-Andersen *et al.*, 2005 Stress granules and processing bodies are dynamically linked sites of mRNP remodeling. *J Cell Biol* 169: 871-884.
- Kedersha, N. L., M. Gupta, W. Li, I. Miller and P. Anderson, 1999 RNA-binding proteins TIA-1 and TIAR link the phosphorylation of eIF-2 alpha to the assembly of mammalian stress granules. *J Cell Biol* 147: 1431-1442.
- Khalfallah, Y., R. Kuta, C. Grasmuck, A. Prat, H. D. Durham and C. Vande Velde, 2018 TDP-43 regulation of stress granule dynamics in neurodegenerative disease-relevant cell types. *Sci Rep* 8: 7551.
- Khan, N. A., J. Nikkanen, S. Yatsuga, C. Jackson, L. Wang *et al.*, 2017 mTORC1 Regulates Mitochondrial Integrated Stress Response and Mitochondrial Myopathy Progression. *Cell Metab* 26: 419-428 e415.
- Khong, A., T. Matheny, S. Jain, S. F. Mitchell, J. R. Wheeler and R. Parker, 2017 The Stress Granule Transcriptome Reveals Principles of mRNA Accumulation in Stress Granules. *Mol Cell* 68: 808-820 e805.
- Kiebler, M., P. Keil, H. Schneider, I. J. van der Klei, N. Pfanner and W. Neupert, 1993 The mitochondrial receptor complex: a central role of MOM22 in mediating preprotein transfer from receptors to the general insertion pore. *Cell* 74: 483-492.

- Kim, J., M. Goldstein, L. Zecchel, R. Ghorayeb, C. A. Maxwell and H. Weidberg, 2024 ATAD1 prevents clogging of TOM and damage caused by un-imported mitochondrial proteins. *Cell Rep* 43: 114473.
- Kim, M., R. A. Serwa, L. Samluk, I. Suppanz, A. Kodron *et al.*, 2023 Immunoproteasome-specific subunit PSMB9 induction is required to regulate cellular proteostasis upon mitochondrial dysfunction. *Nat Commun* 14: 4092.
- King, M. S., K. Thompson, S. Hopton, L. He, E. R. S. Kunji *et al.*, 2018 Expanding the phenotype of de novo SLC25A4-linked mitochondrial disease to include mild myopathy. *Neurol Genet* 4: e256.
- Kliwer, S. A., and D. J. Mangelsdorf, 2019 A Dozen Years of Discovery: Insights into the Physiology and Pharmacology of FGF21. *Cell Metab* 29: 246-253.
- Kliment, C. R., J. M. K. Nguyen, M. J. Kaltreider, Y. Lu, S. M. Claypool *et al.*, 2021 Adenine nucleotide translocase regulates airway epithelial metabolism, surface hydration and ciliary function. *J Cell Sci* 134.
- Kokoszka, J. E., K. G. Waymire, S. E. Levy, J. E. Sligh, J. Cai *et al.*, 2004 The ADP/ATP translocator is not essential for the mitochondrial permeability transition pore. *Nature* 427: 461-465.
- Komaki, H., T. Fukazawa, H. Houzen, K. Yoshida, I. Nonaka and Y. Goto, 2002 A novel D104G mutation in the adenine nucleotide translocator 1 gene in autosomal dominant progressive external ophthalmoplegia patients with mitochondrial DNA with multiple deletions. *Ann Neurol* 51: 645-648.
- Konig, T., H. Nolte, M. J. Aaltonen, T. Tatsuta, M. Krols *et al.*, 2021 MIROs and DRP1 drive mitochondrial-derived vesicle biogenesis and promote quality control. *Nat Cell Biol* 23: 1271-1286.
- Koppenol, R., A. Conceicao, I. T. Afonso, R. Afonso-Reis, R. G. Costa *et al.*, 2023 The stress granule protein G3BP1 alleviates spinocerebellar ataxia-associated deficits. *Brain* 146: 2346-2363.
- Koyano, F., K. Yamano, H. Kosako, K. Tanaka and N. Matsuda, 2019 Parkin recruitment to impaired mitochondria for nonselective ubiquitylation is facilitated by MITOL. *J Biol Chem* 294: 10300-10314.
- Kramer, L., N. Dalheimer, M. Raschle, Z. Storchova, J. Pielage *et al.*, 2023 MitoStores: chaperone-controlled protein granules store mitochondrial precursors in the cytosol. *EMBO J* 42: e112309.
- Kraus, F., E. A. Goodall, I. R. Smith, Y. Jiang, J. C. Paoli *et al.*, 2023 PARK15/FBXO7 is dispensable for PINK1/Parkin mitophagy in iNeurons and HeLa cell systems. *EMBO Rep* 24: e56399.
- Krshnan, L., M. L. van de Weijer and P. Carvalho, 2022 Endoplasmic Reticulum-Associated Protein Degradation. *Cold Spring Harb Perspect Biol* 14.
- Kruger, V., M. Deckers, M. Hildenbeutel, M. van der Laan, M. Hellmers *et al.*, 2012 The mitochondrial oxidase assembly protein1 (Oxa1) insertase forms a membrane pore in lipid bilayers. *J Biol Chem* 287: 33314-33326.
- Kucejova, B., L. Li, X. Wang, S. Giannattasio and X. J. Chen, 2008 Pleiotropic effects of the yeast Sall and Aac2 carriers on mitochondrial function via an activity distinct from adenine nucleotide transport. *Mol Genet Genomics* 280: 25-39.
- Kumar, M., N. Tyagi and M. Faruq, 2023 The molecular mechanisms of spinocerebellar ataxias for DNA repeat expansion in disease. *Emerg Top Life Sci* 7: 289-312.
- Kunji, E. R. S., M. S. King, J. J. Ruprecht and C. Thangaratnarajah, 2020 The SLC25 Carrier Family: Important Transport Proteins in Mitochondrial Physiology and Pathology. *Physiology (Bethesda)* 35: 302-327.
- Kunze, M., and J. Berger, 2015 The similarity between N-terminal targeting signals for protein import into different organelles and its evolutionary relevance. *Front Physiol* 6: 259.
- Labbadia, J., and R. I. Morimoto, 2015 The biology of proteostasis in aging and disease. *Annu Rev Biochem* 84: 435-464.
- Lackey, S. W., R. D. Taylor, N. E. Go, A. Wong, E. L. Sherman and F. E. Nargang, 2014 Evidence supporting the 19 beta-strand model for Tom40 from cysteine scanning and protease site accessibility studies. *J Biol Chem* 289: 21640-21650.

- Laoudj-Chenivesse, D., G. Carnac, C. Bisbal, G. Hugon, S. Bouillot *et al.*, 2005 Increased levels of adenine nucleotide translocator 1 protein and response to oxidative stress are early events in facioscapulohumeral muscular dystrophy muscle. *J Mol Med (Berl)* 83: 216-224.
- Leder, A., G. Mas, V. Szentgyorgyi, R. P. Jakob, T. Maier *et al.*, 2025 A multichaperone condensate enhances protein folding in the endoplasmic reticulum. *Nat Cell Biol* 27: 1422-1430.
- Leonhard, K., J. M. Herrmann, R. A. Stuart, G. Mannhaupt, W. Neupert and T. Langer, 1996 AAA proteases with catalytic sites on opposite membrane surfaces comprise a proteolytic system for the ATP-dependent degradation of inner membrane proteins in mitochondria. *EMBO J* 15: 4218-4229.
- Levy, E., N. El Banna, D. Baille, A. Heneman-Masurel, S. Truchet *et al.*, 2019 Causative Links between Protein Aggregation and Oxidative Stress: A Review. *Int J Mol Sci* 20.
- Li, L., M. Wang, L. Huang, X. Zheng, L. Wang and H. Miao, 2024a Ataxin-2: a powerful RNA-binding protein. *Discov Oncol* 15: 298.
- Li, S. C., and P. M. Kane, 2009 The yeast lysosome-like vacuole: endpoint and crossroads. *Biochim Biophys Acta* 1793: 650-663.
- Li, W., T. Scheel and P. S. Shen, 2025 Mechanism of nascent chain removal by the ribosome-associated quality control complex. *Nat Commun* 16: 5792.
- Li, X., J. Straub, T. C. Medeiros, C. Mehra, F. den Brave *et al.*, 2022 Mitochondria shed their outer membrane in response to infection-induced stress. *Science* 375: eabi4343.
- Li, Y., Y. Liu, X. Y. Yu, Y. Xu, X. Pan *et al.*, 2024b Membraneless organelles in health and disease: exploring the molecular basis, physiological roles and pathological implications. *Signal Transduct Target Ther* 9: 305.
- Li, Y., W. Zheng, Y. Lu, Y. Zheng, L. Pan *et al.*, 2021 BNIP3L/NIX-mediated mitophagy: molecular mechanisms and implications for human disease. *Cell Death Dis* 13: 14.
- Liao, X., and R. A. Butow, 1993 RTG1 and RTG2: two yeast genes required for a novel path of communication from mitochondria to the nucleus. *Cell* 72: 61-71.
- Liao, Y. C., M. S. Fernandopulle, G. Wang, H. Choi, L. Hao *et al.*, 2019 RNA Granules Hitchhike on Lysosomes for Long-Distance Transport, Using Annexin A11 as a Molecular Tether. *Cell* 179: 147-164 e120.
- Lim, K. R. Q., Q. Nguyen and T. Yokota, 2020 DUX4 Signalling in the Pathogenesis of Facioscapulohumeral Muscular Dystrophy. *Int J Mol Sci* 21.
- Lindstrom, M., L. Chen, S. Jiang, D. Zhang, Y. Gao *et al.*, 2022 Lsm7 phase-separated condensates trigger stress granule formation. *Nat Commun* 13: 3701.
- Liu, Y., Y. Li and P. Zhang, 2025 Stress granules and organelles: coordinating cellular responses in health and disease. *Protein Cell* 16: 418-438.
- Liu, Y., X. Wang and X. J. Chen, 2015 Misfolding of mutant adenine nucleotide translocase in yeast supports a novel mechanism of Ant1-induced muscle diseases. *Mol Biol Cell* 26: 1985-1994.
- Liu, Y., X. Wang, L. P. Coyne, Y. Yang, Y. Qi *et al.*, 2019 Mitochondrial carrier protein overloading and misfolding induce aggresomes and proteostatic adaptations in the cytosol. *Mol Biol Cell* 30: 1272-1284.
- Liu, Z., and R. A. Butow, 2006 Mitochondrial retrograde signaling. *Annu Rev Genet* 40: 159-185.
- Lu, B., S. Yadav, P. G. Shah, T. Liu, B. Tian *et al.*, 2007 Roles for the human ATP-dependent Lon protease in mitochondrial DNA maintenance. *J Biol Chem* 282: 17363-17374.
- Lu, Y., Y. Wu, C. Yang, Y. Zhou, X. Ren *et al.*, 2025 Ferredoxins: master regulators in mitochondrial redox homeostasis and programmed cell death. *Redox Biol* 88: 103930.
- Lu, Y. W., M. G. Acoba, K. Selvaraju, T. C. Huang, R. S. Nirujogi *et al.*, 2017 Human adenine nucleotide translocases physically and functionally interact with respirasomes. *Mol Biol Cell* 28: 1489-1506.
- Luo, B., Y. Ma, Y. Zhou, N. Zhang and Y. Luo, 2021 Human ClpP protease, a promising therapy target for diseases of mitochondrial dysfunction. *Drug Discov Today* 26: 968-981.
- Lutz, T., W. Neupert and J. M. Herrmann, 2003 Import of small Tim proteins into the mitochondrial intermembrane space. *EMBO J* 22: 4400-4408.

- Machyna, M., S. Kehr, K. Straube, D. Kappei, F. Buchholz *et al.*, 2014 The coilin interactome identifies hundreds of small noncoding RNAs that traffic through Cajal bodies. *Mol Cell* 56: 389-399.
- Markmiller, S., S. Soltanieh, K. L. Server, R. Mak, W. Jin *et al.*, 2018 Context-Dependent and Disease-Specific Diversity in Protein Interactions within Stress Granules. *Cell* 172: 590-604 e513.
- Martensson, C. U., C. Priesnitz, J. Song, L. Ellenrieder, K. N. Doan *et al.*, 2019 Mitochondrial protein translocation-associated degradation. *Nature* 569: 679-683.
- Martijn, J., J. Vosseberg, L. Guy, P. Offre and T. J. G. Ettema, 2018 Deep mitochondrial origin outside the sampled alphaproteobacteria. *Nature* 557: 101-105.
- Matsumoto, S., K. Nakatsukasa, C. Kakuta, Y. Tamura, M. Esaki and T. Endo, 2019 Msp1 Clears Mistargeted Proteins by Facilitating Their Transfer from Mitochondria to the ER. *Mol Cell* 76: 191-205 e110.
- Mayr, J. A., T. B. Haack, E. Graf, F. A. Zimmermann, T. Wieland *et al.*, 2012 Lack of the mitochondrial protein acylglycerol kinase causes Sengers syndrome. *Am J Hum Genet* 90: 314-320.
- Meisinger, C., M. T. Ryan, K. Hill, K. Model, J. H. Lim *et al.*, 2001 Protein import channel of the outer mitochondrial membrane: a highly stable Tom40-Tom22 core structure differentially interacts with preproteins, small tom proteins, and import receptors. *Mol Cell Biol* 21: 2337-2348.
- Mesecke, N., N. Terziyska, C. Kozany, F. Baumann, W. Neupert *et al.*, 2005 A disulfide relay system in the intermembrane space of mitochondria that mediates protein import. *Cell* 121: 1059-1069.
- Miao, B., J. E. Davis and E. A. Craig, 1997 Mge1 functions as a nucleotide release factor for Ssc1, a mitochondrial Hsp70 of *Saccharomyces cerevisiae*. *J Mol Biol* 265: 541-552.
- Middelberg, R. P., M. A. Ferreira, A. K. Henders, A. C. Heath, P. A. Madden *et al.*, 2011 Genetic variants in LPL, OASL and TOMM40/APOE-C1-C2-C4 genes are associated with multiple cardiovascular-related traits. *BMC Med Genet* 12: 123.
- Mitchell, P., 1961 Coupling of phosphorylation to electron and hydrogen transfer by a chemi-osmotic type of mechanism. *Nature* 191: 144-148.
- Mizushima, N., and M. Komatsu, 2011 Autophagy: renovation of cells and tissues. *Cell* 147: 728-741.
- Mocciaro, E., V. Runfola, P. Ghezzi, M. Pannese and D. Gabellini, 2021 DUX4 Role in Normal Physiology and in FSHD Muscular Dystrophy. *Cells* 10.
- Model, K., T. Prinz, T. Ruiz, M. Radermacher, T. Krimmer *et al.*, 2002 Protein translocase of the outer mitochondrial membrane: role of import receptors in the structural organization of the TOM complex. *J Mol Biol* 316: 657-666.
- More, N., and J. Joseph, 2025 Disruption of ER-mitochondria contact sites induces autophagy-dependent loss of P-bodies through the Ca²⁺-CaMKK2-AMPK pathway. *J Cell Sci* 138.
- Morimoto, R. I., 2011 The heat shock response: systems biology of proteotoxic stress in aging and disease. *Cold Spring Harb Symp Quant Biol* 76: 91-99.
- Muller, V., G. Basset, D. R. Nelson and M. Klingenberg, 1996 Probing the role of positive residues in the ADP/ATP carrier from yeast. The effect of six arginine mutations of oxidative phosphorylation and AAC expression. *Biochemistry* 35: 16132-16143.
- Murdock, D. G., B. E. Boone, L. A. Esposito and D. C. Wallace, 1999 Up-regulation of nuclear and mitochondrial genes in the skeletal muscle of mice lacking the heart/muscle isoform of the adenine nucleotide translocator. *J Biol Chem* 274: 14429-14433.
- Napoli, L., A. Bordoni, M. Zeviani, G. M. Hadjigeorgiou, M. Sciacco *et al.*, 2001 A novel missense adenine nucleotide translocator-1 gene mutation in a Greek adPEO family. *Neurology* 57: 2295-2298.
- Naskar, A., A. Nayak, M. R. Salaikumar, S. S. Vishal and P. P. Gopal, 2023 Phase separation and pathologic transitions of RNP condensates in neurons: implications for amyotrophic lateral sclerosis, frontotemporal dementia and other neurodegenerative disorders. *Front Mol Neurosci* 16: 1242925.
- Neupert, W., and J. M. Herrmann, 2007 Translocation of proteins into mitochondria. *Annu Rev Biochem* 76: 723-749.

- Nguyen-Dien, G. T., K. L. Kozul, Y. Cui, B. Townsend, P. G. Kulkarni *et al.*, 2023 FBXL4 suppresses mitophagy by restricting the accumulation of NIX and BNIP3 mitophagy receptors. *EMBO J* 42: e112767.
- Nikkanen, J., S. Forsstrom, L. Euro, I. Paetau, R. A. Kohnz *et al.*, 2016 Mitochondrial DNA Replication Defects Disturb Cellular dNTP Pools and Remodel One-Carbon Metabolism. *Cell Metab* 23: 635-648.
- Nilsson, R., M. Jain, N. Madhusudhan, N. G. Sheppard, L. Strittmatter *et al.*, 2014 Metabolic enzyme expression highlights a key role for MTHFD2 and the mitochondrial folate pathway in cancer. *Nat Commun* 5: 3128.
- Nimmo, G. A. M., S. Venkatesh, A. K. Pandey, C. R. Marshall, L. N. Hazrati *et al.*, 2019 Bi-allelic mutations of LONP1 encoding the mitochondrial LonP1 protease cause pyruvate dehydrogenase deficiency and profound neurodegeneration with progressive cerebellar atrophy. *Hum Mol Genet* 28: 290-306.
- Ogunbona, O. B., M. G. Baile and S. M. Claypool, 2018 Cardiomyopathy-associated mutation in the ADP/ATP carrier reveals translation-dependent regulation of cytochrome c oxidase activity. *Mol Biol Cell* 29: 1449-1464.
- Onishi, M., K. Yamano, M. Sato, N. Matsuda and K. Okamoto, 2021 Molecular mechanisms and physiological functions of mitophagy. *EMBO J* 40: e104705.
- Orrenius, S., V. Gogvadze and B. Zhivotovsky, 2015 Calcium and mitochondria in the regulation of cell death. *Biochem Biophys Res Commun* 460: 72-81.
- Ostrowski, L. A., A. C. Hall and K. Mekhail, 2017 Ataxin-2: From RNA Control to Human Health and Disease. *Genes (Basel)* 8.
- Pacheu-Grau, D., S. Callegari, S. Emperador, K. Thompson, A. Aich *et al.*, 2018 Mutations of the mitochondrial carrier translocase channel subunit TIM22 cause early-onset mitochondrial myopathy. *Hum Mol Genet* 27: 4135-4144.
- Pakos-Zebrucka, K., I. Koryga, K. Mnich, M. Lujic, A. Samali and A. M. Gorman, 2016 The integrated stress response. *EMBO Rep* 17: 1374-1395.
- Palikaras, K., E. Lionaki and N. Tavernarakis, 2018 Mechanisms of mitophagy in cellular homeostasis, physiology and pathology. *Nat Cell Biol* 20: 1013-1022.
- Palmer, C. S., A. J. Anderson and D. Stojanovski, 2021 Mitochondrial protein import dysfunction: mitochondrial disease, neurodegenerative disease and cancer. *FEBS Lett* 595: 1107-1131.
- Palmieri, F., 2004 The mitochondrial transporter family (SLC25): physiological and pathological implications. *Pflugers Arch* 447: 689-709.
- Palmieri, F., 2013 The mitochondrial transporter family SLC25: identification, properties and physiopathology. *Mol Aspects Med* 34: 465-484.
- Palmieri, F., C. Indiveri, F. Bisaccia and R. Kramer, 1993 Functional properties of purified and reconstituted mitochondrial metabolite carriers. *J Bioenerg Biomembr* 25: 525-535.
- Palmieri, L., S. Alberio, I. Pisano, T. Lodi, M. Meznaric-Petrusa *et al.*, 2005 Complete loss-of-function of the heart/muscle-specific adenine nucleotide translocator is associated with mitochondrial myopathy and cardiomyopathy. *Hum Mol Genet* 14: 3079-3088.
- Parker, R., and U. Sheth, 2007 P bodies and the control of mRNA translation and degradation. *Mol Cell* 25: 635-646.
- Patil, V. A., J. L. Fox, V. M. Gohil, D. R. Winge and M. L. Greenberg, 2013 Loss of cardiolipin leads to perturbation of mitochondrial and cellular iron homeostasis. *J Biol Chem* 288: 1696-1705.
- Petrauskas, A., D. L. Fortunati, A. R. Kandi, S. S. Pothapragada, K. Agrawal *et al.*, 2024 Structured and disordered regions of Ataxin-2 contribute differently to the specificity and efficiency of mRNP granule formation. *PLoS Genet* 20: e1011251.
- Pfanner, N., M. van der Laan, P. Amati, R. A. Capaldi, A. A. Caudy *et al.*, 2014 Uniform nomenclature for the mitochondrial contact site and cristae organizing system. *J Cell Biol* 204: 1083-1086.
- Pfanner, N., B. Warscheid and N. Wiedemann, 2019 Mitochondrial proteins: from biogenesis to functional networks. *Nat Rev Mol Cell Biol* 20: 267-284.

- Pickles, S., P. Vigie and R. J. Youle, 2018 Mitophagy and Quality Control Mechanisms in Mitochondrial Maintenance. *Curr Biol* 28: R170-R185.
- Pierson, T. M., D. Adams, F. Bonn, P. Martinelli, P. F. Cherukuri *et al.*, 2011 Whole-exome sequencing identifies homozygous AFG3L2 mutations in a spastic ataxia-neuropathy syndrome linked to mitochondrial m-AAA proteases. *PLoS Genet* 7: e1002325.
- Pitt, A. S., and S. K. Buchanan, 2021 A Biochemical and Structural Understanding of TOM Complex Interactions and Implications for Human Health and Disease. *Cells* 10.
- Popov-Celeketic, J., T. Waizenegger and D. Rapaport, 2008 Mim1 functions in an oligomeric form to facilitate the integration of Tom20 into the mitochondrial outer membrane. *J Mol Biol* 376: 671-680.
- Protter, D. S. W., and R. Parker, 2016 Principles and Properties of Stress Granules. *Trends Cell Biol* 26: 668-679.
- Pulst, S. M., A. Nechiporuk, T. Nechiporuk, S. Gispert, X. N. Chen *et al.*, 1996 Moderate expansion of a normally biallelic trinucleotide repeat in spinocerebellar ataxia type 2. *Nat Genet* 14: 269-276.
- Qi, L., Q. Wang, Z. Guan, Y. Wu, C. Shen *et al.*, 2021 Cryo-EM structure of the human mitochondrial translocase TIM22 complex. *Cell Res* 31: 369-372.
- Quiros, P. M., T. Langer and C. Lopez-Otin, 2015 New roles for mitochondrial proteases in health, ageing and disease. *Nat Rev Mol Cell Biol* 16: 345-359.
- Rainbolt, T. K., N. Atanassova, J. C. Genereux and R. L. Wiseman, 2013 Stress-regulated translational attenuation adapts mitochondrial protein import through Tim17A degradation. *Cell Metab* 18: 908-919.
- Rainbolt, T. K., J. Lebeau, C. Puchades and R. L. Wiseman, 2016 Reciprocal Degradation of YME1L and OMA1 Adapts Mitochondrial Proteolytic Activity during Stress. *Cell Rep* 14: 2041-2049.
- Rampelt, H., R. M. Zerbes, M. van der Laan and N. Pfanner, 2017 Role of the mitochondrial contact site and cristae organizing system in membrane architecture and dynamics. *Biochim Biophys Acta Mol Cell Res* 1864: 737-746.
- Rapoport, T. A., 2008 Protein transport across the endoplasmic reticulum membrane. *FEBS J* 275: 4471-4478.
- Raval, P. K., S. G. Garg and S. B. Gould, 2022 Endosymbiotic selective pressure at the origin of eukaryotic cell biology. *Elife* 11.
- Rehling, P., K. Model, K. Brandner, P. Kovermann, A. Sickmann *et al.*, 2003 Protein insertion into the mitochondrial inner membrane by a twin-pore translocase. *Science* 299: 1747-1751.
- Roger, A. J., S. A. Munoz-Gomez and R. Kamikawa, 2017 The Origin and Diversification of Mitochondria. *Curr Biol* 27: R1177-R1192.
- Sanpei, K., H. Takano, S. Igarashi, T. Sato, M. Oyake *et al.*, 1996 Identification of the spinocerebellar ataxia type 2 gene using a direct identification of repeat expansion and cloning technique, DIRECT. *Nat Genet* 14: 277-284.
- Sayyed, U. M. H., and R. Mahalakshmi, 2022 Mitochondrial protein translocation machinery: From TOM structural biogenesis to functional regulation. *J Biol Chem* 298: 101870.
- Schreiner, B., H. Westerburg, I. Forne, A. Imhof, W. Neupert and D. Mokranjac, 2012 Role of the AAA protease Yme1 in folding of proteins in the intermembrane space of mitochondria. *Mol Biol Cell* 23: 4335-4346.
- Schuler, M. H., A. M. English, T. Xiao, T. J. Campbell, J. M. Shaw and A. L. Hughes, 2021 Mitochondrial-derived compartments facilitate cellular adaptation to amino acid stress. *Mol Cell* 81: 3786-3802 e3713.
- Schulte, U., F. den Brave, A. Haupt, A. Gupta, J. Song *et al.*, 2023 Mitochondrial complexome reveals quality-control pathways of protein import. *Nature* 614: 153-159.
- Schwarz, D. S., and M. D. Blower, 2016 The endoplasmic reticulum: structure, function and response to cellular signaling. *Cell Mol Life Sci* 73: 79-94.

- Sengers, R. C., A. M. Stadhouders, E. van Lakwijk-Vondrovicova, K. Kubat and W. Ruitenbeek, 1985 Hypertrophic cardiomyopathy associated with a mitochondrial myopathy of voluntary muscles and congenital cataract. *Br Heart J* 54: 543-547.
- Sengers, R. C., J. M. Trijbels, J. L. Willems, O. Daniels and A. M. Stadhouders, 1975 Congenital cataract and mitochondrial myopathy of skeletal and heart muscle associated with lactic acidosis after exercise. *J Pediatr* 86: 873-880.
- Shenton, D., J. B. Smirnova, J. N. Selley, K. Carroll, S. J. Hubbard *et al.*, 2006 Global translational responses to oxidative stress impact upon multiple levels of protein synthesis. *J Biol Chem* 281: 29011-29021.
- Sheth, U., and R. Parker, 2003 Decapping and decay of messenger RNA occur in cytoplasmic processing bodies. *Science* 300: 805-808.
- Shiiba, I., K. Takeda, S. Nagashima and S. Yanagi, 2020 Overview of Mitochondrial E3 Ubiquitin Ligase MITOL/MARCH5 from Molecular Mechanisms to Diseases. *Int J Mol Sci* 21.
- Shpilka, T., and C. M. Haynes, 2018 The mitochondrial UPR: mechanisms, physiological functions and implications in ageing. *Nat Rev Mol Cell Biol* 19: 109-120.
- Siciliano, G., A. Tessa, S. Petrini, M. Mancuso, C. Bruno *et al.*, 2003 Autosomal dominant external ophthalmoplegia and bipolar affective disorder associated with a mutation in the ANT1 gene. *Neuromuscul Disord* 13: 162-165.
- Sies, H., and D. P. Jones, 2020 Reactive oxygen species (ROS) as pleiotropic physiological signalling agents. *Nat Rev Mol Cell Biol* 21: 363-383.
- Silva, J. M., A. Wong, V. Carelli and G. A. Cortopassi, 2009 Inhibition of mitochondrial function induces an integrated stress response in oligodendroglia. *Neurobiol Dis* 34: 357-365.
- Sim, S. I., Y. Chen, D. L. Lynch, J. C. Gumbart and E. Park, 2023 Structural basis of mitochondrial protein import by the TIM23 complex. *Nature* 621: 620-626.
- Simoncini, C., G. Siciliano, G. Tognoni and M. Mancuso, 2017 Mitochondrial ANT-1 related adPEO leading to cognitive impairment: is there a link? *Acta Myol* 36: 25-27.
- Sirrenberg, C., M. F. Bauer, B. Guiard, W. Neupert and M. Brunner, 1996 Import of carrier proteins into the mitochondrial inner membrane mediated by Tim22. *Nature* 384: 582-585.
- Soubannier, V., G. L. McLelland, R. Zunino, E. Braschi, P. Rippstein *et al.*, 2012 A vesicular transport pathway shuttles cargo from mitochondria to lysosomes. *Curr Biol* 22: 135-141.
- Spinelli, J. B., and M. C. Haigis, 2018 The multifaceted contributions of mitochondria to cellular metabolism. *Nat Cell Biol* 20: 745-754.
- Sproviero, W., A. Shatunov, D. Stahl, M. Shoai, W. van Rheenen *et al.*, 2017 ATXN2 trinucleotide repeat length correlates with risk of ALS. *Neurobiol Aging* 51: 178 e171-178 e179.
- Stehling, O., and R. Lill, 2013 The role of mitochondria in cellular iron-sulfur protein biogenesis: mechanisms, connected processes, and diseases. *Cold Spring Harb Perspect Biol* 5: a011312.
- Stephan, T., C. Bruser, M. Deckers, A. M. Steyer, F. Balzarotti *et al.*, 2020 MICOS assembly controls mitochondrial inner membrane remodeling and crista junction redistribution to mediate cristae formation. *EMBO J* 39: e104105.
- Stephen, D. W., S. L. Rivers and D. J. Jamieson, 1995 The role of the YAP1 and YAP2 genes in the regulation of the adaptive oxidative stress responses of *Saccharomyces cerevisiae*. *Mol Microbiol* 16: 415-423.
- Stepien, G., A. Torroni, A. B. Chung, J. A. Hodge and D. C. Wallace, 1992 Differential expression of adenine nucleotide translocator isoforms in mammalian tissues and during muscle cell differentiation. *J Biol Chem* 267: 14592-14597.
- Strauss, K. A., R. N. Jinks, E. G. Puffenberger, S. Venkatesh, K. Singh *et al.*, 2015 CODAS syndrome is associated with mutations of LONP1, encoding mitochondrial AAA+ Lon protease. *Am J Hum Genet* 96: 121-135.
- Sui, J., J. C. Boatz, J. Shi, Q. Hu, X. Li *et al.*, 2023 Loss of ANT1 Increases Fibrosis and Epithelial Cell Senescence in Idiopathic Pulmonary Fibrosis. *Am J Respir Cell Mol Biol* 69: 556-569.

- Sunnucks, P., H. E. Morales, A. M. Lamb, A. Pavlova and C. Greening, 2017 Integrative Approaches for Studying Mitochondrial and Nuclear Genome Co-evolution in Oxidative Phosphorylation. *Front Genet* 8: 25.
- Suzuki, K., 2013 Selective autophagy in budding yeast. *Cell Death Differ* 20: 43-48.
- Swisher, K. D., and R. Parker, 2010 Localization to, and effects of Pbp1, Pbp4, Lsm12, Dhh1, and Pab1 on stress granules in *Saccharomyces cerevisiae*. *PLoS One* 5: e10006.
- Szczepanowska, K., P. Maiti, A. Kukat, E. Hofsetz, H. Nolte *et al.*, 2016 CLPP coordinates mitoribosomal assembly through the regulation of ERAL1 levels. *EMBO J* 35: 2566-2583.
- Szczepanowska, K., and A. Trifunovic, 2022 Mitochondrial matrix proteases: quality control and beyond. *FEBS J* 289: 7128-7146.
- Tang, J., K. Zhang, J. Dong, C. Yan, C. Hu *et al.*, 2020 Sam50-Mic19-Mic60 axis determines mitochondrial cristae architecture by mediating mitochondrial outer and inner membrane contact. *Cell Death Differ* 27: 146-160.
- Taylor, E. B., and J. Rutter, 2011 Mitochondrial quality control by the ubiquitin-proteasome system. *Biochem Soc Trans* 39: 1509-1513.
- Thompson, K., H. Majd, C. Dallabona, K. Reinson, M. S. King *et al.*, 2016 Recurrent De Novo Dominant Mutations in SLC25A4 Cause Severe Early-Onset Mitochondrial Disease and Loss of Mitochondrial DNA Copy Number. *Am J Hum Genet* 99: 1405.
- Tiwari-Heckler, S., S. C. Robson and M. S. Longhi, 2022 Mitochondria Drive Immune Responses in Critical Disease. *Cells* 11.
- Torres, A. K., V. Fleischhart and N. C. Inestrosa, 2024 Mitochondrial unfolded protein response (UPR(mt)): what we know thus far. *Front Cell Dev Biol* 12: 1405393.
- Tort, F., O. Ugarteburu, L. Texido, S. Gea-Sorli, J. Garcia-Villoria *et al.*, 2019 Mutations in TIMM50 cause severe mitochondrial dysfunction by targeting key aspects of mitochondrial physiology. *Hum Mutat* 40: 1700-1712.
- Touvier, T., C. De Palma, E. Rigamonti, A. Scagliola, E. Incerti *et al.*, 2015 Muscle-specific Drp1 overexpression impairs skeletal muscle growth via translational attenuation. *Cell Death Dis* 6: e1663.
- Trivedi, P. C., J. J. Bartlett and T. Pulinilkunnil, 2020 Lysosomal Biology and Function: Modern View of Cellular Debris Bin. *Cells* 9.
- Truscott, K. N., P. Kovermann, A. Geissler, A. Merlin, M. Meijer *et al.*, 2001 A presequence- and voltage-sensitive channel of the mitochondrial preprotein translocase formed by Tim23. *Nat Struct Biol* 8: 1074-1082.
- Tucker, K., and E. Park, 2019 Cryo-EM structure of the mitochondrial protein-import channel TOM complex at near-atomic resolution. *Nat Struct Mol Biol* 26: 1158-1166.
- Tulli, S., A. Del Bondio, V. Baderna, D. Mazza, F. Codazzi *et al.*, 2019 Pathogenic variants in the AFG3L2 proteolytic domain cause SCA28 through haploinsufficiency and proteostatic stress-driven OMA1 activation. *J Med Genet* 56: 499-511.
- Uoselis, L., T. N. Nguyen and M. Lazarou, 2023 Mitochondrial degradation: Mitophagy and beyond. *Mol Cell* 83: 3404-3420.
- Valpadashi, A., S. Callegari, A. Linden, P. Neumann, R. Ficner *et al.*, 2021 Defining the architecture of the human TIM22 complex by chemical crosslinking. *FEBS Lett* 595: 157-168.
- van de Poll, F., B. M. Sutter, M. G. Acoba, D. Caballero, S. Jahangiri *et al.*, 2023 Pbp1 associates with Puf3 and promotes translation of its target mRNAs involved in mitochondrial biogenesis. *PLoS Genet* 19: e1010774.
- van der Laan, M., N. Wiedemann, D. U. Mick, B. Guiard, P. Rehling and N. Pfanner, 2006 A role for Tim21 in membrane-potential-dependent preprotein sorting in mitochondria. *Curr Biol* 16: 2271-2276.
- van Dyck, L., M. Dembowski, W. Neupert and T. Langer, 1998 Mx1p, a ClpX homologue in mitochondria of *Saccharomyces cerevisiae*. *FEBS Lett* 438: 250-254.
- van Wilpe, S., M. T. Ryan, K. Hill, A. C. Maarse, C. Meisinger *et al.*, 1999 Tom22 is a multifunctional organizer of the mitochondrial preprotein translocase. *Nature* 401: 485-489.

- Velazquez-Perez, L. C., R. Rodriguez-Labrada and J. Fernandez-Ruiz, 2017 Spinocerebellar Ataxia Type 2: Clinicogenetic Aspects, Mechanistic Insights, and Management Approaches. *Front Neurol* 8: 472.
- Vitali, D. G., M. Sinzel, E. P. Bulthuis, A. Kolb, S. Zabel *et al.*, 2018 The GET pathway can increase the risk of mitochondrial outer membrane proteins to be mistargeted to the ER. *J Cell Sci* 131.
- von Renesse, A., S. Morales-Gonzalez, E. Gill, G. S. Salomons, W. Stenzel and M. Schuelke, 2019 Muscle Weakness, Cardiomyopathy, and L-2-Hydroxyglutaric Aciduria Associated with a Novel Recessive SLC25A4 Mutation. *JIMD Rep* 43: 27-35.
- Wallace, D. C., 1999 Mitochondrial diseases in man and mouse. *Science* 283: 1482-1488.
- Walther, D. M., and D. Rapaport, 2009 Biogenesis of mitochondrial outer membrane proteins. *Biochim Biophys Acta* 1793: 42-51.
- Wang, F., A. Whynot, M. Tung and V. Denic, 2011 The mechanism of tail-anchored protein insertion into the ER membrane. *Mol Cell* 43: 738-750.
- Wang, J. Y., Y. J. Liu, X. L. Zhang, Y. H. Liu, L. L. Jiang and H. Y. Hu, 2024a PolyQ-expanded ataxin-2 aggregation impairs cellular processing-body homeostasis via sequestering the RNA helicase DDX6. *J Biol Chem* 300: 107413.
- Wang, L., M. Milton, L. G. Fearnley, O. G. Bhalala, M. Bahlo and H. Rafehi, 2025 Identification of expanded and interrupted ATXN2 repeat expansions in Parkinson's disease and Lewy Body Dementia cohorts. *NPJ Parkinsons Dis* 11: 341.
- Wang, Q., J. Zhuang, R. Huang, Z. Guan, L. Yan *et al.*, 2024b The architecture of substrate-engaged TOM-TIM23 supercomplex reveals preprotein proximity sites for mitochondrial protein translocation. *Cell Discov* 10: 19.
- Wang, W., X. Chen, L. Zhang, J. Yi, Q. Ma *et al.*, 2020 Atomic structure of human TOM core complex. *Cell Discov* 6: 67.
- Wang, X., and X. J. Chen, 2015 A cytosolic network suppressing mitochondria-mediated proteostatic stress and cell death. *Nature* 524: 481-484.
- Wang, X., F. A. Middleton, R. Tawil and X. J. Chen, 2022a Cytosolic adaptation to mitochondria-induced proteostatic stress causes progressive muscle wasting. *iScience* 25: 103715.
- Wang, X., K. Salinas, X. Zuo, B. Kucejova and X. J. Chen, 2008 Dominant membrane uncoupling by mutant adenine nucleotide translocase in mitochondrial diseases. *Hum Mol Genet* 17: 4036-4044.
- Wang, X., S. Wang, W. Liu, T. Wang, J. Wang *et al.*, 2019 Epigenetic upregulation of miR-126 induced by heat stress contributes to apoptosis of rat cardiomyocytes by promoting Tomm40 transcription. *J Mol Cell Cardiol* 129: 39-48.
- Wang, X., G. Zhang, S. Dasgupta, E. L. Niewold, C. Li *et al.*, 2022b ATF4 Protects the Heart From Failure by Antagonizing Oxidative Stress. *Circ Res* 131: 91-105.
- Weidberg, H., and A. Amon, 2018 MitoCPR-A surveillance pathway that protects mitochondria in response to protein import stress. *Science* 360.
- Weinhaupl, K., C. Lindau, A. Hessel, Y. Wang, C. Schutze *et al.*, 2018 Structural Basis of Membrane Protein Chaperoning through the Mitochondrial Intermembrane Space. *Cell* 175: 1365-1379 e1325.
- Wek, R. C., H. Y. Jiang and T. G. Anthony, 2006 Coping with stress: eIF2 kinases and translational control. *Biochem Soc Trans* 34: 7-11.
- Wheeler, J. R., T. Matheny, S. Jain, R. Abrisch and R. Parker, 2016 Distinct stages in stress granule assembly and disassembly. *Elife* 5.
- Wiedemann, N., and N. Pfanner, 2017 Mitochondrial Machineries for Protein Import and Assembly. *Annu Rev Biochem* 86: 685-714.
- Wiedemann, N., K. N. Truscott, S. Pfannschmidt, B. Guiard, C. Meisinger and N. Pfanner, 2004 Biogenesis of the protein import channel Tom40 of the mitochondrial outer membrane: intermembrane space components are involved in an early stage of the assembly pathway. *J Biol Chem* 279: 18188-18194.

- Wijegunawardana, D., A. Nayak, S. S. Vishal, N. Venkatesh and P. P. Gopal, 2025 Ataxin-2 polyglutamine expansions aberrantly sequester TDP-43 ribonucleoprotein condensates disrupting mRNA transport and local translation in neurons. *Dev Cell* 60: 253-269 e255.
- Wilson, Z. N., S. S. Balasubramaniam, S. Wong, M. H. Schuler, M. J. Wopat and A. L. Hughes, 2024 Mitochondrial-derived compartments remove surplus proteins from the outer mitochondrial membrane. *J Cell Biol* 223.
- Writzl, K., A. Maver, L. Kovacic, P. Martinez-Valero, L. Contreras *et al.*, 2017 De Novo Mutations in SLC25A24 Cause a Disorder Characterized by Early Aging, Bone Dysplasia, Characteristic Face, and Early Demise. *Am J Hum Genet* 101: 844-855.
- Wrobel, L., U. Topf, P. Bragoszewski, S. Wiese, M. E. Sztolsztener *et al.*, 2015 Mistargeted mitochondrial proteins activate a proteostatic response in the cytosol. *Nature* 524: 485-488.
- Wu, X., L. Li and H. Jiang, 2016 Doa1 targets ubiquitinated substrates for mitochondria-associated degradation. *J Cell Biol* 213: 49-63.
- Xiao, T., V. P. Shakya and A. L. Hughes, 2021 ER targeting of non-imported mitochondrial carrier proteins is dependent on the GET pathway. *Life Sci Alliance* 4.
- Xu, Y. D., X. Y. Zhou, S. D. Wei, F. T. Liu, J. Zhao *et al.*, 2024 Clinical features, disease progression, and nuclear imaging in ATXN2-related parkinsonism in a longitudinal cohort. *Neurol Sci* 45: 3191-3200.
- Xu, Z., T. Fu, Q. Guo, D. Zhou, W. Sun *et al.*, 2022 Disuse-associated loss of the protease LONP1 in muscle impairs mitochondrial function and causes reduced skeletal muscle mass and strength. *Nat Commun* 13: 894.
- Yang, Y. S., M. Kato, X. Wu, A. Litsios, B. M. Sutter *et al.*, 2019 Yeast Ataxin-2 Forms an Intracellular Condensate Required for the Inhibition of TORC1 Signaling during Respiratory Growth. *Cell* 177: 697-710 e617.
- Youle, R. J., and D. P. Narendra, 2011 Mechanisms of mitophagy. *Nat Rev Mol Cell Biol* 12: 9-14.
- Young, J. C., N. J. Hoogenraad and F. U. Hartl, 2003 Molecular chaperones Hsp90 and Hsp70 deliver preproteins to the mitochondrial import receptor Tom70. *Cell* 112: 41-50.
- Yu, Z., Y. Zhu, A. S. Chen-Plotkin, D. Clay-Falcone, L. McCluskey *et al.*, 2011 PolyQ repeat expansions in ATXN2 associated with ALS are CAA interrupted repeats. *PLoS One* 6: e17951.
- Zhang, G., X. Wang, C. Li, Q. Li, Y. A. An *et al.*, 2021a Integrated Stress Response Couples Mitochondrial Protein Translation With Oxidative Stress Control. *Circulation* 144: 1500-1515.
- Zhang, Y., X. Ou, X. Wang, D. Sun, X. Zhou *et al.*, 2021b Structure of the mitochondrial TIM22 complex from yeast. *Cell Res* 31: 366-368.
- Zhao, Q., J. Wang, I. V. Levichkin, S. Stasinopoulos, M. T. Ryan and N. J. Hoogenraad, 2002 A mitochondrial specific stress response in mammalian cells. *EMBO J* 21: 4411-4419.
- Zhu, Z., S. Mallik, T. A. Stevens, R. Huang, E. D. Levy and S. O. Shan, 2025 Principles of cotranslational mitochondrial protein import. *Cell* 188: 5605-5617 e5614.

Chapter 2. Cellular proteostasis during mitochondrial protein import clogging requires the mitochondrial F-box protein 1 and DJ-1 homolog HSP31 in

Saccharomyces cerevisiae

Gargi Mishra¹, Xiaowen Wang¹, Eamon Fitzpatrick¹, Auyon Ghosh², Xin Jie Chen^{1*}

¹Department of Biochemistry and Molecular Biology and ²Department of Medicine, Norton College of Medicine, State University of New York Upstate Medical University, Syracuse, New York 13210, USA

Running title: Mfb1 and Hsp31 protect cells against mPOS

***Corresponding Author:**

Dr. Xin Jie Chen, Department of Biochemistry and Molecular Biology, State University of New York Upstate Medical University, Syracuse, NY 13210, USA. Email: chenx@upstate.edu

Keywords: Yeast, mitochondria, protein import, clogging, mPOS, F-box protein, DJ-1, chaperone, Parkinson's disease.

Chapter 2 (Mishra et al. 2025) was published in GENETICS GSA as an *Advance Article* on December 29, 2025 and can be accessed using the following citation: Mishra G, Wang X, Fitzpatrick E, Ghosh A, Chen XJ. Cellular proteostasis during mitochondrial protein import clogging requires the mitochondrial F-box protein 1 and DJ-1 homolog HSP31 in *Saccharomyces cerevisiae*. *Genetics*. Published online December 29, 2025. doi:10.1093/genetics/iyaf279

2.1] ABSTRACT

Mitochondrial biogenesis requires the import of ~1,000-1,500 nuclear-encoded proteins across the Translocase of Outer Membrane (TOM) and the Translocase of Inner Membrane (TIM) 22 or 23 complexes. Protein import defects cannot only impair mitochondrial respiration but also cause mitochondrial Precursor Overaccumulation Stress (mPOS) in the cytosol. Recent studies have shown that specific mutations in the nuclear-encoded Adenine Nucleotide Translocase 1 (ANT1) cause musculoskeletal and neurological diseases by clogging TOM and TIM22 and inducing mPOS. Here, we found that overexpression of *MFBI*, encoding the mitochondrial F-box protein 1, suppresses cell growth defect caused by a clogger allele of *AAC2*, the yeast homolog of human *Ant1*. Disruption of *MFBI* synergizes with a clogger allele of *aac2* to inhibit cell growth. This is accompanied by increased retention of mitochondrial proteins in the cytosol, suggesting exacerbated defect in mitochondrial protein import. Proximity-dependent biotin identification (BioID) suggested that Mfb1 interacts with several mitochondrial surface proteins including Tom22, a component of the TOM complex. Loss of *MFBI* under clogging conditions activates genes encoding cytosolic chaperones including *HSP31*. Interestingly, disruption of *HSP31* creates a synthetic lethality with protein import clogging under respiring conditions. We propose that Mfb1 functions to maintain mitochondrial protein import competency under clogging conditions, whereas Hsp31 plays an important role in protecting the cytosol against mPOS. Mutations in DJ-1, the human homolog of Hsp31, and mitochondria-associated F-box proteins (eg., Fbxo7) are known to cause early-onset Parkinson's disease. Our work may help to better understand how these mutations affect cellular proteostasis and cause neurodegeneration.

2.2] INTRODUCTION

Mitochondria are essential organelles that perform a wide range of functions, including ATP production, metabolite synthesis, stress signaling, programmed cell death, and immune signaling. Mitochondria possess their own genome, called mitochondrial DNA (mtDNA). While the mitochondrial genome encodes a small number of proteins, the vast majority (approximately 1,000 to 1,500) are encoded by the nuclear genome. These proteins are translated in the cytosol and imported into mitochondria through specialized translocase complexes, with assistance from chaperones, membrane receptors, and motor proteins located on the outer and inner membranes or in the aqueous subcompartments of the mitochondrial matrix and the intermembrane space (WIEDEMANN AND PFANNER 2017). Defects in protein import adversely impact mitochondrial biogenesis and function. Additionally, when import is defective, unimported mitochondrial precursors can accumulate in the cytosol, triggering a form of proteostatic stress known as mitochondrial Precursor Overaccumulation stress (mPOS) (WANG AND CHEN 2015; COYNE AND CHEN 2019). Various forms of mitochondrial damage can indirectly affect protein import efficiency, which in turn causes mPOS and decreases cell viability. Cells respond to mPOS by activating the proteasomal machinery to contain the unimported proteins from accumulating, a mechanism termed Unfolded Protein Response activated by Mistargeting of proteins (UPRam) (WROBEL *et al.* 2015). In addition to genetic mutations that directly affect components of the core protein import machinery, recent studies have shown that mutations in mitochondrial cargo proteins, such as Adenine Nucleotide Translocase 1 (ANT1), can get the protein stuck on import channels, leading to mitochondrial dysfunction, mPOS, and cell death (COYNE *et al.* 2023b). Notably, these “clogging” alleles of *Ant1* have been implicated in human mitochondrial disorders

such as autosomal dominant Progressive External Ophthalmoplegia (adPEO) (KAUKONEN *et al.* 2000; PALMIERI *et al.* 2005).

To counteract import clogging, cells have evolved quality control mechanisms that detect and resolve stalled import events on the mitochondrial surface. These include the mitochondrial Compromised Protein import Response (mitoCPR) and the mitochondrial protein translocation-associated degradation pathway (mitoTAD) (WEIDBERG AND AMON 2018; MARTENSSON *et al.* 2019). In these anti-clogging pathways, AAA-ATPases extract clogged and ubiquitinated precursors from the outer membrane, targeting them for proteasomal degradation in the cytosol. It was previously unclear as to which E3 ligase enzymes are responsible for initially detecting stalled mitochondrial proteins to ubiquitinate them for degradation by the proteasome. A recent study suggested that Rsp5 may be one such E3 ligase since it was found to ubiquitinate mitochondrial preproteins as they were being translated and imported at the outer mitochondrial membrane (SCHULTE *et al.* 2023). However, the full compendium of proteins that maintain protein import efficiency or assist in clearing stalled precursors remains to be defined.

In this study, we identified *MFBI* as a suppressor gene of mitochondrial protein import clogging in a genetic screen in *Saccharomyces cerevisiae*. *MFBI* encodes a mitochondrial F-box protein. Mfb1 has previously been shown to localize to the mitochondrial surface and play roles in maintaining mitochondrial morphology and the yeast replicative lifespan (KONDO-OKAMOTO *et al.* 2006; PERNICE *et al.* 2016). It contains an F-box motif at its N-terminus that is believed to interact with members of a multi-subunit Skp1-Cullin-Fbox (SCF) E3 ligase complex. In a SCF complex, the F-box containing protein acts as a scaffold to which substrate proteins can bind, conferring specificity in ubiquitinating the proteins destined for degradation (NGUYEN AND BUSINO

2020). We found that Mfb1 is required for cell growth under mitochondrial protein import clogging conditions, likely via a SCF-independent mechanism. Strikingly, in the absence of Mfb1, cells activated expression of cytosolic stress-responsive genes, including the chaperone Hsp31. The Hsp31 family of proteins are homologous to human DJ-1, mutations of which are associated with juvenile Parkinsonism (HAGUE *et al.* 2003). Our data suggest that Mfb1 may maintain mitochondrial protein import competency, and that Hsp31/DJ-1 provides a downstream defense line in the cytosol against mPOS.

2.3] Materials and methods

2.3.a] Yeast strains and growth media

The genotypes and sources of yeast strains used in this study are listed in Supplemental Table 5. The *aac2^{AI28P}-mfb1Δ* interaction was studied in the BY4741/4742 strain background, whereas experiments involving the *aac2^{AI28P, AI37D}* allele were carried out in strains of W303-1B background because expression of this severe clogger allele causes cell lethality in BY4741/4742 strains. Yeast cells were cultured in either YPD (1% yeast extract, 2% peptone and 2% dextrose), YPGR (1% yeast extract, 2% peptone, 2% galactose and 2% raffinose), YPGE (1% yeast extract, 2% peptone, 2% glycerol and 2% ethanol), minimal medium (0.67% yeast nitrogenous base without amino acids, 2% dextrose, supplemented with auxotrophic requirements), minimal medium with reduced glucose (0.67% yeast nitrogenous base without amino acids, 0.5% dextrose, supplemented with auxotrophic requirements), and sporulation media (0.5% yeast extract, 1% peptone, 0.05% glucose). All reagents, unless otherwise indicated, were obtained from Sigma-Aldrich.

2.3.b] Gene disruption

The null alleles for *TOM5*, *TOM6*, *TOM7*, *UBX2*, *MFB1* and *HSP31* marked by *kan*, were transferred from strains of the yeast knockout collection into the W303-1B background by PCR amplification and one-step gene replacement by selecting for G418 resistance. For disruption of *AMK1* (or *YNL146C-A*), a *URA3* cassette was used to replace the gene coding region. Correct disruption of the genes was confirmed by PCR, using primers listed in Supplemental Table 5.

2.3.c] Mitochondrial isolation

Depending on the downstream application, mitochondria were isolated using either a glass-bead or Dounce homogenizer protocol. For mini-TurboID proximity ligation and determination of protein ubiquitination levels, 150 ml of yeast cultures were harvested at 5,000 RPM (J-10 rotor) for 10 minutes, washed once with water, and resuspended in 800 μ l of SHP buffer (0.6 M sorbitol, 20 mM HEPES-KOH, PMSF, protease inhibitors and 20 mM NEM). Glass beads (Sigma-Aldrich) were added to the samples, before being vortexed twice for 20 seconds each, and maintained on ice. Samples were spun at 800 x g for 2 minutes to remove cell debris and the glass beads. The supernatant was spun at 12,000 x g for 15 minutes. The resulting supernatant was discarded, and the pellet was resuspended in the miniTurboID lysis buffer (50 mM Tris-HCl pH7.4, 150 mM NaCl, 1 mM EGTA, 1.5 mM MgCl₂, 0.4% SDS and 1% NP-40) and stored at -80°C.

For TMT-MS, 400 ml of yeast cultures grown overnight at 25°C in YPGE were harvested at 5000 RPM (J-10 rotor) for 10 minutes and washed once with water. This was followed by washes with fresh TD buffer (100 mM Tris-SO₄, pH9.4, 10 mM DTT) and SP buffer (1.2 M sorbitol, 20 mM potassium phosphate, pH7.4) buffers. Next, the samples were incubated in 5 mg/ml zymolyase prepared in SP buffer and rotated at 25°C for 2 hours to digest the cell wall. Following this, the samples were washed again with SP buffer and then resuspended in 20 ml of SHP buffer (0.6 M sorbitol, 20 mM HEPES-KOH, pH7.4, PMSF and protease inhibitors). Samples were placed in a Dounce homogenizer one at a time and subjected to 12-14 strokes to mechanically disrupt the cell membrane. Samples were spun at 2,500 x g (J-20 rotor) for 5 minutes to collect any unbroken spheroplasts and the supernatant spun at 12,000xg for 10 minutes to pellet mitochondria. The supernatant containing “unclean” cytosol was spun again at 13,000 x g for 30

minutes to remove any membranous debris and the supernatant was designated as “clean” cytosol to be used for TMT-MS.

2.3.d] MiniTurboID and mass spectrometry

MFBI-MiniTurboID biotin ligase fusion strains: growth, harvest and affinity purification - MiniTurbo biotin ligase ORF was fused to the C-terminal end of the *MFBI* gene immediately before the stop codon in the yeast chromosome. This fusion gene was generated in the WT and *aac2*^{A128P, A137D} background strains. The resulting strains were referred to as WTmT and DMmT, respectively. These strains, as well as untagged wild type (WT) and *aac2*^{A128P, A137D} (DM), were inoculated onto minimal medium supplemented with auxotrophic amino acids and allowed to grow overnight at 30°C. The strains were then inoculated into 150 ml of a non-fermentable medium (YPGE with additional tryptophan) and allowed to grow for 12 hours. Each strain was grown in triplicates. Crude mitochondria were isolated from these strains using the glass-bead protocol described above (see ‘Mitochondrial Isolation’). Bradford assay was performed to quantify mitochondrial yield. For each strain, 600-750 µg mitochondrial lysate was used as input for incubation with 300 µl of 50% slurry of Streptactin-Sepharose beads (IBA Lifesciences). Prior to incubation, the beads were equilibrated by washing twice with lysis buffer (50 mM Tris-HCl, pH7.4, 150 mM NaCl, 1 mM EGTA, 1.5 mM MgCl₂, 0.4% SDS and 1% NP-40). The total volume of input lysate and beads in the lysis buffer was calculated such that lysate would bind the beads at a concentration between 1 – 1,25 µg/µl. Each sample was placed on a rotating drum at 4°C for 2 hours. After this, samples were spun (1000xg, 1 minute) to collect the unbound fraction. The beads were washed twice using wash buffer (1x buffer W) and the washes were kept as controls. After the wash steps, the beads were incubated with elution buffer (1x BXT), rotated using a Nutator mixer at room temperature for 10 minutes, and then spun (1000xg, 1 minute). The elution

step was repeated once more. After confirming the presence of bait protein in the eluates, the elution fractions were combined and subjected to mass spectrometry analysis to obtain label-free quantification of the eluted proteins in the samples.

Sample digestion and cleanup - Fifty μg of proteins were digested using a modification of the FASP method (WISNIEWSKI *et al.* 2009). In-solution proteins were denatured with SDS (1% final concentration), reduced and alkylated with TCEP and chloroacetamide (10 and 40 mM final concentration) at 70°C for 5 minutes. After cooling, the proteins were added to a 10 kDa MWCO membrane filter (Pall, OD010C34) with 200 μL of solution “UA”: 8 M urea with 100 mM tris pH 8.5. The filters were centrifuged at 14,000 x g until nearly dry, then rinse three times with 100 μL of UA solution and three times with 100 μL of 50 mM ammonium bicarbonate. The proteins were digested overnight at 37°C using 0.5 μg of trypsin in 75 μL of 50 mM ammonium bicarbonate. The resulting peptides were recovered from the filtrate by adding 50 μL of 1% TFA and centrifuging across the filter, followed by desalting on 2-core MCX stage tips (3M) (RAPPSILBER *et al.* 2003). The stage tips were activated with ACN followed by 3% ACN with 0.1% TFA. Next, samples were applied, followed by two washes with 3% ACN with 0.1% TFA, and one wash with 65% ACN with 0.1% TFA. Peptides were eluted with 75 μL of 65% ACN with 5% NH_4OH (Millipore, 5.33003), and dried.

LC-MS methods - Samples were dissolved to a concentration of 0.25 $\mu\text{g}/\mu\text{L}$ in water containing 2% ACN and 0.5% formic acid. Two μL were injected onto a pulled tip nano-LC column (New Objective, FS360-75-10-N) with 75 μm inner diameter packed to 25 cm with 3 μm , 120 Å, C18AQ particles (Dr. Maisch, r13.aq.0001). The column was maintained at 50°C with a column oven (Sonation GmbH, PRSO-V2). The peptides were separated using a 120-minute gradient from 3 – 28% ACN, followed by a 7 min ramp to 85% ACN and a 3 min hold at 85% ACN. The column

was connected inline with an Orbitrap Lumos (Thermo) via a nanoelectrospray source operating at 2.5 kV. The mass spectrometer was operated in data-dependent top speed mode with a cycle time of 2.5s. MS1 scans were collected at 120000 resolution with AGC target of 6.0E5 and maximum injection time of 50 ms. CID fragmentation was used followed by MS2 scans in the ion trap with AGC target 2.0E3 and 38 ms maximum injection time.

Database searching and label-free quantification - The MS data was searched using SequestHT in Proteome Discoverer (version 2.4, Thermo Scientific) against the *S. cerevisiae* proteome from Uniprot, containing 6816 sequences and a list of common laboratory contaminant proteins. Enzyme specificity was fully tryptic with up to 2 missed cleavages. Precursor and product ion mass tolerances were 10 ppm and 0.6 Da, respectively. Cysteine carbamidomethylation was set as a fixed modification. Methionine oxidation, lysine biotinylation, protein-terminal methionine loss and acetylation were set as a variable modification. The output was filtered using the Percolator algorithm with strict FDR set to 0.01. Label-free quantification was performed in Proteome Discoverer.

2.3.e] Cytosolic fraction quantitative mass spectrometry

Post-Mitochondrial Cytosolic Fraction Preparation - TMT-MS was performed on the following yeast strains: WT, *mfb1*Δ, *aac2*^{A128P, A137D} and *aac2*^{A128P, A137D} *mfb1*Δ. Each strain was represented in triplicates. Mitochondria were isolated using the ‘Dounce Homogenizer’ protocol as described above and removed from each sample using differential centrifugation to obtain the “mitochondria-free” cytosolic fraction (see above in the ‘Mitochondrial isolation’ section). The cytosolic fractions were quantified using the Bradford Assay, resuspended at a final concentration of 1μg/μL in 1xSHP Buffer (0.6M sorbitol, 20mM HEPES KOH, PMSF, and protease inhibitors) before being analyzed with TMT-MS.

Sample digestion, labeling and cleanup - Samples were prepared for multiplexed quantitative mass spectrometry. Samples were buffer exchanged on a 3 kDa molecular weight cutoff filter (Amicon 3k Ultracel) using 50 mM triethylammonium bicarbonate (Thermo). One hundred µg was taken for digestion using an EasyPep Mini MS sample prep kit (Thermo, A40006). To each buffer-exchanged sample, 65 µL of lysis buffer was added followed by 50 µL of reduction solution and 50 µL of alkylating solution. Samples were incubated at 95°C for 10 minutes, then cooled to room temperature. To each sample 4 µg of trypsin / Lys-C protease was added and the reaction was incubated at 37°C overnight. TMT reagents were reconstituted with 20 µL acetonitrile (ACN) and the contents of each label added to a digested sample. After 60 min, 50 µL of quenching solution was added, consisting of 20% formic acid and 5% hydroxylamine (v/v) in water. The labeled digests were cleaned up by a solid-phase extraction device contained in the EasyPep kit, and dried by speed-vac. The individually labeled samples were dissolved in 100 µL of 3% ACN and 0.2% trifluoroacetic acid (v/v) in water, and 15 µL of each was used to create a pooled sample consisting of 180 µg.

Fractionation - Following an LC-MS experiment to check digestion and labeling quality of the pooled samples, 100 µg of the pooled sample was fractionated using a Pierce High pH Reversed-Phase Peptide Fractionation Kit (part # 84868), per the manufacturer's instructions for TMT-labeled peptides. In brief, samples were dissolved in 300 µL of 0.1% trifluoroacetic acid in water, and applied to the conditioned resin. Samples were washed first with water and then with 300 µL of 5% ACN, 0.1% triethylamine (TEA) in water. The second wash was collected for analysis. Peptides were step eluted from the resin using 300 µL of solvent consisting of 5 to 50% ACN with 0.1% TEA in eight steps. All collected fractions were dried in a speed-vac.

LC-MS/MS - Dried fractions were reconstituted in 25 μ L of load solvent consisting of 3% ACN and 0.5% formic acid in water, and a 5 μ L aliquot was diluted with 7 μ L of the same solvent. Of these 12 μ L, 2 μ L were injected onto a pulled tip nano-LC column (New Objective, FS360-75-10-N) with 75 μ m inner diameter packed to 28 cm with 2.4 μ m, 120 Å, C18AQ particles (Dr. Maisch). The column was maintained at 50°C with a column oven (Sonation GmbH, PRSO-V2). The peptides were separated using a 135-minute gradient consisting of 3 – 12.5% ACN over 60 min, 12.5 – 28% over 60 min, 28 - 85 % ACN over 7 min, a 3 min hold, and 5 min re-equilibration at 3% ACN. The column was connected inline with an Orbitrap Lumos (Thermo) via a nanoelectrospray source operating at 2.5 kV. The mass spectrometer was operated in data-dependent top speed mode with a cycle time of 3s. MS¹ scans were collected from 375 – 1500 m/z at 120,000 resolution and a maximum injection time of 50 ms. HCD fragmentation at 40% collision energy was used followed by MS² scans in the Orbitrap at 50,000 resolution with a 125 ms maximum injection time.

2.3.f] Yeast transcriptomic analysis

Total RNA extraction - For RNA-seq analysis, three biologically independent replicates were used for each strain. Yeast strains were first grown in a minimal medium supplemented with auxotrophic amino acids at 30°C overnight (50 ml). They were then removed from the minimal medium, inoculated into YPGE (100 ml culture), and grown at 25°C until they reached an OD₆₀₀ between 1 and 2. Cells were then harvested and placed immediately on ice followed by a modified chloroform-methanol-based RNA extraction protocol (SCHMITT *et al.* 1990). In this protocol, the cells were suspended in RNA extraction buffer (0.1M NaCl, 10 mM EDTA, 5% SDS, 50 mM Tris-HCl), diluted with equal volumes of PCI (25:24:1 mixture of phenol:chloroform:isoamyl alcohol with phenol at a pH of 4.5) and allowed to sit at room temperature for 5 minutes. The samples

were then incubated with glass beads and subjected to a bead-beater apparatus twice for 30 seconds with a 30-second interval on ice. The homogenized samples were centrifuged (13,000 RPM for 10 minutes) and the aqueous phase was obtained. The aqueous phase was subjected to extraction twice again with PCI and once with 100% chloroform. The final aqueous phase was mixed with 10% volume of 3 M sodium acetate pH 5.2 and 2 volumes of 95% ethanol and the sample allowed to precipitate at -20°C for one hour. The sample mixture was spun at max speed (~16,000xg) for 15 minutes, after which the supernatant was carefully discarded, and the pellet containing precipitated RNA was retained. The pellet was washed with 70% ethanol, resuspended with DEPC-treated water, and stored at -80°C before being submitted for RNA sequencing.

cDNA Library preparation and RNA Sequencing - RNA concentration was confirmed by NanoDrop spectrophotometer, and Agilent Bioanalyzer was used for determining RNA integrity. Sequencing libraries were prepared from samples with the Illumina Stranded mRNA Library Prep kit, using one microgram of RNA as input. The standard protocol was followed and 10 cycles of PCR amplification were. Sequencing was performed on a NextSeq2000 instrument using a paired end 2x100bp read. For sequencing, a P3 sequencing kit was used which had 1.362B reads pass filter. Approximately ~28M reads per sample were obtained.

RNAseq Analysis and Data Visualization - Raw reads and counts generated were processed using the Partek software. The processed dataset containing differentially expressed gene lists was analyzed in R studio using the DESeq2 package (LOVE *et al.* 2014). For stratified analysis, the DESeq model was generated using two groups of samples at a time to allow for a one-to-one comparison. For multifactorial analysis, the DESeq model was generated using all four groups of samples to identify additive genetic interaction effects.

2.3.g] Triton insoluble fraction extraction

A previously described procedure was adapted for extracting triton-insoluble proteins (COYNE *et al.* 2023a). Briefly, cells were resuspended in Triton insoluble lysis buffer (0.5% Triton X-100, 150 mM NaCl, 50 mM HEPES-KOH pH 7.4, 1 mM EDTA with PMSF and protease inhibitors) followed by vigorous bead beating (two rounds of 20 seconds vortexing in the presence of glass beads) and placed on ice. Samples were spun at a low speed (600xg) to collect debris, unbroken cells, etc. The supernatant was placed in a fresh tube and subjected to a 20,000 x g spin for 30 minutes. After discarding the supernatant, the pellet was washed with lysis buffer and spun once more (20,000 x g for 30 minutes). The final pellet was designated as “triton-insoluble” and was resuspended using 8M urea and 5% SDS prior to western blot analysis.

2.3.h] Western blot analyses

Protein lysates were run on SDS-PAGE gels, and proteins were transferred overnight to PVDF membranes. Total protein stain (LICORBio) was performed for all membranes, prior to blocking (5% milk in 1xTBST) and downstream antibody incubation steps. For miniTurboID-MS, the PVDF membranes were probed with either anti-V5 (Cell Signaling cat#E9H80) or anti-Biotin (Milipore Sigma cat#B3640) antibody. For TMT-MS, the PVDF membranes were probed with custom-made or commercially available primary antibodies targeting Porin, Abf2, Aco1, Aac2, or Pgc1, followed by the appropriate secondary antibody (goat anti- rabbit or goat anti-mouse). For the miniTurboID-MS experiment, membranes from the biotinylated protein elution assay were probed with either anti-Biotin (Milipore Sigma cat#B3640) or anti-V5 (Cell Signaling cat#E9H80) antibodies before being probed with Donkey anti-goat secondary, or Goat anti-Mouse secondary antibody, respectively. Finally, for the global ubiquitination measurement, membranes were probed with an anti-ubiquitin (Invitrogen cat#10H4L21) primary antibody before being probed

with Goat anti-Rabbit secondary antibody. Each secondary antibody was HRP-conjugated, which allowed for chemiluminescent detection of protein bands. For complete list of reagents, see Supplemental Table 6.

2.3.i] Fluorescence Microscopy

Strains expressing Hsp31-mNG (chromosomally integrated) were grown in YPGE (1% yeast extract, 2% peptone, 2% glycerol, 2% ethanol) overnight, subcultured for 4 hours in fresh media until mid-log phase (OD_{600} between 0.5-1) and then prepared for imaging. Strains expressing Mfb1-GFP (*URA3*-based multi-copy plasmid) were grown overnight in selective media lacking uracil (YNBCasD+Adenine+Tryptophan), subcultured in YPGR until mid-log phase (OD_{600} between 0.5-1) and then prepared for imaging. Both Hsp31-GFP and Mfb1-GFP expressing cells were stained with MitoTrackerRed CMXRos Dye (final concentration 250 nM) for an hour in the dark, washed twice with sterile water, and then resuspended in fresh media prior to mounting on a glass slide. Cells were inspected and imaged using a 100 \times oil (NA 1.4) objective on a Zeiss Imager.Z1 fluorescence microscope with a Hamamatsu CCD camera. AxioVision software was used to capture and save images. The imaging filter sets included DIC, GFP, and TexasRed which were used for visualizing the general cellular morphology, GFP-fused protein, and mitochondrial profiles respectively. Scale bars were added using FIJI by utilizing the known distance-to-pixels ratio.

2.4] RESULTS

2.4.a] MFB1 overexpression promotes cell growth under conditions of mitochondrial protein import clogging and defects in the protein import process

To investigate mechanisms that counteract mitochondrial import stress, we used a yeast model in which expression of a “pathogenic” *aac2* mutant inhibits cell growth. *AAC2* encodes the major isoform of adenine nucleotide translocase in aerobically grown yeast cells. The Aac2 protein is one of the most abundant mitochondrial proteins involved in ATP/ADP exchange across the inner membrane. Recent studies have shown that the A128P mutation of *AAC2*, equivalent to the pathogenic A114P allele in human *Ant1* that causes autosomal dominant Progressive External Ophthalmoplegia (adPEO) (KAUKONEN *et al.* 2000), increases the retention of the mutant protein at the TOM protein translocase complex on the outer membrane as well as at the TIM22 complex on the inner membrane (COYNE *et al.* 2023b). This causes a partial clogging of mitochondrial protein import. The growth of yeast cells expressing the *aac2*^{A128P} allele from the *GAL10* promoter is strongly inhibited on galactose medium (Figure 2.1A). In a multicopy suppressor screen, we isolated two overlapping genomic clones that restored growth in cells expressing *GAL10-aac2*^{A128P}. Sequence analysis revealed that *MFB1* is the only open reading frame present in the overlapping region between the two suppressor clones (Figure 2.1B). Further, we confirmed that a subcloned version of full-length *MFB1* was sufficient to suppress the cell growth defect (Supplemental Figure S2.1). Multicopy expression of *MFB1* is therefore responsible for suppressing the growth defect of the cells with clogged mitochondrial protein import.

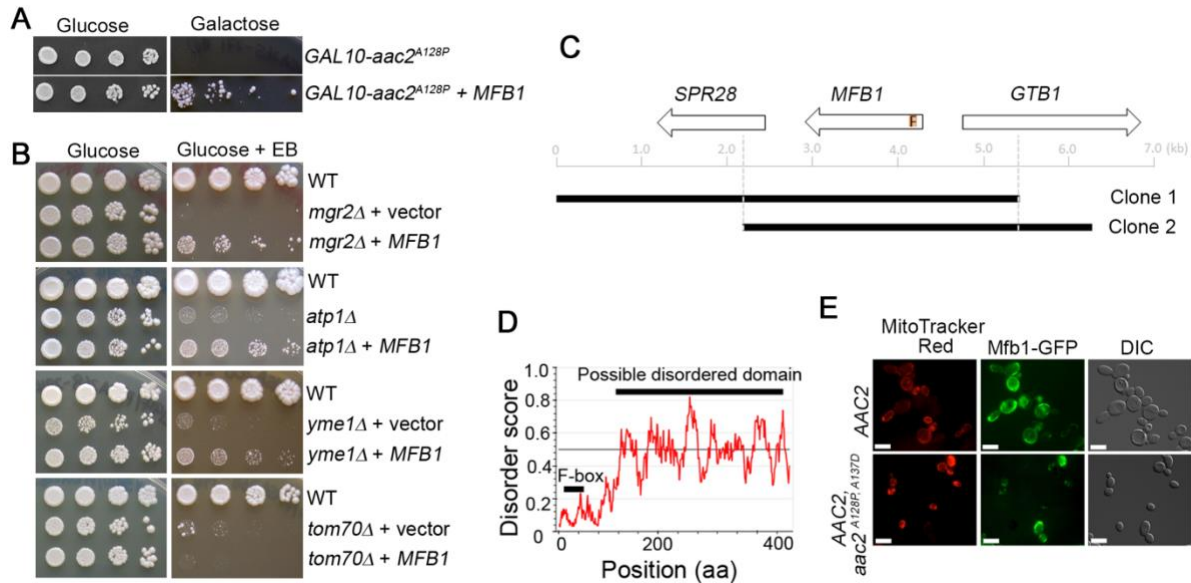


Figure 2.1. *MFB1* overexpression rescues cell growth under a variety of stress conditions with mitochondrial protein import defects. (A) *MFB1* on a multicopy plasmid rescues cell growth in *GAL10-aac2*^{A128P} expressing cells, or in ethidium bromide (EB)-treated *mgr2*Δ, *atp1*Δ, *yme1*Δ but not *tom70*Δ cells (B). These mutant cells are ρ^o-lethal due to low membrane potential and direct effect on protein import. EB eliminates mtDNA and further decreases membrane potential, leading to cell lethality. (C) Physical map of genomic clones on two multicopy plasmids having only *MFB1* as a shared gene that suppresses cell-lethality induced by *GAL10-aac2*^{A128P}. (D) *Mfb1* contains an F-box domain at the N-terminus and a disordered region at the C-terminus as predicted by IUPred2. (E) Fluorescence microscopy showing *Mfb1*-GFP localizing to mitochondria in both wild-type and the *aac2*^{A128P, A137D} clogger cells. Mitochondria were stained by MitoTracker Red dye. Scale bar, 10 μm.

We subsequently found that *MFB1* overexpression can suppress various mutations that affect mitochondrial protein import. *Mgr2* is a subunit of the TIM23 protein translocase (MATTIA *et al.* 2020) and *mgr2*Δ cells cannot tolerate the elimination of mtDNA that reduces membrane potential required for efficient protein import (DUNN *et al.* 2006), a phenotype known as ρ^o-lethality. *ATP1* encodes the α-subunit of F₁-ATPase. In addition to its role in ATP synthesis, F₁-ATPase is also required for the maintenance of mitochondrial membrane potential (and therefore protein import) in ρ^o cells (CHEN AND CLARK-WALKER 2000). As such, *atp1*Δ cells are ρ^o-lethal (CHEN AND CLARK-WALKER 1999). *Yme1* is a chaperone/protease on the mitochondrial inner membrane that is involved in protein quality control and membrane potential maintenance. Loss

of Yme1 is also ρ^0 -lethal (KOMINSKY *et al.* 2002). We found that *MFBI* overexpression from a multicopy vector was able to suppress the ρ^0 -lethal phenotype associated with *mgr2 Δ* , *atp1 Δ* , and *yme1 Δ* cells (Figure 2.1A). These findings suggest that *MFBI* may play a broader role in supporting mitochondrial protein import or in enhancing cell survival under protein import-compromised conditions. Disruption of *TOM70*, encoding a component of the TOM complex that tethers cytosolic chaperones to the outer mitochondrial membrane (BACKES *et al.* 2021), is also known to cause ρ^0 -lethality (DUNN *et al.* 2006). Notably, *MFBI* overexpression failed to suppress the ρ^0 -lethal phenotype of *tom70 Δ* cells, suggesting that Mfb1 function may depend on Tom70 or a related docking site on the mitochondrial surface.

Mfb1 is composed of 465 amino acids. It is predicted to have an F-box domain on its N-terminus, followed by a largely disordered domain on its C-terminus (Figure 2.1C). Many F-box proteins are components of the SKP1-Cullin1-F-box protein (SCF) ubiquitin ligase complex, acting as substrate-recognition subunits that target specific proteins for degradation via the ubiquitin-proteasome pathway. However, some F-box proteins, including the mitochondria-associated Fbxo7 protein in humans are also proposed to be involved in various cellular functions without being part of the SCF complex (NELSON *et al.* 2013; TEIXEIRA *et al.* 2016). Mfb1 has previously been shown to be involved in the maintenance of normal mitochondrial morphology (DURR *et al.* 2006; SCHULTE *et al.* 2023). It also plays a role in anchoring healthier-functioning mitochondria at the mother cell's distal tip throughout the cell cycle and at the bud tip prior to cytokinesis (KONDO-OKAMOTO *et al.* 2006; PERNICE *et al.* 2016). Consistent with a previous report (KONDO-OKAMOTO *et al.* 2008), Mfb1 co-localizes with mitochondria in wild-type cells. Furthermore, Mfb1's mitochondrial localization is not affected even in *aac2^{A128P, A137D}* cells that display a severe clogging of protein import (COYNE *et al.* 2023b) (Figure 2.1D).

2.4.b] Disruption of *MFBI* synergizes with mitochondrial protein import clogging to further inhibit cell growth and destabilize mtDNA

The suppression of the *aac2^{A128P}* clogging allele and *mgr2Δ* by *MFBI* overexpression strongly supports the idea that *MFBI* promotes mitochondrial protein import competency. To further test this, we examined whether loss of *MFBI* synergizes with mitochondrial protein import stress to exacerbate defects in cell growth under clogging conditions. As shown in Figure 2.2A, expression of *aac2^{A128P}* causes a dominant cold-sensitive phenotype, especially at 15°C. The *mfb1Δ* mutant also exhibited mildly reduced growth at 15°C compared to 25°C and 30°C. Importantly, the *aac2^{A128P} mfb1Δ* double mutant showed markedly impaired growth at 15°C, beyond that seen in either single mutant. When single cells were spotted on YPD medium, 48.8% of *aac2^{A128P} mfb1Δ* cells either failed to form colonies or formed microcolonies that could not continue proliferating, compared to 14.4% and 2.2% for *aac2^{A128P}* and *mfb1Δ* single mutants, respectively (Figure 2.2B and 2.2C). These data support a role for Mfb1 in promoting cell growth under conditions of mitochondrial protein import clogging. Since this growth defect was observed on glucose medium, where respiration is dispensable, the data suggest that Mfb1 maintains cell viability under import stress independent of energy metabolism. We speculate that Mfb1 contributes to the maintenance of mitochondrial protein import competency during *aac2^{A128P}*-induced clogging.

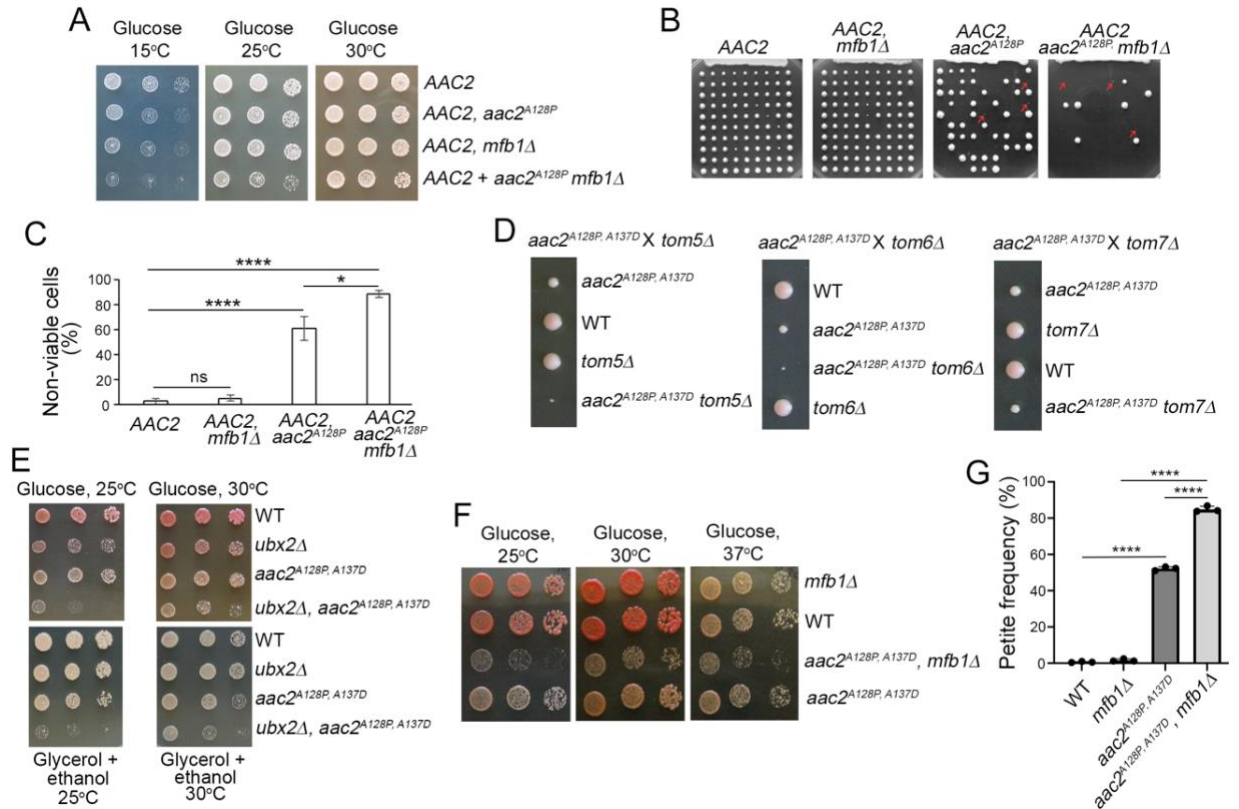


Figure 2.2. Disruption of *MFB1* under import clogging conditions worsens growth defects and decreases mtDNA stability. (A) Five-fold dilution series of yeast cells expressing the dominant single mutant *aac2*^{A128P} clogger allele with or without concurrent *MFB1* deletion on a glucose medium. Plates were incubated for two (30°C), three (25°C) and four days (15°C) before being photographed. (B) Disruption of *MFB1* leads to either complete growth inhibition or non-viable microcolonies (red arrows) in *aac2*^{A128P} background. Single cells from liquid YPD cultures at late-exponential phase (25°C) were spotted onto a YPD agar plate by a Singer dissection microscope. Plates from three biological replicates for each strain were incubated at 30°C for five days before being photographed. (C) Quantification of non-viable cells/colonies shown in (b). (D) Disruption of *TOM5*, *6* and *7* reduces the growth of clogger *aac2*^{A128P, A137D} cells. Asci formed from heterozygous diploids were dissected on synthetic complete glucose medium and a representative tetrad from each cross is shown (E) Disruption of *UBX2* reduces the growth of the clogger *aac2*^{A128P, A137D} cells on fermentable (glucose) or non-fermentable (glycerol plus ethanol) media. (F) Disruption of *MFB1* reduces the growth of the clogger *aac2*^{A128P, A137D} cells on synthetic complete glucose medium. (G) Disruption of *MFB1* increases the formation of petite colonies in the *aac2*^{A128P, A137D} cells. The strains were grown overnight in complete glycerol plus ethanol medium, before being diluted in water and plated on YPD. All the strains are isogenic and harbor the *ade2* mutation which allows the development of red pigment if cells are respiratory competent. The petites were scored based on the development of white colonies due to mutations or loss of mtDNA. Approximately 300 colonies were counted for each strain. Data are from three biological replicates and the error bars represent the standard deviation of means. *P* values were calculated using Student's *t* test. *, *p* < 0.05; ****, *p* < 0.0001.

The Aac2^{A128P} mutant protein impairs import along the protein translocation pathway, from the outer to the inner mitochondrial membrane. In contrast, the double mutant Aac2^{A128P, A137D} preferentially blocks import at the Tom40 channel on the outer membrane (COYNE *et al.* 2023b). In tetrad dissections, the *aac2*^{A128P, A137D} spores showed clearly reduced growth on glucose medium compared to wild-type cells. Supporting the outer membrane-specific import clogging model, growth of *aac2*^{A128P, A137D} cells was further impaired when non-essential components of the TOM40 complex Tom5 and Tom6, and to a lesser extent Tom7, were deleted (Figure 2.2D). Additionally, loss of *UBX2*, which helps cells tolerate outer membrane import clogging (MARTENSSON *et al.* 2019), was synthetically lethal with *aac2*^{A128P, A137D} at 25°C on both fermentable and non-fermentable carbon sources (Figure 2.2E).

Most notably, *MFBI* deletion also severely impaired the growth of *aac2*^{A128P, A137D} cells on glucose medium, especially at 25°C (Figure 2.2F), reinforcing a role for Mfb1 in mitigating import clogging. Furthermore, *aac2*^{A128P, A137D} cells formed petite colonies at high frequency, a hallmark of mtDNA instability. This petite frequency increased even further in *aac2*^{A128P, A137D} *mfb1Δ* cells (Figure 2.2G). These findings suggest that clogging caused by Aac2^{A128P, A137D} disrupts pathways required for mtDNA maintenance, either inside or outside the mitochondria. The additional loss of Mfb1 may intensify import stress, further destabilizing mtDNA and increasing petite formation. Altogether, our genetic data support a role for Mfb1 in preserving mitochondrial protein import and mtDNA stability under stress conditions.

2.4.c] MiniTurboID analysis revealed Mfb1's proximity to the TOM complex and enrichment near inter-organelle contact sites

To better understand the functional relevance of Mfb1 at the mitochondrial surface, we used a proximity labeling approach to identify proteins in its immediate vicinity. We fused a miniTurbo biotin ligase (BRANON *et al.* 2018) to the C-terminus of Mfb1 at the chromosomal locus in both *AAC2* wild-type and *aac2^{A128P, A137D}* (“clogger”) strains. The Mfb1-miniTurbo fusion retained its normal mitochondrial localization (Supplemental Figure S2.2). Given the high-sensitivity nature of the assay, we performed three independent replicates in the wild-type and clogger (*aac2^{A128P, A137D}*) cells expressing Mfb1-miniTurbo (WTmT and DMmT respectively). Consistent with its proximity to mitochondria, the assay revealed numerous mitochondrial proteins that may be proximal to Mfb1 (Figure 2.3A and 2.3B). The total number of Mfb1's potential interactors appeared to be similar between the wild-type and *aac2^{A128P, A137D}* cells. We found 15 and 14 potential interactors that appeared in all the three replicates of WTmT and DMmT cells (Supplemental Figure S2.3). Only four proteins, namely Tom22, Pet10, Ycp4, and Yet3, were consistently identified in all six replicate experiments (three WTmT and three DMmT), strongly suggesting that they reside in stable proximity to Mfb1 (Figure 2.3C).

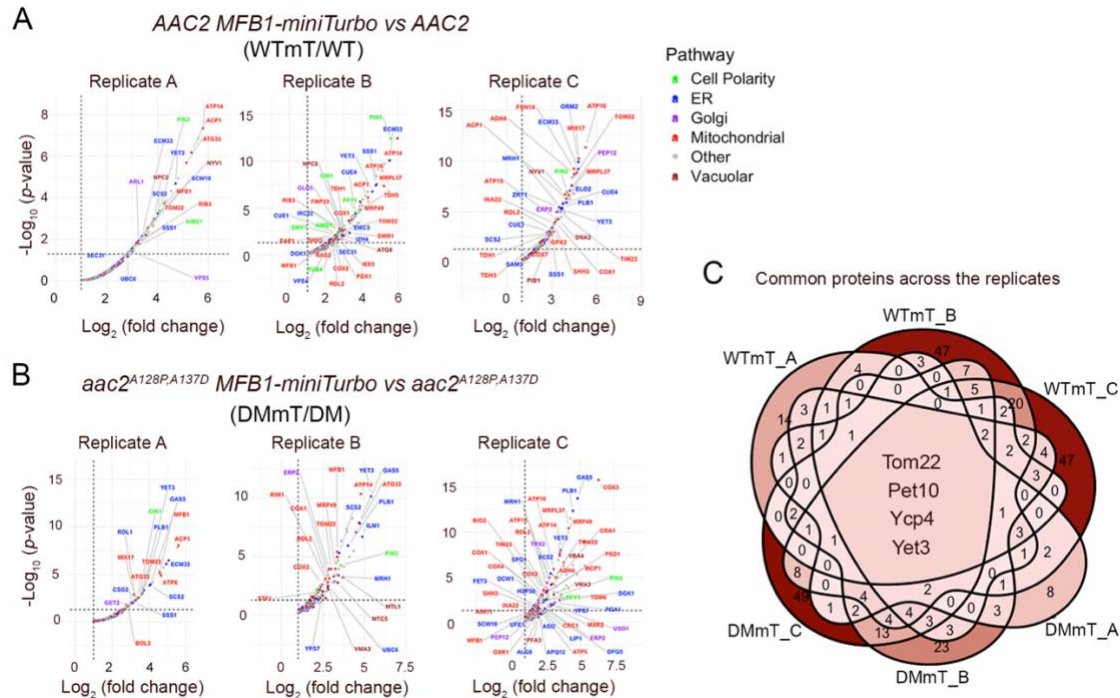


Figure 2.3. Mfb1 interactome analysis reveals its presence on the mitochondrial outer membrane in the proximity of the TOM complex and interorganellar contact sites. (A) Enrichment of biotinylated proteins in the Mfb1-miniTurboID tagged cells in the background of wild type *AAC2*, normalized to untagged wild type. (B) Enrichment of biotinylated proteins in the Mfb1-miniTurboID tagged strains in the clogger cells (*aac2^{A128P, A137D}*), normalized to untagged clogger. (C) Biotinylated proteins common to all replicates (wild type and clogger replicates combined).

Tom22 is a component of the TOM complex on the outer mitochondrial membrane, not only acting as a receptor for precursor proteins that have N-terminal mitochondrial targeting signals but also playing a crucial function in maintaining the integrity of the entire TOM complex (DEKKER *et al.* 1998). Pet10 (or PLN1) is a lipid droplet protein mediating interaction with mitochondria through interactions with outer mitochondrial proteins including Tom22 (PU *et al.* 2011; GAO *et al.* 2017). Yet3 is orthologous to the mammalian endoplasmic reticulum (ER) membrane protein BAP31 involved in ER-mitochondria interaction via Tom40 (NAMBA 2019). Ycp4 is a flavoprotein-like protein associated with mitochondria, but its physiological function is undefined (REINDERS *et al.* 2006). Together with a previous study showing that Mfb1 co-immunoprecipitates with Tom71 (KONDO-OKAMOTO *et al.* 2008), our data further support the idea

that Mfb1 may be peripherally associated with the outer mitochondrial membrane in close proximity to the TOM complex. In support of this, Tom6, which is another TOM subunit, was also identified as a potential interactor in the *aac2^{A128P, A137D}* background (Figure 2.3B). Mitochondrial matrix proteins were also detected, likely because they transiently pass near Mfb1 and the TOM complex during translocation across the outer membrane.

In addition to mitochondrial proteins, the proximity assay also identified numerous candidates from other organelles, including the ER (Cue1, Sec31 and Ubc6), Golgi (Erp2, Trx2 and Glo3), vacuole (Npc2, Nyv1 and Vma3), and cytoskeleton (Pin3, Tub4 and Smy1) (Figure 2.3, Supplemental Figure S2.3). Mfb1's proximity to ER and Golgi proteins is again consistent with its presence on the outer mitochondrial surface and suggests that it may be enriched at inter-organelle contact sites. Finally, Mfb1's proximity to cytoskeletal proteins supports its known role in mitochondrial anchorage during budding, a process important for maintaining the yeast replicative lifespan (PERNICE *et al.* 2016).

2.4.d] Mfb1 loss under clogging conditions leads to increased accumulation of mitochondrial proteins in the cytosol

Given Mfb1's ability to suppress mPOS-mediated growth defects and its proximity to the import machinery, we hypothesized that Mfb1 promotes mitochondrial protein import competency. To test this, we cultured wild-type and *aac2^{A128P, A137D}* (clogger) cells with or without *MFBI* in non-fermentable medium, where the demand for mitochondrial biogenesis is high. We then isolated post-mitochondrial cytosolic fractions and analyzed them using tandem mass-tagged (TMT) mass spectrometry to assess the accumulation of unimported mitochondrial proteins in the cytosol.

In *aac2^{A128P, A137D}* cells, most mitochondrial proteins were reduced in the cytosol, with only a few showing increased levels (Figure 2.4A). This could indicate that the cytosolic proteostatic network can manage mPOS under respiratory conditions. Alternatively, reduced import efficiency and mtDNA instability may activate retrograde signaling pathways that repress mitochondrial biogenesis, thereby decreasing precursor protein synthesis. In contrast, the absence of Mfb1 in *aac2^{A128P, A137D}* cells led to increased accumulation of many mitochondrial proteins in the cytosol (Figure 2.4B, 2.4C), consistent with the exacerbation of mPOS in the cytosol. Notably, Tom20, which is a core component of the import machinery, was among the enriched proteins. This may reflect impaired mitochondrial targeting of Tom20 itself, or a destabilization of the TOM complex upon loss of Mfb1 under clogging conditions. These findings support a model in which Mfb1 safeguards mitochondrial protein import by limiting precursor accumulation in the cytosol and/or maintaining TOM complex integrity.

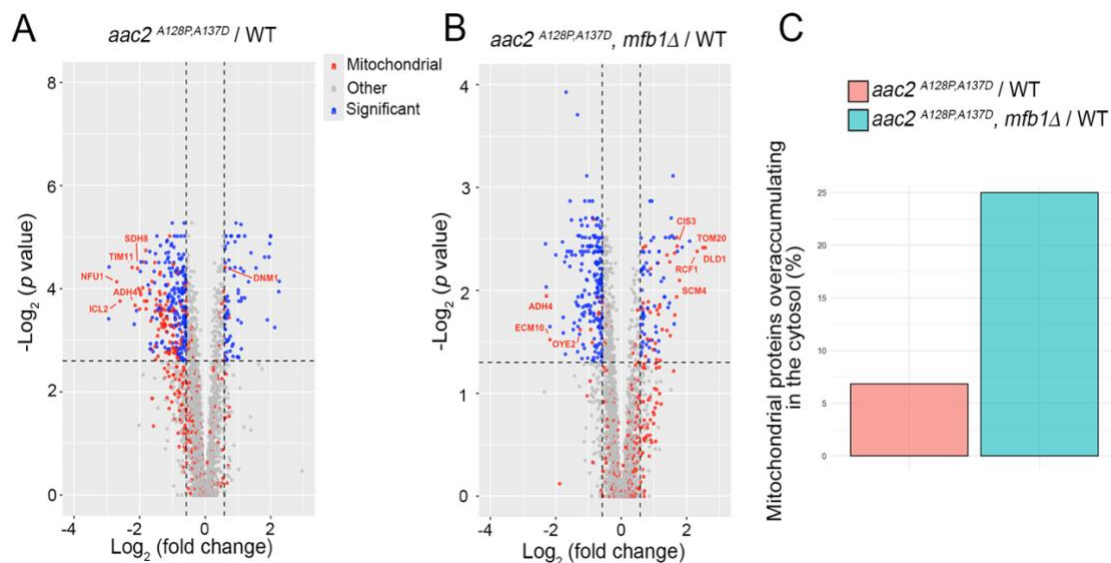


Figure 2.4. Disruption of *MFB1* increases the cytosolic retention of mitochondrial proteins under protein import clogging conditions as revealed by TMT-mass spectrometry analysis of cytosolic fractions. (A) Mitochondrial proteins enriched or depleted in clogger cells (*aac2^{A128P, A137D}*) relative to wild type when grown under non-fermentable conditions. (B) Mitochondrial proteins enriched or depleted in clogger cells lacking *MFB1* (*aac2^{A128P, A137D} mfb1Δ*) relative to wild type. (C) Percentage of mitochondrial proteins enriched relative to all significantly enriched proteins in *aac2^{A128P, A137D}* (pink) or *aac2^{A128P, A137D} mfb1Δ* (blue) cells.

2.4.e] Disruption of *MFBI* activates proteostatic stress responses under mitochondrial protein import clogging conditions

To examine whether Mfb1 influences transcriptional adaptation in the setting of mitochondrial protein import clogging, we performed RNA-seq on wild-type, *mfb1Δ*, *aac2^{A128P, A137D}* (DM), and *aac2^{A128, A137D} mfb1Δ* (DM *mfb1Δ*) strains grown under respiratory conditions. Pairwise comparisons revealed that the clogger (DM) allele by itself strongly induced iron homeostasis genes (e.g., *FET3*, *FRE1*, *FRE6* and *FIT3*) (Figure 2.5A, Supplemental Table 2.1), which is a hallmark of mutants with severe mitochondrial damage (VEATCH *et al.* 2009). Mitochondrial protein import clogging broadly repressed genes encoding ribosomal (e.g., *RPL34A*, *RPL18A*, *RPS16B*, *RPS13*) components, suggesting reduction of protein synthesis as an adaptation to heightened proteostatic stress in the cytosol (Supplemental Figure S2.4A). Several proteasomal components (*PRE6-9*) were also repressed, suggesting remodeling of proteasomal function. Loss of Mfb1 further amplified this transcriptional remodeling. For example, in the DM *mfb1Δ* relative to *mfb1Δ* comparison, stress response programs were expanded to include known mitochondrial quality control factors (*YME1*, *YTA12*, *MSP1* and *RSP5*), autophagic and mitophagic factors (*ATG5*, *ATG11* and *ATG32*) (Figure 2.5B), while genes involved in protein synthesis were repressed (Supplemental Figure S2.4B).

MFBI deletion alone was sufficient to upregulate small heat shock protein genes (*HSP12*, *HSP26* as well as *HSP32* and *HSP33*), redox regulators (*PRX1*, *SOD1*, *SOD2*), and those encoding components of the oxidative phosphorylation pathway (e.g., *COX5A*, *COX8* and *COX13*) (Figure 2.5C), while repressing members of the telomere maintenance gene family *YRF1* (Supplemental Figure S2.4C), indicating a basal role for Mfb1 in maintaining cellular homeostasis. When

clogging was introduced into this background allowing us to compare the DM *mfblΔ* versus DM conditions, we observed a further increase in compensatory proteostatic pathways (Figure 2.5D, Supplemental Table 2.2) including the *HSP70* family members (*SSE2*, *SSA3* and *SSA4*), cytosolic protein deagggregase (*HSP104*), as well as the upregulation of the multifaceted chaperone-coding gene *HSP31* which had not been upregulated in the *mfblΔ* versus WT comparison. *HSP31* belongs to the same family as *HSP32* and *HSP33* (MILLER-FLEMING et al. 2014). However, it appears to have non-redundant roles compared to *HSP32* and *HSP33* (BANKAPALLI et al. 2015). Importantly, *HSP31* is the yeast ortholog for human DJ-1, mutations in which are linked to early-onset autosomal recessive forms of Parkinson's disease (ABOU-SLEIMAN et al. 2003; BONIFATI et al. 2003; HAGUE et al. 2003). While Hsp31 has been shown to act as a responder to oxidative stress and for its glyoxylase activity to reduce mitochondrial damage (BANKAPALLI et al. 2015; ALSHAMMARI 2025), its physiological role as a molecular chaperone is still poorly defined.

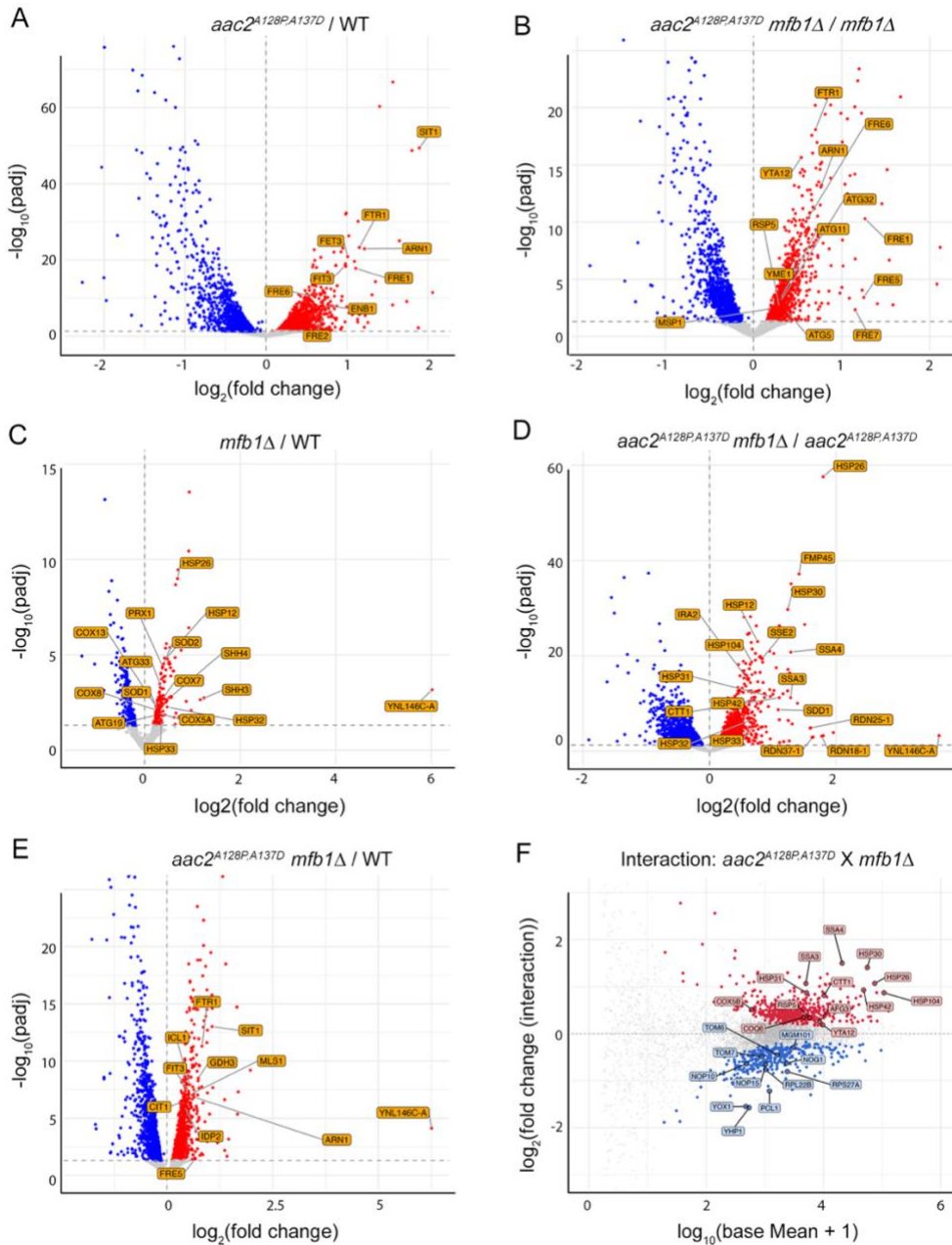


Figure 2.5. Transcriptomic analysis reveals the activation of unique cellular pathways under conditions of protein import clogging and *MFB1* loss. The following four strains in the W303-1B background were included in the bulk RNA-sequencing analysis: wild type, *mfb1Δ*, *aac2^{A128P, A137D}*, and *aac2^{A128P, A137D} mfb1Δ*. Each of these strains was grown as three biologically independent replicates on a nonfermentable carbon source containing glycerol and ethanol (YPGE) at 25°C to an optical density (OD₆₀₀) between 1.1 and 1.6. Total RNA was extracted from these cells and processed for RNA-seq analysis. (A) Volcano plot labeling a subset of genes involved in iron homeostasis that are activated under clogging (*aac2^{A128P, A137D}*) conditions relative to wild type when *MFB1* is present. (B) In addition to iron homeostasis, a subset of mitochondrial quality control genes become activated under clogging conditions relative to wild type when *MFB1* is absent. (C) *MFB1* disruption relative to wild type leads to upregulation of small chaperone

proteins in the cytosol. (D) *MFBI* disruption relative to wild type leads to a drastic upregulation of different chaperone protein families under protein import clogging conditions. (E) Clogging with concurrent *MFBI* disruption compared to wild type reveals the upregulation of genes involved in TCA and glyoxylate cycles, both of which are hallmarks of an activated mitochondrial retrograde signaling response. (F) An MA (Minus Average)-plot showing the genes with the strongest interaction across genotypes in the multifactorial analysis. The y-axis shows the difference, i.e. log normalized fold change resulting from the interaction between *mfbl* Δ and *aac2*^{A128P, A137D}. The x-axis indicates the log-normalized average expression level across all samples for every given gene. Genes labeled in red are more upregulated when comparing in *mfbl* Δ vs *MFBI* wild type under import clogging conditions relative to wild type. Similarly, genes labeled in blue are more downregulated when comparing *mfbl* Δ vs *MFBI* wild type under import clogging conditions relative to wild type.

Next, when comparing the most growth-defective *aac2*^{A128P, A137D} *mfbl* Δ to WT, we noticed an additive effect (Figure 2.5E, Supplemental Table 2.3). In addition to seeing the upregulation of the iron homeostasis genes that we had seen in clogging alone (Figure 2.5A), we also observed the upregulation of genes belonging to various metabolic pathways such as the citric acid cycle, glyoxylate cycle and the glutamate synthesis (eg., *CIT1*, *CIT2*, *CIT3*, *ICL1*, *IDP2* *MLS*, *GDH3*, *PUT1* and *IDP2*). Genes involved in glucose transporters (eg., *HXT1*, *HXT5*, *HXT16* and *HXT2*) are also activated. Activation of the glyoxylate cycle in the peroxisome promotes anaplerotic reactions to supply acetyl-CoA and citrate to mitochondria (KUNZE *et al.* 2006). Increased glutamate biosynthesis provides the nitrogen source used in various biosynthetic reactions (WALKER AND VAN DER DONK 2016). Both these pathways are direct targets of a mitochondria-to-nucleus retrograde signaling response which is activated under ρ^0 conditions (LIU AND BUTOW 2006). Thus, loss of *MFBI* under clogging conditions further heightens cellular stress, which reconfigures anaplerotic reactions and increases carbohydrate scavenging.

Notably, when we compared *mfbl* Δ to wild type *MFBI* with or without the presence of clogging, we consistently observed the upregulation of an uncharacterized open reading frame *YNL146C-A* (Figure 2.5C, 2.5D, and 2.5E). We designated this gene as *AMK1* (Activated by *MFBI*

Knockout). Although *AMK1* deletion did not impair growth or genetically interact with *mfbl1Δ*, *amk1Δ* cells modestly increased petite frequency in the clogger (DM) background (Supplemental Figure S2.5).

Finally, to further validate the genetic interactions, we applied a multifactorial model contrasting the effect of *MFBI* loss in WT versus in the clogger (DM) background. This identified ~825 genes with significant interaction effects, many involved in stress response, protein quality control, and metabolic adaptation (Figure 2.5F, Supplemental Table 2.4). Together, these results indicate that the clogger mutant triggers an iron starvation response, while concomitant loss of *Mfb1* markedly exacerbates cytosolic proteostatic stress and reconfigures cellular transcriptional programs to favor stress tolerance at the expense of growth.

2.4.f] Disruption of *HSP31* is synthetically lethal with *aac2^{A128P, A137D}* under respiring conditions

RNA-sequencing revealed that several cytosolic chaperones were upregulated in *mfbl1Δ* cells under clogging conditions. We speculated that that some of these chaperones may pplay a specific role in maintaining cell viability during severe mitochondrial protein import stress. We focused on Hsp31, the yeast homolog of human DJ-1 due to its direct clinical relevance in contributing to Parkinson's disease (ABOU-SLEIMAN *et al.* 2003; HAGUE *et al.* 2003; ALSHAMMARI 2025). We found that *hsp31Δ*, like *mfbl1Δ*, exacerbated the growth defect of *aac2^{A128P, A137D}* cells at 25°C or 37°C on non-fermentable carbon sources (Figure 2.6A). This effect was not observed on glucose medium that suppresses mitochondrial respiration. The *mfbl1Δ hsp31Δ aac2^{A128P, A137D}* triple mutant cells failed to grow at 37°C. This supports the idea that *HSP31* upregulation in *mfbl1Δ aac2^{A128P, A137D}* cells (Figure 2.5D) is a specific protective response under severe clogging

stress. Although *hsp31Δ* alone does not significantly increase mtDNA instability in the *aac2^{A128P}*, *A137D* background, it markedly enhances petite colony formation when combined with *mfb1Δ* (Figure 2.6B).

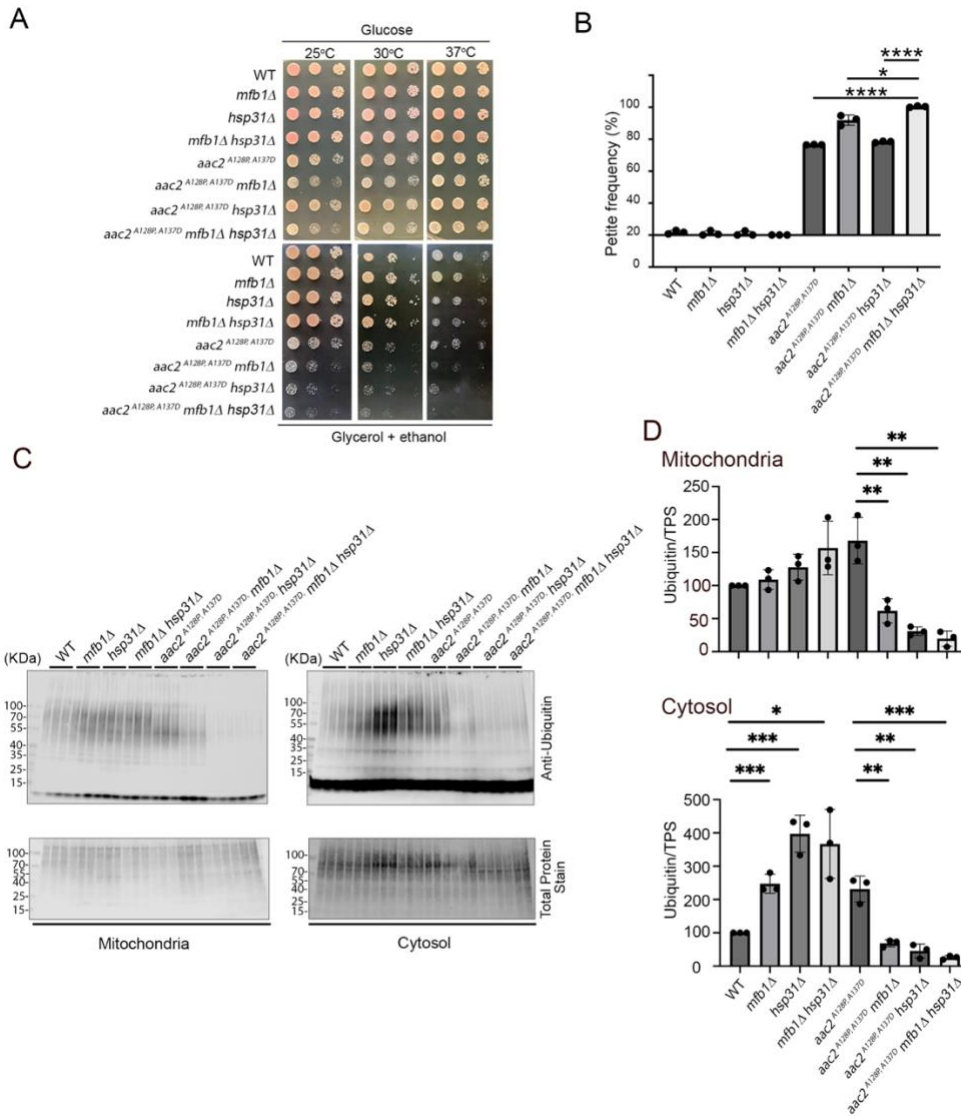


Figure 2.6. Disruption of *HSP31* creates a synthetic growth defect with *aac2^{A128P}*, *A137D* and *aac2^{A128P}*, *A137D* *mfb1Δ* and increases the levels of ubiquitinated proteins in the cytosol under respiring conditions. (A) Five-fold dilution series for cells grown on fermentable YPD (glucose) after two days; or non-fermentable YPGE (glycerol and ethanol) medium after three days (25°C), or two days (30° and 37°C). (B) Petite frequency of yeast strains shown in (A). (C) SDS-PAGE showing protein ubiquitination detected in the mitochondrial and cytosolic fractions from strains as indicated. (D) Quantification of western blots shown in (C). Error bars represent the standard deviation of means with three independent biological replicates. *P* values were calculated using Student's *t* test. *, *p* < 0.05; **, *p* < 0.01; ***, *p* < 0.001; ****, *p* < 0.0001.

Consistent with mitochondrial protein import clogging and the resulting mPOS in the cytosol, western blot analysis showed that both *hsp31Δ* and *mfb1Δ* increased protein ubiquitination in cytosolic but not mitochondrial fractions when compared with wild-type cells (Figure 2.6C and 2.6D). In contrast, cytosolic ubiquitination was reduced in *aac2^{A128P}*, *A137D* mutants lacking *MFBI*, *HSP31*, or both, suggesting that the ubiquitination machinery may be impaired in these cells with severe proteostatic challenges. Importantly, protein ubiquitination was elevated in the Triton X-insoluble fraction of *aac2^{A128P}*, *A137D* and *hsp31Δ* cells (Supplemental Figure S2.6), consistent with increased formation of insoluble protein aggregates. Under the various protein import stress conditions, Hsp31 remained diffusely localized throughout the cytosol (Supplemental Figure S2.7). Together, these findings support an intrinsic role for Hsp31 in maintaining cytosolic proteostasis during mitochondrial import stress, likely by stabilizing or facilitating degradation of unimported mitochondrial preproteins.

2.5] DISCUSSION

In response to oxygen availability, cells upregulate mitochondrial biogenesis and increase the rate of mitochondrial protein import. Defective protein import can be detrimental. In addition to the potential impact on oxidative metabolism, it can also lead to the toxic accumulation of unimported mitochondrial proteins in the cytosol (COYNE AND CHEN 2018). Human adenine nucleotide translocase isoform 1 (ANT1) is primarily involved in ADP/ATP exchange across the inner mitochondrial membrane. It belongs to the mitochondrial carrier protein family (KUNJI *et al.* 2020), expressed mainly in the highly oxidative tissues including the heart, skeletal muscle and brain. Missense mutations in *ANT1* cause dominant pathologies (KAUKONEN *et al.* 1999; KAUKONEN *et al.* 2000; NAPOLI *et al.* 2001; KOMAKI *et al.* 2002; SICILIANO *et al.* 2003; DESCHAUER *et al.* 2005; WANG *et al.* 2008; LIU AND CHEN 2013; THOMPSON *et al.* 2016; SIMONCINI *et al.* 2017). *ANT1* is well conserved across many species, including in yeast where its ortholog is called the ADP/ATP carrier protein 2 or *AAC2*. Genetic manipulation of the yeast *AAC2* has allowed for a meticulous dissection of the mechanisms that underlie human ANT1 pathologies (MISHRA *et al.* 2023). Mutations in *AAC2* that are equivalent to the pathological alleles of *ANT1* not only affect nucleotide transport kinetics (FONTANESI *et al.* 2004), but also cause severe clogging of the mitochondrial protein import pathway, likely through aberrant interactions of the mutant protein with the protein import machinery (COYNE *et al.* 2023b). Import clogging subsequently leads to proteostatic stress in the cytosol (mPOS) that eventually overwhelms the cell's capacity to maintain homeostasis (WANG AND CHEN 2015). In the current study, we used a yeast model to identify cellular pathways that promote cell survival under import clogging conditions. We found that the mitochondrial F-box protein Mfb1 and the cytosolic heat shock

protein Hsp31 play an important role in the survival of respiring cells expressing clinically relevant alleles of *aac2* that clog mitochondrial protein import.

We identified *MFBI* from a genetic screen as a suppressor of *aac2*^{A128P}, equivalent to the pathogenic *ant1*^{A114P} allele in humans. Most of the genetic suppressors identified in this screen were involved in maintaining cytosolic proteostasis (WANG AND CHEN 2015). *MFBI*, however, was unique in that it localizes to the mitochondrial surface, suggesting a more focused role on mitochondria that supports the growth of cells clogged for mitochondrial protein import. Previously, Mfb1 has been characterized for its role in mitochondrial dynamics and the inheritance of mitochondria during cell division. For instance, disruption of *MFBI* has been shown to affect mitochondrial organization and connectivity (KONDO-OKAMOTO *et al.* 2006), the asymmetric inheritance of mitochondria in dividing cells (DURR *et al.* 2006; PERNICE *et al.* 2016), and the replicative lifespan of yeast cells (YANG *et al.* 2022). Our findings add another pertinent layer to Mfb1's function by showing that it also contributes to the maintenance of mitochondrial protein import competency. Specifically, we show that *MFBI* overexpression rescues cell growth under various mPOS-inducing conditions, while its deletion exacerbates precursor accumulation, impairs growth, and contributes to mtDNA instability. Since *MFBI* overexpression suppresses not only *aac2*-induced protein import clogging but also other types of stressors that affect protein import (e.g., *mgr2Δ*, and the ρ^o-lethality phenotype of *atp1Δ* and *yme1Δ* cells), it is likely that Mfb1 plays a more general role in maintaining mitochondrial protein import competency. Since prior studies have established that Mfb1 tethers mitochondria at the mother cell tip throughout the cell cycle and at the bud tip of daughter cells during budding (PERNICE *et al.* 2016; YANG *et al.* 2022), it is thus possible that Mfb1 tethers import-competent mitochondria to cytoskeletal structures, facilitating the transmission of healthy organelles to the daughter cells during aging. We propose

that Mfb1 plays a role in the maintenance of mitochondrial protein import competency, which could have downstream effects on cellular processes such as mitochondrial dynamics. This is reminiscent of a recent study showing that loss of the mitochondrial morphodynamic protein Mitofusin-2 affects the integrity of the mitochondrial protein import machinery (JOAQUIM *et al.* 2025).

So how does Mfb1 contribute to the maintenance of mitochondrial protein import efficiency? Mfb1 is an F-box protein (DURR *et al.* 2006; KONDO-OKAMOTO *et al.* 2006). Classically, F-box proteins act as part of a modular E3 ligase complex called Skp1-Cullin-F box (SCF) complex. However, F-box proteins can have non-SCF functions as well (NELSON *et al.* 2013). Mfb1 seems to interact with Skp1, but not Cdc53, the yeast homolog for Cullin (KONDO-OKAMOTO *et al.* 2006). Skp1 is supposed to interact with F-box proteins through the F-box motif. Interestingly, the F-box motif of Mfb1 has been shown to be dispensable for the maintenance of mitochondrial morphology (KONDO-OKAMOTO *et al.* 2006). This implies that the mitochondrial morphodynamic function of Mfb1 may be independent of SCF complex interaction and protein ubiquitination. This is consistent with our finding that proximity-based biotin ligation followed by mass spectrometry analysis of isolated mitochondria failed to identify Skp1 and Cdc53 as Mfb1's interactors. Notably, the Mfb1-Skp1 interaction was previously observed in a study where authors used whole cell lysates for immunoprecipitation (KONDO-OKAMOTO *et al.* 2006). It therefore remains possible that a smaller cytosolic fraction of Mfb1 may interact with Skp1, while the Mfb1 located on the mitochondrial surface does not.

Mfb1 has been shown to localize to the mitochondrial surface in a Tom70-dependent manner (KONDO-OKAMOTO *et al.* 2008). This suggests that Mfb1 is recruited to mitochondria either via direct interaction with Tom70, or via interaction with another TOM component or

accessory protein with which the interaction is disrupted in the absence of Tom70. Consistent with this, we show that *MFBI* overexpression does not improve the growth of ρ^0 cells in the absence of Tom70, possibly due to a failure to localize to the mitochondrial surface.

Interestingly, our miniTurboID-MS experiment does not suggest a strong interaction between Mfb1 and Tom70. Instead, we identify several other mitochondrial outer membrane proteins in the vicinity of Mfb1. Among these proteins is Tom22, a precursor receptor on the TOM complex. These data provide further support for the idea that Mfb1 is localized in the vicinity of the TOM complex. Mfb1 may directly stabilize the TOM complex under clogging conditions, help unclog the protein translocation channel, and/or improve the microenvironment on the mitochondrial surface to facilitate preprotein targeting. Based on our TMT-MS study, the increased cytosolic accumulation of Tom20 in *aac2^{A128P, A137D} mfb1 Δ* cells supports the idea that Mfb1 may help maintain TOM complex integrity during import stress. Altogether, these functions may help the maintenance of mitochondrial protein import efficiency and cell viability.

It is noteworthy that, in addition to Tom22, Pet10 and Yet3 were also identified as potential interactors of Mfb1. Pet10 is a lipid droplet protein mediating interaction with mitochondria through outer mitochondrial proteins including Tom22 (PU *et al.* 2011; GAO *et al.* 2017). Yet3 is involved in ER-mitochondria interaction via Tom40 (NAMBA 2019). TOM components have been shown to serve as ER-mitochondria tethers (ELLENRIEDER *et al.* 2017), which may facilitate the import of precursor proteins that have been temporarily docked on the ER surface such as in the ER-SURF pathway (KOCH *et al.* 2024). It is possible that Mfb1 localizes to regions engaged in active interactions with other organelles to facilitate inter-organellar communication including protein trafficking, or to sites of greater protein import on the OMM. The latter could be particularly relevant considering a recent study that describes how the mitochondrial membranes

remodel to facilitate the co-translational import of mitochondrial proteins (CHANG *et al.* 2025). The reduced distance observed between OMM and IMM around regions of co-translational protein import could contribute to changes in mitochondrial morphology. If Mfb1 maintains import competency by interacting with the TOM complex, its loss could destabilize regions with higher import frequency, subsequently leading to morphological changes.

Transcriptomic analysis provided further support for a role of Mfb1 in alleviating cellular stress under import clogging conditions. First, we employed a stratified analysis approach comparing WT, *mfb1Δ*, *aac2^{A128P,A137D}* (DM), and DM *mfb1Δ* strains grown under respiratory conditions. This strategy allowed us to identify differences between two genotypes at a time and to determine the effects of *mfb1Δ* and *aac2^{A128P,A137D}* as genetic modifiers. It was interesting that in the *mfb1Δ* background, the additional introduction of import clogging led to an increase in genes that encode proteins which function on or near the mitochondrial surface (*MSP1*, *RSP5*) or within mitochondria (*YME1*, *YTA12*) (Figure 5B). However, in the *aac2^{A128P,A137D}* (DM) background, the additional deletion of *MFBI* led to increased expression of genes that encode a wide variety of cytosolic chaperones (Figure 2.5D). This suggests that under Mfb1-deficient conditions with newly induced clogging, the cell acts to rectify import stress by directly trying to triage/repair damaged mitochondria; while under clogging conditions, Mfb1 loss triggers a “proteostatic crisis” which requires the activation of cytosolic chaperones to counterbalance the stress. Finally, the stress of import clogging alone or concurrently with *MFBI* disruption, led to a downregulation of genes involved in ribosomal biogenesis, nucleolar function, and non-coding RNA processing (Supplemental Figures S2.4A, S2.4B, S2.4D, and S2.4E) which is consistent with reduced cytosolic translation and ribosomal function to alleviate proteostatic stress. Interestingly, Mfb1 loss alone relative to wild type led to a downregulation of the *YRF1* gene family members

(Supplemental Figure S2.4C) which are known to be involved in telomere maintenance (YAMADA *et al.* 1998). The physiological relevance of this transcriptomic adaptation is currently unclear.

Stratified analysis also allowed us to capture an additive interaction effect in our transcriptomic dataset. We found that *Aac2*^{A128P, A137D}-induced clogging activates an iron starvation response. A similar response has been previously observed in ρ^0 cells that have reduced inner membrane potential and defective protein import (VEATCH *et al.* 2009). Interestingly, clogging with concurrent *MFBI* disruption leads to the activation of retrograde (RTG) signaling and increased glucose transport, in addition to the iron starvation response. RTG activation is suggestive of severe mitochondrial damage and drastic metabolic reprogramming, allowing cells to undergo anaplerosis and replenish glutamate stores (LIU AND BUTOW 1999). These data suggest that as the severity of mitochondrial protein import stress increases, there is a corresponding “step-wise” increase in the types of cellular metabolic pathways that get dysregulated.

To be comprehensive in our understanding of the yeast cell’s transcriptional responses to import clogging and *MFBI* disruption, we also employed a multifactorial approach to further validate the genetic interactions within all four yeast strains included in our study. This approach allowed us to define how *MFBI* disruption affects gene expression differently based on whether the cell is undergoing protein import clogging or is in protein import homeostasis. The multifactorial design was able to improve our confidence in the results we obtained from the stratified analysis and help determine which genes are differentially expressed the most in context of the interaction between *mfbl*Δ and *aac2*^{A128P, A137D}. For instance, *SSA4* is drastically upregulated when *MFBI* is deleted under clogging (*aac2*^{A128P, A137D}) conditions but barely changed in expression when *MFBI* is deleted under wild type *AAC2* conditions. Other notable genes that

experience the strongest differences in expression include *HSP30*, *HXT15*, *HSP31*, and *HSP26* among others (Supplemental Table 2.4).

While *HSP31* wasn't the most upregulated gene in our dataset, we decided to focus our downstream validations on it for two primary reasons. First, Hsp31 is known for its role in oxidative stress defense, protein glyoxylation (BANKAPALLI *et al.* 2015), post-diauxic shift growth (MILLER-FLEMING *et al.* 2014), α -synuclein handling (TSAI *et al.* 2015; ASLAM AND HAZBUN 2016), and more recently in redox-dependent mitochondrial dynamics (BISWAS AND D'SILVA 2025), but its role as a molecular chaperone has not been well defined. In our dataset, the entire Hsp31 gene family (*HSP31*, *HSP32*, *HSP33*) was upregulated. The proteins encoded by these genes are localized to the cytosol. However, during times of high oxidative stress they can be associated with mitochondria as well as with membrane-less foci called stress granules (MILLER-FLEMING *et al.* 2014; BANKAPALLI *et al.* 2015). While *HSP32* and *HSP33* have almost complete sequence homology, *HSP31* moderately differs in sequence and performs additional activities compared to its paralogs. The second reason for focusing on Hsp31 was because it is the yeast ortholog of the human DJ-1 protein (PARK7) that is associated with early-onset autosomal recessive Parkinson's disease (BONIFATI *et al.* 2003). DJ-1 has been reported to have many cellular functions in the context of neuronal health (BANKAPALLI *et al.* 2015; ASLAM AND HAZBUN 2016). How these functions contribute to neuronal death remains unresolved (TSAI *et al.* 2015; MAZZA *et al.* 2022; SUSARLA *et al.* 2023).

In our study, we found that *HSP31* is selectively upregulated under conditions of mitochondrial protein import clogging combined with Mfb1 loss, but not in either condition alone. This indicates a specific transcriptional response to severe mPOS. Hsp31 may act as a holdase, preventing protein aggregation and/or facilitating the degradation of unimported mitochondrial

proteins in the cytosol. This idea is supported by the finding that disruption of *HSP31* severely reduces the growth of *aac2^{A128P, A137D}* and *aac2^{A128P, A137D} mfb1 Δ* cells and increases ubiquitinated protein levels in the aggregates formed within these mutant cells. As Hsp31-GFP remains largely cytosolic under clogging conditions, Hsp31 likely defends the cytosol against mPOS. Interestingly, we also observed that global protein ubiquitination is significantly increased even in respiring *hsp31 Δ* cells. This further suggests a protective role of Hsp31 against proteostatic stress and mPOS in cells that have a greater requirement for mitochondrial biogenesis and oxidative metabolism.

Approximately 10% of Parkinson's disease (PD) cases are associated with mutations in single genes including human genes Fbxo7 (or PARK15) and DJ-1 (SHOJAE *et al.* 2008; DI FONZO *et al.* 2009). Fbxo7 is a mitochondria-associated F-box protein. It is known to act either as a substrate adaptor protein in SCF-type E3 ubiquitin ligase complex that regulates proteasomal and other cellular activities, or to function in a SCF-independent manner to promote mitophagy (NELSON *et al.* 2013; JOSEPH *et al.* 2018; KRAUS *et al.* 2023). Interestingly, the SCF-independent function of Fbxo7 is required to stabilize Tomm20, the mammalian homolog of Tom20 (TEIXEIRA *et al.* 2016). Furthermore, loss of Fbxo7 sensitizes cells to proteostatic stress in mitochondria (KRAUS *et al.* 2023). Fbxo7 and Mfb1 share similarities only in the highly conserved F-box motif. Whether Fbxo7 plays a role in the maintenance of mitochondrial protein import competency remains to be tested. This function could become more relevant in actively respiring cells and under pathophysiological conditions with increased mitochondrial protein import stress. On the other hand, Hsp31/DJ-1 may be critical for protecting the cytosol against proteotoxicity caused by unimported mitochondrial proteins. Hence, both Mfb1 and Hsp31 may work in concert at the mitochondrial surface or in the cytosol, respectively, to support cellular proteostasis. Our data therefore draw mechanistic parallels between yeast Mfb1 and human F-box proteins such as

Fbxo7. Additionally, our finding that *HSP31* responds to mitochondrial import stress aligns with DJ-1's broader role in cellular defense mechanisms, potentially providing a functional link between mitochondrial protein import stress, proteostasis, and neurodegeneration.

Altogether, our study reveals a role for Mfb1 in the maintenance of mitochondrial protein import competency. Furthermore, our work clarifies that Mfb1 likely functions in the absence of a SCF complex. It is important to appreciate that our work utilizes an endogenous mitochondrial protein (Aac2) which when mutated causes protein import to partially clog. Thus, discovering an anti-mPOS function for Mfb1 in this cellular setting is clinically relevant. Lastly, our work establishes a link between the disruption of Mfb1 during clogging and the activation of the heat shock protein Hsp31. In summary, we define a novel role for Mfb1 in protecting against mitochondrial precursor overaccumulation stress and show that Hsp31 acts as a downstream proteostatic buffer in Mfb1-deficient cells. This reveals a cooperative axis between mitochondrial surface quality control (Mfb1) and cytosolic chaperone response (Hsp31). Studying this link further may help improve our understanding of how mitochondrial damage, protein import stress and cytosolic proteostasis are intricately connected in the pathogenesis of Parkinson's disease.

2.6] Supporting Information

Data availability – The RNA-Seq data generated as part of this study are presented as supplemental tables. The data have also been deposited to NCBI Gene Expression Omnibus/Sequence Read Archive with the accession numbers GSE298360. The TMT-MS and label-free quantitative proteomic data have been deposited to PRoteomics IDentifications Database (PRIDE) with the accession numbers PXD064566 and PXD065210. All software used in this study is publicly available and there was no code generated as part of this study.

Acknowledgments — We thank Drs. Bruce Knutson, Ryan Palumbo and Ebbing de Jong for help in the MiniTurboID assay and the analysis of proteomic data, Maya Schuldiner for sharing the SWAT-GFP-tagged yeast strains library and Victor Z. Chen for help in RNA-sequencing analysis. We acknowledge the use of the AI tool ChatGPT in assisting us with writing code for computational analysis in RStudio and for suggesting grammar edits to improve the clarity of our manuscript.

Funding — This work was supported by National Institutes of Health grants R01AG063499 and R01AG061204 to X.J.C. The content is solely the responsibility of the authors and does not necessarily represent the official views of the National Institutes of Health. G.M. was the recipient of the American Heart Association Predoctoral Fellowship #1010959.

Conflicts of interest — The authors declare that they have no conflicts of interest with the contents of this article.

Author contributions — **GM**: Conceptualization, Methodology, Formal Analysis, Investigation, Visualization, Data Curation, Writing – Original Draft and Review/Editing, Funding Acquisition. **XW**: Investigation, Data Curation, Validation, Resources, Methodology. **EF**: Investigation, Visualization. **AG**: consultation and supervision for computational analysis of RNAseq data, manuscript revision. **XJC**: Conceptualization, Investigation, Data Curation, Visualization, Formal Analysis, Methodology, Supervision, Writing – Original and Review/Editing, Funding Acquisition.

2.7] Literature cited

- Abou-Sleiman, P. M., D. G. Healy, N. Quinn, A. J. Lees and N. W. Wood, 2003 The role of pathogenic DJ-1 mutations in Parkinson's disease. *Ann Neurol* 54: 283-286.
- Alshammari, Q. A., 2025 Redox modulatory role of DJ-1 in Parkinson's disease. *Biogerontology* 26: 81.
- Aslam, K., and T. R. Hazbun, 2016 Hsp31, a member of the DJ-1 superfamily, is a multitasking stress responder with chaperone activity. *Prion* 10: 103-111.
- Backes, S., Y. S. Bykov, T. Flohr, M. Raschle, J. Zhou *et al.*, 2021 The chaperone-binding activity of the mitochondrial surface receptor Tom70 protects the cytosol against mitoprotein-induced stress. *Cell Rep* 35: 108936.
- Bankapalli, K., S. Saladi, S. S. Awadia, A. V. Goswami, M. Samaddar and P. D'Silva, 2015 Robust glyoxalase activity of Hsp31, a ThiJ/DJ-1/PfpI family member protein, is critical for oxidative stress resistance in *Saccharomyces cerevisiae*. *J Biol Chem* 290: 26491-26507.
- Biswas, S., and P. D'Silva, 2025 Ubp2 modulates DJ-1-mediated redox-dependent mitochondrial dynamics in *Saccharomyces cerevisiae*. *PLoS Genet* 21: e1011353.
- Bonifati, V., P. Rizzu, M. J. van Baren, O. Schaap, G. J. Breedveld *et al.*, 2003 Mutations in the DJ-1 gene associated with autosomal recessive early-onset parkinsonism. *Science* 299: 256-259.
- Branon, T. C., J. A. Bosch, A. D. Sanchez, N. D. Udeshi, T. Svinikina *et al.*, 2018 Efficient proximity labeling in living cells and organisms with TurboID. *Nat Biotechnol* 36: 880-887.
- Chang, Y. T., B. A. Barad, J. Hamid, H. Rahmani, B. M. Zid and D. A. Grotjahn, 2025 Cytoplasmic ribosomes on mitochondria alter the local membrane environment for protein import. *J Cell Biol* 224.
- Chen, X. J., and G. D. Clark-Walker, 1999 Alpha and beta subunits of F₁-ATPase are required for survival of petite mutants in *Saccharomyces cerevisiae*. *Mol Gen Genet* 262: 898-908.
- Chen, X. J., and G. D. Clark-Walker, 2000 The petite mutation in yeasts: 50 years on. *Int Rev Cytol* 194: 197-238.
- Coyne, L. P., and X. J. Chen, 2018 mPOS is a novel mitochondrial trigger of cell death - implications for neurodegeneration. *FEBS Lett* 592: 759-775.
- Coyne, L. P., and X. J. Chen, 2019 Consequences of inner mitochondrial membrane protein misfolding. *Mitochondrion* 49: 46-55.
- Coyne, L. P., A. Rana, X. Wang, S. Bhagwagar, Y. Umino *et al.*, 2023a Mitochondrial protein import stress augments alpha-synuclein aggregation and neurodegeneration independent of bioenergetics. *BioRxiv*. doi: 10.1101/2022.09.20.508793
- Coyne, L. P., X. Wang, J. Song, E. de Jong, K. Schneider *et al.*, 2023b Mitochondrial protein import clogging as a mechanism of disease. *Elife* 12:e84330
- Dekker, P. J., M. T. Ryan, J. Brix, H. Muller, A. Honlinger and N. Pfanner, 1998 Preprotein translocase of the outer mitochondrial membrane: molecular dissection and assembly of the general import pore complex. *Mol Cell Biol* 18: 6515-6524.
- Deschauer, M., G. Hudson, T. Muller, R. W. Taylor, P. F. Chinnery and S. Zierz, 2005 A novel *ANT1* gene mutation with probable germline mosaicism in autosomal dominant progressive external ophthalmoplegia. *Neuromuscul Disord* 15: 311-315.
- Di Fonzo, A., M. C. Dekker, P. Montagna, A. Baruzzi, E. H. Yonova *et al.*, 2009 *FBXO7* mutations cause autosomal recessive, early-onset parkinsonian-pyramidal syndrome. *Neurology* 72: 240-245.
- Dunn, C. D., M. S. Lee, F. A. Spencer and R. E. Jensen, 2006 A genomewide screen for petite-negative yeast strains yields a new subunit of the i-AAA protease complex. *Mol Biol Cell* 17: 213-226.
- Durr, M., M. Escobar-Henriques, S. Merz, S. Geimer, T. Langer and B. Westermann, 2006 Nonredundant roles of mitochondria-associated F-box proteins Mfb1 and Mdm30 in maintenance of mitochondrial morphology in yeast. *Mol Biol Cell* 17: 3745-3755.
- Ellenrieder, L., H. Rampelt and T. Becker, 2017 Connection of Protein Transport and Organelle Contact Sites in Mitochondria. *J Mol Biol* 429: 2148-2160.

- Fontanesi, F., L. Palmieri, P. Scarcia, T. Lodi, C. Donnini *et al.*, 2004 Mutations in *AAC2*, equivalent to human adPEO-associated *ANT1* mutations, lead to defective oxidative phosphorylation in *Saccharomyces cerevisiae* and affect mitochondrial DNA stability. *Hum Mol Genet* 13: 923-934.
- Gao, Q., D. D. Binns, L. N. Kinch, N. V. Grishin, N. Ortiz *et al.*, 2017 Pet10p is a yeast perilipin that stabilizes lipid droplets and promotes their assembly. *J Cell Biol* 216: 3199-3217.
- Hague, S., E. Rogaeva, D. Hernandez, C. Gulick, A. Singleton *et al.*, 2003 Early-onset Parkinson's disease caused by a compound heterozygous DJ-1 mutation. *Ann Neurol* 54: 271-274.
- Joaquim, M., S. Altin, M. B. Bulimaga, T. Simoes, H. Nolte *et al.*, 2025 Mitofusin 2 displays fusion-independent roles in proteostasis surveillance. *Nat Commun* 16: 1501.
- Joseph, S., J. B. Schulz and J. Stegmuller, 2018 Mechanistic contributions of *FBXO7* to Parkinson disease. *J Neurochem* 144: 118-127.
- Kaukonen, J., J. K. Juselius, V. Tiranti, A. Kyttala, M. Zeviani *et al.*, 2000 Role of adenine nucleotide translocator 1 in mtDNA maintenance. *Science* 289: 782-785.
- Kaukonen, J., M. Zeviani, G. P. Comi, M. G. Piscaglia, L. Peltonen and A. Suomalainen, 1999 A third locus predisposing to multiple deletions of mtDNA in autosomal dominant progressive external ophthalmoplegia. *Am J Hum Genet* 65: 256-261.
- Koch, C., S. Lenhard, M. Raschle, C. Prescianotto-Baschong, A. Spang and J. M. Herrmann, 2024 The ER-SURF pathway uses ER-mitochondria contact sites for protein targeting to mitochondria. *EMBO Rep* 25: 2071-2096.
- Komaki, H., T. Fukazawa, H. Houzen, K. Yoshida, I. Nonaka and Y. Goto, 2002 A novel D104G mutation in the adenine nucleotide translocator 1 gene in autosomal dominant progressive external ophthalmoplegia patients with mitochondrial DNA with multiple deletions. *Ann Neurol* 51: 645-648.
- Kominsky, D. J., M. P. Brownson, D. L. Updike and P. E. Thorsness, 2002 Genetic and biochemical basis for viability of yeast lacking mitochondrial genomes. *Genetics* 162: 1595-1604.
- Kondo-Okamoto, N., K. Ohkuni, K. Kitagawa, J. M. McCaffery, J. M. Shaw and K. Okamoto, 2006 The novel F-box protein Mfb1p regulates mitochondrial connectivity and exhibits asymmetric localization in yeast. *Mol Biol Cell* 17: 3756-3767.
- Kondo-Okamoto, N., J. M. Shaw and K. Okamoto, 2008 Tetratricopeptide repeat proteins Tom70 and Tom71 mediate yeast mitochondrial morphogenesis. *EMBO Rep* 9: 63-69.
- Kraus, F., E. A. Goodall, I. R. Smith, Y. Jiang, J. C. Paoli *et al.*, 2023 *PARK15/FBXO7* is dispensable for *PINK1/Parkin* mitophagy in iNeurons and HeLa cell systems. *EMBO Rep* 24: e56399.
- Kunji, E. R. S., M. S. King, J. J. Ruprecht and C. Thangaratnarajah, 2020 The *SLC25* carrier family: important transport proteins in mitochondrial physiology and pathology. *Physiology (Bethesda)* 35: 302-327.
- Kunze, M., I. Pracharoenwattana, S. M. Smith and A. Hartig, 2006 A central role for the peroxisomal membrane in glyoxylate cycle function. *Biochim Biophys Acta* 1763: 1441-1452.
- Liu, Y., and X. J. Chen, 2013 Adenine nucleotide translocase, mitochondrial stress, and degenerative cell death. *Oxid Med Cell Longev* 2013: 146860.
- Liu, Z., and R. A. Butow, 1999 A transcriptional switch in the expression of yeast tricarboxylic acid cycle genes in response to a reduction or loss of respiratory function. *Mol Cell Biol* 19: 6720-6728.
- Liu, Z., and R. A. Butow, 2006 Mitochondrial retrograde signaling. *Annu Rev Genet* 40: 159-185.
- Love, M. I., W. Huber and S. Anders, 2014 Moderated estimation of fold change and dispersion for RNA-seq data with DESeq2. *Genome Biol* 15: 550.
- Martensson, C. U., C. Priesnitz, J. Song, L. Ellenrieder, K. N. Doan *et al.*, 2019 Mitochondrial protein translocation-associated degradation. *Nature* 569: 679-683.
- Matta, S. K., A. Kumar and P. D'Silva, 2020 *Mgr2* regulates mitochondrial preprotein import by associating with channel-forming *Tim23* subunit. *Mol Biol Cell* 31: 1112-1123.
- Mazza, M. C., S. C. Shuck, J. Lin, M. A. Moxley, J. Termini *et al.*, 2022 DJ-1 is not a deglycase and makes a modest contribution to cellular defense against methylglyoxal damage in neurons. *J Neurochem* 162: 245-261.

- Miller-Fleming, L., P. Antas, T. F. Pais, J. L. Smalley, F. Giorgini and T. F. Outeiro, 2014 Yeast DJ-1 superfamily members are required for diauxic-shift reprogramming and cell survival in stationary phase. *Proc Natl Acad Sci USA* 111: 7012-7017.
- Mishra, G., L. P. Coyne and X. J. Chen, 2023 Adenine nucleotide carrier protein dysfunction in human disease. *IUBMB Life* 75: 911-925.
- Namba, T., 2019 BAP31 regulates mitochondrial function via interaction with Tom40 within ER-mitochondria contact sites. *Sci Adv* 5: eaaw1386.
- Napoli, L., A. Bordoni, M. Zeviani, G. M. Hadjigeorgiou, M. Sciacco *et al.*, 2001 A novel missense adenine nucleotide translocator-1 gene mutation in a Greek adPEO family. *Neurology* 57: 2295-2298.
- Nelson, D. E., S. J. Randle and H. Laman, 2013 Beyond ubiquitination: the atypical functions of Fbxo7 and other F-box proteins. *Open Biol* 3: 130131.
- Nguyen, K. M., and L. Busino, 2020 The Biology of F-box Proteins: The SCF Family of E3 Ubiquitin Ligases. *Adv Exp Med Biol* 1217: 111-122.
- Palmieri, L., S. Alberio, I. Pisano, T. Lodi, M. Meznaric-Petrusa *et al.*, 2005 Complete loss-of-function of the heart/muscle-specific adenine nucleotide translocator is associated with mitochondrial myopathy and cardiomyopathy. *Hum Mol Genet* 14: 3079-3088.
- Pernice, W. M., J. D. Vevea and L. A. Pon, 2016 A role for Mfb1p in region-specific anchorage of high-functioning mitochondria and lifespan in *Saccharomyces cerevisiae*. *Nat Commun* 7: 10595.
- Pu, J., C. W. Ha, S. Zhang, J. P. Jung, W. K. Huh and P. Liu, 2011 Interactomic study on interaction between lipid droplets and mitochondria. *Protein Cell* 2: 487-496.
- Rappsilber, J., Y. Ishihama and M. Mann, 2003 Stop and go extraction tips for matrix-assisted laser desorption/ionization, nanoelectrospray, and LC/MS sample pretreatment in proteomics. *Anal Chem* 75: 663-670.
- Reinders, J., R. P. Zahedi, N. Pfanner, C. Meisinger and A. Sickmann, 2006 Toward the complete yeast mitochondrial proteome: multidimensional separation techniques for mitochondrial proteomics. *J Proteome Res* 5: 1543-1554.
- Schmitt, M. E., T. A. Brown and B. L. Trumpower, 1990 A rapid and simple method for preparation of RNA from *Saccharomyces cerevisiae*. *Nucleic Acids Res* 18: 3091-3092.
- Schulte, U., F. den Brave, A. Haupt, A. Gupta, J. Song *et al.*, 2023 Mitochondrial complexome reveals quality-control pathways of protein import. *Nature* 614: 153-159.
- Shojaee, S., F. Sina, S. S. Banihosseini, M. H. Kazemi, R. Kalhor *et al.*, 2008 Genome-wide linkage analysis of a Parkinsonian-pyramidal syndrome pedigree by 500 K SNP arrays. *Am J Hum Genet* 82: 1375-1384.
- Siciliano, G., A. Tessa, S. Petrini, M. Mancuso, C. Bruno *et al.*, 2003 Autosomal dominant external ophthalmoplegia and bipolar affective disorder associated with a mutation in the ANT1 gene. *Neuromuscul Disord* 13: 162-165.
- Simoncini, C., G. Siciliano, G. Tognoni and M. Mancuso, 2017 Mitochondrial ANT-1 related adPEO leading to cognitive impairment: is there a link? *Acta Myol* 36: 25-27.
- Susarla, G., P. Kataria, A. Kundu and P. D'Silva, 2023 *Saccharomyces cerevisiae* DJ-1 paralogs maintain genome integrity through glycation repair of nucleic acids and proteins. *Elife* 12:e88875
- Teixeira, F. R., S. J. Randle, S. P. Patel, T. E. Mevissen, G. Zenkeviciute *et al.*, 2016 Gsk3beta and Tomm20 are substrates of the SCFFbxo7/PARK15 ubiquitin ligase associated with Parkinson's disease. *Biochem J* 473: 3563-3580.
- Thompson, K., H. Majd, C. Dallabona, K. Reinson, M. S. King *et al.*, 2016 Recurrent de novo dominant mutations in Slc25a4 cause severe early-onset mitochondrial disease and loss of mitochondrial DNA copy number. *Am J Hum Genet* 99: 860-876.
- Tsai, C. J., K. Aslam, H. M. Drendel, J. M. Asiago, K. M. Goode *et al.*, 2015 Hsp31 is a stress response chaperone that intervenes in the protein misfolding process. *J Biol Chem* 290: 24816-24834.
- Veatch, J. R., M. A. McMurray, Z. W. Nelson and D. E. Gottschling, 2009 Mitochondrial dysfunction leads to nuclear genome instability via an iron-sulfur cluster defect. *Cell* 137: 1247-1258.

- Walker, M. C., and W. A. van der Donk, 2016 The many roles of glutamate in metabolism. *J Ind Microbiol Biotechnol* 43: 419-430.
- Wang, X., and X. J. Chen, 2015 A cytosolic network suppressing mitochondria-mediated proteostatic stress and cell death. *Nature* 524: 481-484.
- Wang, X., K. Salinas, X. Zuo, B. Kucejova and X. J. Chen, 2008 Dominant membrane uncoupling by mutant adenine nucleotide translocase in mitochondrial diseases. *Hum Mol Genet* 17: 4036-4044.
- Weidberg, H., and A. Amon, 2018 MitoCPR-A surveillance pathway that protects mitochondria in response to protein import stress. *Science* 360: eaan4146
- Wiedemann, N., and N. Pfanner, 2017 Mitochondrial Machineries for Protein Import and Assembly. *Annu Rev Biochem* 86: 685-714.
- Wisniewski, J. R., A. Zougman, N. Nagaraj and M. Mann, 2009 Universal sample preparation method for proteome analysis. *Nat Methods* 6: 359-362.
- Wrobel, L., U. Topf, P. Bragoszewski, S. Wiese, M. E. Sztolsztener *et al.*, 2015 Mistargeted mitochondrial proteins activate a proteostatic response in the cytosol. *Nature* 524: 485-488.
- Yamada, M., N. Hayatsu, A. Matsuura and F. Ishikawa, 1998 Y'-Help1, a DNA helicase encoded by the yeast subtelomeric Y' element, is induced in survivors defective for telomerase. *J Biol Chem* 273: 33360-33366.
- Yang, E. J., W. M. Pernice and L. A. Pon, 2022 A role for cell polarity in lifespan and mitochondrial quality control in the budding yeast *Saccharomyces cerevisiae*. *iScience* 25: 103957.

2.8] Supplemental Figures and Other Supporting Information

The Mitochondrial F-box protein 1 and DJ-1 homolog Hsp31 support cellular proteostasis during mitochondrial protein import clogging in *Saccharomyces cerevisiae*

Gargi Mishra, Xiaowen Wang, Eamon Fitzpatrick, Auyon Ghosh, Xin Jie Chen

The PDF file includes:

Figure S2.1 to S2.7

Other Supplementary Information for this manuscript include the following:

Table S2.1 to S2.6

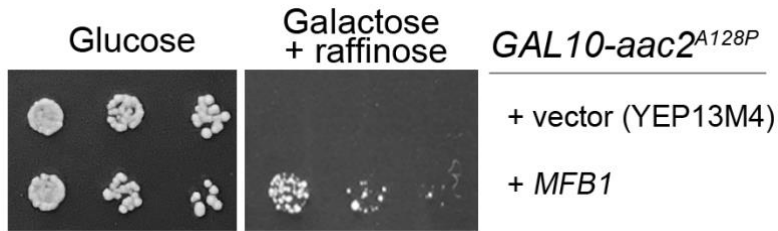


Figure S2.1: A subclone containing only the *MFB1* open reading frame can rescue cell growth defect of a yeast strain expressing *aac2^{A128P}*. The open reading frame of *MFB1* including its endogenous promoter was cloned into the multicopy YEP13M4 vector. This plasmid rescued the growth of cells expressing *GAL10-aac2^{A128P}* at 30°C on complete galactose and raffinose medium. Growth on complete glucose medium represses the expression of *aac2^{A128P}*, which is used as a control.

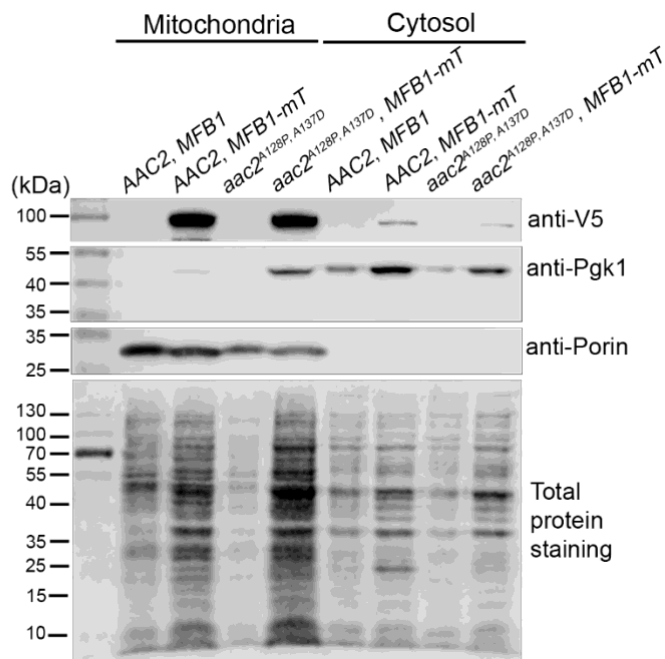


Figure S2.2: Western blot showing the localization of the Mfb1-miniTurboID fusion protein to the mitochondrial fraction. Yeast cells were first cultured on minimal medium before being inoculated in the complete medium with the non-fermentable ethanol plus glycerol as carbon sources. Mitochondrial and cytosolic fractions were prepared and analyzed by SDS-PAGE followed by western blot. Anti-V5 antibody was used to monitor the subcellular distribution of the Mfb1-miniTurboID fusion protein that is tagged with the V5 epitope. Antibodies against Pgk1 and porin were used as markers for cytosolic and mitochondrial fractions, respectively.

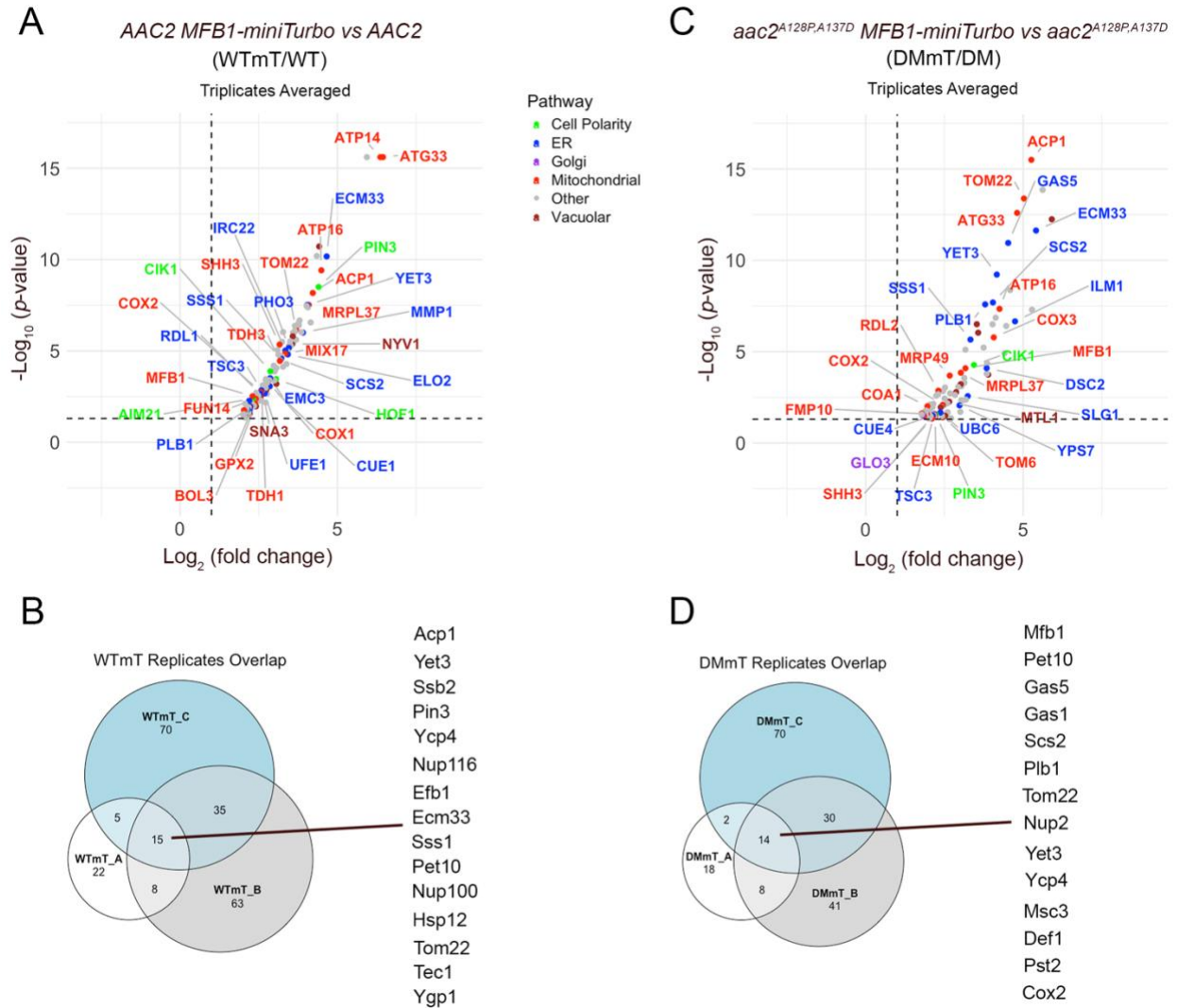


Figure S2.3: Mfb1's interactome as revealed by BioID assay. (A) Volcano plot showing biotinylated proteins in the Mfb1-miniTurboID tagged cells in the background of wild type *AAC2* (WTmT), normalized to untagged wild type after averaging three biologically independent replicates. **(B)** Venn diagram of proteins common across the triplicates described in (A). **(C)** Volcano plot showing biotinylated proteins in the Mfb1-miniTurboID tagged cells in the clogger *aac2^{A128P, A137D}* cells (DMmT), normalized to untagged clogger after averaging three biologically independent replicates. **(D)** Venn diagram of proteins common across the triplicates described in (C).

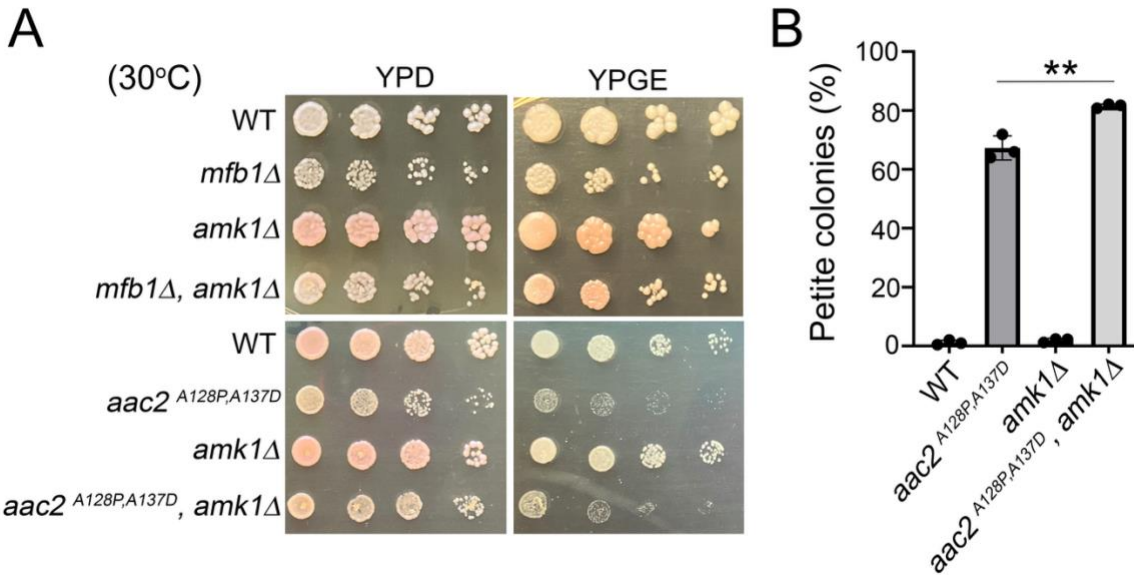


Figure S2.5: Characterization of *AMK1*. (A) Five-fold dilution series for yeast strains lacking either *MFB1* or *AMK1* in the *AAC2* wild type or clogger (*aac2^{A128P, A137D}*) background. *AMK1* disruption does not exacerbate growth defects under clogging conditions for cells grown in either fermentable (YPD) or non-fermentable (YPGE) media. Note that *AMK1*-deficient strains have slightly greater red pigment accumulation when compared to wild type cells, suggesting a potential role for Amk1 in redox homeostasis. (B) Amk1 loss mildly increases petite frequency under import clogging conditions. *P* value was calculated using Student's *t*-test. **, *p*<0.01.

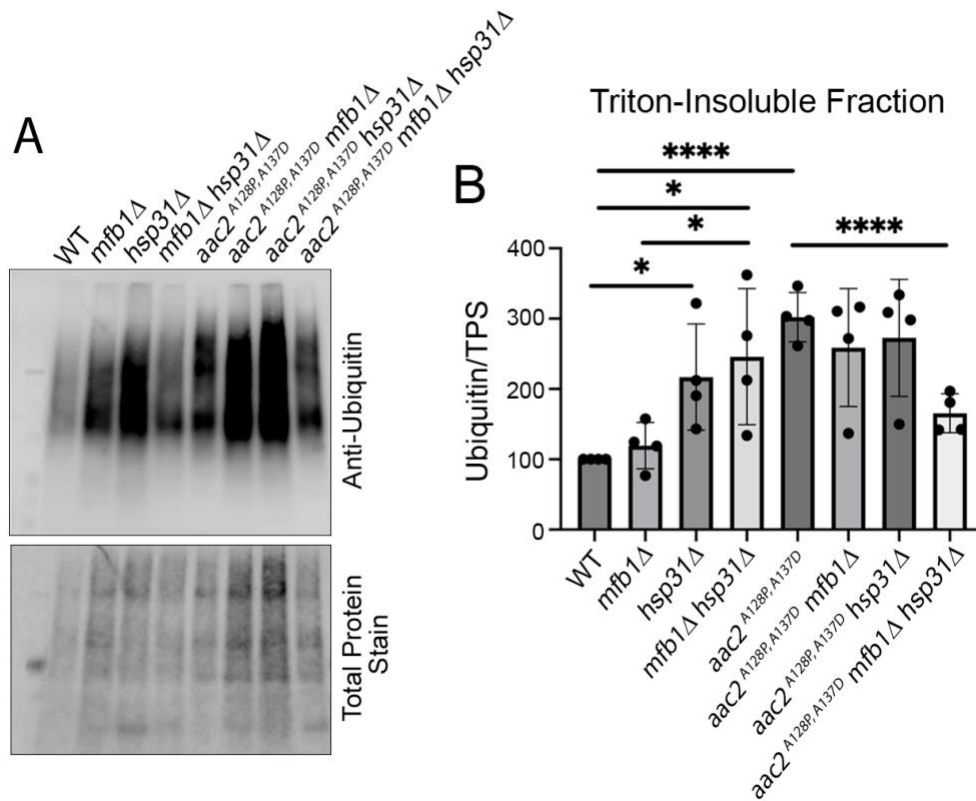


Figure S2.6: Disruption of *HSP31* is sufficient to increase levels of ubiquitinated proteins in Triton-insoluble fractions. (A) Western blot analysis of ubiquitinated proteins sequestered within insoluble aggregates. Samples were obtained from yeast strains grown under respiring conditions. (B) Quantification of western blot shown in (A). *P* values were calculated using Student's t-test. *, $p < 0.05$; ****, $p < 0.0001$.

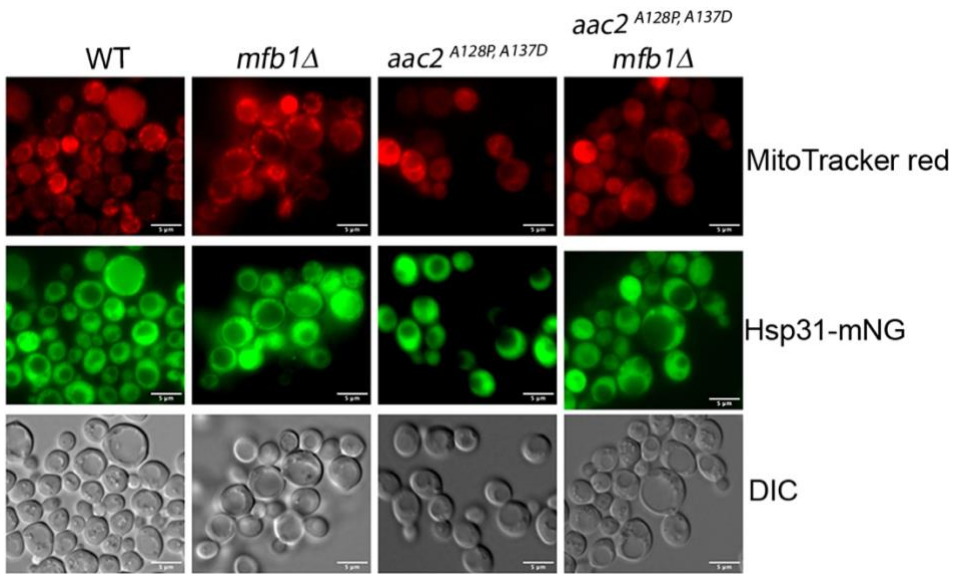


Figure S2.7: Hsp31 remains cytosolic, regardless of clogging conditions or Mfb1-deficiency. Representative images showing Hsp31-mNG fusion protein in the cytosol of all yeast strains visualized. Mitochondria were stained with Mitotracker Red. Scale bar represents 5 μ m.

Legends for Supplemental Tables.

Supplemental Table 2.1: Excel workbook containing pathway analysis results from Funspec for *aac2^{A128P, A137D}* (DM) vs WT comparison. Gene Ontology (GO) terms and Munich Information Center for Protein Sequences (MIPS) classification terms are included. Sheet 1 contains upregulated pathway lists after Bonferroni correction ($p < 0.01$). Sheet 2 contains upregulated pathway lists without Bonferroni correction. Sheet 3 contains downregulated pathway lists after Bonferroni correction ($p < 0.01$). Sheet 4 contains downregulated pathway lists without Bonferroni correction.

Supplemental Table 2.2: Excel workbook containing pathway analysis results from Funspec for *aac2^{A128P, A137D} mfb1 Δ* vs *aac2^{A128P, A137D}* comparison. Gene Ontology (GO) terms and Munich Information Center for Protein Sequences (MIPS) classification terms are included. Sheet 1 contains upregulated pathway lists after Bonferroni correction ($p < 0.01$). Sheet 2 contains upregulated pathway lists without Bonferroni correction. Sheet 3 contains downregulated pathway lists after Bonferroni correction ($p < 0.01$). Sheet 4 contains downregulated pathway lists without Bonferroni correction.

Supplemental Table 2.3: Excel workbook containing pathway analysis results from Funspec for *aac2^{A128P, A137D} mfb1 Δ* vs WT comparison. Gene Ontology (GO) terms and Munich Information Center for Protein Sequences (MIPS) classification terms are included. Sheet 1 contains upregulated pathway lists after Bonferroni correction ($p < 0.01$). Sheet 2 contains upregulated pathway lists without Bonferroni correction. Sheet 3 contains downregulated pathway lists after Bonferroni correction ($p < 0.01$). Sheet 4 contains downregulated pathway lists without Bonferroni correction.

Supplemental Table 2.4: Excel sheet listing the genes and their strength of genetic interaction given the genotype-environment multifactorial analysis of the RNAseq dataset. Each gene's expression level in response to *MFBI* disruption is tested in the *AAC2* wild type and *aac2^{A128P, A137D}* mutant backgrounds. Strength of interaction is the difference in log₂ of the fold change in the mutant vs wild type *AAC2* backgrounds.

Supplemental Table 2.5: Excel workbook containing yeast strains (Sheet 1), plasmids (Sheet 2), and primers (Sheet 3) used in this study.

Supplemental Table 2.6: List of relevant reagents and sources used in this study.

Chapter 3. Pbp1, the yeast homolog of human Ataxin-2, promotes cellular homeostasis and mitochondrial genome stability during mitochondrial protein import clogging

Mishra, Gargi¹; Wang, Xiaowen¹; Chen, Xin Jie¹

1: Department of Biochemistry and Molecular Biology, State University of New York Upstate Medical University
(Manuscript in preparation)

3.1] ABSTRACT

Mitochondria rely on the coordinated expression of both mitochondrial and nuclear genomes to sustain organelle biogenesis and function. Although mitochondrial DNA (mtDNA) encodes only a small fraction of mitochondrial proteins, its integrity is essential for oxidative phosphorylation, iron-sulfur cluster biogenesis, stress signaling, and cellular homeostasis. Efficient mitochondrial biogenesis further requires the faithful import of ~99% of mitochondrial proteins from the cytosol through dedicated translocase machineries. Disruption of this process, including mitochondrial protein import clogging by aberrant precursor proteins, compromises mitochondrial function and destabilizes mtDNA through multiple mechanisms, including impaired mitochondrial membrane potential, defective iron metabolism, and oxidative stress. Despite growing recognition of the reciprocal relationship between protein import and mtDNA maintenance, the cellular pathways that preserve mitochondrial genome stability under import stress remain poorly defined. Here, we investigate mechanisms that safeguard mtDNA integrity during mitochondrial protein import stress using a yeast model expressing pathogenic mutations in the ADP/ATP carrier that induce import clogging and lead to mtDNA loss. Through a multicopy genetic suppressor screen, we identify genes encoding cytosolic RNA-binding proteins associated with stress granule biology, namely *PBPI* and *PABI*, as strong suppressors of mtDNA loss under concurrent clogging conditions. We show that Pbp1 loss exacerbates growth defects and mtDNA instability during import clogging, and that *PBPI* dosage remodels transcriptional programs governing mitochondrial biogenesis, iron homeostasis, and stress adaptation in a mitochondrial import state-dependent manner. At both the protein and RNA levels, mitochondrial protein import clogging profoundly rewires the Pbp1 interactome, revealing a dynamic coupling between cytosolic RNA regulation and mitochondrial proteostasis.

3.2] INTRODUCTION

Mitochondria are ancient organelles found in almost all eukaryotes that contain their own genome which is a remnant phenotype of their bacterial origin. In most animals and certain plants and fungi, the mitochondrial genome, or 'mtDNA', is composed of circular double-stranded DNA (RYCOVSKA *et al.* 2004). The human mtDNA is comprised of 2 ribosomal RNA genes, 22 transfer RNA genes, and 13 genes that encode protein subunits that contribute to different portions of the electron transport chain to facilitate oxidative phosphorylation (TAANMAN 1999). Similarly, the mtDNA of baker's yeast or *Saccharomyces cerevisiae* is also circular and comprises 2 ribosomal RNA genes, 24 transfer RNA genes, a mitoribosomal protein, and 7 proteins that facilitate oxidative phosphorylation (MALINA *et al.* 2018). Despite mtDNA's propensity for accumulating genetic mutations at a faster rate than nuclear DNA, the conservation of its general composition between human and yeast suggests its undeniable role in mitochondrial biogenesis, mitochondrial function, and mitochondrial disease (SHADEL 1999; SEETHASHANKAR *et al.* 2025).

Mitochondrial biogenesis broadly refers to the process by which cells generate new and healthy mitochondria. This process is extremely elaborate and requires the coordinated functioning of cytosolic ribosomes (free-floating as well as those docked on the mitochondrial membrane), cytosolic chaperone proteins such as Hsp70 and Hsp90 that escort nascent polypeptides to the mitochondrial surface, import translocases on the outer and inner mitochondrial membranes, protein motors, and mitochondrial proteases that survey the efficacy of protein import (WIEDEMANN AND PFANNER 2017; DEN BRAVE *et al.* 2024; ZHU *et al.* 2025). This ensures that the nuclear-encoded mitochondrial proteins, comprising 99% of all mitochondrial proteins, reach their correct destination in one of the four different mitochondrial compartments: the outer mitochondrial membrane (OMM), intermembrane space (IMS), inner mitochondrial membrane

(IMM), and the matrix. Indirectly, mtDNA contributes to efficient mitochondrial protein import. This is because mtDNA mutations can impair oxidative phosphorylation leading to alterations in mitochondrial membrane potential ($\Delta\psi$) which in turn can reduce presequence- and carrier-associated import pathways (SZCZEPANOWSKA *et al.* 2012; GARIPLER *et al.* 2014; GOROSPE *et al.* 2023). More generally, effective mitochondrial biogenesis requires the proper replication and maintenance of mtDNA so that daughter mitochondria can each inherit an adequate mtDNA copy number (LEE AND WEI 2005).

Mitochondria perform many functions, of which cellular energy conversion via ATP production is the most well-known. As previously stated, intact mtDNA free from genetic mutations is necessary to ensure that the mtDNA-encoded proteins can contribute to the assembly of the electron transport chain and support the generation of ATP, the energy currency of the cell. Integrity of the mtDNA is also necessary for maintaining proper iron-sulfur cluster (ISC) assembly via an indirect pathway involving nuclear genome stability (VEATCH *et al.* 2009). Proper Fe-S assembly in mitochondria is in turn important for a variety of cellular processes involving both the mitochondrial (electron transport chain, citric acid cycle, mitochondrial iron homeostasis), as well as non-mitochondrial compartments which include Fe-S assembly in the cytosol and the nucleus, DNA repair, replication and gene expression regulation (VALLIERES *et al.* 2024). Finally, defects in mtDNA can trigger the activation of cellular stress responses including the mitochondria-to-nucleus retrograde signaling response (BUTOW AND AVADHANI 2004), innate immune signaling in mammals (HU AND SHU 2023), and proteotoxic stress responses such as UPRmt (MELBER AND HAYNES 2018).

Mitochondrial disease broadly refers to any pathology caused by defects in mitochondrial biogenesis, function, or quality-control (i.e., the timely turnover of aberrant mitochondria).

Mitochondrial diseases can affect any human organ system (WEN *et al.* 2025), reaffirming the importance of these organelles for organismal homeostasis. Since mtDNA mutations can perturb mitochondrial biogenesis as well as cause defects in mitochondrial function, it is not surprising that they have been implicated in a wide variety of mitochondrial diseases, some of the most well-known being Leber hereditary optic neuropathy (LHON), Mitochondrial encephalopathy, lactic acidosis, and stroke-like episodes (MELAS), myoclonus epilepsy with ragged-red fibers (MERRF); neuropathy, ataxia, and retinitis pigmentosa (NARP), Leigh syndrome, Pearson syndrome, Kearns-Sayre syndrome (KSS), and several forms of chronic progressive external ophthalmoplegia (CPEO) (RYZHKOVA *et al.* 2018). Some of these aforementioned diseases are caused by point mutations in mtDNA, while others involve large-scale mtDNA deletions. Besides these, many other mitochondrial diseases caused by defective or unstable mtDNA involve nuclear-encoded mitochondrial genes that are responsible for mtDNA maintenance or more generally for mitochondrial quality control (SHARER 2005; EL-HATTAB AND SCAGLIA 2013; BALLOUT *et al.* 2019). Altogether, directly or indirectly, damaged mtDNA can cause pathology.

Conversely, defects in the mitochondrial protein import process can damage mtDNA. As stated earlier, this may either be due to previously existing mtDNA mutations that disrupt the assembly of respiratory complexes and reduce the import of certain mitochondrial preproteins. However, this may also be due to independent defects in the protein import machinery (FRANCO-IBORRA *et al.* 2018), or due to mutations in the preproteins being imported through the translocase complexes of the outer (TOM) and the inner (TIM) membranes. The latter of the two phenomena can cause mutant proteins to get stuck on the translocases, effectively reducing the import of other mitochondrial proteins, a process referred to as mitochondrial protein import clogging (or simply ‘clogging’) (COYNE *et al.* 2023). This has vast implications for mtDNA stability. First, clogging

may reduce the import of nuclear-encoded mitochondrial proteins directly involved in mtDNA replication and mtDNA maintenance. Secondly, clogging can lead to a reduced import of nuclear-encoded mitochondrial carrier proteins that are involved in nucleotide and phosphate balance between the cytosolic and mitochondrial compartments, which reduces the mitochondrial membrane potential and thus perturbs mtDNA replication and repair (NISHIO *et al.* 2023). Third, clogging may cause reduced assembly of iron-sulfur (Fe-S) cluster (ISC) proteins. These proteins support the functioning of the enzymes involved in mtDNA replication and repair (VALLIERES *et al.* 2024). Finally, defective import associated reactive oxygen species (ROS) production can contribute directly to mtDNA damage. It is important to note that although mitochondrial protein import defects can reduce respiratory chain assembly and can thus lower electron transport chain-derived ROS (LIU *et al.* 2002), they can still lead to mtDNA instability via other ROS-generating mechanisms. These include iron dysregulation resulting from impaired Fe-S cluster biogenesis which promotes Fenton chemistry and hydroxyl radical production, as well as the production of superoxide from misassembled or partially assembled respiratory complexes (CHEN 2019; DE ALMEIDA *et al.* 2022). It is thus clear that defective mitochondrial protein import destabilizes mtDNA integrity through a variety of different molecular mechanisms.

There are several biological systems where mitochondrial protein import is clogged to some severity, whether by precursor overload (WEIDBERG AND AMON 2018; LIU *et al.* 2019), synthetically-designed “clogger” proteins with a mitochondrial targeting signal (MARTENSSON *et al.* 2019) or physiologically occurring mutant preproteins (COYNE *et al.* 2023). Several of these systems have illustrated that protein import clogging causes mtDNA stability. Studies conducted in our lab utilized the mitochondrial carrier protein adenine nucleotide translocase 1 (ANT1) and its corresponding yeast ortholog called the ADP/ATP carrier protein 2 (AAC2) to show that

diseases caused by dominant ANT1 mutations (KAUKONEN *et al.* 2000), such as autosomal dominant progressive external ophthalmoplegia (adPEO) and a form of hypertrophic cardiomyopathy (PALMIERI *et al.* 2005), occur due to mitochondrial protein import clogging. Using a yeast model, our lab showed that the pathogenic mutants *aac2^{A128P}* (orthologous to adPEO-causing human *ANT1^{A114P}*) and *aac2^{A137D}* (orthologous to cardiomyopathy-causing human *ANT1^{A123D}*) decreased yeast cell growth in a dominant manner and increased the formation of ‘petite’ yeast colonies –a readout for respiration insufficiency which can likely occur due to mtDNA loss. A synthetically created “double mutant” (later referred to as DM in this study) that combined the two pathogenic mutations into a single mutant protein-coding gene (*aac2^{A128P, A123D}*) led to a further exacerbation of the growth defect and a further increase in petite colony frequency. An *in vitro* protein import assay showed that the Aac2^{A128P, A137D} protein had increased association with the OMM translocase channel Tom40 (COYNE *et al.* 2023). This finding illustrated that a mutant protein stalling at a translocase channel could contribute to reduced import of other mitochondrial proteins and lead to downstream consequences such as mtDNA destabilization.

Considering the significance mtDNA integrity holds for mitochondrial homeostasis and organismal health, alongside the converse importance of efficient mitochondrial protein import for mtDNA integrity, we sought to identify molecular pathways which could restore mtDNA stability and support protein import efficiency under clogging conditions. To do this we utilized a yeast strain expressing the double mutant clogger allele of AAC2, namely *aac2^{A128P, A123D}* that dominantly inhibits cell growth and causes petite colony formation. We performed a multicopy screen to identify genes that could suppress petite colony formation -using this as a readout for improved mitochondrial protein import efficiency under clogging conditions, as well as improved mtDNA integrity. We identified many protein-coding genes, most of which are expressed in the

cytosol and some that are expressed in mitochondria. Two of the strongest suppressors were *PABI* and *PBPI* which both encode RNA-binding proteins involved in the formation of membraneless organelles in the cytosol called stress granules. In this study, we wanted to test the hypothesis that *PBPI* and *PABI* play a role in maintaining mitochondrial protein import competency under import clogging conditions. The human ortholog for yeast *PBPI* is *Ataxin-2* which is implicated in neurological disorders such as Spinocerebellar ataxia and parkinsonism (OSTROWSKI *et al.* 2017; LAFFITA-MESA *et al.* 2021). Similarly, the human ortholog for yeast *PABI*, namely *PABPC1* is implicated in cardiac hypertrophy, atherosclerosis progression, developmental delays, amyotrophic lateral sclerosis, as well as various forms of cancer (CHORGHAE *et al.* 2017; QI *et al.* 2022; LIN *et al.* 2024). Since *PBPI* is a non-essential gene, while *PABI* is essential, we focused several of our experiments on characterizing Pbp1's function, since it could be genetically manipulated more easily.

Our data revealed that Pbp1 loss exacerbates growth defects and mtDNA instability during import clogging and that *PBPI* dosage remodels transcriptional programs governing mitochondrial biogenesis, iron homeostasis, and stress adaptation in a mitochondrial state-dependent manner. At both the protein and RNA levels, mitochondrial import stress profoundly rewires the Pbp1 interactome, revealing a dynamic coupling between cytosolic RNA regulation and mitochondrial proteostasis. In light of Pbp1's known roles in human health and disease as listed above, our study offers novel insights into Pbp1 function in the context of mitochondrial function and homeostasis

3.3] RESULTS

3.3.a] Multicopy suppressor screen identifies several suppressors of mtDNA loss resulting from import clogging

To identify genes involved in alleviating mitochondrial protein import clogging, we took advantage of the *ade2* mutant colony color assay in the *W303-1B* yeast background (TRON *et al.* 1995; BHARATHI *et al.* 2016). Despite growth at 25 °C, cells with intact mitochondrial function form red colonies due to redox-sensitive pigment accumulation, whereas expression of the pathogenic *aac2*^{A128P,A137D} allele leads to mtDNA loss and the formation of small white (“petite”) colonies, consistent with severe import clogging (Figure 3.1A). We screened for genes that promote mtDNA stability under import-clogging conditions using a multicopy genomic suppressor library (Figure 3.1B).

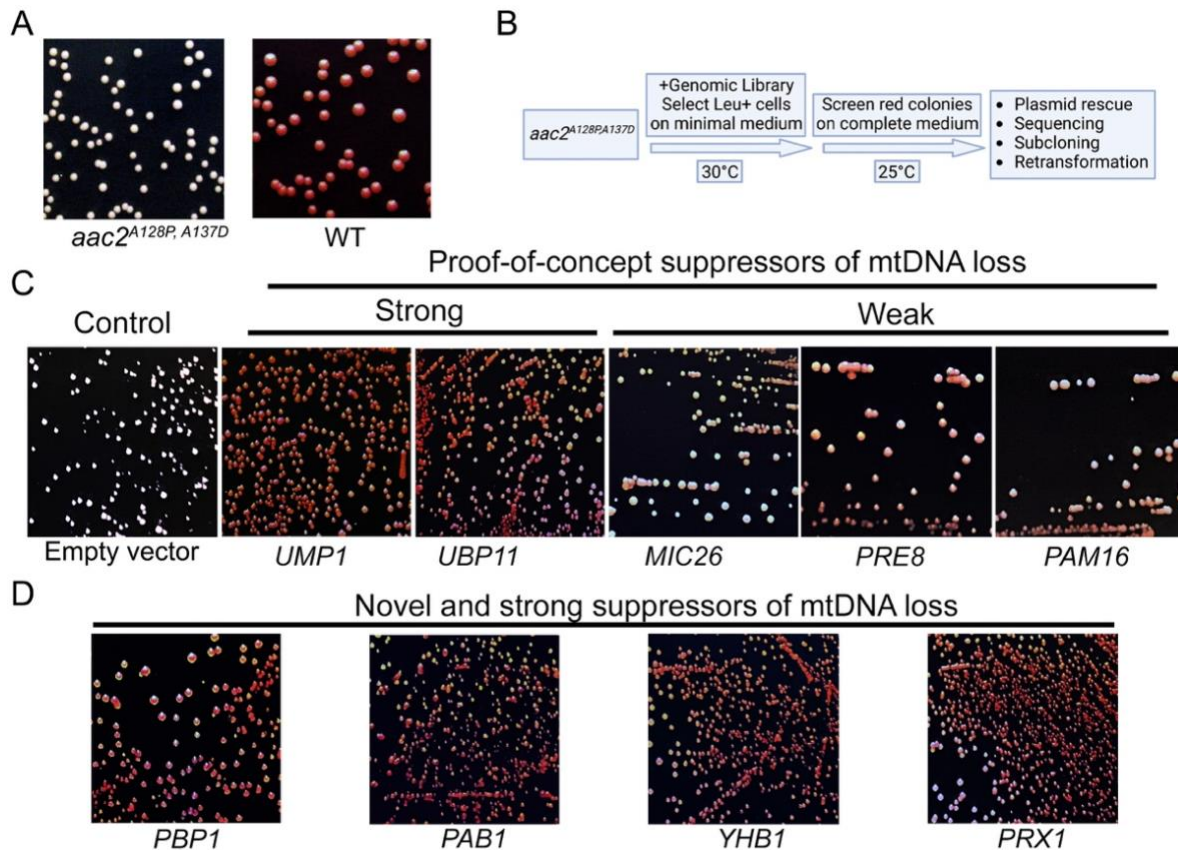


Figure 3.1. Multicopy suppressor screen identifies genetic suppressors of mtDNA instability under import clogging conditions. (A) Representative image of clogger *aac2^{A128P, A137D}* (left) and wild type *AAC2* cells (right). Clogger cells form only small white or petite colonies at 25 °C due to mtDNA loss. Wild type cells appear larger and generate red pigment due to being able to respire. (B) Screening strategy: we transformed clogger cells with a multicopy library and screened for colonies that turned red when grown on glucose at 25 °C (growth conditions where untransformed clogger cells only form petite colonies). Plasmids in the red appearing transformed clogger colonies were rescued and sequenced to identify genes of interest. (C) Proof-of-concept suppressors from the genetic screen included strong suppressors (*UMPI* and *UBP11*), and weak suppressors (*MIC26*, *PRE8*, and *PAM16*). (D) Strong suppressors with novel biological roles with respect to mitochondrial protein import included *PBP1*, *PAB1*, *YHB1*, and *PRX1*.

This screen identified genes encoding components of the ubiquitin-dependent proteasomal machinery (*UMPI*, *UBP11*, and *PRE8*), mitochondrial protein import (*PAM16*), and the MICOS complex (*MIC26*) (Figure 3.1C). The recovery of these factors, which are functionally linked to mitochondrial proteostasis and organization, provided proof-of-concept validation for the suppressor screen. Notably, the most robust suppression of mtDNA loss, as assessed by restoration

of red colony color, was observed upon overexpression of stress granule-associated genes (*PABI* and *PBPI*), as well as genes involved in redox homeostasis (*PRXI* and *YHBI*) (Figure 3.1D).

3.3.b] Genetic suppressors of mtDNA stability improve the tubularity and interconnectedness of mitochondria under import clogging conditions

We next asked whether the red pigment rescue observed in clogger strains expressing multicopy suppressor plasmids reflected a bona fide reduction in mtDNA loss, rather than an unrelated effect on pigment production. Loss of mtDNA is known to impair mitochondrial membrane potential, which in turn compromises protein import, mitochondrial morphology, and overall mitochondrial function (GEISLER *et al.* 2000; KOVERMANN *et al.* 2002; YOULE AND NARENDRA 2011; ZOROVA *et al.* 2018; SATO *et al.* 2019; GUSTAFSON *et al.* 2020; GOTTSCHALK *et al.* 2024). Restoration of mtDNA stability is therefore expected to be accompanied by improved membrane potential-dependent import and recovery of tubular mitochondrial networks.

To directly assess mitochondrial morphology and protein import, we co-transformed the *aac2^{A128P,A137D}* clogger strain expressing individual suppressor plasmids with the pMitoLOC reporter, which encodes two mitochondrial targeting sequences fused to fluorescent proteins: Cox4-mCherry and Su9-GFP (VOWINCKEL *et al.* 2015). The import of Cox4 is dependent on mitochondrial membrane potential and thus relies on the maintenance of mtDNA integrity (BEVIS AND GLICK 2002; VEATCH *et al.* 2009). Su9 on the other hand can be imported into mitochondria independent of mitochondrial membrane potential (WESTERMANN AND NEUPERT 2000). Visualization of both fluorescent markers allows for the quantification of mitochondrial membrane potential and morphological changes concurrently (VOWINCKEL *et al.* 2015). Visualization of these reporters therefore allows concurrent assessment of mitochondrial morphology and membrane

potential-dependent import. Because Su9-GFP import is membrane potential-independent, it was used as the primary marker for quantifying mitochondrial morphology.

As expected, wild-type cells displayed a high proportion of tubular mitochondrial networks, whereas the clogger strain, either untransformed or carrying an empty vector, exhibited predominantly fragmented (or punctate) mitochondria (Figure 3.2A). In contrast, clogger strains expressing the individual multicopy suppressor plasmids showed a significant increase in the proportion of tubular mitochondria, approaching wild-type levels for several suppressors (Figure 3.2B, 3.2C). While Su9-GFP imaging revealed recovery of mitochondrial morphology across all suppressors, Cox4-mCherry import differed among them. Strong suppressors, defined by robust restoration of red colony pigmentation, such as *UMP1*, *UBP11*, *YHB1*, *PRX1*, *PAB1*, and *PBP1*, exhibited Cox4-mCherry localization that closely overlapped with Su9-GFP, consistent with restoration of membrane potential-dependent import. In contrast, clogger strains expressing weaker suppressors, namely *PRE8*, *MIC26*, and *PAM16*, displayed more diffuse cytosolic Cox4-mCherry signal, suggesting partial rescue of mtDNA stability that was insufficient to fully restore membrane potential during import clogging (Figure 3.2B).

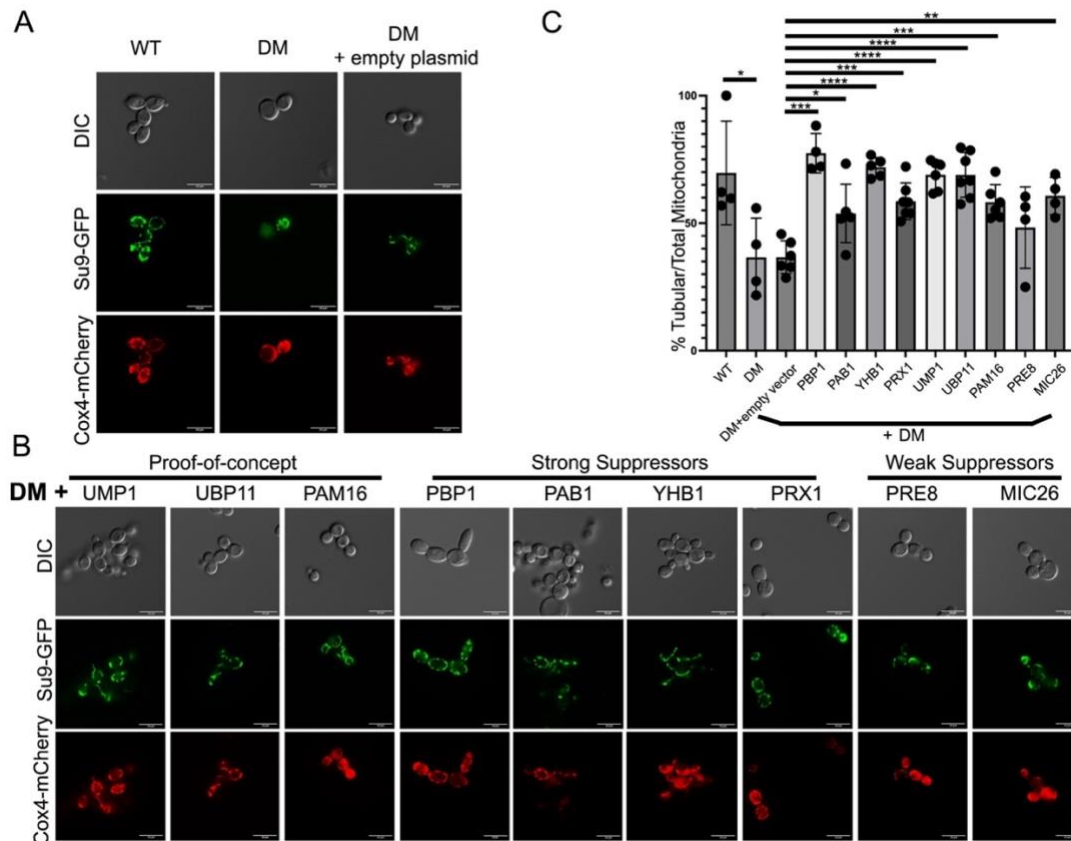


Figure 3.2. Genetic suppressors of mtDNA loss improve mitochondrial morphology. (A) Representative images of AAC2 wild type (WT), clogger (DM), or clogger transformed with empty plasmid, and each strain transformed or co-transformed with pMitoLOC plasmid. WT cells appear to have better connected mitochondrial networks in comparison to clogger cells. (B) Clogger cells transformed with each genetic suppressor identified in our screen, and co-transformed with the pMitoLOC plasmid. All suppressors improve Su9-GFP import, while only strong suppressors improve the import of Cox4-mCherry. (C) Statistical quantification of (A) and (B). Each point represents an independent image. Scale bar denotes 10um. Student's t-test was used to obtain p-values for statistical significance where *, $p < 0.05$; **, $p < 0.01$; ***, $p < 0.001$; ****, $p < 0.0001$.

3.3.c] Loss of *PBP1*, with or without *PAB1*, exacerbates the growth defect of yeast cells undergoing import clogging, especially on a non-fermentable carbon source

Given the suppressors identified in our multicopy genetic screen (Figure 3.1), we focused our subsequent analysis on two genes, namely *PBP1* and *PAB1*. These genes encode RNA-binding proteins that are involved in the formation of stress granules, which are dynamically assembling membraneless organelles found in the cytoplasm in response to a variety of stressors. Although

stress granules have been observed in proximity to mitochondria, their functional contribution to mitochondrial homeostasis remains unclear. Because *PBP1* and *PAB1* suppressed mtDNA instability under import-clogging conditions in our screen, we hypothesized that loss of these factors would exacerbate growth defects when mitochondrial protein import is compromised. To test this hypothesis, we decided to look at yeast cell growth in the absence of these genes under concurrent protein import clogging conditions.

Deletion of *PAB1* is lethal, whereas *PBP1* is non-essential (SACHS *et al.* 1987; DUNN *et al.* 2005; KIMURA *et al.* 2013). However, deletion of *PAB1* in a *pbp1Δ* background restores cell viability (MANGKALAPHIBAN *et al.* 2024). We utilized strains carrying single *pbp1Δ* or combined deletions of *PBP1* and *PAB1* and genetically crossed these with the dominant import-clogging allele *aac2^{A128P,A137D}*. We then assessed growth on fermentable (glucose) and non-fermentable (glycerol plus ethanol) carbon sources across multiple temperatures.

We found that under fermentable and non-fermentable conditions, the growth of mutant strains displayed varying levels of temperature sensitivity. Under fermentable conditions, *pbp1Δ* cells grew comparably to wild type at all temperatures tested, whereas *pab1Δpbp1Δ* cells exhibited reduced growth at 25 °C and 30 °C, and completely failed to grow at 37 °C. On non-fermentable media, *pbp1Δ* cells displayed reduced growth at 25 °C and 37 °C, while *pab1Δ pbp1Δ* cells failed to grow at all temperatures tested (Figure 3.3A, 3.3B).

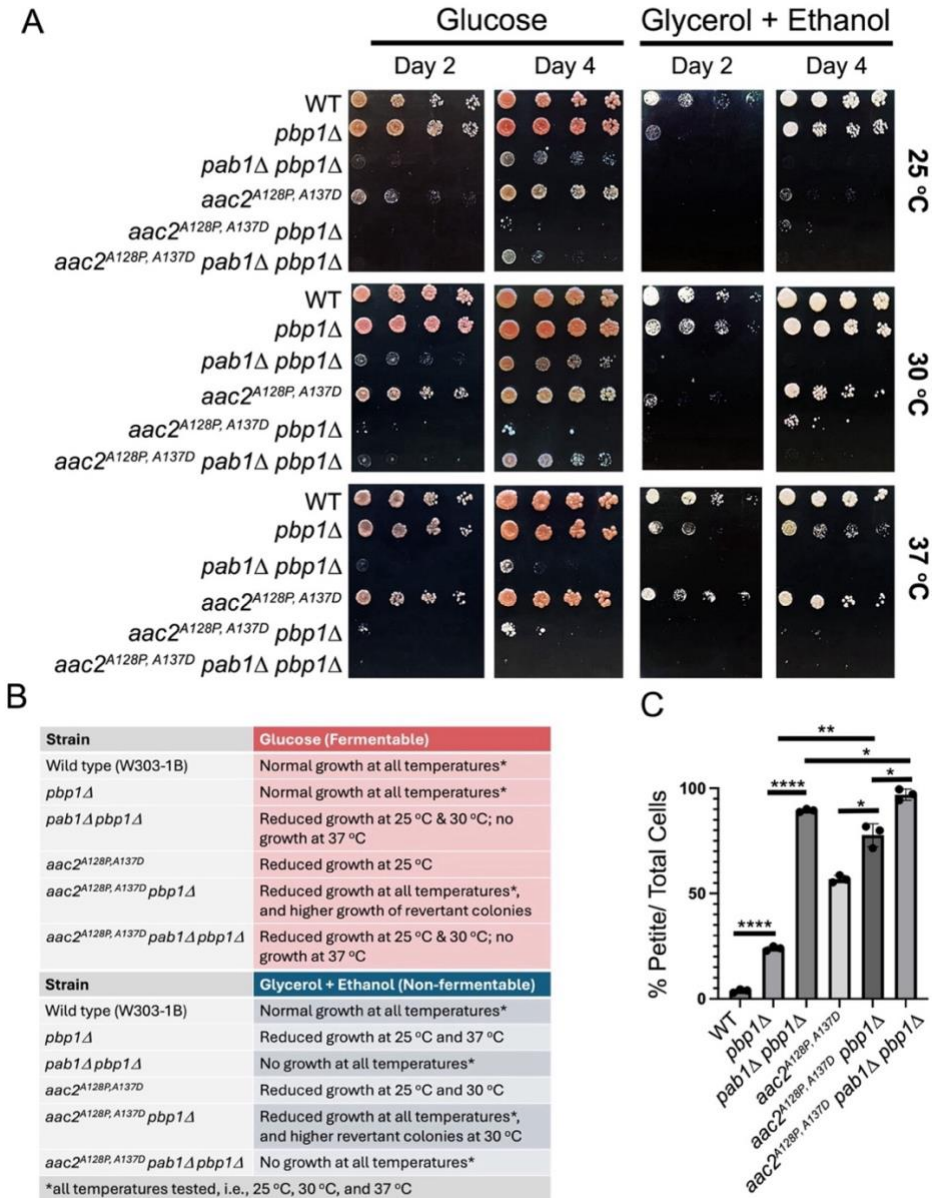


Figure 3.3. Protein import clogging-associated growth defects and mtDNA loss is made worse by the disruption of *PBPI* and *PABI*. (A) Cells from eight different strains were plated onto fermentable (glucose) or nonfermentable (glycerol and ethanol) media and grown at the temperatures of 25 °C, 30 °C, or 37 °C. Plates were imaged on days 2 and 4. (B) Summary of growth defects observed at various growth conditions for all strains tested. (C) Petite frequency quantification for strains shown in (A). All cells in the petite frequency assay were grown on glucose plates (after preculture for 24 hours in minimal glucose conditions) at 30 °C. Three biologically independent replicate plates, each containing 200-400 total cells were counted to quantify petite formation.

Consistent with previous studies from our lab (COYNE *et al.* 2023; MISHRA *et al.* 2025), the *aac2^{A128P, A137D}* clogger strain exhibited reduced growth relative to wild type under both fermentable and non-fermentable conditions at 25 °C and 30 °C, despite retaining an endogenous wild-type copy of *AAC2*, indicating a dominant growth defect. Notably, deletion of *PBP1* in the clogger background markedly exacerbated growth defects on both carbon sources at all temperatures tested. It is important to highlight that while the clogger strain alone grew comparably to wild type at 37 °C, this temperature-dependent growth advantage was abolished upon deletion of *PBP1*, consistent with a role for *PBP1* in supporting stress-adaptive responses under elevated temperatures. Finally, the triple mutant strain (*aac2^{A128P, A137D} pab1Δpbp1Δ*) exhibited the most severe phenotype, displaying slow growth under fermentable conditions, and complete growth arrest on non-fermentable media at all temperatures (Figure 3.3A, 3.3B).

To assess whether these growth defects correlated with mitochondrial dysfunction, we quantified petite colony formation on glucose at 30 °C as a readout of mtDNA loss. Relative to wild-type cells, *pbp1Δ* cells exhibited an approximately 20% increase in petite frequency, which increased to ~75% in *aac2^{A128P, A137D}pbp1Δ* cells, exceeding that observed in the clogger strain alone (~55%). The *pab1Δpbp1Δ* and triple mutant strains exhibited petite frequencies of approximately 85% and 95%, respectively, indicating that loss of *PBP1*, particularly in combination with *PAB1*, strongly exacerbates mtDNA instability during mitochondrial protein import clogging (Figure 3.3C).

3.3.d] *PBP1* differentially remodels transcriptional programs in the presence and absence of mitochondrial protein import clogging

In light of the growth and petite frequency phenotypes, we wanted to determine how *PBP1* affects cellular homeostasis. To study this, we performed bulk RNA sequencing in *AAC2* wild type or clogger *aac2^{A128P, A137D}* cells that either lacked (*pbp1Δ*) or overexpressed *PBP1* from a multicopy vector. These strains were first grown on minimal medium with glucose (YNBD) and then switched to a non-fermentable rich medium containing glycerol and ethanol (YPGE) and grown for 8 hours prior to being harvested and being processed for RNA extraction, cDNA library prep, and sequencing. We excluded the strains lacking *PAB1*, namely the double knockout *pab1Δpbp1Δ* and the triple mutant *aac2^{A128P, A137D} pab1Δpbp1Δ* due to their lack of growth under strict non-fermentable conditions (Figure 3.3).

As previously mentioned, to define how Pbp1 modulates cellular responses to mitochondrial protein import stress, we performed bulk RNA-seq and differential expression analysis across genetic backgrounds and *PBP1* perturbations, including loss-of-function (referred to as “pbp1KO”) and overexpression via a multicopy vector (referred to as “PBP1OE”) in both *AAC2* wild type WT and *aac2^{A128P, A137D}* double mutant (“DM”) clogger backgrounds (Figure 3.4A-F; Supplemental Figures S3.1 and S3.2).

In the WT background, pbp1KO vs WT was characterized by increased expression of genes associated with cation transport and those involved in RNA processing pathways. In contrast, downregulated genes were involved in mitochondrial biogenesis and function, including mitochondrial protein import, aerobic respiration, and mitochondrial genome maintenance,

alongside depletion of protein refolding/chaperone and proteasome-associated functions (Figure 3.4A; Supplemental Figure S3.1A).

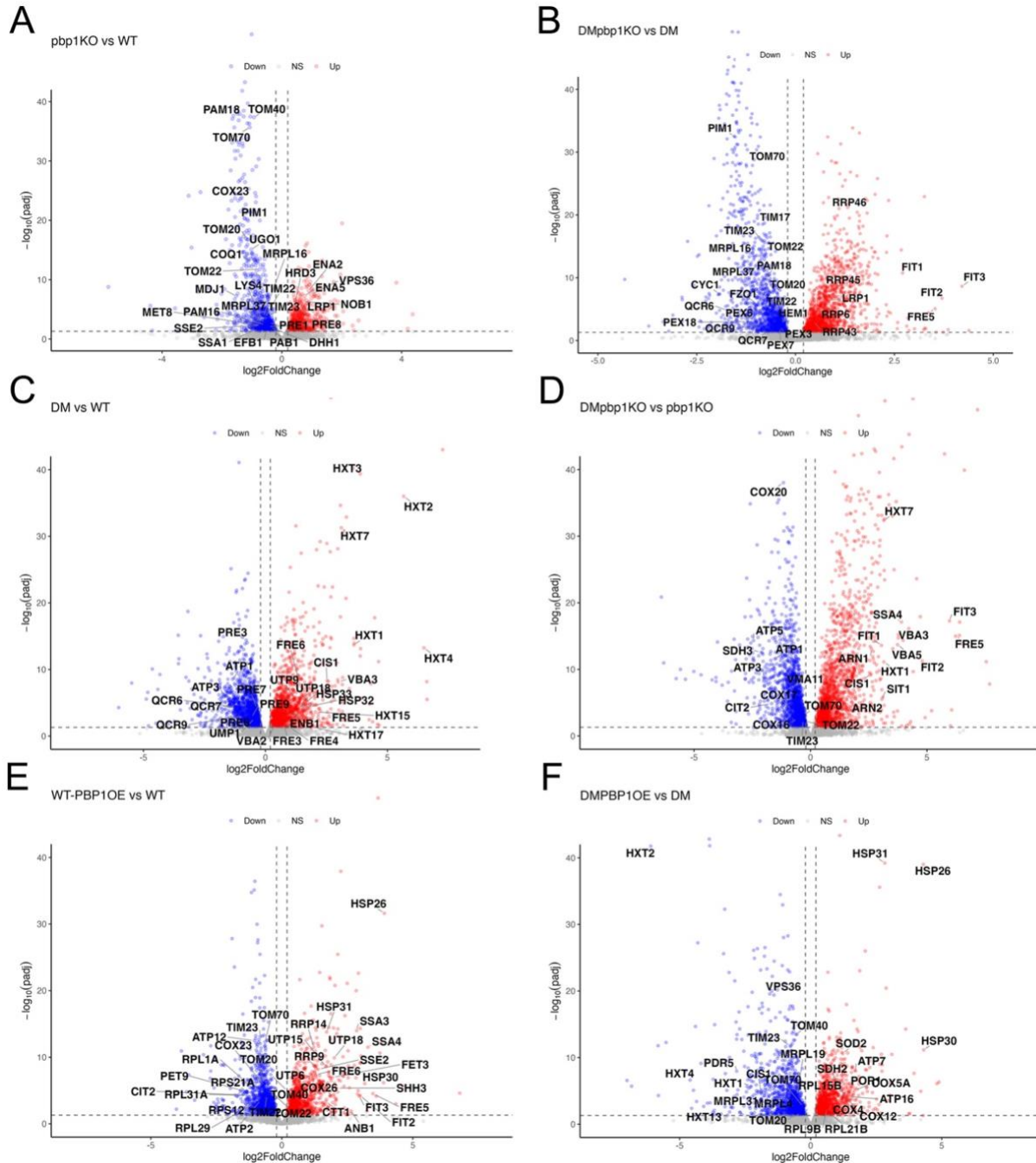


Figure 3.4. Pairwise differential expression analysis for the following contrasts: pbp1KO vs WT (A), DMpbp1KO vs DM (B), DM vs WT (C), DMpbp1KO vs pbp1KO (D), WT-PBP1OE vs WT (E), DM-PBP1OE vs DM (F). The x-intercept lines demarcate absolute log₂-fold change greater than 0.2, y-intercept line demarcates padj<0.05. Both these values are used to arbitrarily assign genes as significantly upregulated (red points) or downregulated (blue points).

In the context of import clogging, DMpbp1KO vs DM showed a pronounced increase in iron homeostasis programs and RNA metabolism signatures, including rRNA processing, nonfunctional RNA decay, and related RNA processing pathways. This transcriptional shift coincided with consistent depletion of mitochondrial biogenesis and functional programs, including protein import, electron transport chain, fatty acid β -oxidation, and other mitochondrial metabolism terms. Additional depleted pathways included vacuolar protein catabolic process and broader transport-associated categories, consistent with widespread remodeling of proteostasis and organelle homeostasis during clogging when PBP1 is absent (Figure 3.4B; Supplemental Figure S3.1A).

As expected from our prior work, DM vs WT exhibited strong upregulation of glucose transporter (*HXT* family) genes and iron starvation genes (*FRE* gene family), along with enrichment of rRNA/snoRNA-associated signatures. The stress-response gene *CISI* was upregulated as well. In contrast, depleted genes included those with mitochondrial respiration-related functions, as well as those involved in proteasomal and vesicle-mediated/ER-to-Golgi transport processes (Figure 3.4C; Supplemental Figure S3.2A).

Comparing DMpbp1KO vs pbp1KO (i.e., to identify transcriptional changes introduced by clogging in a pbp1KO background) further strengthened the iron homeostasis signature and revealed more prominent depletion of mitochondrial biogenesis and function programs than was apparent in DM vs WT alone, consistent with a heightened mitochondrial stress state when clogging occurs in the absence of Pbp1 (Figure 3.4D; Supplemental Figure S3.2B).

PBPI overexpression also elicited context-dependent transcriptional effects. In *AAC2* WT cells, WT-PBP1OE vs WT induced a robust stress response signature (including multiple heat

shock genes), along with enrichment of genes involved in broader RNA regulatory processes (e.g., transcriptional regulation/nucleocytoplasmic transport-type functions), while mitochondrial biogenesis-related genes, including multiple *TOM* and *TIM* import components, were downregulated (Figure 3.4E; Supplemental Figure S3.1C). Strikingly, in the clogger DM background, DMPBP1OE vs DM was associated with an increased expression of multiple mitochondrial respiration-related genes (including several COX/ATP genes), while heat shock genes also remained elevated. Concurrently, several mitochondrial import components remained downregulated (including *TOM20*, *TOM40*, *TIM23*, and *TOM70*). Similarly, genes involved in glucose transport as well as mitochondrial translation were also depleted (Figure 3.4F; Supplemental Figure S3.2C). Together, these data suggested that *PBPI* gene dosage may result in distinct transcriptional outputs in the WT versus import-clogged DM cells, with particularly strong effects on stress adaptation, iron homeostasis, and mitochondrial functional programs.

3.3.e] *PBPI* dosage exerts context-dependent transcriptional effects in WT and import-clogged cells

To directly assess the effects of *PBPI* dosage on cellular transcriptional programs, we compared *PBPI* overexpression (PBP1OE) to *PBPI* deletion (*pbp1KO*) within either an *AAC2* wild-type (WT) or the import-clogged double mutant *aac2^{A128P, A137D}* (DM) background. This contrast was chosen to maximize the dynamic range of Pbp1-dependent effects and to determine whether mitochondrial protein import clogging alters the cellular response to changes in *PBPI* expression (Figure 3.5A-F).

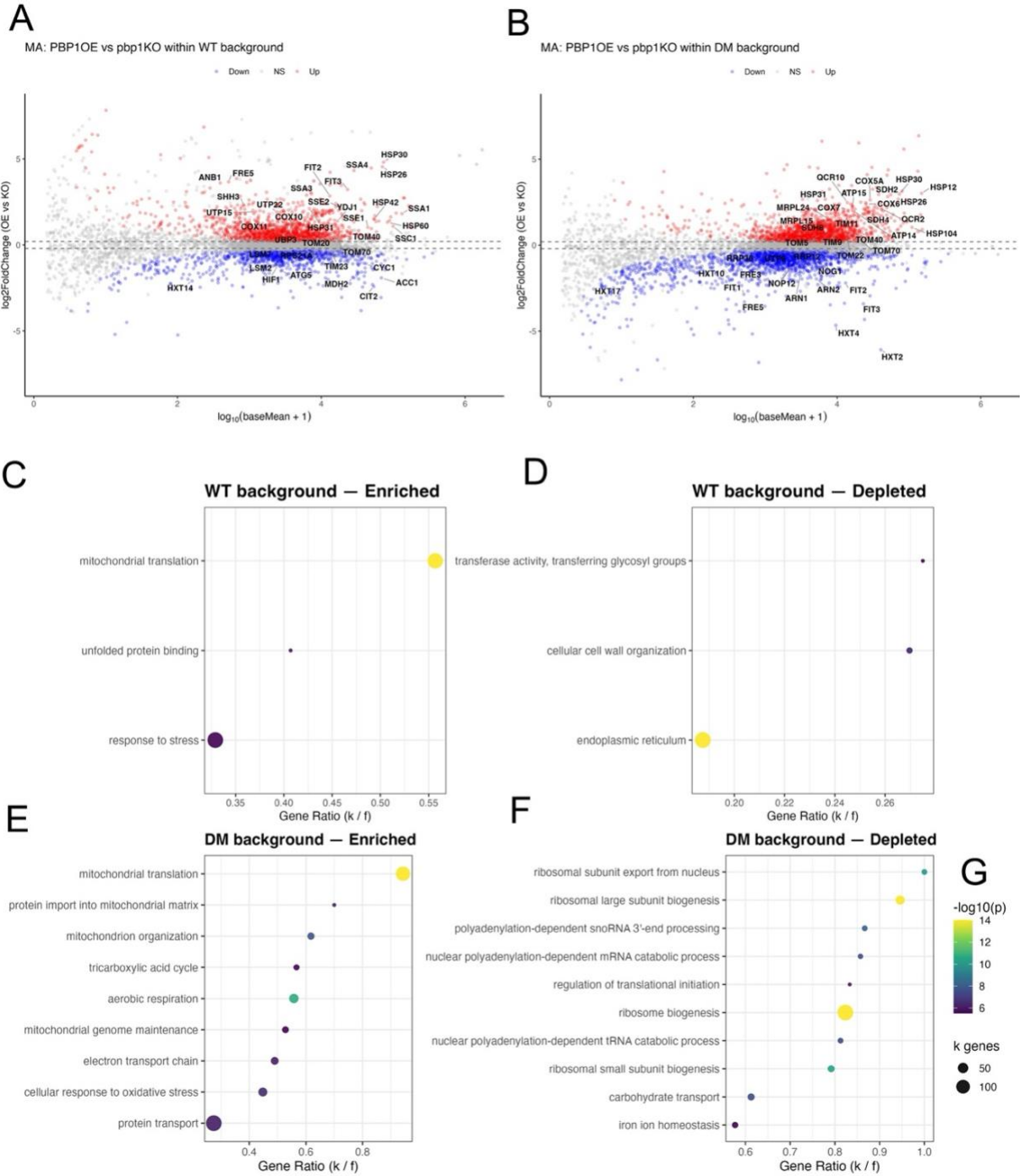


Figure 3.5. Differences in PBP1 gene dosage affect cellular transcription depending on presence or absence of clogging. MA interaction plots showing differential expression in PBP1OE relative to pbp1KO in (A) WT background or (B) DM background. Pathways enriched (C) or depleted (D) in the WT background. Pathways enriched (E) or depleted (F) in the DM background. Pathway analysis was conducting using an online database called Funspec. Gene lists that agreed with the cutoff $\text{padj} < 0.01$ were used for pathway enrichment ($\log_2\text{foldchange} > 0$) or depletion ($\log_2\text{foldchange} < 0$). Bonferroni correction was applied ($p < 0.01$) to obtain significant pathway lists.

In the WT background, comparison of PBP1OE vs *pbp1*KO revealed upregulation of genes associated with protein refolding and heat shock responses, including multiple *HSP* family members. In addition, several mitochondria-associated genes involved in respiration (e.g., *COX10*, *COX11*) and protein import (including *TOM40* and *TOM70*) showed increased expression, whereas the essential import component *TIM23* was downregulated. Genes involved in iron homeostasis (including *FIT2*, *FIT3*, and *FRE5*) were also induced. In contrast, multiple glucose transporter genes were downregulated (Figure 3.5A). These transcriptional changes were similar to, but more robust than those observed in the single-contrast analyses, namely *pbp1*KO vs WT and PBP1OE vs WT (Figure 3.4A and 3.4E). Pathway analysis supported these gene-level trends, revealing enrichment of mitochondrial translation and unfolded protein binding and stress response pathways, alongside depletion of pathways associated with cell wall organization and endoplasmic reticulum-related functions (Figure 3.5C-D).

In the DM background, changes in *PBPI* expression elicited a markedly different transcriptional response. Comparison of PBP1OE vs *pbp1*KO within the DM background revealed strong enrichment of genes involved in mitochondrial biogenesis and function, including in mitochondrial translation, protein import into the mitochondrial matrix, electron transport chain activity, tricarboxylic acid cycle, aerobic respiration, mitochondrial organization, and genome maintenance. Concurrently, genes and pathways associated with cytosolic ribosome biogenesis, cytosolic translation, carbohydrate transport, and iron homeostasis were downregulated (Figure 3.5B, 3.5E-F). Again, these data were consistent with the trends observed in single-contrast analyses, namely DM*pbp1*KO vs DM and DMPBP1OE vs DM (Figure 3.4B and 3.4F).

In addition to analyzing gene dosage-specific effects of PBP1, we also analyzed the reciprocal interaction of the clogger allele *aac2^{A128P, A137D}* (DM) with the *PBPI* expression status, *PBPI*-deletion (*pbp1KO*) environment versus *PBPI*-overexpression (*PBP1OE*) environment, using multifactorial analysis. In the *pbp1KO* environment, the mitochondrial protein import clogger allele (DM), relative to WT, induces a transcriptional response dominated by upregulation of genes involved in iron homeostasis, RNA processing, and protein folding/refolding, consistent with elevated cytosolic stress and compensatory proteostatic pathways. In contrast, genes associated with mitochondrial biogenesis, respiratory chain assembly, and oxidative phosphorylation are more strongly downregulated in the DM cells relative to WT, indicating a blunted or suppressed mitochondrial adaptive response to import clogging when *PBPI* is absent (Supplemental Figure S3.3A). Strikingly, this pattern is reversed when *PBPI* is overexpressed. In the *PBP1OE* environment, the clogger elicits enhanced upregulation of genes involved in mitochondrial biogenesis and respiration, including components of the electron transport chain and ATP synthesis machinery, relative to that in WT cells. Conversely, genes linked to iron homeostasis and glucose transport are preferentially downregulated, suggesting reduced reliance on iron scavenging and fermentative metabolism under clogging conditions when *PBPI* levels are elevated (Supplemental Figure S3.3B).

Together, the *PBPI* dosage and the genetic interaction plots demonstrate that *PBPI* expression state fundamentally reshapes the cellular response to mitochondrial protein import clogging. Loss of *PBPI* biases the response toward cytosolic stress and repression of mitochondrial programs, whereas *PBPI* overexpression promotes a transcriptional shift favoring mitochondrial biogenesis and respiratory capacity during import clogging. Furthermore, these data underscore that *PBPI* interacts differently with wild type *AAC2* versus the clogger *aac2^{A128P, A137D}*.

3.3.f] Pbp1 localization becomes increasingly heterogeneous during respiratory growth, and this heterogeneity is amplified by mitochondrial protein import clogging

The strong gene signatures captured from *PBP1* loss or overexpression under steady and import-compromised states led us to wonder how the Pbp1 protein can rewire cellular transcriptional responses so drastically. It was previously shown that under respiring conditions, Pbp1, an otherwise mostly cytosolic protein, relocalizes to the vicinity of membranous organelles such as mitochondria, and can form foci termed 'nebulous assemblies' (YANG *et al.* 2019). This heterogeneity in localization as well as the formation of nebulous assemblies is distinct from Pbp1's classically described role in stress granule formation (BUCHAN *et al.* 2010; SWISHER AND PARKER 2010; BUCHAN *et al.* 2011). We wanted to test whether mitochondrial protein import state affects Pbp1's localization under fermentable or non-fermentable growth conditions.

To visualize Pbp1 localization under fermentable and non-fermentable growth conditions, we utilized yeast strains expressing chromosomally integrated Pbp1-mNeonGreen, with the tag at the C-terminus, in either the *AAC2* wild-type (WT) or *aac2^{A128P,A137D}* import-clogger (DM) backgrounds. Cells were precultured in minimal glucose medium and subsequently shifted to either rich glucose (fermentable) or glycerol/ethanol-containing (non-fermentable) medium prior to imaging.

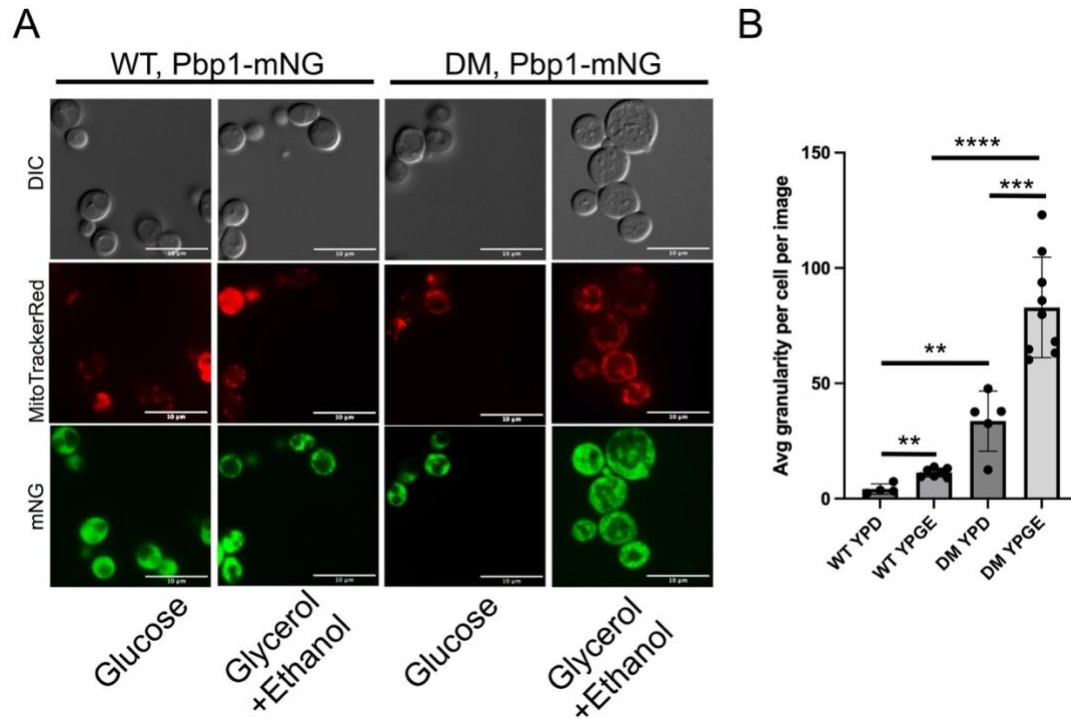


Figure 3.6. Pbp1 protein's localization becomes heterogeneous under respiring conditions, and this is exacerbated by protein import clogging. (A) Representative images of yeast cells expressing Pbp1-mNeonGreen (Pbp1-mNG) fusion protein. MitoTrackerRed staining was performed to visualize mitochondria, and DIC imaging allowed for the visualization of the complete yeast cell. Wild type cells shown on the left and clogger cells on the right, grown in either in glucose or glycerol and ethanol, as indicated. (B) Quantification of average granularity in Pbp1-mNG fluorescent signal. Each point represents an independent image. Scale bar denotes 10um.

In cells expressing wild-type Aac2, Pbp1 exhibited a modest increase in localization heterogeneity upon transition from fermentable to non-fermentable growth, as quantified by an increase in an average granularity value from ~5 to ~12. This observation is consistent with previous reports describing enhanced Pbp1 localization granularity under steady-state respiratory conditions (YANG *et al.* 2019). In contrast, cells expressing the *aac2*^{A128P, A137D} import-clogger protein displayed a markedly greater increase in Pbp1 localization heterogeneity. Upon shifting from fermentable to non-fermentable conditions, the average granularity value increased from ~35 to ~85, indicating a substantial redistribution of Pbp1 during import clogging (Figure 3.6A-B).

Notably, even under fermentable conditions, Pbp1 localization was more heterogeneous in the presence of import clogging compared to wild-type cells grown in either type of media (Figure 3.6B). Together, these data indicate that mitochondrial protein import clogging strongly enhances Pbp1 localization heterogeneity, particularly during respiratory growth, consistent with increased association of Pbp1 in the vicinity of membranous organelles such as mitochondria, as supported by colocalization with MitoTracker Red (Figure 3.6A). These observations raised the possibility that altered Pbp1 localization during mitochondrial protein import clogging reflects changes in its physical interaction network, which we next examined using proteomic approaches.

3.3.g] Pbp1's protein interactome is extensively rewired under mitochondrial protein import stress

While Pbp1 is primarily a cytosolic protein that also shuttles to the nucleus (SALVI *et al.* 2014; SALVI AND MEKHAIL 2015; OSTROWSKI *et al.* 2018), our current results and prior studies from Ben Tu's lab have shown that Pbp1 localization becomes increasingly heterogeneous when yeast cells are switched from fermentable to non-fermentable growth conditions (Figure 6) (YANG *et al.* 2019). We therefore asked which proteins interact with Pbp1 under these respiring conditions, and whether the Pbp1 interactome differs between steady-state and protein import-clogged conditions.

Our preliminary experiments showed that the Pbp1-mNeonGreen fusion protein (referred to as "Pbp1-mNG" or "mNG" throughout the manuscript) is detectable in both whole-cell lysates and membrane-enriched protein fractions but is more prone to degradation in the whole-cell lysates (Supplemental Figure S3.4A). This observation prompted us to use the membrane-enriched protein fraction, obtained by centrifugation at $\sim 21,000 \times g$, for immunoprecipitation of Pbp1 followed by

exploratory mass spectrometry (IP-MS) (Supplemental Figure S3.4B). Protein abundance differences between mNG-tagged strains and untagged controls were analyzed using a limma regression approach to generate adjusted *p-values* and log₂-normalized fold changes.

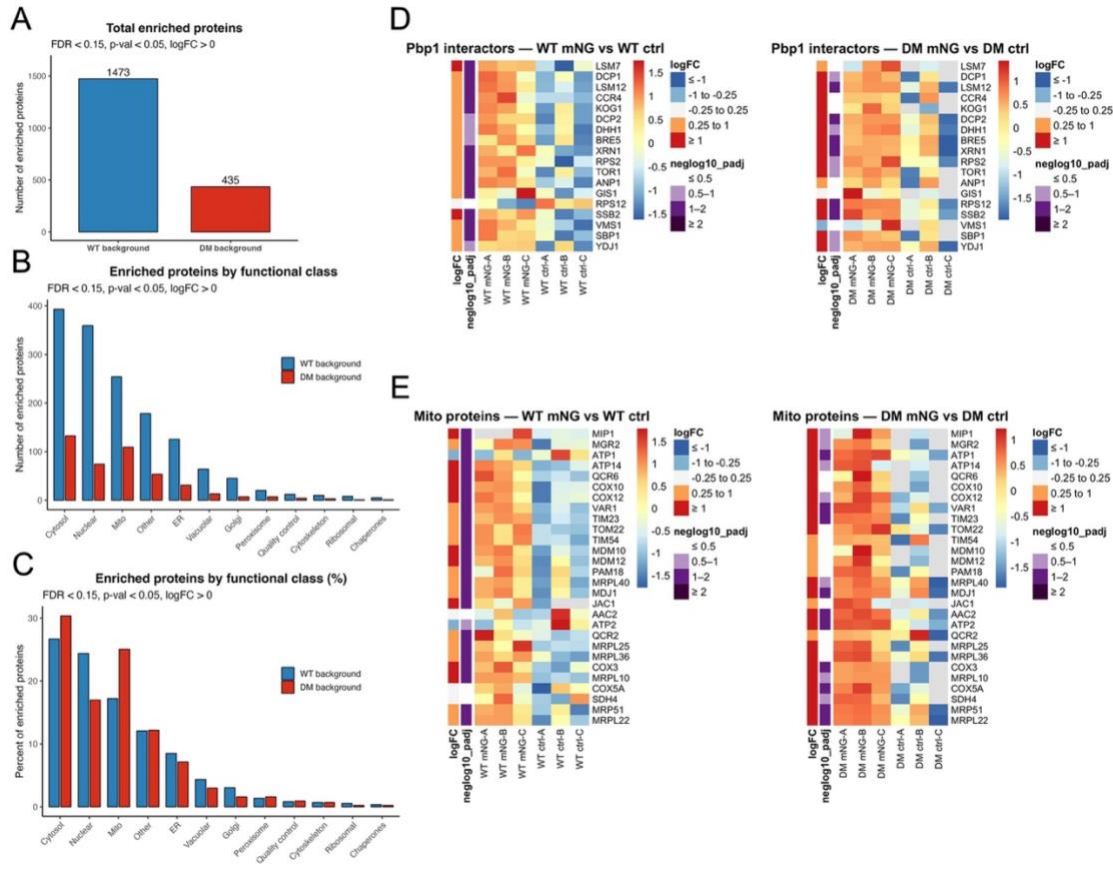


Figure 3.7. Pbp1 immunoprecipitation (IP) reveals the types of proteins Pbp1 interacts with under respiring conditions, with or without import clogging. (A) Total enriched proteins in the Pbp1-IP elution in the Aac2 WT (blue) or clogger DM (red) background. (B) Raw counts of enriched proteins by functional class in the WT (blue) or DM (red) background. (C) Percentage of proteins in each functional class in the WT (blue) or DM (red) background. (D) Known interactors of Pbp1 enriched in the WT background (left) or the DM background (right). (E) Subset of mitochondrial proteins enriched with Pbp1 in the WT background (left) or DM background (right). For (D) and (E), each biological replicate is shown. For each heatmap, the three tagged replicates (containing Pbp1-mNG fusion protein) are shown to the left of the three untagged control replicates.

Our Pbp1 IP-MS analysis revealed that in the *AAC2* wild-type (WT) background, Pbp1 associated with 1,473 proteins, whereas in the *aac2^{A128P, A137D}* import-clogger (DM) background, Pbp1 interacted with only 435 proteins (Figure 3.7A). Of these enriched proteins, 1253 were uniquely enriched in the WT background, 215 were uniquely enriched in the DM background, and 220 were shared in both *Aac2* expression backgrounds (Supplemental Figure S3.5). We next examined the functional categories and cellular compartments represented among these putative interactors. The majority of identified proteins were cytosolic, followed by nuclear and mitochondrial proteins. Additionally, lesser-represented categories included endoplasmic reticulum (ER), vacuolar, Golgi, peroxisomal, cytoskeletal, ribosomal, and proteostasis-associated classes (including quality control factors and chaperones). As expected, the total number of proteins in each functional class was higher in the WT background compared to the DM background (Figure 3.7B). Interestingly, analysis of the percentage of enriched proteins by functional class revealed a distinct trend: the relative proportion of mitochondrial and cytosolic proteins enriched in the DM background was greater than in the WT background (Figure 3.7C).

In addition to generating a global visualization of enriched and depleted proteins across the two datasets (Supplemental Figure S3.6), we curated two focused heatmaps highlighting known Pbp1 interactors acquired from prior studies (CARY *et al.* 2015; CABALLERO *et al.* 2025), and a subset of mitochondrial proteins enriched as putative Pbp1 interactors in our dataset (Figure 3.7D and 3.7E). Finally, pathway analysis of enriched proteins indicated that, in the WT background, Pbp1 interacts with proteins involved in pathways associated with nucleosome mobilization, ribosome biogenesis, mRNA processing, mitochondrial translation and protein transport. In contrast, in the DM background, the Pbp1 interactome, while still including ribosome biogenesis and RNA processing factors, was heavily rewired to include proteins involved in the tricarboxylic

acid cycle, pyridoxal phosphate binding, and redox-related processes (Figure 3.8). Together, these IP-MS data suggest that Pbp1’s interactome is extensively remodeled under mitochondrial protein import-clogging conditions.

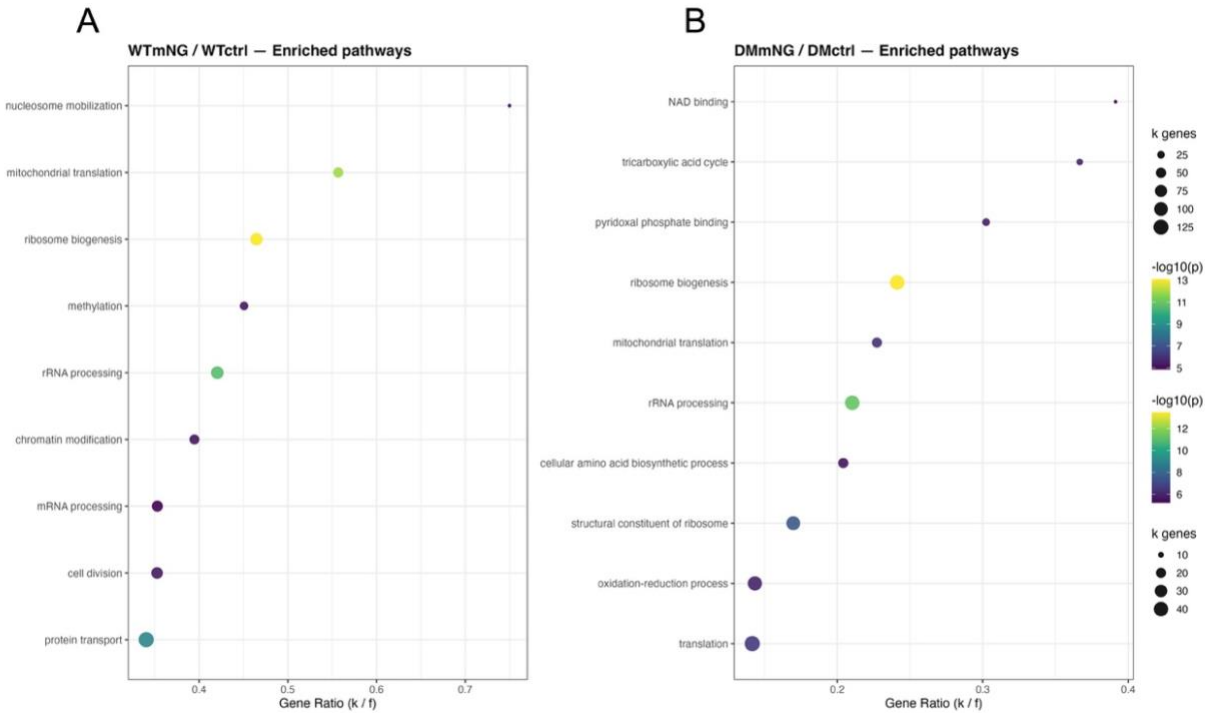


Figure 3.8. Pathways represented by the proteins associating with Pbp1 in the WT background (A), or DM background (B). For IPMS, due to low replicate numbers in the experiment, FDR (padj) cutoff was relaxed to include any protein with padj<0.15, while maintaining p<0.01 and log2-fold change>0. The resulting protein lists were used as input in the online database Funspec to perform pathway analysis with Bonferroni correction on all the pathways discovered (p<0.01).

3.3.h] Pbp1’s RNA interactome is dramatically reduced and rewired under mitochondrial protein import-clogging conditions

Pbp1 is an RNA-binding protein (RBP) that interacts with RNAs and multiple proteins to maintain cellular homeostasis (SWISHER AND PARKER 2010; KIMURA *et al.* 2013; SALVI *et al.* 2014; OSTROWSKI *et al.* 2018; YANG *et al.* 2019; VAN DE POLL *et al.* 2023; CABALLERO *et al.* 2025). In addition to identifying the protein interactors of membrane-associated Pbp1, we sought to define the RNA species that associate with Pbp1 under respiring conditions, either in the presence or

absence of mitochondrial protein import clogging. To this end, we immunoprecipitated Pbp1-mNeonGreen (Pbp1-mNG) using the same methodology as for our IP-MS experiments, followed by RNA extraction from the immunoprecipitated fraction and RNA sequencing. To account for global transcriptional changes, we defined “true RNA interactors” by quantifying RNAs enriched in the immunoprecipitated fraction (“RIP”) relative to total RNA isolated from whole-cell lysates (“Total”).

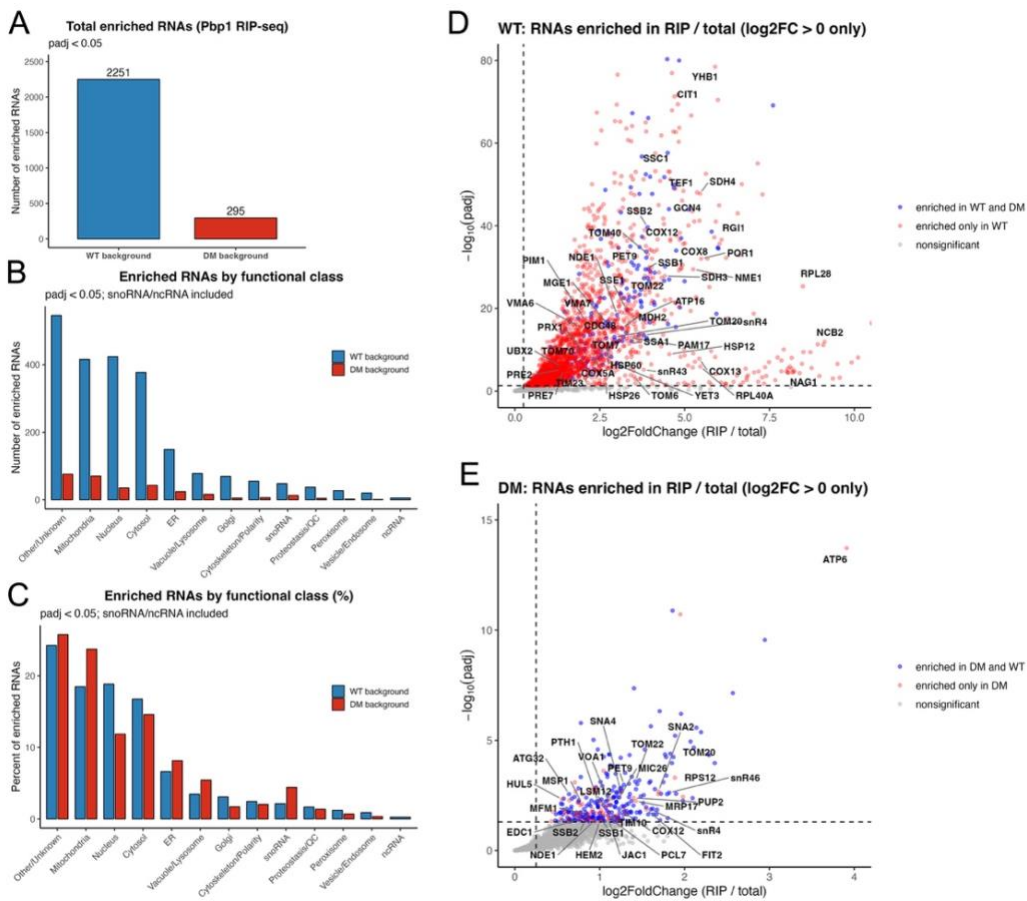


Figure 3.9. RNAs enriched with Pbp1 protein under respiring conditions, with or without protein import clogging. (A) total number of enriched RNAs in WT (blue) or DM (red) backgrounds. (B) total/raw number of enriched RNAs by functional class in WT (blue) or DM (red) backgrounds. (C) Percentage of enriched RNAs by function class in WT (blue) or DM (red) backgrounds. (D) Volcano plot for RNAs enriched in the IP fraction normalized to total RNA in the WT background, labeled for unique hits (red) or genes shared with DM background (blue). (E) Volcano plot for RNAs enriched in the IP fraction normalized to total RNA in the DM background, labeled for unique hits (red) or genes shared with WT background (blue).

Our analysis revealed that Pbp1 associated with 2,251 unique RNA transcripts in cells expressing wild-type Aac2 (WT background), but only 295 transcripts in cells expressing the *aac2^{A128P, A137D}* import-clogger protein (DM background) (Figure 3.9A). Most of these enriched transcript types were protein-coding RNAs, while a small percentage were non-coding RNAs such as snRNAs and snoRNAs (Supplemental Figure S3.7). When subclassified by functional class, the raw number of enriched RNAs was higher in every category in the WT background compared to DM (Figure 3.9B). However, when analyzed as percentages, Pbp1 associated with a greater proportion of transcripts that encoded proteins belonging to the functional class of mitochondria (both nuclear-encoded and mitochondrially encoded), ER, and vacuole in the DM background relative to WT (Figure 3.9C). These trends closely mirrored those observed in our Pbp1 proteomics dataset (Figure 3.7).

Among enriched RNAs, a substantial fraction was shared between the WT and DM backgrounds, while distinct subsets were uniquely enriched in each condition (Supplemental Figure S3.8). In the WT background, Pbp1 associated with transcripts encoding proteins involved in mitochondrial biogenesis (*TOM20, TOM22, TOM70, TIM23, TOM40*), mitochondrial respiration (*COX8, COX12, COX13*), protein folding and refolding (*HSP12, HSP26, SSC1, SSB2*), and ubiquitin-proteasome machinery-associated pathways (*PRE2, PRE7, UBX2, CDC48*) (Figure 3.9D; Supplemental Figure S3.9A). In the DM background, many of these RNA interactions were lost. The interactions that remained included transcripts encoding a select few mitochondrial biogenesis factors (*TOM22, TOM20, TIM10*), respiratory components (*COX12, NDE1*), and protein-folding factors (*SSB1, SSB2*). Notably, RNAs uniquely enriched in the DM background included transcripts encoding known mitochondrial stress-response and protein quality control factors involved in mitoCPR (*MSP1*), polyubiquitination (*HUL5*), and mitoRQC (*PTH1*) (Figure

3.9E; Supplemental Figure S3.9B). Together, these findings indicate that the Pbp1-RNA interactome is both markedly reduced and substantially remodeled in the DM background.

Given the striking differences between the enriched RNA types in the WT and DM backgrounds, we next asked which transcripts exhibited the most pronounced changes in association with Pbp1 under import-clogging conditions relative to steady-state protein import. Transcripts that showed significantly reduced association with Pbp1 in the DM background relative to WT encoded proteins involved in ribosomal subunits, the tricarboxylic acid cycle, the electron transport chain, glycolysis, and endocytosis. In contrast, transcripts that exhibited increased association with Pbp1 in the DM background relative to WT encoded proteins involved in rRNA processing, DNA repair, and ribosome biogenesis, as well as noncoding RNAs such as *snR68* (Figure 3.10A, 3.10B). Thus, our data support the claim that mitochondrial protein import clogging profoundly alters both the composition and functional bias of the Pbp1-RNA interactome.

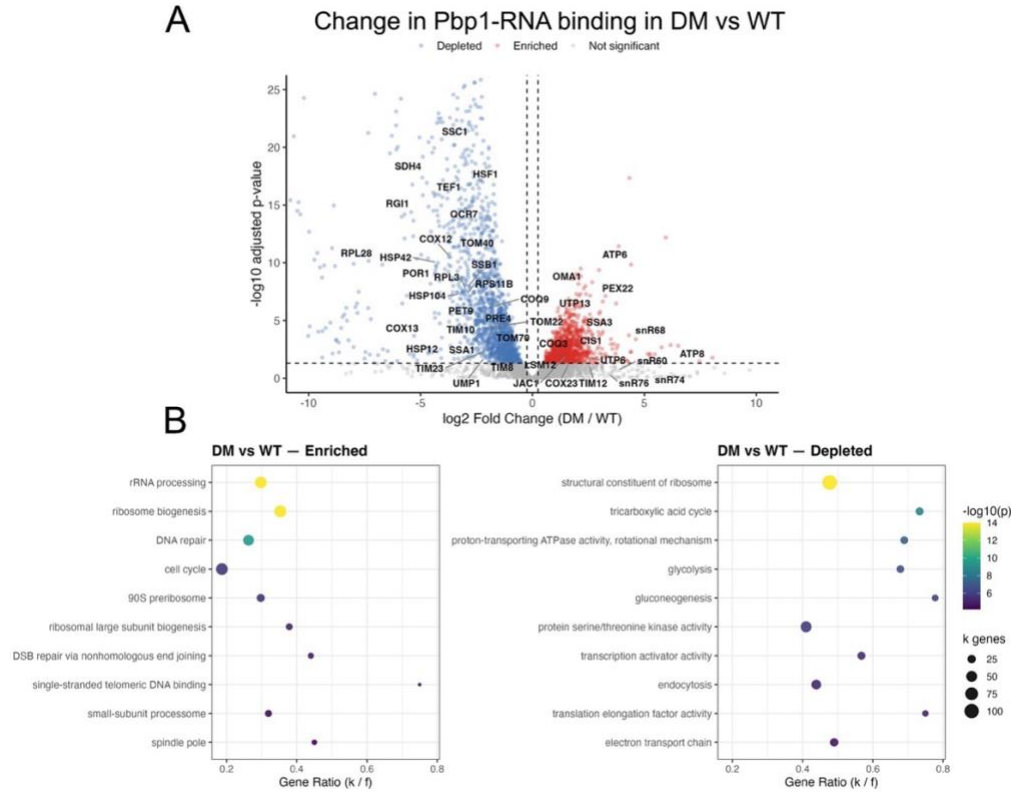


Figure 3.10. A large fraction of RNAs undergo a reduction in binding to Pbp1 under protein import clogging conditions. (A) Volcano plot for RNAs with significant binding alterations in the DM (clogging) background relative to WT. Genes with significantly increased binding are labeled as red points, while those with reduced binding are labeled as blue points. (B) Pathways represented by genes enriched (left) or depleted (right) in the DM background relative to WT. A threshold $p_{adj} < 0.01$ was utilized. Genes with $\log_2\text{-fold change} > 0$, or $\log_2\text{-fold change} < 0$ were used as inputs for pathway enrichment or depletion in the online database Funspec. Bonferroni correction ($p < 0.01$) was applied before generating pathway lists.

3.4] DISCUSSION

The quality of mitochondrial genome integrity directly impacts human health and disease (CASTELLANI *et al.* 2020; GUSTAFSON *et al.* 2020). Recently, mitochondrial protein import clogging has been defined as a mechanism for human disease and a mechanism for mtDNA instability (COYNE *et al.* 2023). Hence there is a dire need to identify novel molecular pathways that can restore mitochondrial protein import efficiency and support mitochondrial genome integrity, as a means to treat mitochondria-induced diseases. Using *Saccharomyces cerevisiae* as a model, we performed a multicopy suppressor screen to identify genes and pathways that suppress petite colony formation, as a readout for improved mtDNA integrity under import clogging conditions.

Our multicopy suppressor screen recovered several classes of factors. First, we identified genes involved in proteostasis, including suppressors that produced strong rescue (e.g., *UMPI*, *UBP11*) and others with weaker suppressor phenotypes (e.g., *PRE8*) (RAMOS *et al.* 1998; AMERIK *et al.* 2000; VELICHUTINA *et al.* 2004). We also recovered suppressors linked to mitochondrial protein import (*PAMI6*) and mitochondrial contact site and cristae organizing system or MICOS complex (*MIC26*), which acted as weaker suppressors in our screen (FRAZIER *et al.* 2004; PFANNER *et al.* 2014). Notably, the strongest suppressors included *PABI* and *PBPI*, which encode RNA binding proteins (RBPs) that are involved in stress granule formation, as well as *YHB1* and *PRX1*, which are well-known antioxidant and redox homeostasis genes (PEDRAJAS *et al.* 2000; CASSANOVA *et al.* 2005; SWISHER AND PARKER 2010). The recovery of proteostasis and mitochondria-associated factors provided proof-of-concept validation for the screen, while the strong suppressor phenotypes associated with *PABI* and *PBPI* suggested a potentially

underappreciated connection between RNA-binding proteins, stress granule biology, and mtDNA stability during mitochondrial protein import clogging (Figure 3.1).

Because the red pigment phenotype used to score suppressor strength could, in principle, arise from effects unrelated to restoration of mtDNA stability, we performed additional assays to directly test whether suppressors improved mitochondrial health. Using pMitoLOC, we quantified mitochondrial morphology and protein import (VOWINCKEL *et al.* 2015). Suppressor-transformed clogger cells showed increased tubularity and mitochondrial network connectedness relative to untransformed or empty-vector-transformed clogger cells, and in many cases approached wild-type morphology. Importantly, this analysis also distinguished strong versus weak suppressors at the level of membrane potential-dependent import. Strong suppressors supported import of both Su9 and the mitochondrial membrane potential-dependent Cox4 reporter, whereas in weak suppressor-transformed clogger cells, Cox4 staining remained more diffuse in the cytosol, suggesting that in weak suppressor-transformed cells, there was only partial rescue of mtDNA loss that was insufficient to adequately restore mitochondrial membrane potential (Figure 3.2). Together, these data support the conclusion that the suppressors identified in our screen can improve mitochondrial homeostasis during import clogging, with strong suppressors exhibiting a more complete restoration of membrane potential-dependent protein import.

Several well-studied mitochondrial toxins and stresses, such as sodium azide, sodium arsenite, hydrogen peroxide, and heat shock, are known to induce stress granule formation (EMARA *et al.* 2012; FRYDRYSKOVA *et al.* 2020; GARG *et al.* 2020; EIERMANN *et al.* 2022). However, a direct role for stress granules in mitochondrial biogenesis and function remains unclear, despite reports linking stress granule-associated factors to processes such as fatty acid β -oxidation,

oxidative stress responses, and mitochondria-associated aging phenotypes (CAO *et al.* 2020; AMEN AND KAGANOVICH 2021). Motivated by the strong suppressor phenotypes of *PAB1* and *PBP1* in our screen, we focused on understanding how these stress granule-associated genes restore mtDNA stability and import efficiency under import clogging conditions.

Genetic analysis supported an important role for *PBP1* and *PAB1* in maintaining cellular fitness when mitochondrial function is required. Deletion of *PAB1* is lethal, whereas *PBP1* is non-essential, and cells can tolerate *PAB1* loss in the background of *PBP1* loss (MANGKALAPHIBAN *et al.* 2024). Consistent with prior studies, mutants lacking both *PAB1* and *PBP1* grew slowly, and in our study the presence of import clogging further exacerbated the growth defect, causing the triple mutant strain *aac2^{A128P, A137D}pab1Δpbp1Δ* to fail to grow under respiring conditions. *PBP1* loss alone also caused a mild defect that was exacerbated at 25°C and 37°C, especially under respiring conditions, and was made worse by the concurrent presence of import clogging. Because 37°C induces heat shock in yeast cells and stress granules are known to form in response to heat shock (BUCHAN *et al.* 2008; TAKAHARA AND MAEDA 2012), loss of *PBP1* and/or *PAB1* under heat shock conditions is expected to compromise growth. In contrast, 25°C induces cold sensitivity in *Aac2* mutants (WANG *et al.* 2008; WANG AND CHEN 2015; COYNE *et al.* 2023; MISHRA *et al.* 2025), providing a plausible explanation for why phenotypes involving the clogger strain were more severe at 25°C. Growth medium also strongly influenced phenotype severity: loss of *PBP1* and *PAB1*, as well as expression of the clogger allele, had a more severe impact on cells under non-fermentable conditions compared to fermentable conditions, consistent with the indispensability of mitochondrial function during respiratory growth. At the same time, the phenotypes observed under fermentable conditions emphasize the essentiality of mitochondria independent of their role in respiration (LILL AND KISPAL 2000; CHEN 2004; TRABA *et al.* 2009). Finally, these growth

defects correlated with mtDNA instability: strains lacking *PBP1* and/or *PABI* displayed increased petite frequency, which was further elevated in the presence of protein import clogging (Figure 3.3). Collectively, these results support the model that *PBP1* and *PABI* function as genetic suppressors of mtDNA instability, and that their disruption compromises growth and mtDNA integrity during mitochondrial protein import clogging.

Next, we wanted to understand how cells adapt to the loss of these RBP-encoding genes, especially under respiring conditions. Since *PABI* loss by itself is deleterious, and because its loss in the setting of *PBP1* deletion does not grow under respiring conditions, we did not include *PABI* deletion strains in our transcriptomic analysis. To understand how *PBP1* modulates cellular homeostasis in the presence and absence of import clogging, we performed bulk RNA-seq in *AAC2* wild type and clogger backgrounds under *PBP1* loss (“pbp1KO”) or *PBP1* overexpression (“PBP1OE”) conditions. Our transcriptomic analysis revealed that *PBP1* exerts context- and gene dosage-dependent effects on cellular transcriptional programs. In the *AAC2* wild-type background, *PBP1* loss was associated with downregulation of mitochondrial biogenesis genes, whereas in the *aac2^{A128P, A137D}* clogging background, pbp1KO was associated with increased expression of iron homeostasis genes alongside consistent downregulation of genes involved in mitochondrial biogenesis and function. PBP1 overexpression also produced context-dependent effects. In *AAC2* wild-type cells, PBP1OE induced the upregulation of protein-folding and iron homeostasis genes, while mitochondrial biogenesis and respiration-associated genes were downregulated. In contrast, in the clogging background, PBP1OE increased expression of genes associated with mitochondrial function and protein stress response, while downregulating gene programs associated with glucose transport and mitochondrial translation (Figure 3.4). Comparisons directly contrasting PBP1OE versus pbp1KO further strengthened these signatures (Figure 3.5). Together, these data indicate

that *PBP1* dosage rewires cellular transcriptional outputs during respiratory growth, and that these outputs are strongly shaped by mitochondrial protein import state, i.e., steady-state or import-clogged state.

The drastic rewiring of transcriptional programs by *PBP1* under respiring conditions, with or without the presence of import clogging, led us to investigate the Pbp1 protein's localization and physical interaction networks. Prior work reported that under respiring conditions, Pbp1, while largely diffuse in the cytosol under fermentable conditions, relocates to the vicinity of membranous organelles such as mitochondria and can form foci termed “nebulous assemblies” (YANG *et al.* 2019). Our imaging data were consistent with this behavior and further showed that mitochondrial protein import clogging amplifies Pbp1 localization heterogeneity. Specifically, even under fermentable growth baseline conditions, Pbp1 localization was more heterogeneous in the presence of import clogging relative to *AAC2* wild type, and this heterogeneity increased markedly during respiratory growth (Figure 3.6). These findings raised the possibility that changes in Pbp1 localization during protein import clogging reflect changes in its physical interaction network, which we examined using proteomic and RNA interactomic approaches.

Strikingly, both the Pbp1 protein interactome and the Pbp1 RNA interactome were dramatically reduced and rewired under import clogging conditions (Figures 3.7-3.10, Supplemental Figure S3.7-S3.9). In our membrane fraction-based IP-MS, Pbp1 associated with substantially fewer proteins in the import-clogger background than in *AAC2* wild type. Similarly, RIP-seq revealed that Pbp1 associated with far fewer RNA transcripts in the clogging (DM) background than in wild type (WT). While the raw numbers of proteins and RNAs associating with Pbp1 was reduced in the DM background, the percentage of proteins and RNA species

belonging to the mitochondrial functional class, i.e., nuclear- and mitochondrially-encoded RNA and proteins, was greater in the DM background compared to that seen in WT (Figure 3.7). This shift is consistent with increased Pbp1 protein associating with, or being in close proximity to, the mitochondrial surface during import clogging conditions under respiratory growth. At the same time, the overall reduction in interactors suggests that mitochondrial protein import clogging may “sequester” Pbp1 near the mitochondrial surface, preventing it from performing its full set of physiological functions (Figure 3.8). If this hypothesis is correct, it may help explain why *PBPI* overexpression rescues mitochondrial biogenesis even under import clogging conditions: increased *PBPI* expression could allow the Pbp1 protein to regain its lost protein-protein and protein-RNA interactions and restore homeostasis despite ongoing import clogging (Figure 3.11).

This interpretation is particularly intriguing in light of recent studies suggesting that up to 20% of the nuclear-encoded mitochondrial proteome is imported co-translationally, as well as reports that RNA-binding proteins (RBPs) interact closely with the TOM complex to buffer RNAs and nascent polypeptides during import (AKRAM *et al.* 2025; BAI *et al.* 2025; ZHU *et al.* 2025). Since import clogging causes a build of unimported mitochondrial proteins in the vicinity of the TOM complex, RBPs such as Pbp1 may become saturated by preprotein buildup, or worse become trapped in aggregates, effectively sequestering them away from performing their cellular duties. Future studies will need to be conducted to shed more light on this proposed mechanism. Alternatively, the reduced protein and RNA interactome that we observed from the membrane-associated Pbp1 immunoprecipitation could be due to proteostatic mechanisms during import clogging that either cause increased protein and RNA turnover, or reduced translation and transcription.

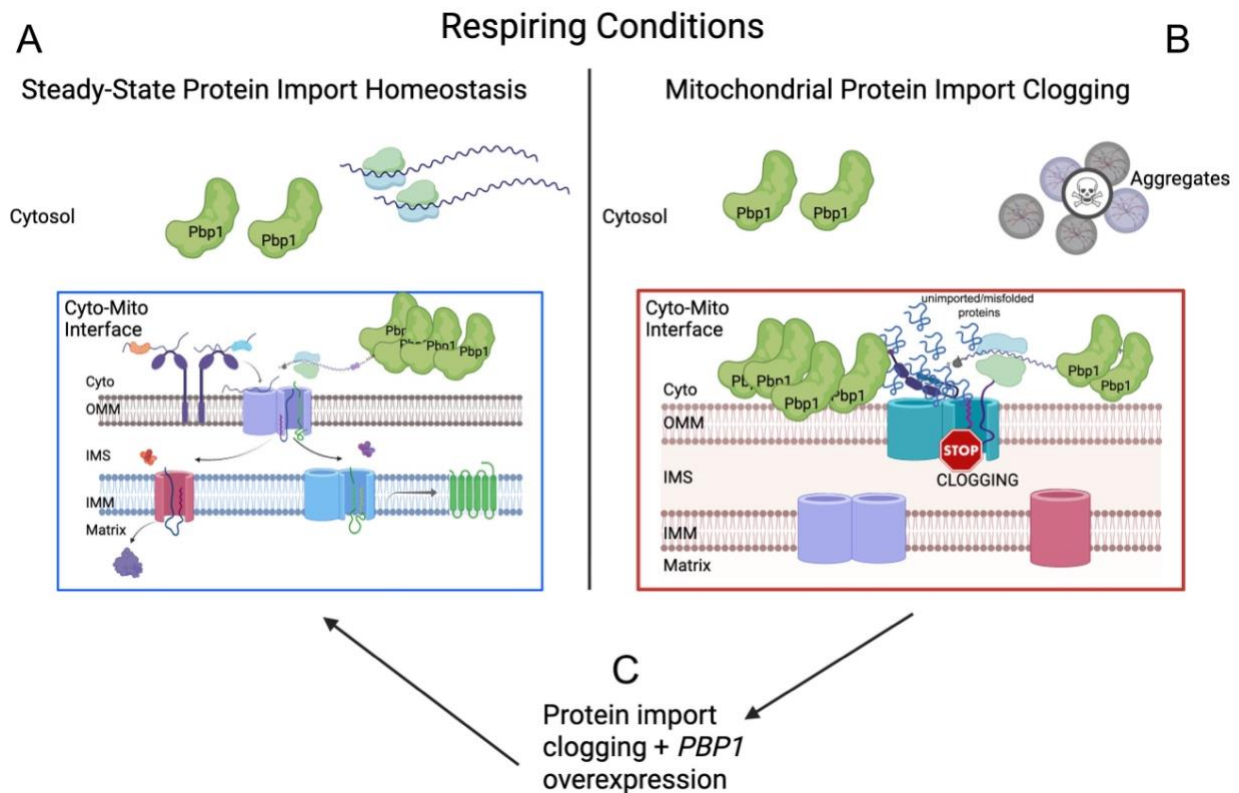


Figure 3.11. Working model for Pbp1's role in maintaining mitochondrial protein import efficiency. (A) Steady state protein import under respiring conditions allow Pbp1 to associate with membranous organelles such as mitochondria, while maintaining cytosolic/nuclear localizations as well. Pbp1 is able to freely interact with other proteins and RNAs that it regulates/modulates. (B) Protein import clogging sequesters Pbp1 on the mitochondrial surface and causes Pbp1 to lose a high majority of its protein and RNA interactions. Pbp1 gains a few unique stress-associated interactions in the clogging background, however due to the severity of import clogging, is unable to protect the growth of cells. (C) *PBP1* overexpression may restore Pbp1's ability to interact with its physiological binding partners, allowing it to restore mitochondrial biogenesis and mitochondrial respiration.

Our IP-MS and RIP-seq datasets also revealed the enrichment of several well-known Pbp1-interacting proteins (e.g., Dcp1, Dcp2, Dhh1, Lsm7, Lsm12), supporting the specificity of our proteomics dataset. However, several additional well-established interactors (including Pab1, Puf3, and Mkt1) were not enriched (SWISHER AND PARKER 2010; VAN DE POLL *et al.* 2023; CABALLERO *et al.* 2025). A likely explanation is the design of our experiment: we immunoprecipitated Pbp1 specifically from a membrane-enriched fraction to focus on the subset

of Pbp1 associated with membranous organelles under respiring conditions, which likely underrepresents Pbp1 complexes that are predominantly cytosolic or nuclear (SALVI *et al.* 2014; SALVI AND MEKHAIL 2015; CABALLERO *et al.* 2025). Thus, an important limitation of our study is that whole-cell lysate immunoprecipitation may have better captured additional canonical Pbp1 interactions that are missed in our membrane fraction enrichments.

Another important limitation of our study is the complicated relationship between suppression of petite colony formation and the stability of the mitochondrial genome. Notably, petite colony formation does not necessarily imply loss of mtDNA. For example, mutants affecting vacuolar function and acidification, including *vma* mutants, exhibit severe oxidative stress sensitivity and poor growth on non-fermentable carbon sources while still retaining mitochondrial DNA (ρ^+). Similarly, vacuolar trafficking mutants such as *vps16 Δ* can form petites associated with mitochondrial genome instability, often retaining mtDNA in an altered ρ^- state rather than becoming fully ρ^0 . Together, these mutants highlight that respiratory growth defects and petite colony phenotypes can arise without complete degradation of the mitochondrial genome (MILGROM *et al.* 2007, FOX AND STAEMPFLI 1982).

On the other hand, nuclear mutations that disrupt mitochondrial nucleotide metabolism or inner membrane homeostasis, such as human ANT1 and yeast AAC2, can destabilize the mitochondrial genome and promote severe mtDNA loss (KAUKONEN *et al.* 2000; FONTANESI *et al.* 2004). In yeast, this instability can ultimately result in ρ^0 derivatives. There exists a small possibility that our *aac2* mutant clogger strain might be causing respiratory deficiency without necessarily fully destabilizing mtDNA. Although our pMitoLOC imaging assay supports the hypothesis that the genetic suppressors of petite colony formation are improving mtDNA which in

turn is improving protein import of Cox4-mCherry and Su9-GFP proteins, we still do not directly show an improvement in mtDNA integrity. To test mtDNA integrity directly in the clogger cells as well as the clogger strain transformed with genetic suppressors, it would be crucial to perform mtDNA-targeted PCR or Southern blot which can distinguish between intact and destabilized mtDNA.

Finally, several questions remain. *PABI* loss is lethal, yet cells can tolerate *PABI* loss in the background of *PBPI* loss. Why? Does this reflect *PBPI* gene dosage effects, changes in Pbp1-dependent translational control, or compensatory remodeling of RNA metabolism when *PABI* is absent? Additionally, does *PBPI* overexpression under steady-state conditions dysregulate aspects of Pbp1 function, potentially contributing to the mild proteostatic stress signatures observed in the *AAC2* wild-type background? Given that the human homolog of Pbp1, Ataxin-2, is mutated in several human diseases (OSTROWSKI *et al.* 2017; LAFFITA-MESA *et al.* 2021), our findings may provide novel insights into how altered dosage or localization of a stress granule-associated RNA-binding protein could influence mitochondrial homeostasis and mtDNA stability.

Overall, our study identified several strong suppressors of mtDNA loss under import clogging conditions. While we focused on the stress granule-associated genes *PBPI* and *PABI*, it will be important in future work to dissect the mechanisms underlying the strong suppression phenotypes displayed by the antioxidant signaling genes *YHB1* and *PRX1* (PEDRAJAS *et al.* 2000; CASSANOVA *et al.* 2005). We validated that disruption of Pbp1/Pab1 expression compromises cell growth, especially under respiring conditions, and destabilizes mtDNA, and we showed that Pbp1 localization becomes increasingly heterogeneous during respiratory growth and this heterogeneity is amplified by mitochondrial protein import clogging. Finally, we characterized global

transcriptomic changes resulting from changes in *PBP1* expression under steady-state and import-clogged conditions and demonstrated that import clogging severely remodels the Pbp1 protein and RNA interactomes. Together, these results establish Pbp1 as a key modulator of mtDNA stability and mitochondrial homeostasis during mitochondrial protein import clogging.

3.5] EXPERIMENTAL PROCEDURES

3.5.a] Yeast strains, plasmids, and transformations

All *Saccharomyces cerevisiae* (yeast) strains used are in the W303-1B strain background, with mating types *a* or α . Mutants lacking PBP1 were generated by PCR-based insertion of the $\Delta pbp1:URA3$ in a WT strain. The resulting $\Delta pbp1$ strain was crossed with the previously generated $aac2^{A128P,A137D}$ (DM) or clogger strain (COYNE *et al.* 2023) to create $aac2^{A128P,A137D}\Delta pbp1$ (DM $\Delta pbp1$, or ‘DMpbp1KO’) by homologous recombination. The strain $\Delta pab1\Delta pbp1$ (KMY07) was a gift from Dr. Allan Jacobsen at UMass Medical School, Worcester, MA. The triple mutant $aac2^{A128P,A137D}\Delta pab1\Delta pbp1$ was generated by homologous recombination in this study.

For Pbp1 fluorescence microscopy experiments, PBP1-mNeonGreen-hygromycinR (*PBP1-mNG-hph*) was PCR amplified from the C-SWAT GFP library generated in the BY4741 background by Dr. Maya Schuldiner and colleagues (WEILL *et al.* 2018). The PCR amplicon was transformed into wild type W303-1B cells by lithium acetate/polyethylene glycol method (GIETZ AND WOODS 2002) and confirmed for chromosomal integration by genotyping PCR. The *PBP1-mNG-hph* strain, henceforth called ‘WTmNG’, was crossed with the clogger strain (DM). This generated $aac2^{A128P,A137D}\text{-}PBP1\text{-}mNG\text{-}hph$ by homologous recombination, henceforth called ‘DMmNG’.

Co-transformation with multicopy suppressors and pMitoLOC plasmid was done in a stepwise manner. First, the clogger strain was transformed with each of the subcloned multicopy plasmids for each genetic suppressor being studied, and transformants were selected using *URA3* or *LEU2* as the markers, based on the plasmid backbone. Next, while maintaining selection for the transformed suppressor plasmids in the clogger strain, the cells were transformed with the pMitoLOC plasmid (VOWINCKEL *et al.* 2015) using the antibiotic nourseuthricin (NAT) as the

selection marker. The dual-transformed cells were grown by maintaining selection pressures for both types of plasmids, namely the multicopy suppressor and pMitoLOC, using selective media (synthetic complete either lacking uracil (SC-Uracil) or (leucine SC-Leucine)) and 100ug/mL NAT, respectively. For controls, the wild type (WT), clogger (DM), and clogger strain transformed with empty plasmid (DM+empty vector), were also transformed with the pMitoLOC plasmid and the resulting transformants were selected as previously described.

3.5.b] Multicopy suppressor screen

Clogger strain was transformed with a *YEP13M4* plasmid-based multicopy suppressor library using *LEU2* gene as selection marker. Transformants were picked from a lawn grown on minimal media containing yeast nitrogenous base and glucose (YNBD) and all auxotrophic amino acids (methionine, lysine, uracil, tryptophan, histidine and adenine) except leucine (SC-Leucine). Transformed single colonies were streaked onto plates containing 1% yeast extract, 2% peptone, and 2% dextrose (YPD) and grown at 25 °C, which is the temperature at which the clogger strain only forms petite colonies, i.e., colonies in which cells have lost mtDNA stability (Figure 3.1).

Suppressors of mtDNA instability were identified by color difference, i.e., clogger cells transformed with a plasmid that suppressed petite colony formation produced red pigment similar to wild type *W303-1B* cells possessing an *ade2* mutation that causes red pigment formation due to reactive oxygen species generated from mitochondrial respiration. The transformed clogger cells that resembled wild type in the red color phenotype were picked and re-plated on the Leucine-minus minimal media plates to purify the transformant by yeast DNA miniprep, bacterial transformation and plasmid miniprep. The plasmids from the miniprep were retransformed back into the clogger strain to reconfirm the red pigment phenotype. Once this was confirmed, the purified, miniprepped, and phenotypically validated plasmid was sent for Sanger sequencing to

confirm the gene(s) present in the plasmid. 325 total colonies were screened, and the sequenced plasmids were subdivided into a list of strong, medium, and weak suppressors based on the intensity and frequency of red pigment development in transformed cells grown on YPD at 25 °C, more intense/frequent the red pigment, the stronger the suppressor of mtDNA instability.

The strongest suppressors that were either “proof-of-concept”, i.e., known to improve cellular proteostasis, or suppressors of novel biological significance were subcloned using HiFi PCR cloning based on the Gibson assembly method (GIBSON *et al.* 2009) such that each plasmid contained the open reading frame from a single gene and its endogenous promoter. After bacterial transformation and miniprep, the amplified plasmids were confirmed by DNA gel electrophoresis to contain the correct sized DNA bands corresponding to each gene insert. The subcloned multicopy plasmids, each containing coding sequence from a unique genetic suppressor, were transformed back into the clogger strain to verify the red pigment phenotype. The clogger strain was transformed with an empty vector as well, and this condition acted as a negative control.

3.5.c] Fluorescence microscopy and quantification with pMitoLOC plasmid

The control strains (WT, DM, and DM transformed with empty vector) as well as the experimental strains (clogger strains transformed with multicopy suppressor plasmids) expressing the pMitoLOC plasmid under NAT selection were grown overnight in rich complete (for WT or DM control), or rich selective media (for clogger strains expressing empty vector, or the multicopy suppressor plasmids) containing glucose at 25 °C to mimic poor growth conditions used for the multicopy suppressor screen. The next day, each strain was subcultured for 4 hours, washed with sterile double deionized water, and then resuspended in fresh medium prior to imaging.

On each glass slide, 5uL of cell mixture was placed. To this, 5uL of 1X concanavalin solution was added to adhere cells to the slide, and a coverslip was placed. Cells were imaged

using the 100X/1.46 oil lens on a Zeiss Imager Z1. The images were captured using the Zeiss software called Zeiss Zen (version 3.10) and saved as .czi files with their metadata. For downstream analysis, images were accessed using the open-source software FIJI (Fiji is Just ImageJ) and saved in .tiff and .jpeg formats for figure representation.

To classify mitochondrial shape as “tubular” or “punctate”, the open-source software called Cell Profiler was used. In Cell Profiler, image files associated with Su9-GFP fluorescence were opened in .tiff format and processed via a pipeline. In this pipeline, each image was first rescaled for intensity and then enhanced for features. To identify mitochondria, the pixel size range between 5 and 20. After detecting mitochondria, several parameters were measured such as diameters (long axis and short axis), area, granularity, eccentricity, etc. Any mitochondrion with an eccentricity less than 0.75, was counted as “punctate”, while all mitochondria with an eccentricity equal to or greater than 0.75 were counted as “tubular”. The percentage of tubular mitochondria relative to total was reported in the form of bar plots using Graphpad Prism, and t-tests were performed to determine statistical significance.

3.5.d] Fluorescence microscopy and quantification for Pbp1-mNG expressing strains

Strains expressing either wild type *AAC2* or clogger *aac2*^{A128P, A137D} were engineered to express Pbp1-mNeonGreen (Pbp1-mNG) fusion protein, via PCR or homologous recombination methods described above. The resulting *AAC2 PBPI-mNG* and *aac2*^{A128P, A137D} *PBPI-mNG* strains were grown on agar plates containing minimal medium and glucose for two days. The day prior to imaging, the strains were moved to liquid minimal medium containing glucose for 12 hours at 30 °C. At the end of this incubation, the strains were moved to either rich medium containing glucose (YPD, fermentable growth medium), or to rich medium containing glycerol and ethanol (YPGE, non-fermentable growth medium) and grown for 8 hours at 30°C. At the end of this incubation,

samples were harvested, stained with MitoTrackerRed (MTR) to label mitochondria with intact membrane potential, and resuspended in fresh medium (YPD or YPGE depending on the final incubation condition). Negative controls were included to identify exposure times where no non-specific autofluorescence could be detected.

On each glass slide, 5uL of cell mixture was placed. To this, 5uL of 1X concanavalin solution was added to adhere cells to the slide, and a coverslip was placed. Cells were imaged using the 100X/1.46 oil lens on a Zeiss Imager Z1. The images were captured using the Zeiss software called Zeiss Zen (version 3.10) and saved as .czi files with their metadata. For downstream analysis, images were accessed using the open-source software FIJI (Fiji is Just ImageJ) and saved in .tiff and .jpeg formats for figure representation.

To measure the heterogeneity of Pbp1's localization, we again made use of a pipeline in the open-source software called Cell Profiler. In this pipeline, image files associated with Pbp1-mNG fluorescence were opened in .tiff format, rescaled for intensity and then enhanced for features. Next the primary objects, in this case the yeast cells, were identified and counted by restricting the pixel size range from 30 to 120 (small cells to very large yeast cells). After the cells were identified, the total granularity of all cells within an image was measured. The average granularity was determined by dividing total granularity by the total number of cells in each field of view. This average was reported in the form of bar plots using Graphpad Prism, and t-tests were performed to determine statistical significance.

3.5.e] Bulk RNA-sequencing of genetically modified strains

3.5.e.1] Cell growth and RNA extraction

The following strains were included for the bulk RNA-sequencing assay: wild type (WT), *pbp1D*, *AAC2*^{WT} + *PBP1_426* overexpression (WT+PBP1^{OE}), *aac2A128P*, *A137D* (DM),

aac2A128P, A137D pbp1D, aac2A128P, A137D + PBP1_426 overexpression (DM+PBP1^{OE}). Each strain was grown as three biologically independent replicate samples at 30 °C at every stage of culture. Strains were first grown in 2mL of minimal medium containing glucose (YNBD) for 12 hours, and then transferred to 50mL flasks at a starting optical density (OD₆₀₀) ranging from 0.1 to 0.4 containing rich non-fermentable medium containing glycerol and ethanol (YPGE). The samples were grown for approximately 8 hours or until they reached an OD₆₀₀ around 1 to 1.4. At this stage, samples were collected and spun down at 2500xg for 15 minutes. Cell pellet was retained, and the supernatant discarded.

The cell pellet from the prior step was transferred to a fresh Eppendorf tube, washed with double deionized water and the mixture spun at 5000xg for 15 minutes to remove water and traces of media. To the resulting pellet, DEPC-treated glass beads (1/3rd of the cell pellet volume) and 300uL of RNA extraction buffer (50mM sodium acetate pH 5.2, 10mM EDTA pH 8.0, and 1% SDS) were added and the contents mixed by inverting the tube several times. To this mixture, an equal volume of 25:24:1 solution of phenol:chloroform:isoamyl alcohol (PCI), with phenol at pH 5.2 were added. The contents were vortexed to disrupt the cell wall, placed on ice, and then spun at 2500xg for 10 minutes. The aqueous phase was extracted into a fresh tube, and mixed again with equal volumes of PCI solution and spun to re-extract the aqueous phase. The resulting aqueous phase was mixed with equal volumes of chloroform, vortexed vigorously, and then spun to collect the aqueous phase. This aqueous phase volume was mixed with 1/10th volume of 3M sodium acetate (pH 5.2), 3 volumes of 100% ethanol, and 2uL of 1ug/uL glycogen to precipitate RNA. To ensure a high RNA yield, the samples were placed at -20 °C for 30 minutes, and then spun at max speed (16,000xg) for 25minutes to precipitate an RNA pellet. The RNA pellet was washed with 70% ethanol, spun again, and then dried for 5 minutes using a speed vacuum

apparatus. The clean RNA pellet was resuspended using DEPC-treated nuclease-free water and quantified on a nanodrop spectrophotometer prior to being submitted to the SUNY Molecular Analysis Core for downstream processing.

3.5.e.2] RNA sequencing for Bulk RNAseq Samples

RNA quality and quantity were assessed with the RNA 6000 Nano chip on the Agilent 2100 Bioanalyzer. For bulk mRNA sequencing, after rRNA depletion step using the QIAseq FastSelect -rRNA Yeast kit (Qiagen), sequencing libraries were prepared with the Illumina Stranded mRNA Prep, using 1ug RNA as input and the standard manufacturer's protocol. Library size and concentration were assessed with the D1000 Screen Tape on the Agilent 4150 TapeStation. All libraries were pooled and sequenced on the Illumina NextSeq 2000 instrument, with paired end 2x100bp reads. We obtained between 40-50 million reads per sample in our sequencing run.

3.5.f] mNeonGreen NanoTrap Immunoprecipitation (IP) for Mass Spectrometry (IP-MS) and RNA-sequencing (RIPseq)

3.5.f.1] Strain types and growth conditions

The following strains were utilized for proteomics and transcriptomics: WTmNG and DMmNG that contained PBP1 fused to mNeonGreen at the C-terminal end in the genome. Each strain was grown as three independent biological replicates at 30 °C with shaking through each stage of culture. For the first 12 hours, each replicate was grown in 2mL volume of liquid minimal media containing 2% glucose (yeast nitrogenous base with dextrose or YNBD) and auxotrophic amino acids required for growth. The strains were then expanded to 100mL YNBD and grown for another 12-14 hours. Finally, the 50mL cultures were spun down to remove YNBD medium and resuspended to grow for 8 hours in 1L of non-fermentable growth medium containing 1% yeast

extract, 2% peptone, 2% glycerol, and 2% ethanol (YPGE) supplemented with additional tryptophan and adenine in excess to suppress the growth of genomic revertant colonies.

3.5.f.2] Cell harvest and lysate preparation

At the end of 8 hours of growth in YPGE, samples from each flask were collected spun at 2500xg for 15 minutes at 4 °C. The cell pellet was retained and washed with 100mL sterilized double deionized water and spun the same way as the prior step. The cell pellet from this spin was resuspended in 20mL volume of 1X phosphate-buffered saline (PBS) and each sample tube placed on ice. Paraformaldehyde solution was added to each sample at a final concentration of 0.25%, and the samples were kept on ice for 10 minutes with gentle shaking. At the end of 10 minutes, the paraformaldehyde was quenched by adding glycine at a final concentration of 250mM. This step was done with vigorous shaking.

The sample mixture containing paraformaldehyde and glycine was diluted by adding 50mL of 1X PBS and spun at 5000xg for 10 minutes. The supernatant was discarded, and the cell pellet retained. DEPC-treated and autoclaved glass beads were added to the cell pellet at an approximate volumetric ratio of 1:3. Next, each sample received 800uL of lysis buffer (10mM Tris-Cl, 150mM NaCl, 0.5mM EDTA, 0.5% NP-40, RNase inhibitor, and protease inhibitors) and was then subjected to three rounds of bead beating for 45 seconds each (samples were kept on ice in between each round of bead-beating). The bead-beated samples were spun at low speed (2500xg) for 10 minutes to collect cell debris, unbroken cells, and glass beads. The supernatant from this spin was either kept as a small aliquot that acted as the whole cell lysate (WCL) or placed into another fresh tube which was subjected to a high-speed spin at 21,000xg for 1 hour at 4 °C. The pellet from this high-speed spin was the “membrane-associated 21,000xg fraction”, henceforth called “21kg fraction”. The supernatant was the “post-21kg cytosolic fraction”. The fusion protein Pbp1-mNG

was best detected in the 21kg fraction, and hence this fraction was used to immunoprecipitate the protein and RNA interactors of Pbp1.

3.5.f.3] mNeonGreen NanoTrap-IP for proteomics

Prior to performing the IP, two preclearing steps were utilized. The anti-mNeonGreen agarose beads slurry was aliquoted into 20uL volume tubes (one tube per sample) and incubated with 1mL of 1% BSA (bovine serum albumin) made in lysis buffer and placed on a nutator at 4 °C for 1 hour. At the end of the incubation, the anti-mNeonGreen beads were spun at 1000xg for 2 minutes to remove the 1% BSA and other debris, washed with fresh lysis buffer, and spun again to remove supernatant, and retain the pre-blocked and equilibrated anti-mNeonGreen agarose beads. Second, 260ug of “21kg fraction” lysate for each sample was incubated with 10uL of binding control agarose beads and placed on a rotator for 1 hour at 4 °C. At the end of the incubation, the lysate and control beads were spun at a very low speed (600xg) for 2 minutes to collect control beads and debris, and the supernatant was carefully collected which retained the pre-cleared lysate. Of this, 10ug of lysate was kept as “input fraction” for IP validation western blot. The remaining 250ug of precleared lysate was incubated with the 20uL of pre-blocked anti-mNeonGreen beads and rotated at 4 °C for 4 hours.

At the end of four hours, the lysate and beads mixture was spun at 1000xg and the supernatant was collected and saved as the “unbound” fraction. The beads were washed with 150uL of wash buffer (10mM Tris-Cl, 150mM NaCl, 0.5mM EDTA, 0.1% NP-40, RNase inhibitor, and protease inhibitors) and spun at 1000xg for 2 minutes, for a total of five washes. Wash fractions were collected and saved. The final pellet containing the anti-mNeonGreen beads after the 5th wash was incubated with 60uL of sample buffer containing beta-mercaptoethanol, glycerol, and 2% SDS at 95 °C for 2 minutes. The elution fractions were measured for their protein

concentrations using the Bradford assay. All samples were prepared at a concentration of 1 µg/µL by dilution if necessary. These normalized samples at a uniform concentration of 1 µg/µL were submitted to proteomics core at SUNY Upstate for further processing and mass spectrometry.

3.5.f.4] Sample digestion and cleanup for IP-MS

Fifty to 100 µg of proteins were digested using a modification of the FASP method (WISNIEWSKI *et al.* 2009). In-solution proteins were denatured with SDS (1% final concentration), reduced and alkylated with TCEP and chloroacetamide (10 and 40 mM final concentration) at 70°C for 5 minutes. After cooling, the proteins were added to a 10 kDa MWCO membrane filter (Pall, OD010C34) with 200 µL of solution “UA”: 8 M urea with 100 mM tris pH 8.5. The filters were centrifuged at 14,000 x g until nearly dry, then rinse three times with 100 µL of UA solution and three times with 100 µL of 50 mM ammonium bicarbonate. The proteins were digested overnight at 37°C using 0.5 µg of trypsin in 75 µL of 50 mM ammonium bicarbonate. The resulting peptides were recovered from the filtrate by adding 50 µL of 1% TFA and centrifuging across the filter, followed by desalting of 20 µg on 2-core MCX stage tips (RAPPSILBER *et al.* 2003) (3M, 2241). The stage tips were activated with ACN followed by 3% ACN with 0.1% TFA. Next, samples were applied, followed by two washes with 3% ACN with 0.1% TFA, and one wash with 65% ACN with 0.1% TFA. Peptides were eluted with 75 µL of 65% ACN with 5% NH₄OH (Millipore, 5.33003), and dried.

3.5.f.5] LC-MS methods

Samples were dissolved to a concentration of 0.25 µg/µL in water containing 2% ACN and 0.5% formic acid. Two µL were injected onto a pulled tip nano-LC column (New Objective, FS360-75-10-N) with 75 µm inner diameter packed to 25 cm with 3 µm, 120 Å, C18AQ particles (Dr. Maisch, r13.aq.0001). The column was maintained at 50°C with a column oven (Sonation

GmbH, PRSO-V2). The peptides were separated using a 120-minute gradient from 3 – 28% ACN, followed by a 7 min ramp to 85% ACN and a 3 min hold at 85% ACN. The column was connected inline with an Orbitrap Lumos (Thermo) via a nanoelectrospray source operating at 2.5 kV. The mass spectrometer was operated in data-dependent top speed mode with a cycle time of 2.5s. MS1 scans were collected at 120000 resolution with AGC target of 6.0E5 and maximum injection time of 50 ms. CID fragmentation was used followed by MS2 scans in the ion trap with AGC target 2.0E3 and 38 ms maximum injection time.

3.5.f.6] mNeonGreen NanoTrap-IP for RNA-sequencing

The initial steps of the NanoTRAP-IP for RNA sequencing (RIPseq) were identical to IP-MS, and consisted of pre-blocking the anti-mNeonGreen beads with 1% BSA, preclearing the “21kg fraction” lysates with the binding control agarose beads, and then incubating the precleared lysates with the pre-blocked anti-mNeonGreen agarose beads for 4 hours on a rotator at 4 °C. The only thing different was that instead of using 250ug of pre-cleared lysate with 20uL bead slurry, we used 350ug of precleared lysate with 30uL of bead slurry per sample. This was done to account for RNA degradation during sample handling.

At the end of the incubation, the lysate and beads mixture was spun and the unbound supernatant fraction was carefully removed. The beads were washed with 150uL of wash buffer similarly to that done for IP-MS but with the addition of an RNase inhibitor in the wash buffer (10mM Tris-Cl, 150mM NaCl, 0.5mM EDTA, 0.1% NP-40, RNaseIN, and protease inhibitors) and spun at 1000xg for 2 minutes, for a total of five washes. Wash fractions were collected and saved. The final pellet containing the anti-mNeonGreen beads bound to enriched lysate after the 5th wash were incubated with 250uL of proteinase K buffer (10mM Tris-Cl pH 7.5, 5mM EDTA, 1% SDS, 100ug/mL Proteinase K, 1M urea) per sample and placed at 55 °C for 30 minutes to

digest any proteins and help increase RNA yield. At the end of this incubation, samples were incubated at a temperature between 65 °C and 70 °C (it was ensured that the temperature did not exceed 70 °C) for 30 minutes to reverse any RNA-RNA or RNA-DNA crosslinks and increase RNA yield in our extraction.

3.5.f.7] RNA extraction steps for RIPseq

At the end of this incubation, an equal volume of PCI (25:24:1 of acidic buffered phenol:chloroform:isoamyl alcohol) was added to the samples, the samples were inverted several times to ensure mixing and then spun at max speed for 10 minutes. The aqueous phase was extracted and an additional extraction with PCI was performed. After the second PCI extraction, the resulting aqueous phase was incubated with an equal volume of chloroform, inverted several times, and spun. The resulting aqueous phase was placed in a tube containing 1/10th aqueous phase volume of 3M sodium acetate pH 5.2, 3 volumes of 100% ethanol, and 2uL of glycogen (1ug/uL stock concentration) and the samples incubated at -20 °C for an hour to ensure complete RNA precipitation.

The precipitated RNA samples were spun at max speed at 4 °C for 30 minutes. The supernatant was discarded and the crude RNA pellet was washed with 70% ethanol and spun again at max speed for 10 minutes. The clean RNA pellet was acquired post-spin after discarding supernatant, air dried for 15 minutes, and then dried using a speed-vacuum apparatus for 5 minutes to ensure removal of any trace ethanol. Drying time was controlled to make sure the pellet wasn't overdried and flaky. The dry RNA pellet was resuspended in nuclease-free DEPC treated water and analyzed for concentration and purity (by acquiring 260/280 and 260/230 ratios) on a nanodrop spectrophotometer. After this step, samples were clearly labeled and stored at -80 °C until being

transported to the SUNY Molecular Analysis Core for downstream processing and RNA-IP sequencing (RIPseq).

In parallel, total RNA was extracted from the whole cell lysate using the same methodology involving proteinase K incubation, PCI and chloroform extractions, and sodium acetate/ethanol/glycogen precipitation of RNA as mentioned above. The Total RNA samples acted as the background RNA signal from the cell, while the immunoprecipitated RNA (or RIP) was enriched for the RNA species associating with Pbp1. Additionally, untagged strains processed identically served as negative controls to account for nonspecific RNA binding to the anti-mNeonGreen NanoTRAP beads during immunoprecipitation. In summary, the experimental design comprised four strain backgrounds (WTmNG, DMmNG, ctrlWT, ctrlDM), two RNA fractions (RIP and Total), and three biological replicates per condition, yielding 24 samples.

3.5.f.8] RNA Sequencing steps for RIPseq

RNA quality and quantity were assessed with the RNA 6000 Nano chip on the Agilent 2100 Bioanalyzer. For RIP-seq samples, the QIAseq FastSelect -rRNA Yeast kit (Qiagen) was used to deplete ribosomal RNA, following manufacturer's instructions to incorporate the rRNA depletion step with the Illumina Stranded Total RNA Prep to prepare sequencing libraries, using 100ng RNA as input. Library size and concentration were assessed with the D1000 Screen Tape on the Agilent 4150 TapeStation. All libraries were pooled and sequenced on the Illumina NextSeq 2000 instrument, with paired end 2x100bp reads. Untagged control RIPseq samples resulted in 10-30 million reads per sample, while Pbp1-mNG tagged RIPseq samples resulted in 30 to ~50 million reads per sample. Total RNA samples from either the untagged control or tagged Pbp1-mNG strains resulted in ~30 to 55 million reads per sample.

3.5.g] Computational Analysis for Bulk RNAsequencing

Raw sequencing data (FASTQ files) were downloaded from Illumina BaseSpace and preprocessed using Partek Flow. Adapter sequences and low-quality bases were removed using Partek's built-in trimming pipeline. Trimmed reads were aligned to the *Saccharomyces cerevisiae* reference genome using Bowtie2, and aligned reads were assigned to annotated gene features using the *S. cerevisiae* annotation model. Gene-level read counts were exported from Partek Flow as comma-separated value (CSV) files for downstream analysis.

Gene count files were imported into R (version 4.2.1). Count values were coerced to integers as required for downstream differential expression analysis. Sample metadata, including genotype and experimental condition, were manually curated and used to construct a count matrix with genes as rows and samples as columns. Genes with fewer than 10 total counts across all samples were excluded prior to model fitting. Differential gene expression analysis was performed using the DESeq2 package. The DESeq2 design formula was specified as: $\sim aac2 + pbp1 + aac2:pbp1$, where *aac2* represented *AAC2* genotype (*AAC2*-WT or *AAC2*-DM) and *pbp1* represented *PBP1* status (WT, *pbp1Δ*, or *PBP1OE*), enabling assessment of main effects and genotype-dependent interaction effects. DESeq2 size-factor normalization and dispersion estimation were performed using default settings, and Wald tests were used to assess differential expression for specific contrasts of interest. Resulting p-values were adjusted for multiple hypothesis testing using the Benjamini-Hochberg method.

Differential expression results were visualized in the form of volcano plots, displaying log₂ fold change versus -log₁₀ adjusted p-value, and MA plots, displaying log₂ fold change as a function of mean normalized expression by using the ggplot2 package. Significance thresholds

were applied as described in the figure legends. To interpret transcriptional changes at the pathway level, significantly enriched and depleted gene sets were analyzed using FunSpec, and the Bonferroni correction was applied on all the pathways identified (Robinson et al. 2002). Functional categories and pathway terms identified by FunSpec were visualized using dot plots, with dot size representing gene counts or gene ratios and color representing statistical significance. All downstream data manipulation, visualization, and statistical analyses were performed in R using packages from the tidyverse ecosystem and custom scripts.

3.5.h] Computational Analysis for Pbp1 IP-MS proteomics

3.5.h.1] Database searching and label-free quantification

The MS data was searched using SequestHT in Proteome Discoverer (version 2.4, Thermo Scientific) against the *S. cerevisiae* proteome from Uniprot, containing 6816 sequences and a list of common laboratory contaminant proteins. Enzyme specificity was fully tryptic with up to 2 missed cleavages. Precursor and product ion mass tolerances were 10 ppm and 0.6 Da, respectively. Cysteine carbamidomethylation was set as a fixed modification. Methionine oxidation, protein-terminal methionine loss and acetylation were set as a variable modifications. The output was filtered using the Percolator algorithm with strict FDR set to 0.01. The results were exported in Microsoft Excel workbooks.

3.5.h.2] Proteomics data analysis and visualization

Protein abundance tables exported from Proteome Discoverer were analyzed in R (version 4.2.1). Grouped protein abundance values provided for each biological replicate were log₂-transformed prior to downstream analysis. Differential protein enrichment was assessed using linear modeling and empirical Bayes moderation implemented in the limma package. Enrichment

analyses were performed separately for WTmNG versus WT control samples and DMmNG versus DM control samples, allowing identification of proteins significantly enriched or depleted within each genetic background. Statistical significance was assessed using moderated p -values, with a nominal cutoff of $p < 0.05$. For visualization and summary analyses, including global heatmaps and bar plots, a relaxed false discovery rate threshold ($FDR < 0.15$) was applied while maintaining $p < 0.05$ to capture broader enrichment trends across replicates. Functional classification of enriched proteins was based on curated UniProt subcellular localization annotations and functional keywords.

Global heatmaps were generated using log₂-transformed grouped abundances across replicates with row-wise scaling, using pheatmap package. Data manipulation and plotting were performed using tidyverse and ggplot2 packages. In addition to unbiased global heatmaps, curated heatmaps were generated to highlight biologically relevant protein subsets. Known Pbp1 interactors were compiled from prior published studies (CARY *et al.* 2015; VAN DE POLL *et al.* 2023; CABALLERO *et al.* 2025) and the BioGRID database, and were explicitly labeled within focused heatmaps. A separate curated heatmap was generated to visualize mitochondrial proteins enriched in the proteomics datasets based on established mitochondrial annotations. Finally, pathway enrichment analysis was performed using FunSpec, using proteins with log₂ fold change greater than zero, $p < 0.05$, and $FDR < 0.15$ as input.

3.5.i] Computational Analysis for Pbp1 RIPseq

3.5.i.1] FASTQ preprocessing and read alignment

Raw sequencing reads (FASTQ files) were imported from Illumina BaseSpace into Partek Flow for preprocessing. Adapter sequences and low-quality bases were trimmed using default

Partek Flow settings. Trimmed reads were aligned to the *Saccharomyces cerevisiae* reference genome using Bowtie2, and aligned reads were annotated using the *S. cerevisiae* annotation model. Gene-level read counts were then generated within Partek Flow and exported as comma-separated value (CSV) files for downstream statistical analysis in R.

3.5.i.2] Read quantification and preprocessing

Gene-level read counts were generated using Partek Flow, with genomic features represented as rows and sequencing samples as columns. Gene annotations included systematic gene identifiers, transcript names, gene symbols, and gene and transcript biotypes. To retain both protein-coding and noncoding RNA species (including snoRNAs, tRNAs, and other ncRNAs), features lacking an annotated transcript name were assigned their corresponding systematic gene identifiers prior to downstream analysis. Partek-exported count tables contained non-integer values due to internal normalization during quantification. After importing these files into R (version 4.2.1) and prior to performing differential analysis, count values corresponding to sequencing samples were rounded and converted to integers to satisfy the assumptions of negative binomial modeling implemented in DESeq2.

3.5.i.3] Construction of count matrix and sample metadata

An integer-rounded count matrix was constructed with genes as rows and samples as columns. Sample metadata were derived from sample identifiers and encoded genotype (Aac2-WT or Aac2-DM), RNA fraction (RIP or Total), and biological replicate. All variables were treated as categorical factors, and sample ordering was verified to match the count matrix prior to model

fitting. Genes with fewer than 10 total counts across all samples were excluded prior to downstream analyses.

3.5.i.4] Identification and removal of background-associated (“sticky”) RNAs

To minimize nonspecific RNA recovery during immunoprecipitation, an initial background filtering step was performed using untagged control samples. Size factor-normalized counts were calculated for all genes, and normalized RIP vs Total ratios were computed separately for WT and DM untagged controls. Genes were classified as background-associated (“sticky”) if they exhibited both (i) reproducible RIP signal above a minimum abundance threshold (≥ 10 normalized counts) and (ii) ≥ 2 -fold enrichment in RIP relative to Total RNA in control samples. To ensure conservative background removal, only genes meeting these criteria in both genotypes were flagged as background associated. These genes were excluded from downstream hit calling but retained for quality-control analyses.

3.5.i.5] Differential RNA enrichment analysis using DESeq2

Following background RNA filtering, differential RNA enrichment was analyzed in R using DESeq2. A generalized linear model was fitted to compare RIP versus Total RNA within each genotype: \sim genotype + fraction + genotype:fraction

This design enabled identification of RNAs enriched or depleted in the Pbp1 RIP fraction relative to Total RNA while accounting for genotype-dependent differences in transcript abundance. Size factors and dispersion parameters were estimated using default DESeq2 settings, and statistical significance was assessed using Wald tests with Benjamini–Hochberg correction for multiple testing.

3.5.i.6] *Definition of contrasts*

Three primary contrasts were extracted from the fitted model:

1. WT RIP enrichment, defined as RNAs enriched or depleted in WT RIP relative to WT Total RNA.
2. DM RIP enrichment, defined as RNAs enriched or depleted in DM RIP relative to DM Total RNA.
3. Differential RNA binding in DM versus WT, defined by the interaction between genotype and RNA fraction, identifying RNAs whose association with Pbp1 was significantly altered (increased or decreased) due to mitochondrial protein import clogging.

Log₂ fold changes reflect relative enrichment or depletion in the RIP fraction or differential binding between genotypes.

3.5.i.7] *Visualization and downstream analyses*

Differential enrichment results were annotated with gene symbols and biotype information to facilitate visualization. Volcano plots were generated for the three contrasts defined above using background-filtered results for hit classification with the help of the ggplot2 package in R. Pathway enrichment analyses were performed using Funspec on significantly enriched or depleted gene sets (FDR < 0.05) and the discovered pathway lists were generated after performing the Bonferroni correction. Additional summary visualizations included bar plots depicting raw counts and percentages of enriched RNAs by functional class, as well as Venn diagrams illustrating RNAs uniquely enriched in the WT or DM backgrounds or shared between the two conditions.

3.6] Supporting Information

Acknowledgments - We thank Drs. Bruce Knutson and Ryan Palumbo for their help with subcloning the multicopy suppressor plasmids using HiFi PCR technique, Maya Schuldiner for sharing the SWAT-GFP-tagged yeast strains library and Dr. Allan Jacobsen for sharing the *pab1Δpbp1Δ* double knockout strain. We acknowledge the use of the AI tool ChatGPT in assisting us with writing code for computational analysis in R and for suggesting grammar edits to improve the clarity of this study.

Funding - This work was supported by National Institutes of Health grants R01AG063499 and R01AG061204 to X.J.C. The content is solely the responsibility of the authors and does not necessarily represent the official views of the National Institutes of Health. G.M. was the recipient of the American Heart Association Predoctoral Fellowship #1010959.

Conflicts of interest - The authors declare no conflicts of interest with the contents of this study.

Author contributions - **GM**: Conceptualization, Methodology, Formal Analysis, Investigation, Visualization, Data Curation, Writing, Funding Acquisition. **XW**: Resources, Methodology. **XJC**: Conceptualization, Investigation, Data Curation, Visualization, Formal Analysis, Methodology, Supervision, Funding Acquisition.

3.7] References for Chapter 3

- Akram, S., K. I. Zittlau, K. Sharma, J. C. Fitzgerald, N. Rafiq *et al.*, 2025 Proximity Labeling Reveals RNA-Binding Proteins Associating with the Human Mitochondrial Import Receptor TOMM20. *J Proteome Res.*
- Amen, T., and D. Kaganovich, 2021 Stress granules inhibit fatty acid oxidation by modulating mitochondrial permeability. *Cell Rep* 35: 109237.
- Amerik, A. Y., S. J. Li and M. Hochstrasser, 2000 Analysis of the deubiquitinating enzymes of the yeast *Saccharomyces cerevisiae*. *Biol Chem* 381: 981-992.
- Bai, Y., T. Ma, S. Zhao, S. Li, X. Wang *et al.*, 2025 Mitochondria-associated condensates maintain mitochondrial homeostasis and promote lifespan. *Nat Aging* 5: 1983-2002.
- Ballout, R. A., C. Al Alam, P. E. Bonnen, M. Huemer, A. W. El-Hattab and R. Shbarou, 2019 FBXL4-Related Mitochondrial DNA Depletion Syndrome 13 (MTDPS13): A Case Report With a Comprehensive Mutation Review. *Front Genet* 10: 39.
- Bevis, B. J., and B. S. Glick, 2002 Rapidly maturing variants of the *Discosoma* red fluorescent protein (DsRed). *Nat Biotechnol* 20: 83-87.
- Bharathi, V., A. Girdhar, A. Prasad, M. Verma, V. Taneja and B. K. Patel, 2016 Use of *ade1* and *ade2* mutations for development of a versatile red/white colour assay of amyloid-induced oxidative stress in *saccharomyces cerevisiae*. *Yeast* 33: 607-620.
- Buchan, J. R., D. Muhlrud and R. Parker, 2008 P bodies promote stress granule assembly in *Saccharomyces cerevisiae*. *J Cell Biol* 183: 441-455.
- Buchan, J. R., T. Nissan and R. Parker, 2010 Analyzing P-bodies and stress granules in *Saccharomyces cerevisiae*. *Methods Enzymol* 470: 619-640.
- Buchan, J. R., J. H. Yoon and R. Parker, 2011 Stress-specific composition, assembly and kinetics of stress granules in *Saccharomyces cerevisiae*. *J Cell Sci* 124: 228-239.
- Butow, R. A., and N. G. Avadhani, 2004 Mitochondrial signaling: the retrograde response. *Mol Cell* 14: 1-15.
- Caballero, D., B. M. Sutter, Z. Xing, C. Wang, E. Choo *et al.*, 2025 The yeast Mkt1/Pbp1 complex promotes adaptive responses to respiratory growth. *J Cell Biol* 224.
- Cao, X., X. Jin and B. Liu, 2020 The involvement of stress granules in aging and aging-associated diseases. *Aging Cell* 19: e13136.
- Cary, G. A., D. B. Vinh, P. May, R. Kuestner and A. M. Dudley, 2015 Proteomic Analysis of Dhh1 Complexes Reveals a Role for Hsp40 Chaperone Ydj1 in Yeast P-Body Assembly. *G3 (Bethesda)* 5: 2497-2511.
- Cassanova, N., K. M. O'Brien, B. T. Stahl, T. McClure and R. O. Poyton, 2005 Yeast flavohemoglobin, a nitric oxide oxidoreductase, is located in both the cytosol and the mitochondrial matrix: effects of respiration, anoxia, and the mitochondrial genome on its intracellular level and distribution. *J Biol Chem* 280: 7645-7653.
- Castellani, C. A., R. J. Longchamps, J. Sun, E. Guallar and D. E. Arking, 2020 Thinking outside the nucleus: Mitochondrial DNA copy number in health and disease. *Mitochondrion* 53: 214-223.
- Chen, H. Y., 2019 Why the Reactive Oxygen Species of the Fenton Reaction Switches from Oxoiron(IV) Species to Hydroxyl Radical in Phosphate Buffer Solutions? A Computational Rationale. *ACS Omega* 4: 14105-14113.
- Chen, X. J., 2004 Sal1p, a calcium-dependent carrier protein that suppresses an essential cellular function associated with the Aac2 isoform of ADP/ATP translocase in *Saccharomyces cerevisiae*. *Genetics* 167: 607-617.
- Chorghade, S., J. Seimetz, R. Emmons, J. Yang, S. M. Bresson *et al.*, 2017 Poly(A) tail length regulates PABPC1 expression to tune translation in the heart. *Elife* 6.
- Coyne, L. P., X. Wang, J. Song, E. de Jong, K. Schneider *et al.*, 2023 Mitochondrial protein import clogging as a mechanism of disease. *Elife* 12.

- de Almeida, A., J. de Oliveira, L. V. da Silva Pontes, J. F. de Souza Junior, T. A. F. Goncalves *et al.*, 2022 ROS: Basic Concepts, Sources, Cellular Signaling, and its Implications in Aging Pathways. *Oxid Med Cell Longev* 2022: 1225578.
- den Brave, F., U. Schulte, B. Fakler, N. Pfanner and T. Becker, 2024 Mitochondrial complexome and import network. *Trends Cell Biol* 34: 578-594.
- Dunn, E. F., C. M. Hammell, C. A. Hodge and C. N. Cole, 2005 Yeast poly(A)-binding protein, Pab1, and PAN, a poly(A) nuclease complex recruited by Pab1, connect mRNA biogenesis to export. *Genes Dev* 19: 90-103.
- Eiermann, N., G. Stoecklin and B. Jovanovic, 2022 Mitochondrial Inhibition by Sodium Azide Induces Assembly of eIF2alpha Phosphorylation-Independent Stress Granules in Mammalian Cells. *Int J Mol Sci* 23.
- El-Hattab, A. W., and F. Scaglia, 2013 Mitochondrial DNA depletion syndromes: review and updates of genetic basis, manifestations, and therapeutic options. *Neurotherapeutics* 10: 186-198.
- Emara, M. M., K. Fujimura, D. Sciaranghella, V. Ivanova, P. Ivanov and P. Anderson, 2012 Hydrogen peroxide induces stress granule formation independent of eIF2alpha phosphorylation. *Biochem Biophys Res Commun* 423: 763-769.
- Fontanesi, F., L. Palmieri, P. Scarcia, T. Lodi, C. Donnini *et al.*, 2004 Mutations in AAC2, equivalent to human adPEO-associated ANT1 mutations, lead to defective oxidative phosphorylation in *Saccharomyces cerevisiae* and affect mitochondrial DNA stability. *Hum Mol Genet* 13: 923-934.
- Fox, T.D. and S. Staempfli, 1982 Suppressor of yeast mitochondrial ochre mutations that maps in or near the 15S ribosomal RNA gene of mtDNA. *Proc Natl Acad Sci USA* 79(5): 1583-1587
- Franco-Iborra, S., T. Cuadros, A. Parent, J. Romero-Gimenez, M. Vila and C. Perier, 2018 Defective mitochondrial protein import contributes to complex I-induced mitochondrial dysfunction and neurodegeneration in Parkinson's disease. *Cell Death Dis* 9: 1122.
- Frazier, A. E., J. Dudek, B. Guiard, W. Voos, Y. Li *et al.*, 2004 Pam16 has an essential role in the mitochondrial protein import motor. *Nat Struct Mol Biol* 11: 226-233.
- Frydryskova, K., T. Masek and M. Pospisek, 2020 Changing faces of stress: Impact of heat and arsenite treatment on the composition of stress granules. *Wiley Interdiscip Rev RNA* 11: e1596.
- Garg, M., G. Poornima and P. I. Rajyaguru, 2020 Elucidation of the RNA-granule inducing sodium azide stress response through transcriptome analysis. *Genomics* 112: 2978-2989.
- Garipler, G., N. Mutlu, N. A. Lack and C. D. Dunn, 2014 Deletion of conserved protein phosphatases reverses defects associated with mitochondrial DNA damage in *Saccharomyces cerevisiae*. *Proc Natl Acad Sci U S A* 111: 1473-1478.
- Geissler, A., T. Krimmer, U. Bomer, B. Guiard, J. Rassow and N. Pfanner, 2000 Membrane potential-driven protein import into mitochondria. The sorting sequence of cytochrome b(2) modulates the deltapsi-dependence of translocation of the matrix-targeting sequence. *Mol Biol Cell* 11: 3977-3991.
- Gibson, D. G., L. Young, R. Y. Chuang, J. C. Venter, C. A. Hutchison, 3rd and H. O. Smith, 2009 Enzymatic assembly of DNA molecules up to several hundred kilobases. *Nat Methods* 6: 343-345.
- Gietz, R. D., and R. A. Woods, 2002 Transformation of yeast by lithium acetate/single-stranded carrier DNA/polyethylene glycol method. *Methods Enzymol* 350: 87-96.
- Gorospe, C. M., G. Carvalho, A. Herrera Curbelo, L. Marchhart, I. C. Mendes *et al.*, 2023 Mitochondrial membrane potential acts as a retrograde signal to regulate cell cycle progression. *Life Sci Alliance* 6.
- Gottschalk, B., Z. Koshenov, R. Malli and W. F. Graier, 2024 Implications of mitochondrial membrane potential gradients on signaling and ATP production analyzed by correlative multi-parameter microscopy. *Sci Rep* 14: 14784.
- Gustafson, M. A., E. D. Sullivan and W. C. Copeland, 2020 Consequences of compromised mitochondrial genome integrity. *DNA Repair (Amst)* 93: 102916.
- Hu, M. M., and H. B. Shu, 2023 Mitochondrial DNA-triggered innate immune response: mechanisms and diseases. *Cell Mol Immunol* 20: 1403-1412.

- Kaukonen, J., J. K. Juselius, V. Tiranti, A. Kytölä, M. Zeviani *et al.*, 2000 Role of adenine nucleotide translocator 1 in mtDNA maintenance. *Science* 289: 782-785.
- Kimura, Y., K. Irie and K. Irie, 2013 Pbp1 is involved in Ccr4- and Khd1-mediated regulation of cell growth through association with ribosomal proteins Rpl12a and Rpl12b. *Eukaryot Cell* 12: 864-874.
- Kovermann, P., K. N. Truscott, B. Guiard, P. Rehling, N. B. Sepuri *et al.*, 2002 Tim22, the essential core of the mitochondrial protein insertion complex, forms a voltage-activated and signal-gated channel. *Mol Cell* 9: 363-373.
- Laffita-Mesa, J. M., M. Paucar and P. Svenningsson, 2021 Ataxin-2 gene: a powerful modulator of neurological disorders. *Curr Opin Neurol* 34: 578-588.
- Lee, H. C., and Y. H. Wei, 2005 Mitochondrial biogenesis and mitochondrial DNA maintenance of mammalian cells under oxidative stress. *Int J Biochem Cell Biol* 37: 822-834.
- Lill, R., and G. Kispal, 2000 Maturation of cellular Fe-S proteins: an essential function of mitochondria. *Trends Biochem Sci* 25: 352-356.
- Lin, M., L. Hu, S. Shen, J. Liu, Y. Liu *et al.*, 2024 Atherosclerosis-related biomarker PABPC1 predicts pan-cancer events. *Stroke Vasc Neurol* 9: 108-125.
- Liu, Y., G. Fiskum and D. Schubert, 2002 Generation of reactive oxygen species by the mitochondrial electron transport chain. *J Neurochem* 80: 780-787.
- Liu, Y., X. Wang, L. P. Coyne, Y. Yang, Y. Qi *et al.*, 2019 Mitochondrial carrier protein overloading and misfolding induce aggresomes and proteostatic adaptations in the cytosol. *Mol Biol Cell* 30: 1272-1284.
- Malina, C., C. Larsson and J. Nielsen, 2018 Yeast mitochondria: an overview of mitochondrial biology and the potential of mitochondrial systems biology. *FEMS Yeast Res* 18.
- Mangkalaphiban, K., R. Ganesan and A. Jacobson, 2024 Pleiotropic effects of PAB1 deletion: Extensive changes in the yeast proteome, transcriptome, and translome. *PLoS Genet* 20: e1011392.
- Martensson, C. U., C. Priesnitz, J. Song, L. Ellenrieder, K. N. Doan *et al.*, 2019 Mitochondrial protein translocation-associated degradation. *Nature* 569: 679-683.
- Melber, A., and C. M. Haynes, 2018 UPR(mt) regulation and output: a stress response mediated by mitochondrial-nuclear communication. *Cell Res* 28: 281-295.
- Milgrom, E., Diab, H., Middleton, F. and P.M. Kane, 2007 Loss of vacuolar proton-translocating ATPase activity in yeast results in chronic oxidative stress. *J Biol Chem* 282 (10): 7125-7136
- Mishra, G., X. Wang, E. Fitzpatrick, A. Ghosh and X. J. Chen, 2025 Cellular proteostasis during mitochondrial protein import clogging requires the mitochondrial F-box protein 1 and DJ-1 homolog HSP31 in *Saccharomyces cerevisiae*. *Genetics*.
- Nishio, K., T. Kawarasaki, Y. Sugiura, S. Matsumoto, A. Konoshima *et al.*, 2023 Defective import of mitochondrial metabolic enzyme elicits ectopic metabolic stress. *Sci Adv* 9: eadf1956.
- Ostrowski, L. A., A. C. Hall and K. Mekhail, 2017 Ataxin-2: From RNA Control to Human Health and Disease. *Genes (Basel)* 8.
- Ostrowski, L. A., A. C. Hall, K. J. Szafranski, R. Oshidari, K. J. Abraham *et al.*, 2018 Conserved Pbp1/Ataxin-2 regulates retrotransposon activity and connects polyglutamine expansion-driven protein aggregation to lifespan-controlling rDNA repeats. *Commun Biol* 1: 187.
- Palmieri, L., S. Alberio, I. Pisano, T. Lodi, M. Meznaric-Petrusa *et al.*, 2005 Complete loss-of-function of the heart/muscle-specific adenine nucleotide translocator is associated with mitochondrial myopathy and cardiomyopathy. *Hum Mol Genet* 14: 3079-3088.
- Pedrajas, J. R., A. Miranda-Vizuete, N. Javanmardy, J. A. Gustafsson and G. Spyrou, 2000 Mitochondria of *Saccharomyces cerevisiae* contain one-conserved cysteine type peroxiredoxin with thioredoxin peroxidase activity. *J Biol Chem* 275: 16296-16301.
- Pfanner, N., M. van der Laan, P. Amati, R. A. Capaldi, A. A. Caudy *et al.*, 2014 Uniform nomenclature for the mitochondrial contact site and cristae organizing system. *J Cell Biol* 204: 1083-1086.
- Qi, Y., M. Wang and Q. Jiang, 2022 PABPC1--mRNA stability, protein translation and tumorigenesis. *Front Oncol* 12: 1025291.

- Ramos, P. C., J. Hockendorff, E. S. Johnson, A. Varshavsky and R. J. Dohmen, 1998 Ump1p is required for proper maturation of the 20S proteasome and becomes its substrate upon completion of the assembly. *Cell* 92: 489-499.
- Rappsilber, J., Y. Ishihama and M. Mann, 2003 Stop and go extraction tips for matrix-assisted laser desorption/ionization, nanoelectrospray, and LC/MS sample pretreatment in proteomics. *Anal Chem* 75: 663-670.
- Robinson, M.D., Grigull, J., Mohammad, N., and T.R. Hughes, 2002 FunSpec: a web-based cluster interpreter for yeast. *BMC Bioinformatics Epub volume 3*- pages 35.
- Rycovska, A., M. Valach, L. Tomaska, M. Bolotin-Fukuhara and J. Nosek, 2004 Linear versus circular mitochondrial genomes: intraspecies variability of mitochondrial genome architecture in *Candida parapsilosis*. *Microbiology (Reading)* 150: 1571-1580.
- Ryzhkova, A. I., M. A. Sazonova, V. V. Sinyov, E. V. Galitsyna, M. M. Chicheva *et al.*, 2018 Mitochondrial diseases caused by mtDNA mutations: a mini-review. *Ther Clin Risk Manag* 14: 1933-1942.
- Sachs, A. B., R. W. Davis and R. D. Kornberg, 1987 A single domain of yeast poly(A)-binding protein is necessary and sufficient for RNA binding and cell viability. *Mol Cell Biol* 7: 3268-3276.
- Salvi, J. S., J. N. Chan, K. Szafranski, T. T. Liu, J. D. Wu *et al.*, 2014 Roles for Pbp1 and caloric restriction in genome and lifespan maintenance via suppression of RNA-DNA hybrids. *Dev Cell* 30: 177-191.
- Salvi, J. S., and K. Mekhail, 2015 R-loops highlight the nucleus in ALS. *Nucleus* 6: 23-29.
- Sato, T. K., S. Kawano and T. Endo, 2019 Role of the membrane potential in mitochondrial protein unfolding and import. *Sci Rep* 9: 7637.
- Seethashankar, S., S. Hariharan and V. D. Parvathi, 2025 Implications of mtDNA in human health and diseases. *BioTechnologia (Pozn)* 106: 209-222.
- Shadel, G. S., 1999 Yeast as a model for human mtDNA replication. *Am J Hum Genet* 65: 1230-1237.
- Sharer, J. D., 2005 The adenine nucleotide translocase type 1 (ANT1): a new factor in mitochondrial disease. *IUBMB Life* 57: 607-614.
- Swisher, K. D., and R. Parker, 2010 Localization to, and effects of Pbp1, Pbp4, Lsm12, Dhh1, and Pab1 on stress granules in *Saccharomyces cerevisiae*. *PLoS One* 5: e10006.
- Szczepanowska, J., D. Malinska, M. R. Wieckowski and J. Duszynski, 2012 Effect of mtDNA point mutations on cellular bioenergetics. *Biochim Biophys Acta* 1817: 1740-1746.
- Taanman, J. W., 1999 The mitochondrial genome: structure, transcription, translation and replication. *Biochim Biophys Acta* 1410: 103-123.
- Takahara, T., and T. Maeda, 2012 Transient sequestration of TORC1 into stress granules during heat stress. *Mol Cell* 47: 242-252.
- Traba, J., J. Satrustegui and A. del Arco, 2009 Transport of adenine nucleotides in the mitochondria of *Saccharomyces cerevisiae*: interactions between the ADP/ATP carriers and the ATP-Mg/Pi carrier. *Mitochondrion* 9: 79-85.
- Tron, T., M. Yang, F. A. Dick, M. E. Schmitt and B. L. Trumpower, 1995 QSR1, an essential yeast gene with a genetic relationship to a subunit of the mitochondrial cytochrome bc1 complex, is homologous to a gene implicated in eukaryotic cell differentiation. *J Biol Chem* 270: 9961-9970.
- Vallieres, C., O. Benoit, O. Guittet, M. E. Huang, M. Lepoivre *et al.*, 2024 Iron-sulfur protein odyssey: exploring their cluster functional versatility and challenging identification. *Metallomics* 16.
- van de Poll, F., B. M. Sutter, M. G. Acoba, D. Caballero, S. Jahangiri *et al.*, 2023 Pbp1 associates with Puf3 and promotes translation of its target mRNAs involved in mitochondrial biogenesis. *PLoS Genet* 19: e1010774.
- Veatch, J. R., M. A. McMurray, Z. W. Nelson and D. E. Gottschling, 2009 Mitochondrial dysfunction leads to nuclear genome instability via an iron-sulfur cluster defect. *Cell* 137: 1247-1258.
- Velichutina, I., P. L. Connerly, C. S. Arendt, X. Li and M. Hochstrasser, 2004 Plasticity in eucaryotic 20S proteasome ring assembly revealed by a subunit deletion in yeast. *EMBO J* 23: 500-510.
- Vowinckel, J., J. Hartl, R. Butler and M. Ralsler, 2015 MitoLoc: A method for the simultaneous quantification of mitochondrial network morphology and membrane potential in single cells. *Mitochondrion* 24: 77-86.

- Wang, X., and X. J. Chen, 2015 A cytosolic network suppressing mitochondria-mediated proteostatic stress and cell death. *Nature* 524: 481-484.
- Wang, X., K. Salinas, X. Zuo, B. Kucejova and X. J. Chen, 2008 Dominant membrane uncoupling by mutant adenine nucleotide translocase in mitochondrial diseases. *Hum Mol Genet* 17: 4036-4044.
- Weidberg, H., and A. Amon, 2018 MitoCPR-A surveillance pathway that protects mitochondria in response to protein import stress. *Science* 360.
- Weill, U., I. Yofe, E. Sass, B. Stynen, D. Davidi *et al.*, 2018 Genome-wide SWAp-Tag yeast libraries for proteome exploration. *Nat Methods* 15: 617-622.
- Wen, H., H. Deng, B. Li, J. Chen, J. Zhu *et al.*, 2025 Mitochondrial diseases: from molecular mechanisms to therapeutic advances. *Signal Transduct Target Ther* 10: 9.
- Westermann, B., and W. Neupert, 2000 Mitochondria-targeted green fluorescent proteins: convenient tools for the study of organelle biogenesis in *Saccharomyces cerevisiae*. *Yeast* 16: 1421-1427.
- Wiedemann, N., and N. Pfanner, 2017 Mitochondrial Machineries for Protein Import and Assembly. *Annu Rev Biochem* 86: 685-714.
- Wisniewski, J. R., A. Zougman, N. Nagaraj and M. Mann, 2009 Universal sample preparation method for proteome analysis. *Nat Methods* 6: 359-362.
- Yang, Y. S., M. Kato, X. Wu, A. Litsios, B. M. Sutter *et al.*, 2019 Yeast Ataxin-2 Forms an Intracellular Condensate Required for the Inhibition of TORC1 Signaling during Respiratory Growth. *Cell* 177: 697-710 e617.
- Youle, R. J., and D. P. Narendra, 2011 Mechanisms of mitophagy. *Nat Rev Mol Cell Biol* 12: 9-14.
- Zhu, Z., S. Mallik, T. A. Stevens, R. Huang, E. D. Levy and S. O. Shan, 2025 Principles of cotranslational mitochondrial protein import. *Cell* 188: 5605-5617 e5614.
- Zorova, L. D., V. A. Popkov, E. Y. Plotnikov, D. N. Silachev, I. B. Pevzner *et al.*, 2018 Mitochondrial membrane potential. *Anal Biochem* 552: 50-59.

3.8] Supplemental Figures and Tables for Chapter 3

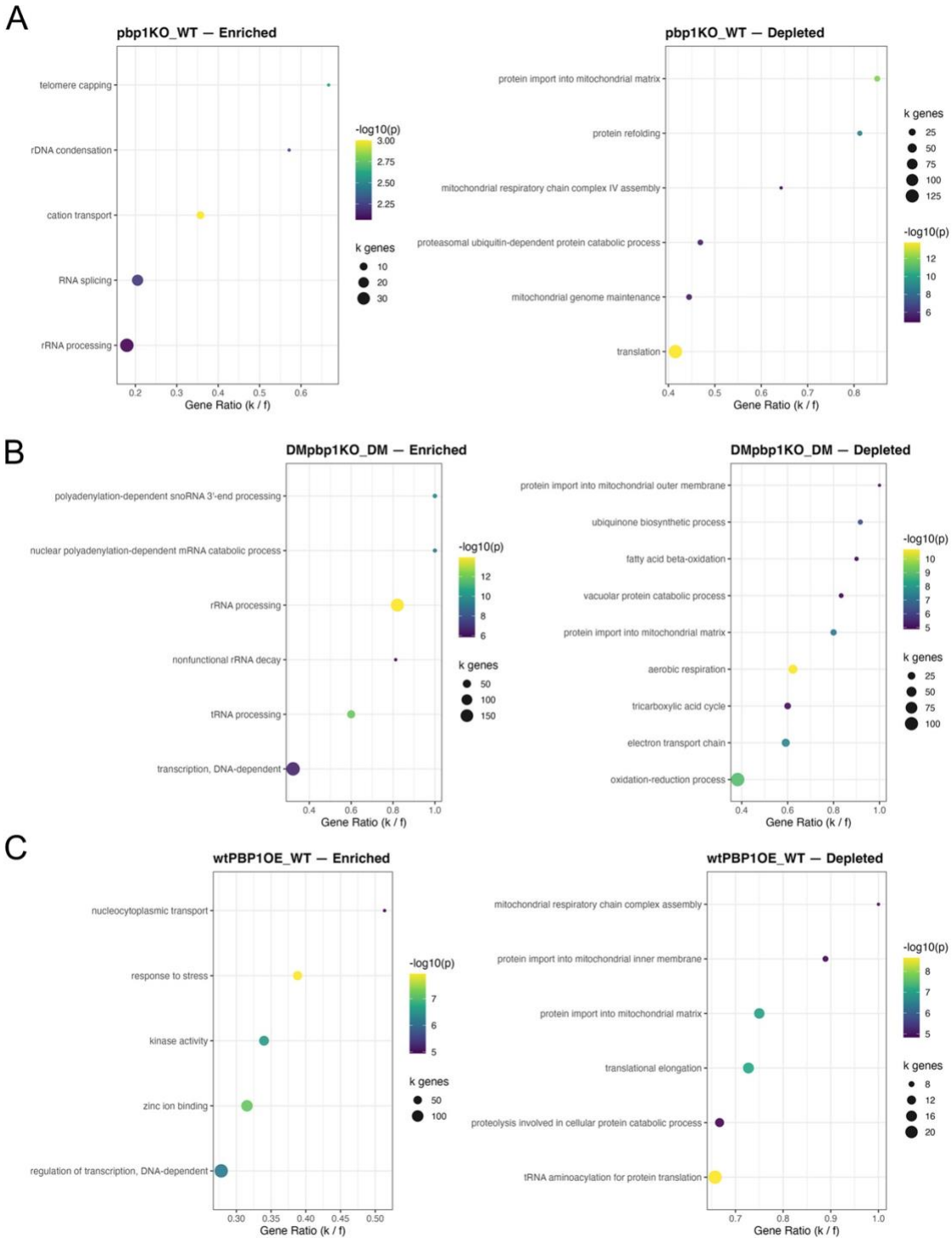


Figure S3.1: Pathways enriched and depleted in Bulk RNAseq (part 1) for the following contrasts pbp1KO vs WT (A), DMpbp1KO vs DM (B), wtPBP1OE vs WT (C). To generate enriched pathway lists, genes with log2-fold change >0, and padj <0.01 were used as input in Funspec. Bonferroni correction of p = 0.05 was applied.

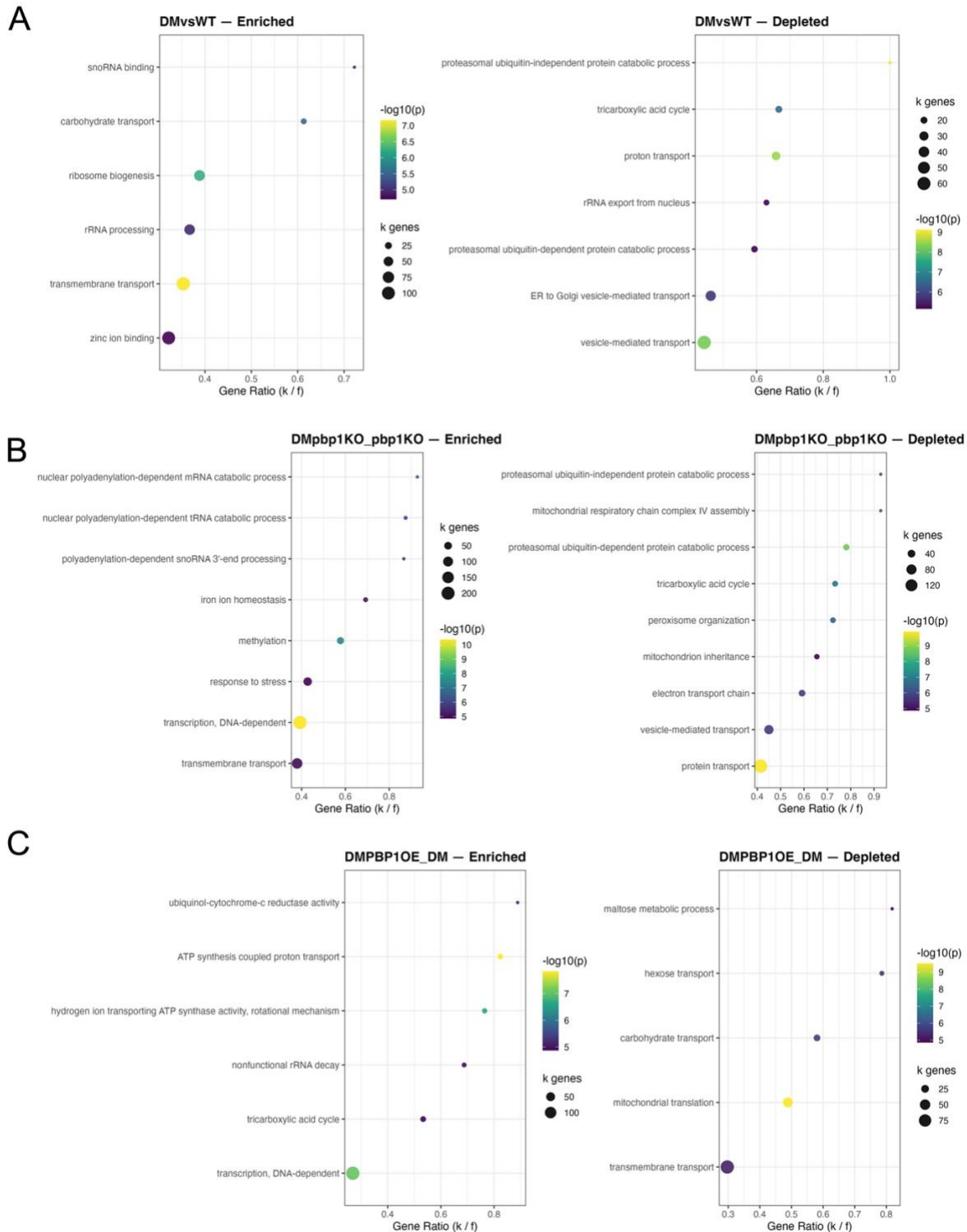


Figure S3.2: Pathways enriched and depleted in Bulk RNAseq (part 2) for the following contrasts DM vs WT (A), DMpbp1KO vs pbp1KO (B), DMPBP1OE vs DM (C). To generate enriched pathway lists, genes with \log_2 -fold change >0 , and $p_{adj} < 0.01$ were used as input in the online Funspec software. Bonferroni correction of $p = 0.05$ was applied.

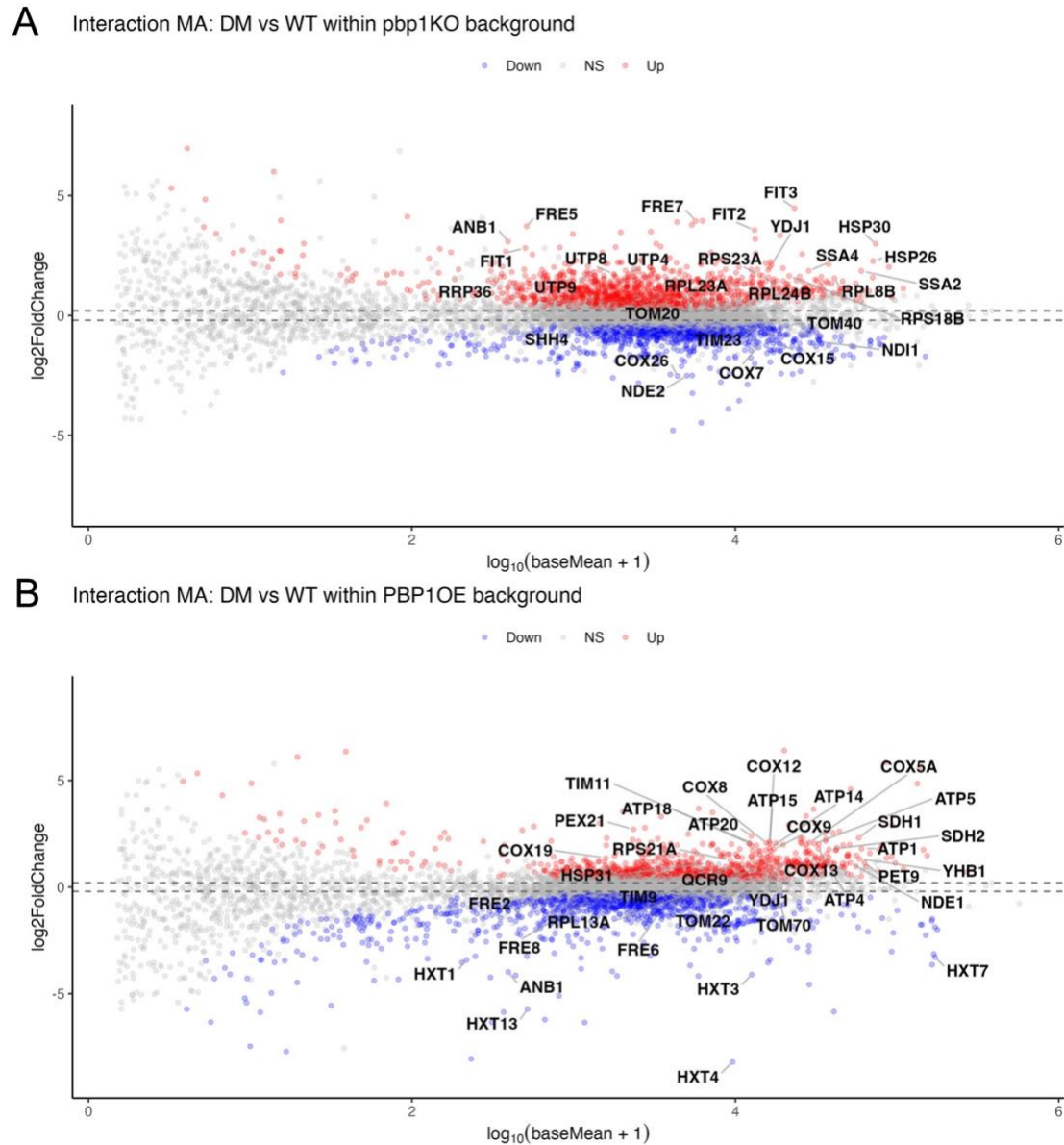


Figure S3.3. Genotype-Environment Interaction MA plots. (A) MA plot showing the genes differentially expressed in clogger cells relative to wild type, in the *pbp1* Δ environment or background. (B) (MA) plot showing the genes differentially expressed in clogger cells relative to wild type, in the *PBP1* overexpression environment or background.

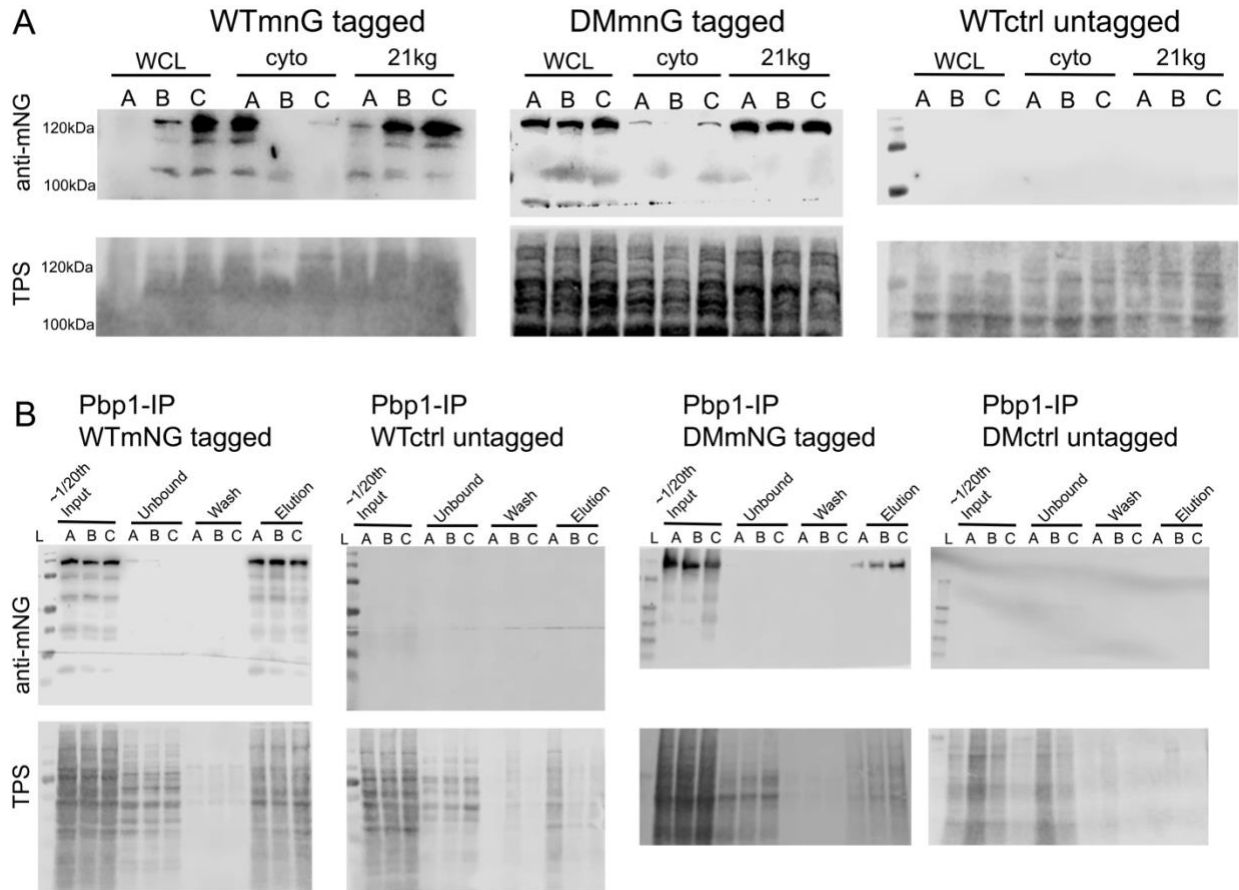


Figure S3.4. Western blot analysis for Pbp1 protein localization and immunoprecipitation. (A) Pbp1 protein is prone to degradation in the whole cell lysate (WCL), and post 21,000xg – cytosolic fraction (cyto). The 21,000xg (21kg) fraction preserves the Pbp1-mNeonGreen (Pbp1-mNG) fusion protein the most from degradation. From left to right, showing Pbp1-mNG tagged strains in *AAC2* wild type (WTmnG), Pbp1-mNG tagged strains in clogger *aac2^{A128P, A137D}* (DMmnG), and untagged wild type control strains (WTctrl) to show the specificity of the anti-mNeonGreen antibody. Top panels show antibody staining, while bottom panel shows total protein stain (TPS). **(B)** Immunoprecipitation of Pbp1 from the membrane-associated (“21kg”) fractions. From left to right: WTmnG tagged, WTmnG untagged (negative control), DMmnG tagged, DMmnG untagged (negative control). Approximately 1/20th of the input lysate was run on the western blot. Unbound and wash fractions were also run, followed by the Elution fraction. Top panels show anti-mNeonGreen (anti-mNG) antibody staining, while bottom panels show total protein stain (TPS), corresponding to each membrane.

Proteins enriched with Pbp1

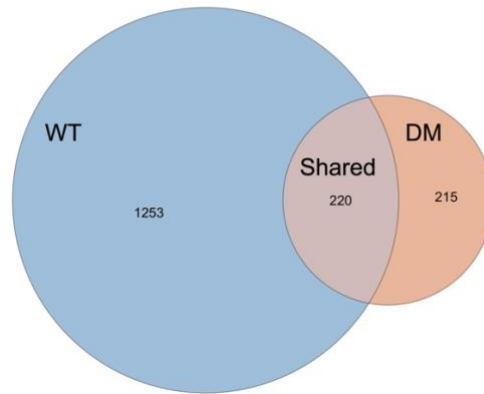


Figure S3.5. Venn diagram of shared and unique proteins enriched with Pbp1 (IPMS).

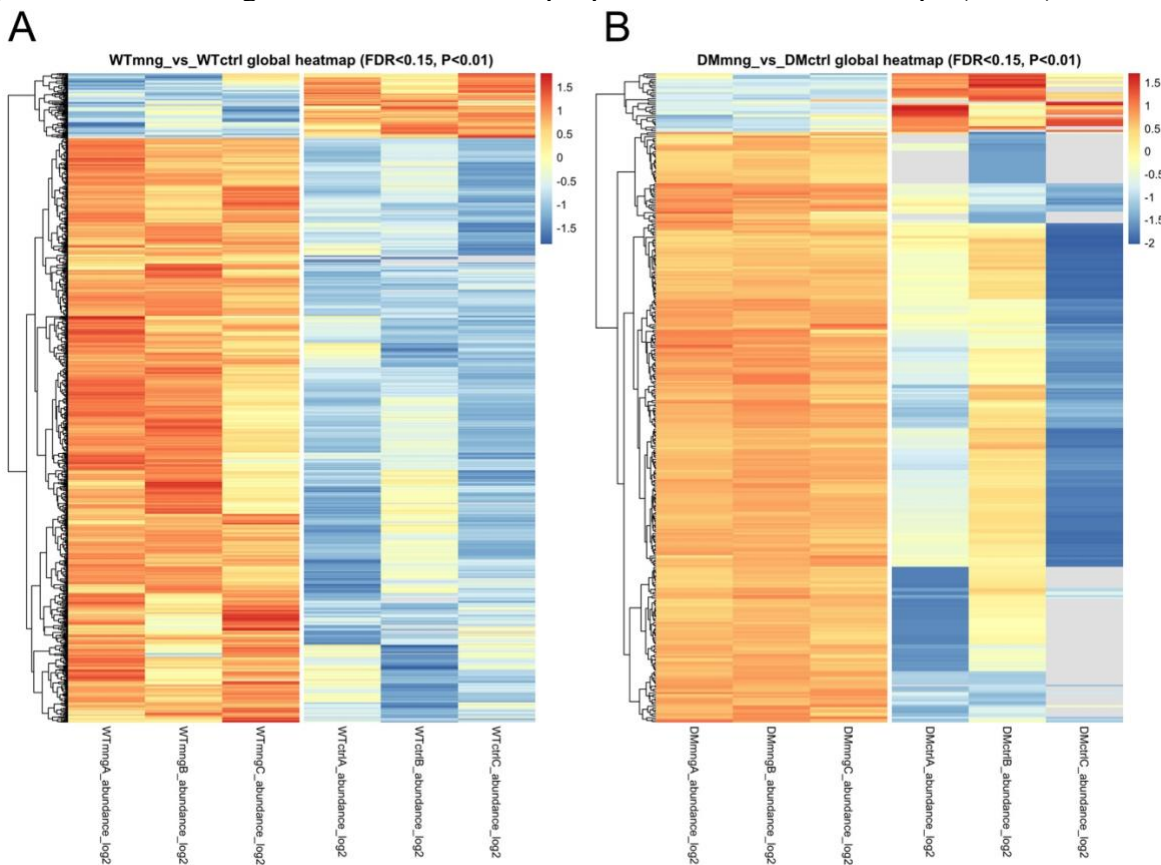


Figure S3.6. Global heatmaps of enriched or depleted proteins in the Pbp1 immunoprecipitation (IP-MS). **(A)** Pbp1-associated proteins in the *AAC2* wild type background. Tagged replicates (“WTmng”) are shown on the left, and untagged controls (“WTctrl”) are shown on the right. **(B)** Pbp1-associated proteins in the *aac2*^{A128P, A137D} clogger background. Tagged replicates (“DMmng”) are shown on the left, and untagged controls (“DMctrl”) are shown on the right. *FDR* (*padj*) threshold was set at <0.15 to allow for any missed interactors due to low replicate numbers in our experiment. *p-value* was set at <0.01.

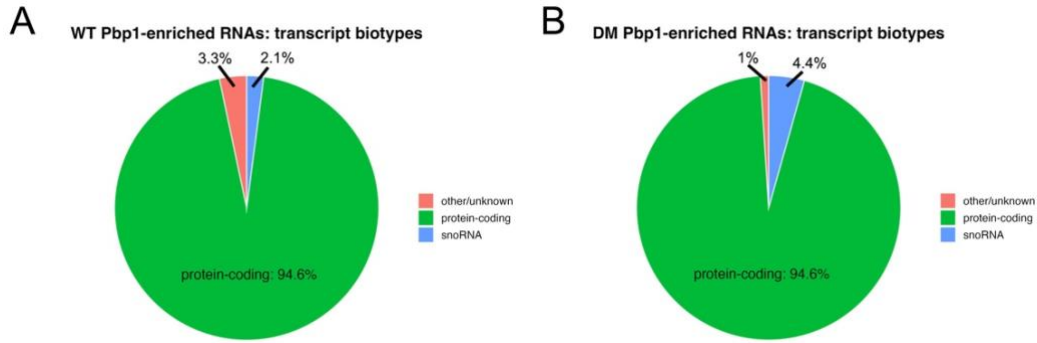


Figure S3.7. Types of RNA (transcript “biotypes”) enriched with Pbp1 in (A) WT background, or (B) DM background.

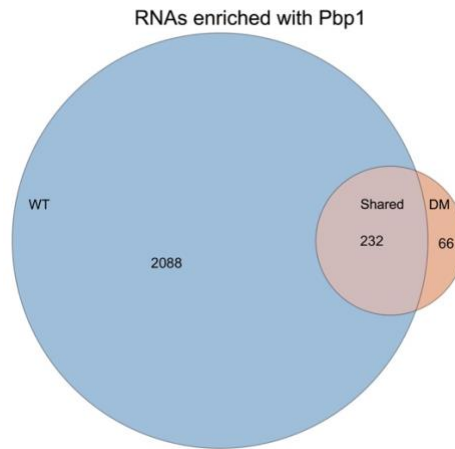


Figure S3.8. Venn diagram of shared and unique RNAs enriched with Pbp1 (RIPseq).

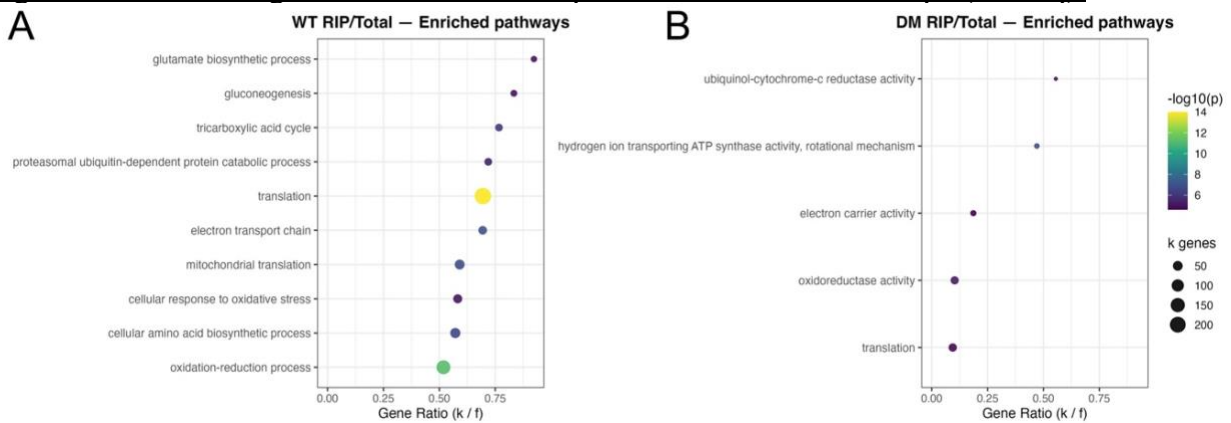


Figure S3.9. Pathways enriched or depleted in RIPseq for the RNAs associating with Pbp1 in the (A) WT background, or (B) DM background.

Table 3.1 Excel Workbook for yeast strains, plasmids, primers and reagents.

Table 3.1a. Excel Workbook Sheet 1: Yeast strains used in this study.

Strain ID	Detailed Genotype	Reference
CY5626	<i>aac2-A128P,A137D-KAN::Δlys2; AAC2</i>	Coyne et al. 2023
CY884	<i>AAC2; alpha mating type W303-1B</i>	Chen lab strain
PBP1KO	<i>pbp1Δ-URA3</i>	This study
KMY07	<i>pbp1Δ-URA3; pab1Δ-KAN</i>	Gift from Dr. Allan Jacobson at UMass Worcester
GM15_13B	<i>aac2-A128P,A137D-KAN::Δlys2; AAC2; pbp1Δ-URA3</i>	This study
GM17-24C	<i>aac2-A128P,A137D-KAN::Δlys2; AAC2; pbp1Δ-URA3; pab1Δ-KAN</i>	This study
WTmNG	<i>AAC2; PBP1-mNeonGreen-hph</i>	This study
DMmNG (GM16_12D)	<i>aac2-A128P,A137D-KAN::Δlys2; AAC2; PBP1-mNeonGreen-hph</i>	This study

Table 3.1b. Excel Workbook Sheet 2: List of plasmids used in this study.

Plasmid ID	Source
pRS425_empty	Addgene
pRS426_empty	Addgene
PAB1_pRS425	Chen lab
RGI1_pRS425	Chen lab
RCA1_pRS425	Chen lab
PBP1_pRS426	Chen lab
YHB1_pRS426	Chen lab
PRX1_pRS426	Chen lab
UMP1_pRS426	Chen lab
UBP11_pRS426	Chen lab
MIC26_pRS426	Chen lab
PRE8_pRS426	Chen lab
PAM16_pRS426	Chen lab
pMitoLOC	Addgene

Table 3.1c. Excel Workbook Sheet 3: List of primers used in this study.

Primer	Forward/Reverse	Purpose(s)
PBP1_P1	Forward	knockout, and Pbp1-mNG PCR
PBP1_P2	Reverse	knockout, and Pbp1-mNG PCR
PBP1_P5	Forward	Genotyping for knockout and Pbp1-mNG
PBP1_P6	Reverse	Genotyping for knockout and Pbp1-mNG
PRE8_fwd	Forward	HiFi PCR for Subcloning
PRE8_rev	Reverse	HiFi PCR for Subcloning
MIC26_fwd	Forward	HiFi PCR for Subcloning
MIC26_rev	Reverse	HiFi PCR for Subcloning
UMP1_fwd	Forward	HiFi PCR for Subcloning
UMP1_rev	Reverse	HiFi PCR for Subcloning
UBP11_fwd	Forward	HiFi PCR for Subcloning
UBP11_rev	Reverse	HiFi PCR for Subcloning
YHB1_fwd	Forward	HiFi PCR for Subcloning
YHB1_rev	Reverse	HiFi PCR for Subcloning
PRX1_fwd	Forward	HiFi PCR for Subcloning
PRX1_rev	Reverse	HiFi PCR for Subcloning
RPM2_fwd	Forward	HiFi PCR for Subcloning
RPM2_rev	Reverse	HiFi PCR for Subcloning

Table 3.1d. Excel Workbook Sheet 4: List of important commercial reagents used in this study.

Reagent name	Source
Mitotracker Red CMXRos	Invitrogen/ThermoFisher
Concanavalin A	Sigma
Binding control agarose beads	Proteintech/BullDogBio
Nanotrap mNeonGreen Agarose beads	Proteintech
Anti-mNeonGreen Primary Antibody	Cell Signaling
Glycogen	Invitrogen/ThermoFisher

Chapter 4. Discussion and Future Directions

Gargi Mishra

Department of Biochemistry and Molecular Biology

SUNY Upstate Medical University

4.1] Key Findings and Immediate Future Directions

In this thesis, we used the power of yeast genetics to identify and characterize two biological pathways that support cellular homeostasis during mitochondrial precursor overaccumulation stress (mPOS) and severe mitochondrial protein import clogging. The first pathway identified centers around the identification of the F-box protein Mfb1 as a suppressor of mutant *aac2*-induced cell death, while the second arises from the discovery of the RNA-binding protein Pbp1 as a suppressor of mtDNA loss under severe import-clogging conditions. Together, these pathways highlight distinct yet complementary strategies by which cells maintain mitochondrial proteostasis when protein import is compromised. Below, I discuss the broader implications of these findings and outline important open questions that remain to be addressed.

A substantial body of prior work established Mfb1 as a regulator of mitochondrial morphology, distribution, and inheritance (KONDO-OKAMOTO *et al.* 2006; KONDO-OKAMOTO *et al.* 2008; PERNICE *et al.* 2016; YANG *et al.* 2022). A previous genetic screen conducted in our lab had found *MFBI* overexpression to rescue cell growth in cells overexpressing a mutant form of Aac2 protein. Despite the main suppressors from this screen being genes that act in the cytosol to modulate global translational rates in response to mPOS (WANG AND CHEN 2015), *MFBI* was a unique suppressor since it localized and functioned on the mitochondrial surface. After extensive genetic, biochemical, and molecular assays, our findings extended Mfb1's functional repertoire by directly linking it to cellular proteostasis during mitochondrial protein import stress (Chapter 2).

Despite this expanded role, the precise mechanism by which Mfb1 promotes cellular survival under clogging conditions remains unresolved. Proximity proteomics showed us that Mfb1 is enriched at the outer mitochondrial membrane and associates with core components of the

TOM complex, suggesting a potential role in either surveying or stabilizing the TOM-associated mitochondrial protein import machinery. In addition, Mfb1 proximity interactions included proteins linked to lipid droplet formation and ER-mitochondria contact sites, raising the possibility that Mfb1 functions at membrane interfaces where lipid composition, protein quality control, and import efficiency converge (PU *et al.* 2011; ELLENRIEDER *et al.* 2017; GAO *et al.* 2017; NAMBA 2019; MISHRA *et al.* 2025). Whether Mfb1 stabilizes the TOM complex directly, influences the lipid environment surrounding import channels, or facilitates local proteostatic mechanisms at mitochondrial contact sites remains an open question. Future studies employing cross-linking-based mass spectrometry, structure-guided interaction mapping, or in vitro mitochondrial protein import assays will be critical for resolving these possibilities.

In addition to its independent role in proteostasis, our data revealed a profound genetic interaction between Mfb1 and the stress-responsive protein Hsp31. Transcriptomic analysis demonstrated that *HSP31* mRNA levels increase upon loss of *MFBI* under mitochondrial protein import clogging conditions, suggesting activation of a compensatory proteostatic stress response when Mfb1-mediated proteostatic function is compromised. Consistent with this model, simultaneous deletion of *MFBI* and *HSP31* resulted in exacerbated growth defects, particularly under conditions of concurrent import stress, indicating that these factors act in parallel or partially overlapping pathways to support cellular survival (MISHRA *et al.* 2025).

Hsp31 is a multifunctional protein with reported roles not only as a molecular chaperone, but also in redox homeostasis, detoxification of reactive metabolites, and protein glycation control. Its induction in the absence of Mfb1 may therefore reflect an attempt to buffer the combined proteostatic and oxidative stress associated with mitochondrial precursor accumulation. This might

explain the increased levels of ubiquitinated proteins in the triton-insoluble fractions of clogger mutants lacking *HSP31* (Supporting information, Chapter 2). Thus, the identification of Hsp31 as a genetic modifier of mitochondrial import stress provides a potential mechanistic framework for understanding how loss of DJ-1 function may sensitize cells to mitochondrial protein mismanagement and highlights mitochondrial import stress as a previously underappreciated contributor to DJ-1-associated disease pathogenesis (MISHRA *et al.* 2025). Despite the discovery of Hsp31 as a key responder to mPOS, our study did not expand upon the role of several other chaperones and heat shock proteins that were also upregulated in response to MFB1 loss under import clogging conditions. These heat shock/chaperone-encoding genes included small chaperones (*HSP12*, *HSP26*) and the cytosolic deaggregase *HSP104* (SUSEK AND LINDQUIST 1990; GLOVER AND LINDQUIST 1998; WELKER *et al.* 2010). It would be important to follow up on these chaperones and determine whether they triage unique substrates when mPOS gets induced due to severe import clogging.

Next, as part of our effort to identify genes that suppress mitochondrial genome instability under severe import clogging stress, we stumbled upon a role for Pbp1 as a regulator of mitochondrial biogenesis and function. It is important to note that our genetic screen isn't unique in identifying a role for Pbp1 in mitochondrial homeostasis. A prior screen from our lab, which had identified *MFBI* among various suppressors of mutant-Aac2-induced cell death, had also identified *PBPI* as a genetic suppressor (WANG AND CHEN 2015). Another study in the field of yeast genetics had utilized a Tim18 mutant to identify suppressors of mitochondrial protein import defects and discovered *PBPI* as a suppressor of Tim18 deficiency (DUNN AND JENSEN 2003). More recent work has shown that Pbp1 interacts with proteins that mediate the translation of several nuclear-encoded mitochondrial proteins (VAN DE POLL *et al.* 2023). That said, our current study

adds an important nuance to Pbp1's role in supporting mitochondrial health, which is that severe mitochondrial protein import clogging can prevent Pbp1 from being effective in carrying out its functions, which may help provide an explanation for the severe growth defects that we observe in our clogger cells, especially under clogging conditions, when cells have to rely on mitochondrial respiration.

Pbp1's role in supporting mitochondrial biogenesis and function raises several important mechanistic questions. Under non-fermentable growth conditions, Pbp1 displays heterogeneous subcellular localization, suggesting that metabolic state influences its assembly, interactions, or functional engagement (Chapter 3). What drives this localization heterogeneity remains unclear and may reflect changes in translational demand, RNA availability, or stress-responsive condensate formation. Moreover, under concurrent respiratory growth and import-clogging conditions, Pbp1 loses interactions with a broad set of proteins and RNAs, indicating a rewiring of its interactome (Chapter 3). How import stress triggers this loss of interaction, and whether it reflects active regulatory remodeling versus collapse of RNA-protein assemblies due to reduced synthesis or increased turnover, is not yet clear. Notably, overexpression of *PBPI* significantly restores cellular homeostasis under clogging conditions, raising the possibility that increased Pbp1 abundance compensates for reduced interaction efficiency or promotes the formation of functional assemblies that buffer unimported mitochondrial preproteins and RNA species that may encode such preproteins (Chapter 3). Elucidating the molecular determinants of Pbp1 interaction dynamics and their relationship to mitochondrial stress signaling will be an important avenue for future investigation. Finally, an important limitation of our bulk RNA-seq experiment was that we did not include *PABI* deletion strains in our analysis. We could have utilized previously described temperature-sensitive (ts)-mutants of Pab1 and genetically crossed these with the clogger allele to

identify the resulting transcriptional signatures (SACHS AND DAVIS 1989). Alternatively, we could have utilized the *pab1Δpbp1Δ*, as well as the triple mutant *aac2^{A128P, A137D} pab1Δpbp1Δ* in media that is permissive to both fermentation and respiration to assess transcriptional changes. This is because a previous study has shown that *PABI* loss causes drastic changes to the transcriptome and proteomes of cells, especially by dysregulating translational initiation, translational termination, and mRNA decay processes (MANGKALAPHIBAN *et al.* 2024). Given this, it would be important to determine further transcriptional and translational changes to *PABI* loss concurrent with import clogging.

In addition to *PBPI*, our multicopy suppressor screen for mtDNA stabilizing genes identified genes involved in antioxidant signaling such as *YHB1* and *PRX1*. Prx1 is a yeast mitochondrial peroxiredoxin that reduces hydroperoxides and regulates redox balance (CALABRESE *et al.* 2019). Yhb1 is a yeast nitric oxide oxidoreductase that protects against protein nitration during nitrosative and oxidative stress (LEWINSKA *et al.* 2008). We hypothesize that these proteins may have direct or indirect roles in supporting mitochondrial protein import and mitochondrial genome maintenance.

As a direct function, Prx1 and Yhb1 may help establish a reducing environment along the mitochondrial protein import pathway, thereby preventing premature oxidative folding of mitochondrial precursor proteins and facilitating their import. As an indirect role, a more reduced cytosolic and mitochondrial environment generated by these proteins may preserve redox-sensitive components of the import machinery, help maintain mitochondrial membrane potential, and limit secondary oxidative damage to mitochondrial proteins and DNA. Interestingly, *YHB1* mRNA is upregulated in clogger cells relative to wild type within the *PBPI* overexpression (*PBPIOE*)

background (Supplemental Figure S3.3, Chapter 3). Altogether, these findings suggest that redox homeostasis plays an important modulatory role during mPOS. In future work, it will be important to genetically disrupt *YHB1* and *PRX1* to determine their effects on mtDNA stability during import clogging. Furthermore, identifying pathways that compensate for Prx1/Yhb1 deficiency will be an important area for future investigation.

It is also possible that *YHB1* and *PRX1* suppress mtDNA instability during import clogging through redox-independent mechanisms, as both proteins have been shown to possess proteostatic functions. For example, Prx1 has been reported to act as a molecular chaperone in addition to being a peroxidase (JANG *et al.* 2004; AVELLANEDA PENATTI *et al.* 2025). Similarly, neuroglobin, the human ortholog of Yhb1, has been implicated in protecting cells against cytotoxicity resulting from α -synuclein protein aggregates (KLEINKNECHT *et al.* 2016). In addition, proteomic studies in yeast have revealed physical interactions of both Prx1 and Yhb1 with mitochondrial proteins, components of the mitochondrial import machinery, and cytosolic chaperones (GAVIN *et al.* 2006; KAUR AND STUART 2011; HILL *et al.* 2016; LORENZI *et al.* 2016). Using redox-dead mutants of Prx1 and Yhb1 (EL HAMMI *et al.* 2012; KLEINKNECHT *et al.* 2016; AVELLANEDA PENATTI *et al.* 2025), it will be possible to determine whether *PRX1* and *YHB1* can still suppress mtDNA instability under clogging conditions. Partial or complete rescue of mtDNA loss by redox-compromised variants of *PRX1* and *YHB1* would support a direct protein quality control-based mechanism underlying their contribution to mitochondrial protein import efficiency, whereas a lack of rescue would suggest that these proteins function primarily through antioxidant signaling pathways.

Taking a step back, two more things need to be discussed. First, it is interesting that *PBPI* was identified in both multicopy suppressor screens performed in our lab, while *MFBI* was only identified in the growth defect suppression screen. Thus, it appears that *PBPI* can suppress both clogging associated mtDNA-instability but also suppress mPOS-associated growth defects in Aac2 mutants. On the other hand, *MFBI* suppresses mPOS-associated growth defects induced by the overexpression of Aac2 mutants, or those induced by general defects in import machinery. This suggests that *MFBI* plays a focused role in promoting protein import competency and anti-mPOS signaling, while *PBPI* can more broadly support mitochondrial biogenesis and function. Mfb1 is a well-characterized morphodynamic protein associated with the mitochondrial surface, while Pbp1 is an RNA-binding protein involved in the assembly of condensates such as cytosolic stress granules, but can associate with the mitochondrial surface under respiratory growth conditions. It is likely that due to their differential localization and roles in mitochondrial morphology versus RNA binding, Mfb1 and Pbp1 affect mitochondrial biogenesis and function differently.

Second, we had observed that Pbp1 protein enriches more strongly with several mtDNA-encoded RNAs and proteins under import clogging conditions relative to steady-state import conditions. We previously speculated that this could either be an artefact or due to a triage function performed by Pbp1 under clogging conditions (Chapter 3). If Pbp1's interaction with mitochondrially-encoded RNAs and proteins reflects true biology, then the follow-up question is what's causing Pbp1 to have access to these mtDNA-encoded genes? First, it may be possible that a small fraction of Pbp1 gets imported into mitochondria during clogging conditions, but this seems counter-intuitive, especially during conditions of severe clogging. Another possibility is that during import clogging conditions, mtDNA-encoded proteins and RNAs get released into the cytosol to get accessed by Pbp1. This possibility seems much more likely. One way that this could

happen is if the toxic protein aggregates in the cytosol formed by unimported mitochondrial proteins disturb the intracellular osmotic balance which could cause lysis of intact mitochondria, leading to release of mtDNA-encoded RNAs and proteins. Besides this hypothesis, there are well-established phenomena where mtDNA, dsRNA, mtRNA, and proteins get released into mitochondria, leading to downstream immune consequences involving the cGAS-STING and RIG-1/MDA5-MAVS pathways, especially in higher-order eukaryotes (LINDER AND HORNING 2018; HU AND SHU 2023; LYU *et al.* 2023).

It would be important to study these two open questions described above. First, it would be important to study the genetic interaction between *MFBI* and *PBPI* using yeast genetics as well as transcriptomic and proteomic approaches, as this would reveal whether these two genes act independently, or if they are epistatic. Next, determining how Pbp1 increases its association with mtDNA-encoded RNAs and proteins during import clogging conditions will help answer whether mitochondria are inherently “leakier” during clogging. To study this, we could make use of inducible clogger strains. Using these strains, we can first determine Pbp1’s interactome in the uninduced or steady state import condition. Next, we can determine how Pbp1’s interactome changes when clogging is induced in the same strains. Additionally, measuring other “leakage” parameters such as mitochondrial membrane potential measurements using fluorescent dyes, mitochondrial swelling by light scattering, and measurements of membrane coupling via patch-clamp technique would provide further data to test this phenotype (SIVANDZADE *et al.* 2009, JOHNSON *et al.* 2002, KIRICHOK *et al.* 2004).

4.2] Future directions for the study of mitochondrial biogenesis and human health

In the past several decades, mitochondria have emerged as important guardians of human health, owing to their diverse cellular functions and not merely their role in energy production (BAKER *et al.* 2014; SUOMALAINEN AND NUNNARI 2024). Furthermore, over the past decade, there has been a paradigm shift in how mitochondria-induced cellular damage is understood. It is now well appreciated that mitochondrial damage can occur in multiple forms and that this damage can be communicated to other topological compartments of the cell in a bioenergetics-independent manner (SCHULZ AND HAYNES 2015). Diseases characterized by chronic proteostatic stress, impaired mitochondrial dynamics, or age-associated decline in import efficiency may therefore be particularly sensitive to import clogging-associated pathology (MACKENZIE AND PAYNE 2007; PALMER *et al.* 2021; CALAIS AND BERTOLIN 2025).

In light of these insights from the field of mitochondrial biology, several efforts have been made to target mitochondria in the context of human disease using molecular approaches such as adenoviral or adeno-associated virus (AAV)-mediated gene delivery, CRISPR-Cas9-based gene editing, mRNA-based therapies, as well as small molecules (SIEGEL *et al.* 2013; ZHANG *et al.* 2013; HU *et al.* 2021; CHERNEGA *et al.* 2022; SOLDATOV *et al.* 2022; ZACHARIOUDAKIS AND GAVATHIOTIS 2023; SONG *et al.* 2024). While many of these approaches continue to focus on restoring mitochondrial bioenergetic function, more recent strategies have begun to diverge by targeting mitochondrial protein quality control pathways and organelle dynamics (ZHANG *et al.* 2013; HU *et al.* 2021; ZACHARIOUDAKIS AND GAVATHIOTIS 2023).

In the context of these molecular advances, genetic screens conducted in model organisms such as baker's yeast (*Saccharomyces cerevisiae*), roundworm (*Caenorhabditis elegans*), or fruit

fly (*Drosophila melanogaster*) enable rapid discovery of conserved genetic pathways that may respond to general protein import stress and severe forms of import clogging. The identified pathways can then be further screened and validated in mammalian systems before being translated into therapies for mitochondrial diseases. In parallel, computational and synthetic approaches aimed at designing modular proteins and small molecules may also be harnessed to generate artificial proteins that support mitochondrial biogenesis, quality control, or function (MI *et al.* 2025; NASH *et al.* 2025).

The molecular pathways identified in this study, namely those mediated by Mfb1/Hsp31 and Pbp1, serve as proofs of concept for the types of cellular mechanisms that could be therapeutically targeted in human diseases where mitochondrial protein import is compromised. In future work, it will be important to validate these findings in pre-clinical models in which protein import clogging is implicated. As discussed previously, several mammalian F-box proteins (FBXL4, FBXO7, etc.), as well as DJ-1 and Ataxin-2 (homologs of Hsp31 and Pbp1, respectively), have been implicated in several human diseases (OSTROWSKI *et al.* 2017; BALLOUT *et al.* 2019; ZHANG *et al.* 2020; HUANG AND CHEN 2021; LAFFITA-MESA *et al.* 2021; ZHONG *et al.* 2023; SKOU *et al.* 2024). If the phenomenon of protein import clogging synergizes with the physiological roles of these mammalian proteins, this would provide a strong rationale for developing therapies that improve the function of these proteins in disease settings.

4.3] References for Chapter 4

- Avellaneda Penatti, N. M., M. H. Barros, F. Gomes, L. E. Soares Netto, K. de Jesus Maciel *et al.*, 2025 Decreased levels of Prx1 are associated with proteasome impairment and mitochondrial dysfunction in the yeast *Saccharomyces cerevisiae*. *Arch Biochem Biophys* 768: 110406.
- Baker, M. J., C. S. Palmer and D. Stojanovski, 2014 Mitochondrial protein quality control in health and disease. *Br J Pharmacol* 171: 1870-1889.
- Ballout, R. A., C. Al Alam, P. E. Bonnen, M. Huemer, A. W. El-Hattab and R. Shbarou, 2019 FBXL4-Related Mitochondrial DNA Depletion Syndrome 13 (MTDPS13): A Case Report With a Comprehensive Mutation Review. *Front Genet* 10: 39.
- Calabrese, G., E. Peker, P. S. Amponsah, M. N. Hoehne, T. Riemer *et al.*, 2019 Hyperoxidation of mitochondrial peroxiredoxin limits H₂O₂-induced cell death in yeast. *EMBO J* 38: e101552.
- Calais, H., and G. Bertolin, 2025 Stress at the gates: Mitochondrial import dysfunctions, response pathways, and therapeutic potential. *Mitochondrion* 87: 102107.
- Chernega, T., J. Choi, L. Salmena and A. C. Andreazza, 2022 Mitochondrion-targeted RNA therapies as a potential treatment strategy for mitochondrial diseases. *Mol Ther Nucleic Acids* 30: 359-377.
- Dunn, C. D., and R. E. Jensen, 2003 Suppression of a defect in mitochondrial protein import identifies cytosolic proteins required for viability of yeast cells lacking mitochondrial DNA. *Genetics* 165: 35-45.
- El Hammi, E., E. Warkentin, U. Demmer, N. M. Marzouki, U. Ermler and L. Baciou, 2012 Active site analysis of yeast flavohemoglobin based on its structure with a small ligand or econazole. *FEBS J* 279: 4565-4575.
- Ellenrieder, L., H. Rampelt and T. Becker, 2017 Connection of Protein Transport and Organelle Contact Sites in Mitochondria. *J Mol Biol* 429: 2148-2160.
- Gao, Q., D. D. Binns, L. N. Kinch, N. V. Grishin, N. Ortiz *et al.*, 2017 Pet10p is a yeast perilipin that stabilizes lipid droplets and promotes their assembly. *J Cell Biol* 216: 3199-3217.
- Gavin, A. C., P. Aloy, P. Grandi, R. Krause, M. Boesche *et al.*, 2006 Proteome survey reveals modularity of the yeast cell machinery. *Nature* 440: 631-636.
- Glover, J. R., and S. Lindquist, 1998 Hsp104, Hsp70, and Hsp40: a novel chaperone system that rescues previously aggregated proteins. *Cell* 94: 73-82.
- Hill, S. M., X. Hao, J. Gronvall, S. Spikings-Nordby, P. O. Widlund *et al.*, 2016 Asymmetric Inheritance of Aggregated Proteins and Age Reset in Yeast Are Regulated by Vac17-Dependent Vacuolar Functions. *Cell Rep* 16: 826-838.
- Hu, D., Z. Liu and X. Qi, 2021 Mitochondrial Quality Control Strategies: Potential Therapeutic Targets for Neurodegenerative Diseases? *Front Neurosci* 15: 746873.
- Hu, M.M. and H.B. Shu, 2023 Mitochondrial DNA-triggered innate immune response: mechanisms and diseases. *Cell Mol Immunol* 20(12): 1403-1412
- Huang, M., and S. Chen, 2021 DJ-1 in neurodegenerative diseases: Pathogenesis and clinical application. *Prog Neurobiol* 204: 102114.
- Jang, H. H., K. O. Lee, Y. H. Chi, B. G. Jung, S. K. Park *et al.*, 2004 Two enzymes in one; two yeast peroxiredoxins display oxidative stress-dependent switching from a peroxidase to a molecular chaperone function. *Cell* 117: 625-635.
- Johnson, L.J., Chung, W., Hanley, D.F. and N.V. Thakor, 2002 Optical scatter imaging detects mitochondrial swelling in living tissue slices. *Neuroimage* 17(3):1649-1657.
- Kaur, J., and R. A. Stuart, 2011 Truncation of the Mrp20 protein reveals new ribosome-assembly subcomplex in mitochondria. *EMBO Rep* 12: 950-955.
- Kirichok, Y., Krapivinsky, G. and D.E. Clapham, 2004 The mitochondrial calcium uniporter is a highly selective ion channel. *Nature* 427(6972):360-364.

- Kleinknecht, A., B. Popova, D. F. Lazaro, R. Pinho, O. Valerius *et al.*, 2016 C-Terminal Tyrosine Residue Modifications Modulate the Protective Phosphorylation of Serine 129 of alpha-Synuclein in a Yeast Model of Parkinson's Disease. *PLoS Genet* 12: e1006098.
- Kondo-Okamoto, N., K. Ohkuni, K. Kitagawa, J. M. McCaffery, J. M. Shaw and K. Okamoto, 2006 The novel F-box protein Mfb1p regulates mitochondrial connectivity and exhibits asymmetric localization in yeast. *Mol Biol Cell* 17: 3756-3767.
- Kondo-Okamoto, N., J. M. Shaw and K. Okamoto, 2008 Tetratricopeptide repeat proteins Tom70 and Tom71 mediate yeast mitochondrial morphogenesis. *EMBO Rep* 9: 63-69.
- Laffita-Mesa, J. M., M. Paucar and P. Svenningsson, 2021 Ataxin-2 gene: a powerful modulator of neurological disorders. *Curr Opin Neurol* 34: 578-588.
- Lewinska, A., A. Grzelak and G. Bartosz, 2008 Application of a YHB1-GFP reporter to detect nitrosative stress in yeast. *Redox Rep* 13: 161-171.
- Linder A. and V. Hornung, 2018 Mitochondrial dsRNA: A new DAMP for MDA5. *Dev Cell* 46(5): 530-532
- Lorenzi, I., S. Oeljeklaus, C. Ronsor, B. Bareth, B. Warscheid *et al.*, 2016 Ribosome-Associated Mba1 Escorts Cox2 from Insertion Machinery to Maturing Assembly Intermediates. *Mol Cell Biol* 36: 2782-2793.
- Lyu Y., Wang T., Huang S., and Z. Zhang, 2023 Mitochondrial Damage-Associated Molecular Patterns and Metabolism in the Regulation of Innate Immunity. *J Innate Immun* 15(1): 665-679
- MacKenzie, J. A., and R. M. Payne, 2007 Mitochondrial protein import and human health and disease. *Biochim Biophys Acta* 1772: 509-523.
- Mangkalaphiban, K., R. Ganesan and A. Jacobson, 2024 Pleiotropic effects of PAB1 deletion: Extensive changes in the yeast proteome, transcriptome, and translome. *PLoS Genet* 20: e1011392.
- Mi, L., Y. X. Li, X. Lv, Z. L. Wan, X. Liu *et al.*, 2025 Computational design of a high-precision mitochondrial DNA cytosine base editor. *Nat Struct Mol Biol* 32: 2575-2586.
- Mishra, G., X. Wang, E. Fitzpatrick, A. Ghosh and X. J. Chen, 2025 Cellular proteostasis during mitochondrial protein import clogging requires the mitochondrial F-box protein 1 and DJ-1 homolog HSP31 in *Saccharomyces cerevisiae*. *Genetics*.
- Namba, T., 2019 BAP31 regulates mitochondrial function via interaction with Tom40 within ER-mitochondria contact sites. *Sci Adv* 5: eaaw1386.
- Nash, P. A., K. M. Turner, C. A. Powell, L. Van Haute, P. Silva-Pinheiro *et al.*, 2025 Clinically translatable mitochondrial gene therapy in muscle using tandem mtZFN architecture. *EMBO Mol Med* 17: 1222-1237.
- Ostrowski, L. A., A. C. Hall and K. Mekhail, 2017 Ataxin-2: From RNA Control to Human Health and Disease. *Genes (Basel)* 8.
- Palmer, C. S., A. J. Anderson and D. Stojanovski, 2021 Mitochondrial protein import dysfunction: mitochondrial disease, neurodegenerative disease and cancer. *FEBS Lett* 595: 1107-1131.
- Pernice, W. M., J. D. Vevea and L. A. Pon, 2016 A role for Mfb1p in region-specific anchorage of high-functioning mitochondria and lifespan in *Saccharomyces cerevisiae*. *Nat Commun* 7: 10595.
- Pu, J., C. W. Ha, S. Zhang, J. P. Jung, W. K. Huh and P. Liu, 2011 Interactomic study on interaction between lipid droplets and mitochondria. *Protein Cell* 2: 487-496.
- Sachs, A. B., and R. W. Davis, 1989 The poly(A) binding protein is required for poly(A) shortening and 60S ribosomal subunit-dependent translation initiation. *Cell* 58: 857-867.
- Schulz, A. M., and C. M. Haynes, 2015 UPR(mt)-mediated cytoprotection and organismal aging. *Biochim Biophys Acta* 1847: 1448-1456.
- Siegel, M. P., S. E. Kruse, J. M. Percival, J. Goh, C. C. White *et al.*, 2013 Mitochondrial-targeted peptide rapidly improves mitochondrial energetics and skeletal muscle performance in aged mice. *Aging Cell* 12: 763-771.

- Sivandzade, F., Bhalerao, A., and L. Cucullo, 2019 Analysis of the Mitochondrial Membrane Potential Using the Cationic JC-1 Dye as a Sensitive Fluorescent Probe. *Bio-protocol*, 9(1): e3128.
- Skou, L. D., S. K. Johansen, J. Okarmus and M. Meyer, 2024 Pathogenesis of DJ-1/PARK7-Mediated Parkinson's Disease. *Cells* 13.
- Soldatov, V. O., M. V. Kubekina, M. Y. Skorkina, A. E. Belykh, T. V. Egorova *et al.*, 2022 Current advances in gene therapy of mitochondrial diseases. *J Transl Med* 20: 562.
- Song, M., L. Ye, Y. Yan, X. Li, X. Han *et al.*, 2024 Mitochondrial diseases and mtDNA editing. *Genes Dis* 11: 101057.
- Suomalainen, A., and J. Nunnari, 2024 Mitochondria at the crossroads of health and disease. *Cell* 187: 2601-2627.
- Susek, R. E., and S. Lindquist, 1990 Transcriptional derepression of the *Saccharomyces cerevisiae* HSP26 gene during heat shock. *Mol Cell Biol* 10: 6362-6373.
- van de Poll, F., B. M. Sutter, M. G. Acoba, D. Caballero, S. Jahangiri *et al.*, 2023 Pbp1 associates with Puf3 and promotes translation of its target mRNAs involved in mitochondrial biogenesis. *PLoS Genet* 19: e1010774.
- Wang, X., and X. J. Chen, 2015 A cytosolic network suppressing mitochondria-mediated proteostatic stress and cell death. *Nature* 524: 481-484.
- Welker, S., B. Rudolph, E. Frenzel, F. Hagn, G. Liebisch *et al.*, 2010 Hsp12 is an intrinsically unstructured stress protein that folds upon membrane association and modulates membrane function. *Mol Cell* 39: 507-520.
- Yang, E. J., W. M. Pernice and L. A. Pon, 2022 A role for cell polarity in lifespan and mitochondrial quality control in the budding yeast *Saccharomyces cerevisiae*. *iScience* 25: 103957.
- Zacharioudakis, E., and E. Gavathiotis, 2023 Mitochondrial dynamics proteins as emerging drug targets. *Trends Pharmacol Sci* 44: 112-127.
- Zhang, L., J. Wang, J. Wang, B. Yang, Q. He and Q. Weng, 2020 Role of DJ-1 in Immune and Inflammatory Diseases. *Front Immunol* 11: 994.
- Zhang, L. N., H. Y. Zhou, Y. Y. Fu, Y. Y. Li, F. Wu *et al.*, 2013 Novel small-molecule PGC-1 α transcriptional regulator with beneficial effects on diabetic db/db mice. *Diabetes* 62: 1297-1307.
- Zhong, Y., J. Li, M. Ye and X. Jin, 2023 The characteristics of FBXO7 and its role in human diseases. *Gene* 851: 146972.